
Geometric Description of Scattering Amplitudes

Exploring the Amplituhedron

Andrea Orta



München 2017

Geometric Description of Scattering Amplitudes

Exploring the Amplituhedron

Andrea Orta

Dissertation
an der Fakultät für Physik
der Ludwig-Maximilians-Universität
München

vorgelegt von
Andrea Orta
aus Torino, Italien

München, den 30. Oktober 2017

Erstgutachterin: Prof. Dr. Livia Ferro

Zweitgutachter: Prof. Dr. Dieter Lüst

Tag der mündlichen Prüfung: 15. Dezember 2017

Contents

Zusammenfassung	xi
Summary	xiii
Acknowledgements	xv
0 Introduction	1
1 Scattering amplitudes in massless quantum field theories	9
1.1 General framework	9
1.2 Large- N limit and colour decomposition	14
1.2.1 Properties of tree-level colour-ordered amplitudes	16
1.3 $\mathcal{N} = 4$ super Yang–Mills	19
1.3.1 The superspace formalism	22
2 On-shell methods for $\mathcal{N} = 4$ SYM theory and its symmetries	25
2.1 Spinor-helicity variables	25
2.2 Symmetries of tree-level superamplitudes and the Yangian	31
2.2.1 Superconformal symmetry	31
2.2.2 Dual superconformal symmetry	33
2.2.3 Yangian symmetry	36
2.3 Twistor variables	38
2.3.1 Spacetime supertwistors	38
2.3.2 Momentum supertwistors	39
2.3.3 Yangian generators in supertwistor formulation	42
2.4 BCFW recursion relations	43
2.5 Grassmannian formulation of scattering amplitudes	54

2.5.1	Geometric interpretation of momentum conservation	56
2.5.2	Grassmannian integrals	58
2.5.3	On-shell diagrams	63
3	The Amplituhedron proposal	79
3.1	Positive geometry in arbitrary dimensions	80
3.2	Tree amplituhedron and scattering amplitudes	85
3.3	Loop-level amplituhedron	91
3.4	An $i\epsilon$ -prescription for volume functions	94
3.4.1	A mathematical prelude: multivariate residues	94
3.4.2	NMHV amplitudes	96
3.4.3	N ² MHV amplitudes	105
4	Volume of the dual tree-level amplituhedron	107
4.1	Symmetries of the volume function and the Capelli differential equations .	108
4.2	Solution for the $k = 1$ case	110
4.3	Applying the master formula	114
4.3.1	Volume in the $m = 2$ case	114
4.3.2	Volume in the $m = 4$ case	117
4.4	Deformations and higher- k amplituhedron volumes	120
5	Yangian symmetry for the tree-level amplituhedron	123
5.1	The Heisenberg isotropic spin chain and the algebraic Bethe ansatz	124
5.1.1	Introduction	124
5.1.2	Lax operators, R-matrices, monodromy and transfer matrix	128
5.1.3	The ansatz and the Bethe equations	130
5.2	Construction of amplituhedron volume functions	133
5.2.1	From scattering amplitudes to the amplituhedron	134
5.2.2	On-shell diagrammatics	136
5.3	Spin chain picture for the amplituhedron volume	139
5.3.1	Proof of the monodromy relation	143
5.3.2	Yangian invariance for the amplituhedron volume	144
6	Summary and outlook	147

A	More on the $i\epsilon$-prescription	151
A.1	Even distribution of poles: a proof	151
A.2	The five-point N^2 MHV volume function	154
B	Details on the solution of the Heisenberg spin chain	161
B.1	Permutation and shift operators	162
B.2	\mathcal{U}_N and \mathcal{H}_N from the transfer matrix	163
B.3	On the ansatz and the Bethe equations	164
C	Yangian for the tree amplituhedron	167
C.1	Construction of volume functions	167
C.2	Seed mutations	168
C.3	Intertwining relations	169
C.4	Action of the monodromy matrix on the seed	170

Zusammenfassung

Die vorliegende Dissertation befasst sich mit einigen der neuesten Entwicklungen im Themengebiet der Streuamplituden in schwach gekoppelten Eichtheorien. Der traditionelle störungstheoretische Zugang, der Feynman-Diagramme verwendet, hat sich durchgesetzt und großen Erfolg erzielt, jedoch er ist zunehmend ungeeignet geworden, um mit der Komplexität der Präzisionsberechnungen umzugehen, die heutzutage benötigt sind. Neue Techniken, die zusammenfassend als *on-shell Methoden* bezeichnet werden, sind entwickelt worden, um die Nachteile und Engpässe dieses Zugangs zu vermeiden. Sie enthüllen eine inhärente (und manchmal unerwartete) Einfachheit der Streuamplituden, oft in Verbindung zur Symmetrien; daneben, erlaubten sie die Entwicklung eines grundverschiedenen, geometrischen Verständnis von Amplituden, bei dem Grassmann-Mannigfaltigkeiten eine zentrale Rolle spielen. Dieses Programm hat sich sehr gut im Rahmen eines speziellen Modells bewährt, der planaren $\mathcal{N} = 4$ super Yang–Mills Theorie. Im Jahr 2013 ist eine bemerkenswerte Vermutung vorgelegt worden, die besagt, dass jede Amplitude ist insgeheim das Volumen eines verallgemeinerten Polytops, das *Amplituhedron* heißt.

In dieser Doktorarbeit, untersuchen wir, nach einer detaillierten Einführung in die on-shell Methoden, den Amplituhedron-Vorschlag ausführlich auf Baumniveau und wir berichten über mehrere Ergebnisse, die zusammen mit anderen Mitarbeitern erreicht worden sind. Wir führen eine Formel ein, die NMHV-Baumniveau Volumenfunktionen als Integrale über eine duale Grassmann-Mannigfaltigkeit darstellt, und damit Triangulationen des Amplituhedrons vermeidet; dann leiten wir eine $i\epsilon$ -Vorschrift her, die uns erlaubt, sie als Summe von Residuen eines Grassmannschen Integrals aufzubauen, das im Geiste ähnlich zu dem für Amplituden relevanten ist. Anschließend, angeregt von den Schwierigkeiten bei der Verallgemeinerung unserer Ergebnisse, suchen wir nach einer Realisation der Yangschen Symmetrie im Rahmen des Amplituhedrons. Wir zeigen, dass mit den Volumenfunktionen eng verwandte Objekte wirklich invariant unter den Transformationen des Yangians $Y(\mathfrak{gl}(m+k))$ sind und denken über die Implikationen davon nach.

Summary

This dissertation is concerned with some of the most recent developments in the understanding of gauge theory scattering amplitudes at weak coupling. The traditional perturbative approach in terms of Feynman diagrams is well established and has achieved great triumphs, however it has become increasingly unsuited to handle the complexity of the precision calculations needed nowadays. In looking for new ways to avoid its drawbacks and bottlenecks, new techniques have been developed, collectively going under the name of *on-shell methods*. Beyond unveiling an inherent (and at times unexpected) simplicity of scattering amplitudes – often in connection to symmetries – they helped the rise of a radically different, geometric understanding of them, in which Grassmannian manifolds play a central role. This program has proven very successful in the context of a special model, planar $\mathcal{N} = 4$ super Yang–Mills theory. In 2013 a striking conjecture was put forward, stating that every amplitude is secretly the volume of a generalised polytope, called the *amplituhedron*.

In this thesis, after providing a broad introduction about on-shell methods, we investigate this proposal at tree-level in detail and report on several new results that were obtained in collaboration with other authors. In particular, we present a closed formula for expressing NMHV tree-level volume functions as integrals over a dual Grassmannian, avoiding triangulations of the amplituhedron; we subsequently derive an $i\epsilon$ -prescription that allows to alternatively construct them as a sum of residues of a Grassmannian integral, similar in spirit to the one relevant for scattering amplitudes. Motivated by the difficulties in moving to more general tree-level volume functions, we then look for a realisation of Yangian symmetry in the framework of the amplituhedron. We prove that objects closely related to the volume functions are in fact invariant under the Yangian $Y(\mathfrak{gl}(m+k))$ and ponder on the implications of this result.

Acknowledgements

First and foremost, I am very grateful to my supervisor, Livia Ferro, who introduced me to a thriving field to investigate a fascinating problem. Beyond always being available to answer my questions and sharing her deep knowledge, she was supportive and encouraging throughout the difficulties of my first research experiences. Moreover, she gave me the opportunity to travel to attend schools and conferences, where I had the opportunity to learn from numerous outstanding scientists: in relation to this, I would like to thank Nima Arkani-Hamed for a kind invitation to the IAS in Princeton.

It has been a pleasure to share my research projects with Tomek Łukowski, whose expertise and insight have been of inspiration and who contributed to create a pleasant atmosphere throughout our collaborations. I also want to thank Matteo Parisi for the many fruitful discussions that improved my understanding.

This dissertation has been heavily influenced by many people: I am indebted to Reinke Isermann for helping me gain familiarity with the on-shell methods; to Josè Francisco Morales and Congkao Wen for collaborating on my first project; to Nils Kanning for sharing his knowledge on integrability and proofreading the *Zusammenfassung* of this thesis (any remaining mistake is of course my own!). I also wish to thank Jake Bourjaily, Hugh Thomas and Jaroslav Trnka for useful discussions about details of this work; finally, I owe Matteo Rosso and especially Michela Amicone for helping me code a complicated matrix in L^AT_EX.

I thoroughly enjoyed my time in Munich, also thanks to the lively atmosphere created by all members of the *Mathematical physics and String theory* research group. I want to personally thank for the time spent together my fellow PhD students Enrico Brehm, Fabrizio Cordonier-Tello, Nicolás Gonzalez, Daniel Jaud, Benedikt Richter and the Post-Docs Reinke Isermann, Daniel Junghans, Nils Kanning, Emanuel Malek, Stefano Massai, Christoph Mayrhofer, Erik Plauschinn, Felix Rudolph, Cornelius Schmidt-Colinet, Angnis Schmidt-May, as well as Michael Haack for the friendly help and advice on many technical issues. Finally, I express my gratitude to Dieter Lüst, for agreeing to be my second

Gutachter.

I would like to thank Ruth Britto for giving me the chance to continue my career in Dublin as a PostDoc. In this regard, I am grateful to Livia Ferro, Lorenzo Magnea, Dieter Lüst and Tomek Lukowski for supporting my applications with their recommendation letters, as well as to Reinke Isermann, Matteo Rosso, Cornelius Schmidt-Colinet and Johannes Broedel for sharing their experience and offering me their friendly advice on the matter.

Ich bin Andreas und Veronika herzlich dankbar: ihr seid nicht nur voll nette Mitbewohner, sondern auch ganz engagierte und geduldige Deutschlehrer gewesen, aber insbesondere gute Freunde geworden. Ich freue mich darauf, euch wiederzusehen und Musik zusammenzuspielen!

Un grande grazie agli amici italiani. A quelli di Torino, perché mi scrivete regolarmente e – quando la distanza tra noi diventa piccola a sufficienza – rimediate sempre almeno un pomeriggio o una serata libera; a quelli conosciuti a Monaco, in particolare Anna, Elisabetta, Michela, Alberto e Angelo: tra chiacchierate, giochi da tavolo e (ardite) spedizioni in montagna, il vostro affetto ha reso speciale questo tempo insieme.

In conclusione, un doveroso pensiero va ai miei genitori, Marilena e Renato, e a mio fratello Federico. Pur discretamente, siete stati sempre presenti in questi tre anni: grazie per avermi reso capace di camminare con le mie gambe, grazie perché continuate a sostenermi nel mio percorso.

Chapter 0

Introduction

It is difficult to overestimate the role that symmetry principles have played in the development of physics. A good example of this can be found in two of the most fundamental problems in classical and quantum mechanics, both instances of the Kepler problem *i.e.* a two-body problem characterised by a central potential of the form $V(r) \sim 1/r$. In a classical context, it arises in the description of the trajectories of two celestial bodies orbiting each other, whereas in quantum mechanics it is relevant to understand the motion of an electron around a proton in a hydrogen atom. Despite pertaining to completely different length scales, the two situations are alike and in both cases an exact solution could be found – albeit by very different means. Focusing on the classical setting, the particular dependence of the potential on the distance between the two masses implies that all bound orbits are closed ellipses, *i.e.* they do not precess. As this property is spoiled even by slight modifications to the power law of the potential, we are led to think that there must be some conserved quantity preventing changes in the orientation of the major axis of the ellipse. This is indeed the case and such constant of motion is the *Laplace–Runge–Lenz vector* [1]. As first pointed out by Pauli [2], an operator version of the same vector is also conserved quantum mechanically in the hydrogen atom: this enhances the standard three-dimensional rotational symmetry of the system to a four-dimensional one, allowing to recover the spectrum of energy eigenvalues without solving the Schrödinger equation [3]. The upshot of this parable is that sometimes unveiling hidden properties of the problem under consideration can yield powerful insights, allowing to move beyond known results, especially when the traditional techniques have already been fully exploited.

A central problem in quantum field theory (QFT) is the computation of scattering amplitudes, which are strictly related to the probabilities of any interaction among elementary

particles to occur. Such processes are probed at colliders, the most powerful of which – the Large Hadron Collider (LHC) – is now operating at CERN. Scattering hadrons allows to access high-energy regimes, however it also produces a very large background that needs to be understood as much as possible in order to reliably identify potential signals in the host of collected data. The mathematical model within which theoretical calculations are performed is a gauge theory called *Standard Model*. It is the best theory describing the elementary constituents of nature and its predictions have been verified often at unprecedented levels of precision. One of its sectors, namely quantum chromodynamics (QCD), is most responsible for the background processes at the LHC. The enhanced sensitivity of modern detectors has called for theoretical predictions of comparable quality: this has triggered much theoretical research and the last decades have witnessed astounding progress in different directions. In particular, the knowledge of many formal aspects of gauge theories has improved significantly, also through the study of non-realistic models, such as the one that will prominently appear in this work, $\mathcal{N} = 4$ super Yang–Mills theory ($\mathcal{N} = 4$ SYM), particularly when restricted to the planar sector. In light of the previous discussion, it seems fitting that the latter is often referred to as *the hydrogen atom of the 21st century!* The hope is that even those new ideas that seem inextricably tied to the simplified setting in which they were conceived could one day be employed to compute observables of direct phenomenological interest.

In the next section we will review the most relevant recent developments in the field of scattering amplitudes, focusing on those that will play a central role in this dissertation.

Overview of recent developments

In 1949 Feynman proposed a new formalism to compute scattering amplitudes in quantum electrodynamics (QED), introducing his eponymous diagrams [4]. They quickly became the standard tool for performing perturbative calculations in QFT and achieved tremendous success. Within a few decades, however, it became clear that they had some serious drawbacks: even at leading order, the number of diagrams contributing to a process is generally very large, so that even modern computers can be of little help if one is interested in an analytic result; moreover – besides not having physical meaning (*i.e.* not corresponding to any physical observable) by themselves – they typically evaluate to more complicated expressions than the amplitude they are meant to compute, signalling that the theory has more structure than what is manifest at the level of the Lagrangian. A clear example of

this is the extremely compact form that the so-called maximally-helicity-violating (MHV) amplitudes of QCD take, which was originally advocated by Parke and Taylor (it is instructive to compare the result they first obtained in the six-gluon case [5] with the form they proposed in [6] for any number of gluons).

In the Sixties there was an attempt to understand scattering amplitudes based only on their singularity structure and symmetry properties, a program called *Analytic S-matrix* [7]. Inspired by it, people tried to circumvent Feynman diagrams altogether and construct the amplitudes by other means, the so-called *on-shell methods*. For instance, building on the work of Cutkosky [8], the modern *unitarity method* was introduced by Bern, Dixon, Dunbar and Kosower to construct one-loop gauge theory amplitudes by gluing together tree-level ones. They first applied this technique to determine all $\mathcal{N} = 4$ SYM one-loop amplitudes [9] and then extended it to encompass several others, in particular those of $\mathcal{N} = 1$ SYM [10]: these results significantly simplified the computation of QCD one-loop amplitudes, exposing once again unexpected simplicity in the structure of the final result. The technique has since then been upgraded, allowing more than two internal lines to be put on-shell, deserving the name *generalised unitarity*. This was done first at one loop [11] and then extended to higher loop orders: a recent result in QCD is the computation of the two-loop six-point all-plus-helicity amplitude [12, 13]. Much more has been said about higher loops in $\mathcal{N} = 4$ SYM, at least at the level of the integrand [14, 15]. This story is deeply interwoven with the so-called BDS-ansatz [16], conjecturing an iterative structure governing the planar part of the amplitudes: the proposal is correct for $n = 4, 5$ scattering particles and – despite being incomplete starting at six-point – it proved extremely fruitful, sparking a lot of research in the mathematics of scattering amplitudes as well. Additional details about unitarity methods may be found *e.g.* in [17, 18].

Much progress, especially concerning more formal aspects of gauge theories, was initiated by Witten’s seminal paper [19]. He reconsidered the problem of expressing perturbative scattering amplitudes in terms of twistors [20, 21] and found that they are non-vanishing only if they are supported on some holomorphic curve in twistor space. This revealed a correspondence between the perturbative expansion of $\mathcal{N} = 4$ SYM and the D-instanton expansion of a particular string theory, the topological B-model, on supertwistor space (Berkovits showed shortly after that one can alternatively consider the standard perturbative expansion of an open string theory [22]). Explicit checks of the proposal were originally provided only for tree-level MHV amplitudes: shortly after, it received confirmation for the conjugate tree-level $\overline{\text{MHV}}$ ones [23] and further strong evidence

in its favour was presented in [24].

One of the most influential ideas that stemmed from Witten’s twistor string theory is that of constructing amplitudes recursively. One of the approaches is a direct consequence of the twistor transform of tree-level amplitudes analysed in [19] and consists in constructing them by sewing MHV amplitudes as if they were interaction vertices, as shown by Cachazo, Svrček and Witten in [25]. Alternatively, it is possible to take advantage of the analytic structure of any tree-level amplitude to obtain it as a product of lower-point ones: this technique was pioneered by Britto, Cachazo and Feng [26] and proven shortly after [27]. Both recursions have been generalised to the supersymmetric setting of $\mathcal{N} = 4$ SYM and solved for all tree-level amplitudes by Elvang, Freedman and Kiermaier [28] and by Drummond and Henn [29] respectively. In the planar limit, moreover, the latter allowed the authors of [30] to determine the integrand of scattering amplitudes for any number of particles at any number of loops.

The aforementioned strict connection between gauge theory and string theory resonates well with one of the most groundbreaking works of the last decades, namely Maldacena’s conjecture of the AdS/CFT correspondence [31]. According to it, there exists a duality between string theories defined on an Anti-de Sitter background and conformal field theories living on its flat boundary: despite the lack of a formal proof, much evidence has been collected in favour of this proposal, the most studied instance of it being the duality between type IIB superstring theory on an $AdS_5 \times S^5$ background and $\mathcal{N} = 4$ SYM theory. However, as opposed to the one previously presented, AdS/CFT is a strong-weak duality, meaning that the strongly coupled regime of gauge theory is captured by the perturbative expansion of string theory (and viceversa). Thanks to this feature, the correspondence has lent itself to the investigation of $\mathcal{N} = 4$ SYM amplitudes at strong coupling [32, 33] as well as of problems coming from very different areas of physics, such as condensed matter theory, nuclear physics and even fluid dynamics [34].

Another major theme in the modern approach to $\mathcal{N} = 4$ SYM theory is that of symmetries. The model is the most symmetric QFT in four dimensions, enjoying maximal supersymmetry and conformal symmetry. In particular, every amplitude is invariant under the action of the generators of $\mathfrak{psu}(2, 2|4)$. Moreover, in the planar limit, $\mathcal{N} = 4$ SYM enjoys an even bigger symmetry: upon introducing new dual variables, Drummond, Henn, Korchemsky and Sokatchev showed that tree-level amplitudes are invariant under another copy of the $\mathfrak{psu}(2, 2|4)$ algebra [35], completely hidden from the point of view of the Lagrangian. The interplay with the previously mentioned one gives rise to an infinite-

dimensional symmetry, the Yangian $Y(\mathfrak{psu}(2,2|4))$, as proven by Drummond, Henn and Plefka [36]. Such strong symmetry constraints constitute compelling evidence that planar $\mathcal{N} = 4$ SYM can be solved exactly and is therefore amenable to methods proper to the theory of integrable systems, see *e.g.* the review [37]. This can be further understood in light of the AdS/CFT correspondence, dictating that it is dual to a two-dimensional non-linear sigma model on a symmetric coset space, which commonly exhibits integrability. Furthermore, the two-point correlators of gauge-invariant operators could be determined by mapping the problem to an integrable Heisenberg spin chain [38, 39] (see also [40]). These and other works paved the way for studying $\mathcal{N} = 4$ SYM from the perspective of integrability. Finally, aside from the previously discussed computations at strong coupling, we should mention that a non-perturbative proposal for calculating scattering amplitudes at finite coupling was advanced in [41].

Twistor variables make the symmetries of $\mathcal{N} = 4$ SYM as manifest as possible. Hodges was the first to introduce dual variables to the ones employed by Witten, associated to momentum space instead of ordinary spacetime and hence called momentum twistors [42]. By expressing the kinematic degrees of freedom in terms of either set of twistors, it was shown that amplitudes can be represented via contour integrals on Grassmannian manifolds. The first proposal in this sense – employing ordinary twistors – came from Arkani-Hamed, Cachazo, Cheung and Kaplan [43]; shortly after, Mason and Skinner worked out the analogue for momentum twistors [44]; the two formulations were exposing ordinary and dual superconformal symmetry respectively and were shown to be related by a change of variables in [45]. Drummond and Ferro [46] proved that the two Grassmannian formulae are dual to each other and explicitly Yangian-invariant. Furthermore, they were able to prove that their form is in fact essentially dictated by the requirement of Yangian invariance [47], see also [48] for a different approach.

The remarkable results listed in the previous paragraph suggested unexpected ties between the physics of scattering and areas of geometry and combinatorics. A new kind of Grassmannian space was considered, called positive Grassmannian and already well known to mathematicians [49]: its cell decomposition – deeply interwoven with the permutation group – was put in one-to-one correspondence with the newly introduced on-shell diagrams. Very different from Feynman diagrams, they allow to represent the amplitude in accordance with the recursion relations of [27] and their combinatorial properties make them an efficient computational tool [50]. On a different note, a class of tree-level amplitudes had been interpreted in [42] as volumes of polytopes in twistor space. This idea was

further explored in [51] and elicited the amplituhedron conjecture of Arkani-Hamed and Trnka [52, 53]. The (tree-level) amplituhedron is a region of a high-dimensional (Grassmannian) space, obtained from momentum twistor space by bosonisation of the fermionic coordinates: it is believed that any (integrand of a) scattering amplitude is computed as the volume of an appropriately defined dual object and that different triangulations correspond to different ways of obtaining the amplitude by means of recursion relations. From this picture of scattering amplitudes, in particular, known properties such as locality and unitarity are emergent from the geometry, instead of having to be postulated. Despite the compelling simplicity and highly non-trivial evidence in its favour, the amplituhedron is not yet a viable alternative to more established computational tools. Triangulations of the amplituhedron are not known in general and the definition of its dual is unclear, hence the need for new strategies circumventing the difficulties. The work presented in this thesis contributes to filling this gap, in the hope that phenomenologically interesting computations could be tackled soon.

Plan of the thesis

This dissertation is organised as follows:

- In Chapter 1 we review the definition of scattering amplitudes in a generic massless quantum field theory, following the textbook approach. Working with pure Yang–Mills theory, we present the colour decomposition technique and the properties fulfilled by colour-ordered amplitudes, and explain what obstructions prevent the efficient computation of arbitrary scattering amplitudes via Feynman diagrams. Finally, we introduce $\mathcal{N} = 4$ SYM theory and the superspace formalism.
- Chapter 2 constitutes a review of the on-shell methods which will be relevant later on. We introduce the spinor-helicity formalism and twistor variables, useful to expose interesting properties of gauge theories. We discuss the symmetries of $\mathcal{N} = 4$ SYM amplitudes, coming to the definition of Yangian symmetry in the planar limit. After working out the on-shell recursion of Britto, Cachazo, Feng and Witten [26, 27], we present the Grassmannian formulation of scattering amplitudes, discussing Grassmannian integrals [43, 44] and on-shell diagrams [50].
- Chapter 3 is devoted to introducing the amplituhedron [52, 53] both at tree- and loop-level. Moreover, after presenting an amplituhedron version of the Grassmannian

contour integral for tree-level amplitudes – first appeared in [54] – we discuss our attempt at introducing an $i\epsilon$ -prescription to identify the correct set of residues to consider, without any additional input from *e.g.* recursion relations [55]. Further details are included in Appendix A.

- In Chapter 4 – following [54] – we exploit general symmetry properties of the amplituhedron volume to partially constrain an ansatz for it. In particular, we discuss a set of PDEs called Capelli differential equations. For a particular class of tree-level amplitudes we are able to fully specify the volume and correctly compute the expected result. We conclude commenting on what prevents us from applying our strategy to more general classes of amplitudes.
- Chapter 5 – drawing from [56] – addresses the shortcomings of the technique employed in [54] and investigates a notion of Yangian symmetry in the amplituhedron setting. Since we make use of various concepts coming from the integrability realm, we find it useful to open with an introduction to the Heisenberg isotropic spin chain, complemented by Appendix B. Building on the results of [57] for scattering amplitudes, we first obtain a new formula for the amplituhedron volume, yielding an on-shell diagrammatics similar to that of [50]; we then proceed to construct a spin chain for the amplituhedron, such that objects closely related to its volume are invariant under the Yangian $Y(\mathfrak{gl}(m+k))$. Some technical aspects of the derivations are included in Appendix C.
- In Chapter 6 we conclude, indicating a few directions for future research.

Chapter 1

Scattering amplitudes in massless quantum field theories

In this first chapter we want to discuss the main features of the standard methods used to perturbatively compute scattering amplitudes, making use of Feynman diagrams. We will start by reviewing the traditional formalism focusing on pure Yang–Mills theory, together with its most immediate drawbacks in the context of tree-level high-multiplicity processes. Then we will explain how decoupling the kinematics from the colour information can significantly speed up the calculations. Finally, we will introduce the maximally supersymmetric generalisation of Yang–Mills theory, namely $\mathcal{N} = 4$ super Yang–Mills, which will be the framework of a large part of this dissertation.

1.1 General framework

The basic quantity that can be measured at collider experiments is the probability for a given process among elementary particles to happen. Suppose we have an initial state in the Hilbert space \mathcal{H} of our QFT and we want to measure the probability for it to evolve to a final state. To this end, we will first have to calculate the corresponding probability amplitude, defined as the inner product of the two:

$$A(\text{in} \rightarrow \text{out}) = \langle \text{out}; t = +\infty | \text{in}; t = -\infty \rangle_S = \langle \text{out} | S | \text{in} \rangle_H . \quad (1.1)$$

We can see how in the Schrödinger picture – where states are functions of time – the amplitude is the overlap between the initial and final states taken to be far apart in time. This is based on the assumption that every interaction occurs in a finite time interval:

long before and after it, the scattering particles are free. One speaks of *asymptotic states*, namely on-shell, one-particle momentum eigenstates described by plane waves. On the other hand, in the Heisenberg picture the temporal dependence is encoded in the operators and therefore one thinks of scattering amplitudes as elements of the *S(cattering)-matrix* S .

Once the amplitude is known, to obtain the desired probability, *e.g.* a cross section, we will have to

- compute its modulus squared $|\mathbf{A}(\text{in} \rightarrow \text{out})|^2$;
- sum over the quantum numbers of the outgoing particles and average over those of the incoming particles;
- integrate the result over the phase space of the outgoing particles.

Although the last step of this algorithm is far from trivial in general, it is however clear how the *scattering amplitude* $\mathbf{A}(\text{in} \rightarrow \text{out})$ is the building block of the theoretical prediction.

The Lehmann–Symanzik–Zimmermann (LSZ) reduction formula relates S-matrix elements to vacuum expectation values (v.e.v.’s) of time-ordered products of fields: assuming for simplicity to be working with a scalar theory and neglecting normalisation factors, for a $n_{\text{in}} \rightarrow n - n_{\text{in}}$ process we have

$$\begin{aligned} \langle \text{out} | S | \text{in} \rangle &\sim \prod_{i=1}^{n_{\text{in}}} \left[i \int d^4 x_i e^{-ip_i \cdot x_i} (\square_{x_i} + m^2) \right] \prod_{j=n_{\text{in}}+1}^n \left[i \int d^4 x_j e^{+ip_j \cdot x_j} (\square_{x_j} + m^2) \right] \times \\ &\quad \times \langle \Omega | T \{ \phi(x_1) \phi(x_2) \phi(x_3) \cdots \phi(x_n) \} | \Omega \rangle . \end{aligned} \quad (1.2)$$

The two products distinguish incoming states – carrying momenta $p_1, \dots, p_{n_{\text{in}}}$ – from outgoing ones – carrying momenta $p_{n_{\text{in}}+1}, \dots, p_n$. When performing the Fourier transforms, the operators $\square_{x_i} + m^2$ produce – up to constants – factors of the form $p_i^2 - m^2$: since they vanish when the external particles are on-shell, the LSZ formula precisely singles out from the many terms involved in $T\{\phi(x_1)\phi(x_2)\phi(x_3)\cdots\phi(x_n)\}$ those having the pole structure corresponding to the desired configuration of asymptotic states.

Observe also that the fields appearing in the time-ordered product are interacting; moreover, the vacuum $|\Omega\rangle$ is that of the interacting theory, in general different from that of the free theory $|0\rangle$. Luckily, both difficulties can be overcome *perturbatively* thanks to a result due to Gell–Mann and Low [58]:

$$\langle \Omega | T \{ \phi(x_1) \phi(x_2) \phi(x_3) \cdots \phi(x_n) \} | \Omega \rangle = \frac{\langle 0 | T \{ \phi_0(x_1) \cdots \phi_0(x_n) e^{i \int d^4 z \mathcal{L}_{\text{int}}[\phi_0]} \} | 0 \rangle}{\langle 0 | T \{ e^{i \int d^4 z \mathcal{L}_{\text{int}}[\phi_0]} \} | 0 \rangle} \quad (1.3)$$

The problem is now reduced to the computation of v.e.v.'s of time-ordered products of *free* fields, with respect to the free-theory vacuum: the interactions are accounted for expanding the exponentials to the desired order in the coupling constant g . Furthermore, Wick's theorem states that the only non-vanishing contributions will come from full contractions of the fields in the T -product, *i.e.* products of time-ordered product of two free fields, the *Feynman propagators*

$$D_F(x, y) = \langle 0 | T \{ \phi_0(x) \phi_0(y) \} | 0 \rangle = \lim_{\epsilon \rightarrow 0} \int \frac{d^4 k}{(2\pi)^4} \frac{i}{k^2 - m^2 + i\epsilon} e^{ik \cdot (x-y)} . \quad (1.4)$$

This all looks very involved, but admits an efficient representation in terms of *Feynman diagrams*, matching the individual terms of the expansion of time-ordered products: the nodes of these graphs will be the external points x_i and the internal ones z_i , where the interactions take place. In fact, one can avoid computing T -products altogether and start instead from the diagrams: each graph can be easily converted to an integral through a set of *position space Feynman rules*. Plugging the result into the LSZ formula accounts for a Fourier transform to momentum space and a so-called *amputation* of the Feynman diagrams, by which we mean that the external legs have been put on the mass shell (at loop level also taking into account higher-order corrections).

The upshot of this procedure is that any amplitude $A(\text{in} \rightarrow \text{out})$ is computable evaluating a set of (amputated) Feynman diagrams via *momentum space Feynman rules*, which can be read off from the Lagrangian of the theory. An important remark to be done is that the set of relevant diagrams to consider restricts to fully connected graphs, *i.e.* those for which any external leg can be reached from any other: diagrams involving vacuum bubbles are removed by the denominator of (1.3), whereas partially connected diagrams are obtained as products of fully connected ones, with respect to which they are suppressed.

We now specialise our discussion to the pure Yang–Mills gauge theory with colour group $SU(N)$. This is the restriction of QCD (although we allow $N \neq 3$) to the pure-gluon sector and it bears interesting similarities with the most symmetric QFT in four dimensions, $\mathcal{N} = 4$ SYM; its classical Lagrangian density reads

$$\mathcal{L}_{\text{YM}}^{(\text{cl})} = -\frac{1}{4} \text{tr} (F_{\mu\nu} F^{\mu\nu}) \quad , \quad F_{\mu\nu} = \partial_\mu A_\nu - \partial_\nu A_\mu - ig[A_\mu, A_\nu] . \quad (1.5)$$

The elementary *gluon* fields are matrix valued and can be expanded as $(A_\mu)_j^i = A_\mu^a (T_a)_j^i$, where the T_a ($a = 1, \dots, N^2 - 1$) are the (Hermitian, traceless) generators of the colour group in the adjoint representation. Quantising Yang–Mills theory as in (1.5) is not possible, because $\mathcal{L}_{\text{YM}}^{(\text{cl})}$ is singular and a propagator for the gluon field cannot be defined.

To remedy this issue, a gauge-fixing term \mathcal{L}_{gf} must be added, which however breaks the gauge symmetry. To restore it for the quantities of physical interest we need to add yet another piece \mathcal{L}_{gh} to the Lagrangian: it comes from the Faddeev–Popov procedure and introduces unphysical states, called *ghosts*, essential for loop-level calculations. For the sake of simplicity, in the following we will restrain from spelling out its form in full: on the one hand, ghosts only enter in loop-level computations, which will not concern us; more importantly, we will soon enough depart from the traditional approach to the problem, hence additional details would be redundant. Choosing \mathcal{L}_{gf} so that the Lagrangian retains manifest covariance, we arrive at

$$\mathcal{L}_{\text{YM}} = -\frac{1}{4} \text{tr} (F_{\mu\nu} F^{\mu\nu}) - \frac{1}{2\xi} \text{tr} (\partial_\mu A^\mu \partial_\nu A^\nu) + \mathcal{L}_{\text{gh}} , \quad (1.6)$$

which can now be quantised and yields – up to the ghost sector – the Feynman rules of Figure 1.1, having set $\xi = 1$ (Feynman gauge) and denoted with f^{abc} the structure constants of $\text{SU}(N)$. It should be noted how the non-Abelian gauge group allows for self-interactions of the gauge fields.

The figure displays three Feynman rules for pure Yang–Mills theory, neglecting ghosts. Each rule is represented by a diagram of red wavy lines and an associated mathematical expression.

- Propagator:** A horizontal red wavy line with momentum p and indices a, μ at the left end and b, ν at the right end. The corresponding expression is $\frac{-i\eta^{\mu\nu}}{p^2 + i\epsilon} \delta^{ab}$.
- Trivalent Vertex:** A vertex where three red wavy lines meet. The incoming lines from the top-left and bottom-left have momenta p and q and indices a, μ and b, ν respectively. The outgoing line to the right has momentum r and index c, ρ . The corresponding expression is $-gf^{abc}(\eta^{\mu\nu}(p-q)^\rho + \eta^{\nu\rho}(q-r)^\mu + \eta^{\rho\mu}(r-p)^\nu)$.
- Quartic Vertex:** A vertex where four red wavy lines meet. The incoming lines from the top-left and bottom-left have momenta p and q and indices a, μ and b, ν respectively. The outgoing lines to the top-right and bottom-right have momenta r and s and indices c, ρ and d, σ respectively. The corresponding expression is $-ig^2(f^{abe}f^{cde}(\eta^{\mu\rho}\eta^{\nu\sigma} - \eta^{\mu\sigma}\eta^{\nu\rho}) + f^{ace}f^{bde}(\eta^{\mu\nu}\eta^{\rho\sigma} - \eta^{\mu\sigma}\eta^{\nu\rho}) + f^{ade}f^{bce}(\eta^{\mu\nu}\eta^{\rho\sigma} - \eta^{\mu\rho}\eta^{\nu\sigma}))$.

Figure 1.1: Feynman rules for pure Yang–Mills theory, neglecting the ghosts. All momenta have been taken to be outgoing, as will be done throughout this work. Trivalent and quartic vertices contribute six terms to the evaluation of any Feynman diagram they appear into.

Consider one of the most common processes happening at the LHC, namely $2 \rightarrow 2$ gluon scattering. At tree-level, we have to evaluate the four diagrams in Figure 1.2.

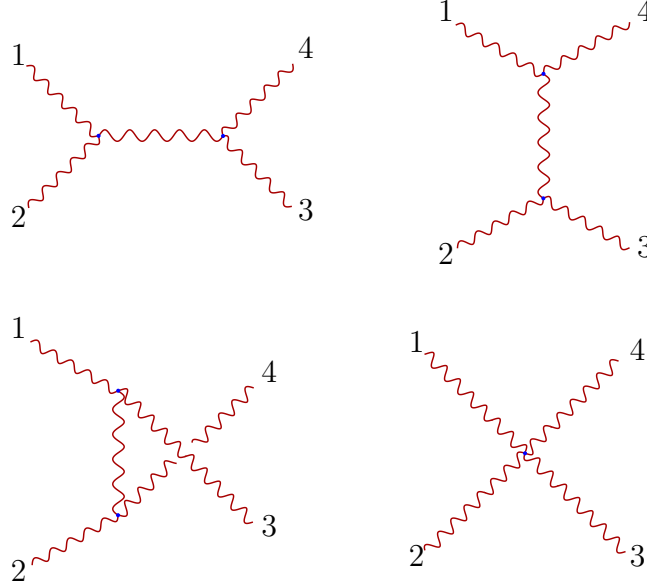


Figure 1.2: Feynman diagrams contributing to the tree-level four-point gluon amplitude. The diagrams involving trivalent vertices only are typically referred to as s -, t -, u -channel.

Given the Feynman rules written above, it is easy to realise that the amplitude computation is not quick, and yet the answer is simple: after combining many terms, the modulus squared of the amplitude – summed over the final states and averaged over the initial ones – reads

$$\frac{1}{4(N^2 - 1)} \sum_{\text{pol., col.}} |\mathcal{A}^{\text{tree}}(2 \rightarrow 2)|^2 = g^4 \frac{4N^2}{(N^2 - 1)} \left(3 - \frac{tu}{s^2} + \frac{su}{t^2} + \frac{st}{u^2} \right), \quad (1.7)$$

where $s = (p_1 + p_2)^2$, $t = (p_1 - p_4)^2$, $u = (p_1 - p_3)^2$ are the Mandelstam variables, satisfying $s + t + u = 0$ since gluons are massless. The situation worsens dramatically (in fact, factorially) when considering a higher number of particles. Table 1.1 shows how many diagrams contribute to the $2 \rightarrow n$ gluon amplitude, computed in an appendix of [59].

n	2	3	4	5	6	7	8
# diagrams	4	25	220	2485	34300	559405	10525900

Table 1.1: In [59] one can also read how many of these diagrams include up to four quartic vertices and find a recursive formula to count their number.

1.2 Large- N limit and colour decomposition

Even for tree-level amplitudes, a brute force approach to their calculation is ruled out. Nevertheless, it is possible to simplify one's life by disentangling *kinematic* degrees of freedom (momenta and polarisations of gluons) and *colour* degrees of freedom. Looking at the Feynman rules spelled out previously, we see that the colour dependence arises from contractions of the structure constants of $SU(N)$. Let us fix the normalisation of the generators as $\text{tr}(T^a T^b) = \delta^{ab}$ and recall the completeness relation they satisfy, known as $SU(N)$ *Fierz identity*:

$$(T^a)_j^i (T^a)_l^k = \delta_l^i \delta_j^k - \frac{1}{N} \delta_j^i \delta_l^k . \quad (1.8)$$

It is easy to show that

$$[T^a, T^b] = i f^{abc} T^c \quad \longrightarrow \quad f^{abc} = -i \text{tr}(T^a [T^b, T^c]) , \quad (1.9)$$

as well as the less trivial

$$f^{abe} f^{cde} = \text{tr}([T^a, T^b][T^c, T^d]) . \quad (1.10)$$

It is then clear that the colour contributions of any given diagram can be written as (products of) traces of generators. The Kronecker δ 's of the propagators force colour indices to be the same at the two ends of internal gluon lines, further simplifying the expressions, and in the end we are left with a small set of terms, forming a basis in the space of all possible colour structures. At tree-level, it consists of single-trace terms only, involving as many generators as the external legs. A graphical notation can be set up, allowing these colour factors to be computed more easily: in Figure 1.3 we illustrate the prescription to deal with the cubic vertices, whereas in Figure 1.4 we provide the pictorial version of the Fierz identity (1.8). The latter justifies the introduction of the so-called *double-line notation* for the gluon propagator, originally due to 't Hooft [60].

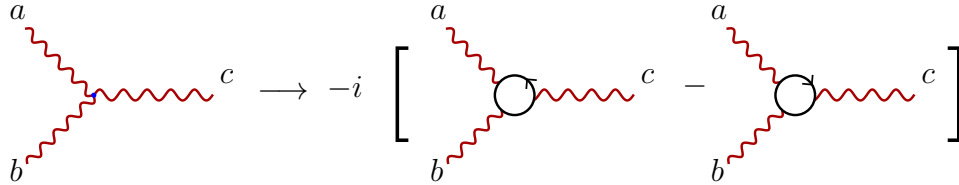


Figure 1.3: Graphical representation of the trivalent vertex. For the quartic one, we would have to expand the product of two structure constants into four traces.

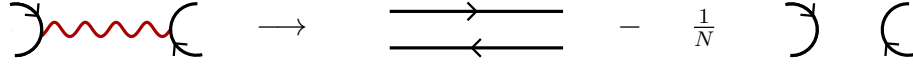


Figure 1.4: Graphical representation of the Fierz identity, providing a decomposition of the propagator in double-line notation.

There exists a particular limit of gauge theory in which at every loop order only single-trace colour structures are present, because every other contribution is subleading. This is called the *large- N limit* and was first considered by 't Hooft in [60]. To define it properly, we first need to operate a simple rescaling of the fields and the coupling constant appearing in the Yang–Mills Lagrangian, namely

$$A_\mu \rightarrow \frac{\sqrt{N}}{g} A_\mu \quad \text{and} \quad g \rightarrow \frac{g}{\sqrt{N}}. \quad (1.11)$$

It is straightforward to check that (1.6) transforms as

$$\mathcal{L}_{\text{YM}} \rightarrow \frac{N}{g^2} \left(-\frac{1}{4} \text{tr} (F_{\mu\nu} F^{\mu\nu}) - \frac{1}{2} (\partial_\mu A^\mu \partial_\nu A^\nu) + \mathcal{L}_{\text{gh}} \right), \quad (1.12)$$

where now both the field strength and the ghost Lagrangian are free from any occurrence of the coupling constant. The Feynman rules come with an extra factor of N^{-1} for each gluon propagator and of N for each gluon vertex and the perturbative expansion of an amplitude can be organised in powers of $1/N$, making the $N \rightarrow \infty$ limit well defined.¹ As anticipated, 't Hooft's double line notation allows to associate to any Feynman diagram a “colour diagram” drawn with double lines, clarifying the colour flow. Finally, observing that any loop of colour provides a factor of N – since it corresponds to $\text{tr}(\mathbb{1}_N)$ – we can perform a power counting on each Feynman diagram, keeping track of all factors of N . One then discovers that at every loop order non-planar diagrams are suppressed with respect to planar ones, implying that they can be neglected as $N \rightarrow \infty$. For this reason the large- N limit is also called *planar limit*.

Based on the previous discussion, we can encode the colour structure of any tree-level amplitude in single-trace terms and come to the following colour decomposition:

$$A_n^{\text{tree}}(\{a_i, p_i, h_i\}) = g^{n-2} \sum_{\sigma \in S_n / \mathbb{Z}_n} \text{tr}(T^{a_{\sigma(1)}} \dots T^{a_{\sigma(n)}}) A_n^{\text{tree}}(\{p_{\sigma(i)}, h_{\sigma(i)}\}). \quad (1.13)$$

The sum runs over non-cyclic permutations of the external legs; it could equivalently be written as a sum over the permutations of $n-1$ legs, once *e.g.* the first one has been singled

¹To be precise, the large- N limit also requires the 't Hooft coupling $\lambda = g^2 N$ to remain finite.

out. The colour information has been disentangled from the kinematics (gluon momenta and helicities), encoded in the gauge-invariant² *colour-ordered amplitudes* A_n^{tree} (also called *partial amplitudes*). At one-loop level, instead, new terms appear and the relevant formula reads [62, 10]

$$\begin{aligned} A_n^{1\text{L}}(\{a_i, p_i, h_i\}) &= g^n \sum_{\sigma \in S_n/\mathbb{Z}_n} N \text{tr}(T^{a_{\sigma(1)}} \dots T^{a_{\sigma(n)}}) A_{n;1}^{1\text{L}}(\{p_{\sigma(i)}, h_{\sigma(i)}\}) + \\ &+ g^n \sum_{c=3}^{\lfloor \frac{n}{2} \rfloor + 1} \sum_{\sigma \in S_n/S_{n;c}} \text{tr}(T^{a_{\sigma(1)}} \dots T^{a_{\sigma(c-1)}}) \text{tr}(T^{a_{\sigma(c)}} \dots T^{a_{\sigma(n)}}) A_{n;c}^{1\text{L}}(\{p_{\sigma(i)}, h_{\sigma(i)}\}) . \end{aligned} \quad (1.14)$$

The sum is over the elements of the quotient group $S_n/S_{n;c}$, with $S_{n;c}$ the residual symmetry group of $\text{tr}(T^{a_{\sigma(1)}} \dots T^{a_{\sigma(c)}}) \text{tr}(T^{a_{\sigma(c+1)}} \dots T^{a_{\sigma(n)}})$, *i.e.* the set of permutations leaving such product invariant; $S_{n;c}$ is typically some product of cyclic groups, *e.g.* $S_{8;4} = \mathbb{Z}_3 \times \mathbb{Z}_5$, $S_{8;5} = \mathbb{Z}_4 \times \mathbb{Z}_4 \times \mathbb{Z}_2$ (expressing the cyclicity of the trace and, in the latter case, the commutativity of the two factors). The $A_{n;1}^{1\text{L}}$ are colour-ordered one-loop amplitudes, used to construct all other $A_{n;c>2}^{1\text{L}}$, by taking sums over permutations of the external legs [9]. Notice how non-planar contributions are indeed subleading in N . Both formulae (1.13) and (1.14) are natural from a string-theoretical point of view and have to do with Chan–Paton factors for open strings scattering [63], of which gluon scattering is the field theory limit. Let us finally mention that the leading term of the previous expansions straightforwardly generalises to any number ℓ of loops: as $N \rightarrow \infty$,

$$A_n^{\ell\text{-L}}(\{a_i, p_i, h_i\}) = g^{n-2} (g^2 N)^\ell \sum_{\sigma \in S_n/\mathbb{Z}_n} \text{tr}(T^{a_{\sigma(1)}} \dots T^{a_{\sigma(n)}}) A_n^{\ell\text{-L}}(\{p_{\sigma(i)}, h_{\sigma(i)}\}) , \quad (1.15)$$

for $A_n^{\ell\text{-L}}$ ℓ -loop colour-ordered amplitudes. We will from now on usually focus on this limit, although this work will be mainly concerned with tree-level amplitudes, which are trivially insensitive to the matter.

1.2.1 Properties of tree-level colour-ordered amplitudes

Colour-ordered amplitudes can be computed via colour-ordered Feynman rules. These are simpler than the regular ones, in that they are stripped off of any colour dependence (by definition) and have fewer terms: the quartic vertex, in particular, only involves three, which can even be reduced to one by picking the Gervais–Neveu gauge [64] (contrast this with the situation of Figure 1.1). Furthermore, the number of contributing Feynman

²Gauge invariance is a consequence of some partial orthogonality property of the colour traces, see [61].

diagrams drops significantly: we only need to retain those whose external legs display the desired ordering, without any crossing, see Table 1.2.

n	2	3	4	5	6	7	8
# diagrams	3	10	38	154	654	2871	12925

Table 1.2: Colour-ordered Feynman diagrams contributing to a tree-level $2 \rightarrow n$ amplitude.

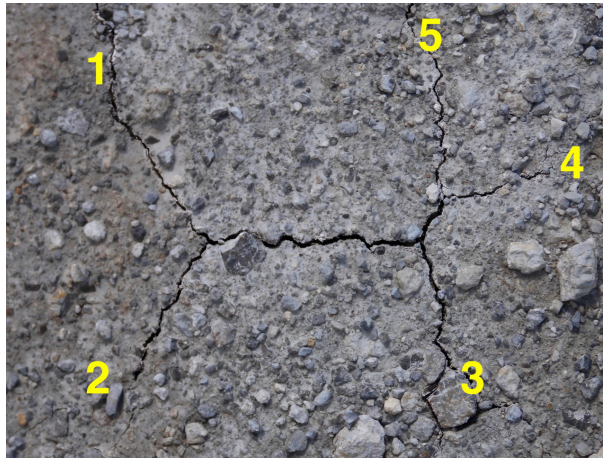


Figure 1.5: One of the ten diagrams contributing to the colour-ordered amplitude A_5^{tree} , spotted in the Tyrolean Alps.

Importantly, not all $n!$ partial amplitudes need to be calculated from Feynman diagrams, because a web of linear relations exists, allowing to express a subset of them in terms of the others, possibly yielding more compact representations of the full amplitude. We present them without proof, employing the shorthand notation

$$\begin{aligned} A_n^{\text{tree}}(1, 2, \dots, n) &= A_n^{\text{tree}}(p_1, h_1; p_2, h_2; \dots; p_n, h_n) \\ A_n^{\text{tree}}(\sigma(1, 2, \dots, n)) &= A_n^{\text{tree}}(\sigma(1), \sigma(2), \dots, \sigma(n)) \end{aligned} \quad (1.16)$$

Cyclicity identities

$$A_n^{\text{tree}}(1, 2, \dots, n) = A_n^{\text{tree}}(\sigma(1, 2, \dots, n)) \quad \text{for } \sigma \text{ cyclic} , \quad (1.17)$$

reducing the number of independent colour-ordered amplitudes by a factor of n .

Reflection identities

$$A_n^{\text{tree}}(1, 2, \dots, n) = (-1)^n A_n^{\text{tree}}(n, n-1, \dots, 1) , \quad (1.18)$$

which leave us with at most $\frac{(n-1)!}{2}$ independent partial amplitudes.

U(1) decoupling identities

$$\sum_{\sigma \text{ cyclic}} A_n^{\text{tree}}(1, \sigma(2, \dots, n)) = 0 . \quad (1.19)$$

The result can be understood enlarging the symmetry group of the theory to $U(N)$. Since $U(N) = SU(N) \times U(1)$, the added generator would correspond to a photon, which does not couple to gluons, forcing any amplitude involving a photon leg to vanish.

Kleiss–Kuijf relations [59]

$$A_n^{\text{tree}}(1, \mathbf{A}, n, \mathbf{B}) = (-1)^{|\mathbf{B}|} \sum_{\sigma \in \text{OP}(\mathbf{A} \cup \mathbf{B}^\top)} A_n^{\text{tree}}(1, \sigma(2, \dots, n-1), n) , \quad (1.20)$$

where \mathbf{A}, \mathbf{B} are two ordered sets of labels, $|\mathbf{B}|$ is the cardinality of the latter, \mathbf{B}^\top is \mathbf{B} with oppositely ordered elements and the sum is over *ordered permutations* of the elements of $\mathbf{A} \cup \mathbf{B}^\top$, *i.e.* those preserving the ordering of labels within \mathbf{A} and \mathbf{B}^\top . These relations imply both reflection and U(1) decoupling identities and cut down the number of independent colour-ordered amplitudes to $(n-2)!$ (two legs are fixed in the RHS of (1.20)).

Incidentally, Kleiss–Kuijf relations are encoded in a different colour decomposition of tree-level amplitudes in terms of $SU(N)$ structure constants, introduced in [65] and proven in [66]:

$$\begin{aligned} A_n^{\text{tree}}(g_1, \dots, g_n) &= \\ &= (ig)^{n-2} \sum_{\sigma \in S_{n-2}} f^{a_1 a_{\sigma(2)}}_{x_1} f^{x_1 a_{\sigma(3)}}_{x_2} \dots f^{x_{n-3} a_{\sigma(n-1)} a_n} A_n^{\text{tree}}(1, \sigma(2, \dots, n-1), n) = \\ &= g^{n-2} \sum_{\sigma \in S_{n-2}} (F^{a_{\sigma(2)}} F^{a_{\sigma(3)}} \dots F^{a_{\sigma(n-1)}})_{a_n}^{a_1} A_n^{\text{tree}}(1, \sigma(2, \dots, n-1), n) , \end{aligned} \quad (1.21)$$

where the matrices $(F^a)_c^b = if^{bac}$, are the $SU(N)$ generators in the adjoint representation.

Bern–Carrasco–Johansson relations [67]

$$A_n^{\text{tree}}(1, 2, \mathbf{A}, 3, \mathbf{B}) = \sum_{\sigma \in \text{POP}(\mathbf{A} \cup \mathbf{B})} \left(\prod_{k=4}^n \frac{\mathcal{F}_k(3, \sigma, 1)}{s_{2,4,\dots,k}} \right) A_n^{\text{tree}}(1, 2, 3, \sigma) . \quad (1.22)$$

Without providing too many details, let us remark that we are now summing over the *partially ordered permutations* of the set $\mathbf{A} \cup \mathbf{B}$, *i.e.* those preserving the ordering of labels only within \mathbf{B} . The function \mathcal{F}_k associated to the k -th leg depends on the Mandelstam invariants $s_{i,j} = (p_i + p_j)^2$ or their generalisation $s_{i,j,\dots,k} = (p_i + p_j + p_{j+1} + \dots + p_k)^2$. The upshot is that only $(n-3)!$ partial amplitudes, *e.g.* the $A_n^{\text{tree}}(1, 2, 3, \sigma)$, are linearly independent.

The fact that one requires the knowledge of only $(n-3)!$ partial amplitudes to construct the full amplitude A_n^{tree} is a very remarkable computational advantage, see Table 1.3.

n	4	5	6	7	8	9	10
$n!$	24	120	720	5040	40320	362880	3628800
$(n-3)!$	1	2	6	24	120	720	5040

Table 1.3: Number of distinct colour-ordered amplitudes $A_n^{\text{tree}}(1, \dots, n)$ and of those which actually need to be computed from Feynman diagrams or by other means.

1.3 $\mathcal{N} = 4$ super Yang–Mills theory

In this section we aim to give a concise introduction to the model that will be mainly investigated in this work, $\mathcal{N} = 4$ super Yang–Mills theory with $\text{SU}(N)$ gauge group ($\mathcal{N} = 4$ SYM for short). We refer to [68, 64] for additional details. As already discussed in the introductory chapter, supersymmetric models can be very useful to consider – despite the lack of any experimental evidence in their favour so far. So numerous and noteworthy are the features of $\mathcal{N} = 4$ SYM, and its advantages compared *e.g.* to pure Yang–Mills, that it can be regarded as *the simplest quantum field theory* in four dimensions [69], at least if we require renormalisability of the interactions.

Supersymmetric theories are not trivial to construct, due to the delicate balance between bosonic and fermionic degrees of freedom that they demand. In particular, the number of spacetime dimensions is crucial to determine which models are allowed and

which are not. In four dimensions we can construct $\mathcal{N} = 1, 2, 4$ supersymmetric theories (to avoid the appearance of spins higher than 1), but we will focus on the maximal amount of supersymmetry for the added constraints that this implies. The classical Lagrangian of the theory reads

$$S_{\mathcal{N}=4}^{(\text{cl})} = \frac{1}{g^2} \int d^4x \, \text{tr} \left(-\frac{1}{4} F_{\mu\nu} F^{\mu\nu} - D_\mu \phi_{AB} D^\mu \phi^{AB} - \frac{1}{2} [\phi_{AB}, \phi_{CD}] [\phi^{AB}, \phi^{CD}] + \right. \\ \left. + i \bar{\psi}_\alpha^A \sigma_\mu^{\dot{\alpha}\alpha} D^\mu \psi_{\alpha A} - \frac{i}{2} \psi_A^\alpha [\phi^{AB}, \psi_{\alpha B}] - \frac{i}{2} \bar{\psi}_\alpha^A [\phi_{AB}, \bar{\psi}^{\dot{\alpha}B}] \right). \quad (1.23)$$

All fields are massless and transform in the adjoint representation of the gauge group. Beyond the implicit adjoint indices, the expression above involves Lorentz, spinor and $\text{SU}(4)$ indices: the range of the last ones is dictated by the number of supercharges, *i.e.* by the value of \mathcal{N} . In the spectrum of the theory we find a gauge field A , which is analogous to the pure Yang–Mills gluon and therefore will bear the same name; its superpartners are the four gluinos $\psi_A, \bar{\psi}^A$, which must satisfy $\bar{\psi}_\alpha^A = (\psi_{\alpha A})^*$; finally, closure of the supersymmetry algebra demands the presence of six real scalar fields $\phi_{AB} = -\phi_{BA}$, such that $\phi_{AB} = \frac{1}{2} \epsilon_{ABCD} \phi^{CD}$. Therefore, $\mathcal{N} = 4$ SYM has eight bosonic and eight fermionic degrees of freedom, recalling that non-scalar fields come in two helicities (± 1 for the gluons and $\pm \frac{1}{2}$ for (anti)gluinos).

It should be noted that (1.23) is the unique four-dimensional action consistent with $\mathcal{N} = 4$ supersymmetry and it can be obtained by dimensional reduction of an $\mathcal{N} = 1$ SYM theory in ten dimensions, upon compactification on a six-dimensional torus [70]: the procedure enhances the symmetry giving rise to the internal *R-symmetry* group $\text{SU}(4)_R$, rotating the supercharges into each other. With respect to this internal invariance, gluons transform in the trivial representation, fermions in the (anti)fundamental, scalars in the antisymmetric one. For more details, see for example [71].

Beyond local $\text{SU}(N)$ invariance and maximal supersymmetry, what makes $\mathcal{N} = 4$ SYM special is the existence of conformal symmetry at the quantum level, extending Poincaré invariance to include transformations such as dilations and special conformal transformations. This highly non-trivial property corresponds to the β -function vanishing at all loop orders, implying that there are no ultraviolet (UV) divergences in the theory and thus no running of the coupling constant g , which is the only tunable parameter of the theory beside the number of colours N , often taken to be very large to study the planar limit. Based on the field content of $\mathcal{N} = 4$ SYM we can explicitly see the vanishing of the β -function at one loop, using the following formula, valid for any $\text{SU}(N)$ gauge theory

with n_{ferm} fermions and n_{scal} scalars in the spectrum:

$$\beta^{1\text{L}}(g) = -\frac{g^3}{16\pi^2} \left(\frac{11}{3}C_2(R_{\text{adj}}) - \frac{1}{6}n_{\text{scal}}C(R_{\text{scal}}) - \frac{2}{3}n_{\text{ferm}}C(R_{\text{ferm}}) \right), \quad (1.24)$$

where the constants $C(R), C_2(R)$ are defined for a generic representation R through

$$\text{tr}(T_R^a T_R^b) = C(R)\delta^{ab} \quad , \quad T_R^a T_R^a = C_2(R) \cdot \mathbb{1} \quad (1.25)$$

and happen to be equal to N if every field transforms in the adjoint representation. It should be noted that infrared (IR) divergences affect radiative corrections nonetheless.

An important point must be addressed, concerning an ingredient of the action $S_{\mathcal{N}=4}$, namely the scalar potential $V_{\text{scal}} = [\phi_{AB}, \phi_{CD}][\phi^{AB}, \phi^{CD}]$: indeed, to avoid breaking supersymmetry, it is necessary that V_{scal} vanishes, when working in a flat background. Consider the moduli space of $\mathcal{N} = 4$ supersymmetric vacua, where v.e.v.'s of the scalar fields live: at its origin V_{scal} is clearly zero, all fields are massless and the theory is conformally invariant, as anticipated. It appears meaningless to talk about scattering amplitudes in $\mathcal{N} = 4$ SYM, since the very definition of the S -matrix is hindered from the start by the impossibility of defining asymptotic states. Rather than moving away from four dimensions, which would break conformal invariance but also obscure a host of symmetries otherwise manifest, consider the theory on the *Coulomb branch*, where scalars acquire v.e.v.'s – albeit guaranteeing $V_{\text{scal}} = 0$ – and then take the zero-v.e.v. limit of the Coulomb branch S -matrix.

It can be argued that $\mathcal{N} = 4$ SYM theory is a supersymmetric version of QCD. One of the points of contact is that tree-level gluon amplitudes are identical in the two models. This can be seen working out the Feynman rules from (1.23): since gluons couple only to pairs of fermions or scalars, no diagram with only external gluons allows the propagation of other particles along the internal lines. Simplifications occur at one-loop level as well, where QCD gluon amplitudes can be advantageously decomposed as

$$A_n^{1\text{L}} = A_n^{\mathcal{N}=4} - 4A_n^{\mathcal{N}=1} + A_n^{\text{scal}}. \quad (1.26)$$

Here $A_n^{\mathcal{N}=1,4}$ are the analogous amplitudes computed in supersymmetric (hence simpler) theories, whereas A_n^{scal} is the original one with a scalar replacing the gluon running in the loop. Furthermore, for ℓ -loop *planar* amplitudes, the $\mathcal{N} = 4$ piece is conjectured to be the *maximally transcendental* part of the result [50] (roughly speaking, the one involving the highest order polylogarithms or the highest powers of the logarithms). One might worry that amplitudes involving fermions are bound to be different in the two theories,

since gluinos transform in the adjoint representation, unlike quarks, transforming in the fundamental. However, this difference affects the colour factors only: thanks to colour decomposition formulae similar to (1.13) and (1.21) – to be found in previously referenced papers – we can thus safely compute partial amplitudes in the more symmetric framework as well.

1.3.1 The superspace formalism

In the case of extended supersymmetry $\mathcal{N} > 1$, massless supermultiplets include $2^{\mathcal{N}}$ states. In the case of $\mathcal{N} = 2$ supersymmetry, one supermultiplet consists of an helicity +1 photon, two photino superpartners of helicity $+\frac{1}{2}$ and one scalar; by CPT symmetry, also the conjugate supermultiplet must be present, grouping non-positive-helicity states. $\mathcal{N} = 4$ SYM has instead a single CPT-self-dual supermultiplet, involving sixteen massless states. It is very useful to group them all in a *superfield*

$$\Phi(\eta) = g^+ + \eta^A \psi_A^+ + \frac{1}{2!} \eta^A \eta^B S_{AB} + \frac{1}{3!} \eta^A \eta^B \eta^C \epsilon_{ABCD} \bar{\psi}^{-D} + \frac{1}{4!} \eta^A \eta^B \eta^C \eta^D \epsilon_{ABCD} g^- , \quad (1.27)$$

where we employed the auxiliary Grassmann-odd variables η^A [72], transforming in the fundamental representation of $SU(4)_R$. Observe that if we assign them helicity $+\frac{1}{2}$, then the superfield carries uniform helicity +1. An equally legitimate choice would have been to consider the parity-conjugate fermionic variables $\bar{\eta}_A$, transforming in the antifundamental representation of $SU(4)_R$ and carrying helicity $-\frac{1}{2}$, yielding the following expansion of the superfield:

$$\bar{\Phi}(\bar{\eta}) = g^- + \bar{\eta}_A \bar{\psi}^{-A} + \frac{1}{2!} \bar{\eta}^A \bar{\eta}^B S^{AB} + \frac{1}{3!} \bar{\eta}^A \bar{\eta}^B \bar{\eta}^C \epsilon^{ABCD} \psi_D^+ + \frac{1}{4!} \bar{\eta}^A \bar{\eta}^B \bar{\eta}^C \bar{\eta}^D \epsilon^{ABCD} g^+ . \quad (1.28)$$

The two expansions are related by a Grassmann Fourier transform (see *e.g.* [73]), namely

$$\bar{\Phi}(\bar{\eta}) = \int d^4\eta \, e^{\eta\bar{\eta}} \Phi(\eta) , \quad (1.29)$$

however we will always stick to the expression (1.27) and hence to the η^A .

So far we refrained from making all variables at play explicit, particularly those parametrising the kinematics: the reason is that ordinary four-momenta and polarisation vectors are not optimally suited for the computation of scattering amplitudes in a massless theory. In fact, we will devote much of Chapter 2 to addressing this issue. We mention in passing that the introduction of the anticommuting variables allows us to associate to any one-particle state of $\mathcal{N} = 4$ SYM a point in the *superspace*.

The fields appearing in (1.27) have to be thought as annihilation operators, producing the corresponding excitation with given momentum when acting on the out-vacuum $\langle 0|$. Then we can think of scattering n superfields and defining a *superamplitude* $\mathcal{A}_n(\Phi_1, \dots, \Phi_n)$ to be the S -matrix element between the in-vacuum $|0\rangle$ and n outgoing states created by the various Φ_i . The (generalised) function \mathcal{A}_n depends polynomially on the auxiliary fermionic variables, which allow to keep track of the contribution of each state of the supermultiplet within the scattering process: the *component amplitude* of a specific set of states can be extracted taking an appropriate number of derivatives with respect to the η_i^A . For example, we can compute the amplitude of 2 negative-helicity and $n - 2$ positive-helicity gluons as

$$A_n(g_1^+, \dots, g_i^-, \dots, g_j^-, \dots, g_n^+) = \left(\prod_{A=1}^4 \frac{\partial}{\partial \eta_i^A} \right) \left(\prod_{B=1}^4 \frac{\partial}{\partial \eta_j^B} \right) \mathcal{A}_n(\Phi_1, \dots, \Phi_n) , \quad (1.30)$$

which evaluates to the already mentioned Parke–Taylor formula. This makes the super-space formalism remarkably powerful.

Finally, let us mention that any amount of supersymmetry gives rise to a set of linear relations among different component amplitudes. They are valid at any loop order and go under the collective name of *supersymmetric Ward identities* [74, 75]. We give a brief sketch of the proof. $\mathcal{N} = 4$ supersymmetry transformations are generated by four pairs of fermionic supercharges, satisfying³

$$\{q^A, \bar{q}_B\} = \delta_B^A p . \quad (1.31)$$

It can be shown that the q^A raise the helicity of the states they act on by $\frac{1}{2}$, whereas the \bar{q}_A lower it by the same amount:

$$\begin{aligned} \delta_q g^+ &= 0 \quad , \quad \delta_q \psi_A \sim g^+ \quad , \quad \dots \quad , \quad \delta_q g^- \sim \bar{\psi}^{-A} \\ \delta_{\bar{q}} g^+ &\sim \psi_A^+ \quad , \quad \delta_{\bar{q}} \psi_A^+ \sim S_{AB} \quad , \quad \dots \quad , \quad \delta_{\bar{q}} g^- = 0 \end{aligned} . \quad (1.32)$$

Let the superamplitude be defined by $\mathcal{A}_n = \langle 0| \mathcal{O}_1 \mathcal{O}_2 \cdots \mathcal{O}_n |0\rangle$, where the \mathcal{O}_i are annihilation operators for arbitrary states. Demanding supersymmetry of the vacuum, *i.e.* $q^A |0\rangle = \bar{q}_A |0\rangle = 0$, we trivially have

$$\langle 0| [q^A, \mathcal{O}_1 \mathcal{O}_2 \cdots \mathcal{O}_n] |0\rangle = 0 \quad , \quad \langle 0| [\bar{q}_A, \mathcal{O}_1 \mathcal{O}_2 \cdots \mathcal{O}_n] |0\rangle = 0 . \quad (1.33)$$

³We are keeping notation to a minimum, omitting for the moment the spinor indices. Moreover, unlike standard conventions, we do not use capital letters for these operators: the reason will be clear later on.

The two equalities can be finally expanded as

$$\begin{aligned} \sum_{i=1}^n (-1)^{\sum_{j<i} |\mathcal{O}_j|} \langle 0 | \mathcal{O}_1 \cdots [q^A, \mathcal{O}_i] \cdots \mathcal{O}_n | 0 \rangle &= 0 , \\ \sum_{i=1}^n (-1)^{\sum_{j<i} |\mathcal{O}_j|} \langle 0 | \mathcal{O}_1 \cdots [\bar{q}_A, \mathcal{O}_i] \cdots \mathcal{O}_n | 0 \rangle &= 0 . \end{aligned} \tag{1.34}$$

As a consequence of (1.32), the LHSs are a linear combination of component amplitudes, where the relative signs are determined by the number of fermionic operators \mathcal{O}_j that had to hop past the supercharges to exit the commutators.

The upshot of this discussion is that supersymmetric Ward identities allow us to regard the gluon amplitudes of $\mathcal{N} = 4$ SYM as fundamental, since any other amplitude can be immediately related to those via (1.34).

Chapter 2

On-shell methods for $\mathcal{N} = 4$ SYM theory and its symmetries

This Chapter aims at introducing the main tools that allow to compute amplitudes in planar $\mathcal{N} = 4$ SYM by more efficient means than “brute force” Feynman diagram calculations. We will discuss the variables that are best suited to describe massless scattering processes: following the development of the field, we will initially present the spinor-helicity formalism [76, 77, 78], which will allow us to introduce the manifest symmetries of $\mathcal{N} = 4$ SYM; afterwards, we will review twistor variables, both in their spacetime and momentum space incarnation [42, 44, 45], and the hidden symmetries. We will emphasise the geometric character of these constructions, which will culminate in the Grassmannian description of scattering amplitudes [50] and eventually in the amplituhedron proposal [52]. As a prelude to that, we will discuss on-shell recursion techniques [25, 26, 27], which have proven extremely valuable.

2.1 The spinor-helicity formalism

It is often argued that picking the right variables is of paramount importance in solving a physics problem. Although the final result is of course independent of it, an inconvenient choice might introduce unnecessary redundancies and make an analytic solution way more difficult to find (if not preventing it completely). For instance, a point particle moving in a spherically symmetric potential is easiest to describe in terms of spherical, rather than *e.g.* Cartesian, coordinates.

In the context of scattering amplitudes in massless theories, the usual four-momenta and

polarisation vectors are in fact a redundant description. Indeed, both on-shell conditions and momentum conservation are not built-in, but rather must be imposed by hand; moreover, polarisation states are embedded in four-dimensional vectors subject to transversality conditions and some other normalisation requirements, namely for each leg

$$\varepsilon_{\pm}(p) \cdot p = 0 \quad ; \quad \varepsilon_{\pm}(p) \cdot (\varepsilon_{\pm}(p))^* = -1 \quad , \quad \varepsilon_{\pm}(p) \cdot (\varepsilon_{\mp}(p))^* = 0 . \quad (2.1)$$

The situation can be much improved.¹

Massless scattering involves null momenta: to make this property manifest, the *spinor-helicity formalism* is introduced. Instead of representing a four-momentum through a four-vector p^μ , we can employ the Pauli matrices – supplemented by the identity – to provide a two-dimensional matrix representation. Setting $(\bar{\sigma}_\mu)^{\dot{\alpha}\alpha} = (\mathbb{1}_2, \sigma_1, \sigma_2, \sigma_3)^{\dot{\alpha}\alpha}$,

$$p^{\dot{\alpha}\alpha} = p^\mu (\bar{\sigma}_\mu)^{\dot{\alpha}\alpha} = \begin{pmatrix} p^0 + p^3 & p^1 - ip^2 \\ p^1 + ip^2 & p^0 - p^3 \end{pmatrix} = p_\mu (\bar{\sigma}^\mu)^{\dot{\alpha}\alpha} . \quad (2.2)$$

Spinor indices can be raised and lowered by means of the $\epsilon_{\alpha\beta}, \epsilon_{\dot{\alpha}\dot{\beta}}$ invariant symbols, yielding

$$p_{\alpha\dot{\alpha}} = \epsilon_{\alpha\beta} \epsilon_{\dot{\alpha}\dot{\beta}} (\bar{\sigma}_\mu)^{\dot{\beta}\beta} p^\mu = (\sigma_\mu)_{\alpha\dot{\alpha}} p^\mu = \begin{pmatrix} p^0 - p^3 & -p^1 + ip^2 \\ -p^1 - ip^2 & p^0 + p^3 \end{pmatrix} = (\sigma^\mu)_{\alpha\dot{\alpha}} p_\mu , \quad (2.3)$$

with $(\sigma^\mu)_{\alpha\dot{\alpha}} = (\mathbb{1}, \sigma_1, \sigma_2, \sigma_3)_{\alpha\dot{\alpha}}$.

From (2.2), it is immediate to verify that $\det p^{\dot{\alpha}\alpha} = p^2$ and therefore $p^{\dot{\alpha}\alpha}$ has full rank if and only if the four-momentum is not lightlike. Conversely, any null p^μ admits a *bispinor representation*

$$p^{\dot{\alpha}\alpha} = \tilde{\lambda}^{\dot{\alpha}} \lambda^\alpha \quad , \quad p_{\alpha\dot{\alpha}} = \lambda_\alpha \tilde{\lambda}_{\dot{\alpha}} . \quad (2.4)$$

The *spinor-helicity* variables λ and $\tilde{\lambda}$ are two-dimensional commuting Weyl spinors of opposite chirality, transforming respectively in the $(\frac{1}{2}, 0)$ and $(0, \frac{1}{2})$ representations of the Lorentz group. They go under the name of *angle* and *square* spinors, after a shorthand notation that reads

$$\lambda_{i\alpha} \rightarrow |i\rangle \quad , \quad \lambda_i^\alpha \rightarrow \langle i| \quad , \quad \tilde{\lambda}_{i\dot{\alpha}} \rightarrow |i] \quad , \quad \tilde{\lambda}_{i\dot{\alpha}} \rightarrow [i] . \quad (2.5)$$

The basic Lorentz invariants can be formed via contractions of the helicity spinors with the ϵ -symbols:

$$\langle ij \rangle = \lambda_i^\alpha \lambda_{j\alpha} = \epsilon_{\alpha\beta} \lambda_i^\alpha \lambda_j^\beta \quad , \quad [ij] = \tilde{\lambda}_{i\dot{\alpha}} \tilde{\lambda}_{j\dot{\alpha}} = \epsilon_{\dot{\alpha}\dot{\beta}} \tilde{\lambda}_i^{\dot{\beta}} \tilde{\lambda}_j^{\dot{\alpha}} . \quad (2.6)$$

¹We will follow the conventions of [68].

It should be noted that these are antisymmetric quantities, *i.e.* $\langle ii \rangle = [ii] = 0$: this is unsurprising, since both kinds of brackets have the structure of a determinant. To make contact with more standard notation, let us recall the positive/negative helicity spinors for *outgoing* particles \bar{u}_\pm and antiparticles v_\pm , since we will find it practical to consider scattering of n outgoing states, which are related by crossing symmetry to the physical $2 \rightarrow n - 2$ amplitudes. Then it is then easy to see that the λ and $\tilde{\lambda}$ are the building blocks of the solutions to the Dirac equations in the massless limit. Considering the chiral representation of the γ -matrices, which can be compactly written as

$$\gamma^\mu = \begin{pmatrix} 0 & (\sigma^\mu)_{\alpha\dot{\alpha}} \\ (\bar{\sigma}^\mu)^{\dot{\alpha}\alpha} & 0 \end{pmatrix} \longrightarrow \not{p} = p_\mu \gamma^\mu = \begin{pmatrix} 0 & p_{\alpha\dot{\alpha}} \\ p^{\dot{\alpha}\alpha} & 0 \end{pmatrix}, \quad (2.7)$$

it can be checked that

$$\not{p} \begin{pmatrix} |\lambda\rangle \\ 0 \end{pmatrix} = \not{p} v_-(p) = 0 \quad , \quad \not{p} \begin{pmatrix} 0 \\ |\tilde{\lambda}] \end{pmatrix} = \not{p} v_+(p) = 0 \quad ; \quad (2.8)$$

$$\begin{pmatrix} 0 & |\tilde{\lambda}] \end{pmatrix} \not{p} = \bar{u}_+(p) \not{p} = 0 \quad , \quad \begin{pmatrix} \langle \lambda | & 0 \end{pmatrix} \not{p} = \bar{u}_-(p) \not{p} = 0. \quad (2.9)$$

It can be shown that the helicity spinors corresponding to a real four-momentum are – up to a sign – one the complex conjugate of the other:

$$\tilde{\lambda}^{\dot{\alpha}} = (\text{sgn } p^0) (\lambda^\alpha)^* \quad \text{for } p = \lambda \tilde{\lambda} \in \mathbb{R}^4, \quad (2.10)$$

an explicit realisation being given by

$$\lambda^\alpha = \frac{1}{\sqrt{p^0 + p^3}} \begin{pmatrix} p^0 + p^3 \\ p^1 + ip^2 \end{pmatrix}, \quad \tilde{\lambda}^{\dot{\alpha}} = \frac{1}{\sqrt{p^0 + p^3}} \begin{pmatrix} p^0 + p^3 \\ p^1 - ip^2 \end{pmatrix} \quad (2.11)$$

This is evidently not the only one, since any phase transformation

$$\lambda^\alpha \rightarrow e^{i\phi} \lambda^\alpha, \quad \tilde{\lambda}^{\dot{\alpha}} \rightarrow e^{-i\phi} \tilde{\lambda}^{\dot{\alpha}} \quad (2.12)$$

would yield equally good representatives. Such an ambiguity in the definition of the helicity spinors is referred to as *little group scaling*, because the transformations leaving the four-momentum invariant are the rotations in the transverse plane and their group is isomorphic to $U(1)$. Soon enough we will find it extremely convenient to continue four-momenta to the complex plane: in this case, λ and $\tilde{\lambda}$ are independent quantities. Moreover, the little group scaling freedom (2.12) is extended to the whole multiplicative group \mathbb{C}^* :

$$\lambda^\alpha \rightarrow t \lambda^\alpha, \quad \tilde{\lambda}^{\dot{\alpha}} \rightarrow t^{-1} \tilde{\lambda}^{\dot{\alpha}}, \quad (2.13)$$

i.e. the scaling factor need not be unimodular anymore.

Based on formulae (2.2), (2.3) and (2.6), one can verify that scalar products of lightlike four-momenta are conveniently expressed as

$$p_i \cdot p_j = \frac{1}{2}(p_i + p_j)^2 = \frac{1}{2}p_i^{\dot{\alpha}\alpha}p_{j\alpha\dot{\alpha}} = \frac{1}{2}\langle ij \rangle[ji] . \quad (2.14)$$

The equation for momentum conservation can be cast as

$$\sum_{i=1}^n p_i = 0 \quad \longleftrightarrow \quad \sum_{i=1}^n \lambda_i \tilde{\lambda}_i = 0 \quad \longleftrightarrow \quad \sum_{i=1}^n \langle ai \rangle [ib] = 0 , \quad (2.15)$$

after appropriate contractions with arbitrary λ_a and $\tilde{\lambda}_b$. Moreover, a very useful identity follows from a simple observation: since the helicity spinors are two-dimensional objects, any three of them must be linearly dependent. The derived result is the *Schouten identity*: for arbitrary lightlike momenta $p_{i,j,k} = \lambda_{i,j,k} \tilde{\lambda}_{i,j,k}$,

$$\begin{aligned} \langle ij \rangle \lambda_k^\alpha + \langle jk \rangle \lambda_i^\alpha + \langle ki \rangle \lambda_j^\alpha &= 0 , \\ [ij] \tilde{\lambda}_k^{\dot{\alpha}} + [jk] \tilde{\lambda}_i^{\dot{\alpha}} + [ki] \tilde{\lambda}_j^{\dot{\alpha}} &= 0 . \end{aligned} \quad (2.16)$$

It is possible to provide a bispinor representation for the polarisation vectors as well. The prescription for the i -th leg, carrying momentum $p_i = \lambda_i \tilde{\lambda}_i$, reads

$$\varepsilon_{i+}^{\dot{\alpha}\alpha} = -\sqrt{2} \frac{\tilde{\lambda}_i^{\dot{\alpha}} \mu_i^\alpha}{\langle \lambda_i \mu_i \rangle} , \quad \varepsilon_{i-}^{\dot{\alpha}\alpha} = +\sqrt{2} \frac{\lambda_i^\alpha \tilde{\mu}_i^{\dot{\alpha}}}{[\lambda_i \mu_i]} , \quad (2.17)$$

satisfying (2.1). A lightlike reference momentum $q_i = \mu_i \tilde{\mu}_i$ not proportional to p_i was introduced: the freedom in choosing it can be traced back to the gauge invariance of the theory. Indeed, shifting $\mu_i \rightarrow \mu_i + \delta\mu_i$ changes the polarisation vectors by an amount proportional to p_i , bound to give a vanishing contribution by the Ward identity. We stress that a different reference spinor may be chosen for each leg of a given amplitude: this can be exploited to make certain diagrams vanish.

We have thus seen how good variables exist, automatically putting the momenta of the external particles on the mass shell and allowing an explicit (and flexible, thanks to the reference spinors) representation of the polarisation vectors. By construction, the spinor-helicity formalism directly computes colour-ordered *helicity amplitudes* – of the form $A_n(1^{h_1}, \dots, n^{h_n})$ – where every leg carries a definite helicity: the full amplitude is obtained summing over all possible helicity assignments. Far from being an obstacle, this can further elucidate the structure of the problem. For instance, helicity amplitudes obey

$$\left(\lambda_i^\alpha \frac{\partial}{\partial \lambda_i^\alpha} - \tilde{\lambda}_i^{\dot{\alpha}} \frac{\partial}{\partial \tilde{\lambda}_i^{\dot{\alpha}}} \right) A_n(1^{h_1}, \dots, n^{h_n}) = -2h_i A_n(1^{h_1}, \dots, n^{h_n}) \quad , \quad i = 1, \dots, n . \quad (2.18)$$

These relations can be quickly checked observing that the operator on the LHS annihilates the scalar products $p_i \cdot p_j$ and maps $\varepsilon_{i h_i} \cdot \varepsilon_{j h_j}$ to $-2h_i \varepsilon_{i h_i} \cdot \varepsilon_{j h_j}$. Equation (2.18) is the infinitesimal version of

$$A_n(\dots, t\lambda_i, t^{-1}\tilde{\lambda}_i, \dots) = t^{-2h_i} A_n(\dots, \lambda_i, \tilde{\lambda}_i, \dots) , \quad (2.19)$$

displaying the nice behaviour of helicity amplitudes under little group transformations. Equation (2.19) also provides a quick plausibility check for a candidate answer: by rescaling the i -th spinor we can read off the helicity of the i -th particle. We can now naturally define the *helicity operator*

$$h = \sum_{i=1}^n \left(-\frac{1}{2} \lambda_i^\alpha \frac{\partial}{\partial \lambda_i^\alpha} + \frac{1}{2} \tilde{\lambda}_i^{\dot{\alpha}} \frac{\partial}{\partial \tilde{\lambda}_i^{\dot{\alpha}}} \right) \quad (2.20)$$

and even extend it to a *superhelicity* operator, by supplementing its definition with the η_i^A (which carry helicity $+\frac{1}{2}$ and transform as $\tilde{\lambda}_i$ under little group scaling):

$$h = \sum_{i=1}^n h_i = \sum_{i=1}^n \left(-\frac{1}{2} \lambda_i^\alpha \frac{\partial}{\partial \lambda_i^\alpha} + \frac{1}{2} \tilde{\lambda}_i^{\dot{\alpha}} \frac{\partial}{\partial \tilde{\lambda}_i^{\dot{\alpha}}} + \frac{1}{2} \eta_i^A \frac{\partial}{\partial \eta_i^A} \right) . \quad (2.21)$$

Then, since superfields carry uniform superhelicity $+1$, we find that the superamplitudes satisfy leg by leg

$$h_i \mathcal{A}_n(1, \dots, n) = \mathcal{A}_n(1, \dots, n) \quad , \quad i = 1, \dots, n . \quad (2.22)$$

Let us focus on some component amplitudes to discuss a few important examples: it can be shown that any Yang–Mills amplitude involving all (or all but one) like-helicity gluons vanishes at tree-level:

$$A_n^{\text{tree}}(1^\pm, 2^\pm, \dots, n^\pm) = 0 \quad , \quad A_n^{\text{tree}}(1^\mp, 2^\pm, \dots, n^\pm) = 0 . \quad (2.23)$$

A proof can be found in [64] and relies on the fact that we are free to choose the reference spinors in the polarisations at will: let us stress that this is a very non-trivial statement from the traditional point of view. Supersymmetric Ward identities provide an alternative proof and much stronger implications for the corresponding supersymmetric gluon amplitudes: they vanish identically at all loops! We remark that strictly speaking (2.23) holds for $n \geq 4$: in fact, three-point amplitudes are exceptional, since $A_3^{\text{tree}}(i^-, j^\mp, k^+) \neq 0$, at least when allowing for complex momenta. We will come back to this when discussing BCFW recursion relations.

This is a good point to introduce a bit of terminology which will be extensively used in the rest of this work. From (2.23) we see that the first non-zero helicity amplitudes are those involving exactly two negative-helicity gluons: these are called *maximally helicity violating* (MHV) amplitudes² and evaluate to the renowned Parke–Taylor formula

$$A_n^{\text{tree}}(1^+, \dots, i^-, \dots, j^-, \dots, n^+) = \frac{\langle ij \rangle^4}{\langle 12 \rangle \langle 23 \rangle \dots \langle n1 \rangle}, \quad (2.24)$$

first conjectured in [6], then proven in [79]. The class of gluon amplitudes involving three negative-helicity states is called *next-to-MHV* (NMHV) and in general we denote with $N^k\text{MHV}$ an amplitude with $k + 2$ negative-helicity and $n - k - 2$ positive-helicity gluons. Applying a parity transformation, all helicities are flipped and the amplitude can be immediately written down just by trading angle brackets for square ones and viceversa, up to a sign:

$$A_n(1^{-h_1}, 2^{-h_2}, \dots, n^{-h_n}) = (-1)^n A_n(1^{h_1}, 2^{h_2}, \dots, n^{h_n})|_{\langle \rangle \leftrightarrow []} \quad (2.25)$$

This can be generalised to the realm of maximal supersymmetry, where we can talk about the $N^k\text{MHV}$ sector as the set of component amplitudes of \mathcal{A}_n related by supersymmetric Ward identities, for $k = 0, 1, \dots, n - 2$. At each sector belongs in particular the $N^k\text{MHV}$ gluon amplitude, which is fundamental in the sense that all other $N^k\text{MHV}$ component amplitudes are proportional to it.

We already explained how the superamplitude is a polynomial in the Grassmann variables η_i^A . In order for \mathcal{A}_n to be $\text{SU}(4)_R$ -symmetric (no free $\text{SU}(4)$ index), the expansion may only include terms of a degree divisible by 4; moreover it must start at order $\mathcal{O}(\eta^8)$ (MHV sector) and end at order $\mathcal{O}(\eta^{4(n-2)})$ ($N^{n-4}\text{MHV}$ or $\overline{\text{MHV}}$, *i.e.* anti-MHV sector). We have for example

$$\begin{aligned} \mathcal{A}_n^{\text{MHV}} = & (\eta_1^1 \eta_1^2 \eta_1^3 \eta_1^4) (\eta_2^1 \eta_2^2 \eta_2^3 \eta_2^4) A_n(g^-, g^-, g^+, g^+, \dots, g^+) + \\ & + (\eta_1^1 \eta_1^2 \eta_1^3 \eta_1^4) \left(\frac{1}{3!} \epsilon_{ABCD} \eta_2^A \eta_2^B \eta_2^C \eta_2^D \right) A_n(g^-, \psi^{-D}, \bar{\psi}_E^+, g^+, \dots, g^+) + \dots, \end{aligned} \quad (2.26)$$

where the second term is an $\text{SU}(4)_R$ singlet only if the gluino and the antigluino have the same flavour, *i.e.* $D = E$ (see also the $g\bar{\psi}\psi$ -vertex in the Lagrangian (1.23)).

²The reason for the name is understood when looking at the physical $2 \rightarrow n - 2$ picture of the scattering process: in this case the helicity of the incoming particles is the opposite of the one assigned in our $0 \rightarrow n$ picture; say it is negative. The amplitudes such that all (or all but one) outgoing particles carry positive helicity are those that “violate” helicity the most, but we have seen that they vanish; so the biggest non-trivial helicity violation we can achieve is of the form $1^- 2^- \rightarrow 3^- 4^- 5^+ \dots n^+$, which by crossing symmetry corresponds to partial amplitudes featuring exactly two negative-helicity gluons.

2.2 Symmetries of tree-level superamplitudes and the Yangian

We already mentioned that $\mathcal{N} = 4$ SYM is a superconformal field theory at the quantum level, the symmetry superalgebra being $\mathfrak{psu}(2, 2|4)$. As we will review in this section, there is a much richer story to this already non-trivial result. Indeed, a second, hidden copy of the same superconformal invariance was identified in the large- N limit: when combined with the first one, an infinite-dimensional symmetry algebra arises, the Yangian $Y(\mathfrak{psu}(2, 2|4))$. In fact, this enormous amount of symmetry strongly hints at the integrability of planar $\mathcal{N} = 4$ SYM. Despite the lack of a proof thereof, many results seem to point in this direction.

2.2.1 Superconformal symmetry

Tree-level superamplitudes are invariant under the $\mathfrak{psu}(2, 2|4)$ superalgebra, see [19] for a discussion of the MHV case in the bosonic sector. Here we present the realisation of the symmetry generators in terms of the superspace variables $\lambda_i, \tilde{\lambda}_i, \eta_i$.

Poincaré and conformal sector The four generators of translations are

$$p^{\dot{\alpha}\alpha} = \sum_i \lambda_i^\alpha \tilde{\lambda}_i^{\dot{\alpha}}, \quad (2.27)$$

whereas the six generators of Lorentz transformations are given by

$$m_{\alpha\beta} = \sum_i \frac{1}{2} \left(\lambda_{i\alpha} \frac{\partial}{\partial \lambda_i^\beta} + \lambda_{i\beta} \frac{\partial}{\partial \lambda_i^\alpha} \right), \quad (2.28)$$

$$\bar{m}_{\dot{\alpha}\dot{\beta}} = \sum_i \frac{1}{2} \left(\tilde{\lambda}_{i\dot{\alpha}} \frac{\partial}{\partial \tilde{\lambda}_i^{\dot{\beta}}} + \tilde{\lambda}_{i\dot{\beta}} \frac{\partial}{\partial \tilde{\lambda}_i^{\dot{\alpha}}} \right). \quad (2.29)$$

Beside translations, boosts and rotations, we have dilations and special conformal transformations, whose generators are

$$d = \sum_i \left(\frac{1}{2} \lambda_i^\alpha \frac{\partial}{\partial \lambda_i^\alpha} + \frac{1}{2} \tilde{\lambda}_i^{\dot{\alpha}} \frac{\partial}{\partial \tilde{\lambda}_i^{\dot{\alpha}}} + 1 \right) \quad (2.30)$$

(notice the inhomogeneity given by the +1!) and the four

$$k_{\alpha\dot{\alpha}} = \sum_i \frac{\partial^2}{\partial \lambda_i^\alpha \partial \tilde{\lambda}_i^{\dot{\alpha}}} = \sum_i \partial_{i\alpha} \partial_{i\dot{\alpha}}. \quad (2.31)$$

The set $\{p^{\dot{\alpha}\alpha}, m_{\alpha\beta}, \bar{m}_{\dot{\alpha}\dot{\beta}}, d, k_{\alpha\dot{\alpha}}\}$ generates the conformal algebra $\mathfrak{so}(2, 4) \sim \mathfrak{su}(2, 2)$, a bosonic subalgebra of $\mathfrak{psu}(2, 2|4)$.

Supersymmetric sector The (anti)commutation relations of supersymmetry state that the combination of two supersymmetry transformations is a translation, $\{q, \bar{q}\} \sim p$, hence the representation of the sixteen q, \bar{q} generators in terms of superspace coordinates is

$$q^{\alpha A} = \sum_i \lambda_i^\alpha \eta_i^A, \quad \bar{q}_{\dot{A}} = \sum_i \tilde{\lambda}_i^{\dot{\alpha}} \frac{\partial}{\partial \eta_i^{\dot{A}}}. \quad (2.32)$$

Commuting the supercharges with the special conformal transformations gives rise to the sixteen conformal supercharges

$$s_{\alpha A} = \sum_i \frac{\partial^2}{\partial \lambda_i^\alpha \partial \eta_i^A}, \quad \bar{s}_{\dot{A}} = \sum_i \frac{\partial}{\partial \tilde{\lambda}_i^{\dot{\alpha}}} \eta_i^{\dot{A}} \quad (2.33)$$

and the closure of the algebra is ensured by the fifteen R-symmetry generators

$$r_{\mathbf{B}}^{\mathbf{A}} = \sum_i \left(\eta_i^{\mathbf{A}} \frac{\partial}{\partial \eta_i^{\mathbf{B}}} - \frac{1}{4} \delta_{\mathbf{B}}^{\mathbf{A}} \eta_i^{\mathbf{C}} \frac{\partial}{\partial \eta_i^{\mathbf{C}}} \right). \quad (2.34)$$

Observe how the second term, proportional to $\delta_{\mathbf{B}}^{\mathbf{A}}$, makes the $r_{\mathbf{B}}^{\mathbf{A}}$ traceless.

Altogether we have found that

$$j_a \mathcal{A}_n = 0, \quad \text{for } j_a \in \{p^{\dot{\alpha}\alpha}, m_{\alpha\beta}, \bar{m}_{\dot{\alpha}\dot{\beta}}, d, k_{\alpha\dot{\alpha}}, q^{\alpha A}, \bar{q}_{\dot{A}}, s_{\alpha A}, \bar{s}_{\dot{A}}, r_{\mathbf{B}}^{\mathbf{A}}\}. \quad (2.35)$$

We observe that two of the generators listed in (2.35), namely $p^{\dot{\alpha}\alpha}, q^{\alpha A}$, act multiplicatively. Hence \mathcal{A}_n must be proportional to one bosonic and one fermionic δ -functions, enforcing momentum and supermomentum conservation respectively. It is customary to write the n -point superamplitude as

$$\mathcal{A}_n(\{\lambda_i, \tilde{\lambda}_i, \eta_i\}) = \frac{\delta^4(\sum_i \lambda_i \tilde{\lambda}_i) \delta^{0|8}(\sum_i \lambda_i \eta_i)}{\langle 12 \rangle \langle 23 \rangle \cdots \langle n1 \rangle} \mathcal{P}_n(\{\lambda_i, \tilde{\lambda}_i, \eta_i\}), \quad (2.36)$$

where the denominator was chosen for convenience and the Grassmann-odd δ -function is defined as

$$\delta^{0|8} \left(\sum_i \lambda_i^\alpha \eta_i^A \right) = \prod_{\alpha=1}^2 \prod_{A=1}^4 \left(\sum_{i=1}^n \lambda_i^\alpha \eta_i^A \right) = \prod_{A=1}^4 \sum_{i < j} \langle ij \rangle \eta_i^A \eta_j^A \sim \mathcal{O}(\eta^8) \quad (2.37)$$

and the \mathcal{P}_n function can be expanded at each loop order according to

$$\mathcal{P}_n = \mathcal{P}_n^{\text{MHV}} + \mathcal{P}_n^{\text{NMHV}} + \mathcal{P}_n^{\text{N}^2\text{MHV}} + \cdots + \mathcal{P}_n^{\overline{\text{MHV}}}. \quad (2.38)$$

Each $\mathcal{P}_n^{\text{N}^k\text{MHV}}$ is a monomial in the η 's of degree $4k$, which means that $\mathcal{P}_n^{\text{MHV}}$ does not depend on the auxiliary variables because the required ones already appear in $\delta^{0|8}(q)$. In particular, suppose to be interested in the tree-level MHV gluon amplitude $A_n(i^-, j^-)$, component amplitude of $\mathcal{A}_n^{\text{MHV}}$ multiplying the structure $(\eta_i)^4(\eta_j)^4$. Then from (2.37) it is immediate to see that $\delta^{0|8}(q) \rightarrow \langle ij \rangle^4$, so that the prefactor of $\mathcal{P}_n^{\text{MHV}}$ in (2.36) is precisely the RHS of the Parke–Taylor formula.

It should also be pointed out that the statement of superconformal invariance of the superamplitude presents some subtleties. In particular, it was shown in [80] that the invariance holds only up to terms supported on collinear configurations of the momenta: this fact is referred to as the *holomorphic anomaly*.³ If the issue can be dismissed at tree-level arguing that one is only interested in general kinematics, it definitely cannot be ignored at loop-level (since the momenta of the internal gluons are unconstrained, they may well go collinear with the external ones). In fact, in [81, 82] it was turned into a feature, allowing the computation of certain unitarity cuts of one-loop gluon amplitudes; furthermore, the authors of [83] proved that one can deform the superconformal generators by terms which change the number of external legs and re-obtain (2.35) as an exact equality; in [84] the extension of exact superconformal invariance to loop-level was discussed.

2.2.2 Dual superconformal symmetry

Inspired by what was achieved with the spinor-helicity formalism, we can ask whether even better variables exist, already encoding the information enforced by the δ 's, *i.e.* fulfilling the momentum and supermomentum conservation constraints. The answer is affirmative, as long as we restrict ourselves to the planar sector of the theory, since we are going to need an unambiguous notion of ordering of external momenta: as already mentioned elsewhere, this is no loss of generality at tree-level, but is of course a significant *caveat* for loop amplitudes.

We will first define the dual variables to the p_i 's. From a geometrical point of view, momentum conservation means that the four-vectors p_i define a closed polygonal contour in momentum space, see Figure 2.1. Let us therefore introduce the *dual variables* x_i, θ_i such that

$$p_i^{\dot{\alpha}\alpha} = \lambda_i^\alpha \tilde{\lambda}_i^{\dot{\alpha}} = (x_i - x_{i+1})^{\dot{\alpha}\alpha} \quad \text{and} \quad q_i^{\alpha A} = \lambda_i^\alpha \eta_i^A = (\theta_i - \theta_{i+1})^{\alpha A}, \quad (2.39)$$

³The holomorphicity refers to the fact that MHV gluon amplitudes are a function of λ_i variables only, up to the momentum-conserving $\delta^4(\sum \lambda_i \tilde{\lambda}_i)$.

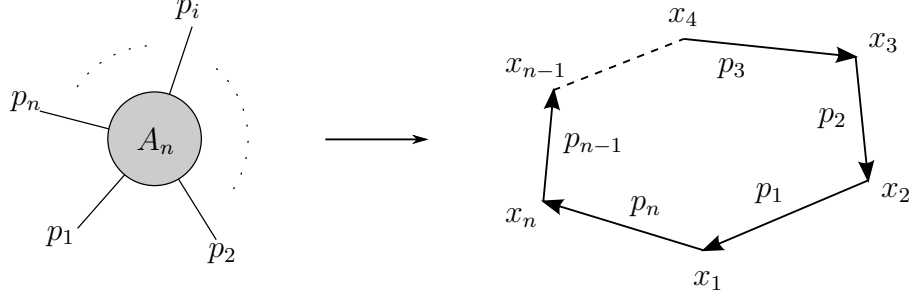


Figure 2.1: A polygon may be equivalently described via its edges or its vertices. This motivates the definitions (2.39).

where by analogy we introduced new variables for the supermomentum as well. Since the p_i are lightlike vectors, the vertices of the polygon in Figure 2.1 are null-separated. The above definitions clearly turn the (super)momentum conservation conditions in cyclicity constraints on the dual variables:

$$\sum_i \lambda_i \tilde{\lambda}_i = \sum_i \lambda_i \eta_i = 0 \quad \longleftrightarrow \quad x_1 = x_{n+1}, \quad \theta_1 = \theta_{n+1}. \quad (2.40)$$

The above dual variables, together with the λ_i , parametrise the *dual on-shell superspace*. As explained in [35], this can also be viewed as a section of the full on-shell superspace of coordinates $\{\lambda_i, \tilde{\lambda}_i, x_i, \eta_i, \theta_i\}$, where $\tilde{\lambda}_i, \eta_i$ are compatible with the constraints (2.39): solving them, we find

$$\tilde{\lambda}_i^{\dot{\alpha}} = \frac{(x_i - x_{i+1})^{\dot{\alpha}\alpha} \lambda_{i+1\alpha}}{\langle i \ i+1 \rangle}, \quad \eta_i^A = \frac{(\theta_i - \theta_{i+1})^{\alpha A} \lambda_{i+1\alpha}}{\langle i \ i+1 \rangle}. \quad (2.41)$$

The last equation allows to quickly re-express the superamplitude in dual space: we simply find

$$\mathcal{A}_n(\{\lambda_i, x_i, \theta_i\}) = \frac{\delta^4(x_1 - x_{n+1}) \delta^{0|8}(\theta_1 - \theta_{n+1})}{\langle 12 \rangle \langle 23 \rangle \cdots \langle n1 \rangle} \mathcal{P}_n(\{\lambda_i, x_i, \theta_i\}), \quad (2.42)$$

where

$$\mathcal{P}_n(\{\lambda_i, x_i, \theta_i\}) = \mathcal{P}_n(\{\lambda_i, \tilde{\lambda}_i(\lambda_j, x_j), \eta_i(x_j, \theta_j)\}). \quad (2.43)$$

Dual variables make it possible to exhibit a novel, hidden symmetry of $\mathcal{N} = 4$ SYM, generated by another copy of the $\mathfrak{psu}(2, 2|4)$ algebra. First hints of it were observed in [85, 16], whose authors were classifying and computing planar loop integrals contributing to the four-gluon MHV amplitude; in [86] it was then shown that they display conformal covariance, albeit formal, as it is broken by the regulator of IR divergencies. Additional evidence in favour of this symmetry was progressively obtained both at weak coupling

[87, 88, 89] as well as at strong coupling [32, 33], until the authors of [35] could prove that all scattering amplitudes of $\mathcal{N} = 4$ SYM are dual superconformal invariants. Remarkably, this observation fully explained how the so-called *BDS-ansatz* [16] for loop amplitudes would be violated starting at two loops, six points (the MHV result was first computed in [90]).

We will denote the generators of dual superconformal symmetry with capital letters to distinguish them from the previously discussed ones. In terms of dual variables,

$$\begin{aligned}
P_{\alpha\dot{\alpha}} &= \sum_i \frac{\partial}{\partial x_i^{\dot{\alpha}\alpha}} \quad , \quad K^{\dot{\alpha}\alpha} = \sum_i \left(x_i^{\dot{\alpha}\beta} x_i^{\dot{\beta}\alpha} \frac{\partial}{\partial x_i^{\dot{\beta}\beta}} + x_i^{\dot{\alpha}\beta} \theta_i^{\alpha\mathbf{B}} \frac{\partial}{\partial \theta_i^{\beta\mathbf{B}}} + x_i^{\dot{\alpha}\beta} \lambda_i^\alpha \frac{\partial}{\partial \lambda_i^\beta} \right) \quad , \\
D &= \sum_i \left(x_i^{\dot{\alpha}\alpha} \frac{\partial}{\partial x_i^{\dot{\alpha}\alpha}} + \frac{1}{2} \theta_i^{\alpha\mathbf{A}} \frac{\partial}{\partial \theta_i^{\alpha\mathbf{A}}} + \frac{1}{2} \lambda_i^\alpha \frac{\partial}{\partial \lambda_i^\alpha} \right) \quad , \\
M_{\alpha\beta} &= \sum_i \left(x_{i(\alpha} \frac{\partial}{\partial x_i^{\beta)\dot{\alpha}}} + \theta_{i(\alpha}^{\mathbf{A}} \frac{\partial}{\partial \theta_i^{\beta)\mathbf{A}}} + \lambda_{i(\alpha} \frac{\partial}{\partial \lambda_i^{\beta)}} \right) \quad , \quad \bar{M}_{\dot{\alpha}\dot{\beta}} = \sum_i x_{i(\dot{\alpha}} \frac{\partial}{\partial x_i^{\dot{\beta})\alpha}} \quad , \\
Q_{\alpha\mathbf{A}} &= \sum_i \frac{\partial}{\partial \theta_i^{\alpha\mathbf{A}}} \quad , \quad \bar{Q}_{\dot{\alpha}}^{\mathbf{A}} = \sum_i \theta_i^{\alpha\mathbf{A}} \frac{\partial}{\partial x_i^{\dot{\alpha}\alpha}} \quad , \quad R_{\mathbf{B}}^{\mathbf{A}} = \sum_i \left(\theta_i^{\alpha\mathbf{A}} \frac{\partial}{\partial \theta_i^{\alpha\mathbf{B}}} - \frac{1}{4} \delta_{\mathbf{B}}^{\mathbf{A}} \theta_i^{\alpha\mathbf{C}} \frac{\partial}{\partial \theta_i^{\alpha\mathbf{C}}} \right) \quad , \\
S^{\alpha\mathbf{A}} &= \sum_i \left(\theta_i^{\alpha\mathbf{B}} \theta_i^{\beta\mathbf{A}} \frac{\partial}{\partial \theta_i^{\beta\mathbf{B}}} + x_i^{\dot{\beta}\alpha} \theta_i^{\beta\mathbf{A}} \frac{\partial}{\partial x_i^{\dot{\beta}\beta}} + \lambda_i^\alpha \theta_i^{\beta\mathbf{A}} \frac{\partial}{\partial \lambda_i^\beta} \right) \quad , \quad \bar{S}_{\mathbf{A}}^{\dot{\alpha}} = \sum_i x_i^{\dot{\alpha}\alpha} \frac{\partial}{\partial \theta_i^{\alpha\mathbf{A}}} \quad .
\end{aligned} \tag{2.44}$$

It can be checked that the first and the second copy of the $\mathfrak{psu}(2,2|4)$ algebra are inequivalent: indeed, one can construct expressions which are invariant under the former but not the latter, an example of this being the “wrong MHV gluon amplitude”

$$B_n = \frac{\langle 12 \rangle^4 \delta^4(p)}{\langle 13 \rangle \langle 23 \rangle \langle 24 \rangle \langle 45 \rangle \cdots \langle n1 \rangle} = \frac{\langle 12 \rangle \langle 34 \rangle}{\langle 13 \rangle \langle 24 \rangle} A_n^{\text{tree}}(1^-, 2^-, 3^+, \dots, n^+) \quad . \tag{2.45}$$

In fact, we have been slightly imprecise, in that the dual superconformal generators of (2.44) only satisfy

$$J_a \mathcal{P}_n = 0 \quad , \quad \text{for } J_a \in \{P_{\alpha\dot{\alpha}}, M_{\alpha\beta}, \bar{M}_{\dot{\alpha}\dot{\beta}}, D, K^{\dot{\alpha}\alpha}, Q_{\alpha\mathbf{A}}, \bar{Q}_{\dot{\alpha}}^{\mathbf{A}}, S^{\alpha\mathbf{A}}, \bar{S}_{\mathbf{A}}^{\dot{\alpha}}, R_{\mathbf{B}}^{\mathbf{A}}\} \quad . \tag{2.46}$$

Exact invariance is spoiled by the denominator of the MHV prefactor of \mathcal{P}_n . In particular, one finds the anomalies

$$K^{\dot{\alpha}\alpha} \mathcal{A}_n = - \left(\sum_i x_i^{\dot{\alpha}\alpha} \right) \mathcal{A}_n \quad , \quad S^{\alpha\mathbf{A}} \mathcal{A}_n = - \left(\sum_i \theta_i^{\alpha\mathbf{A}} \right) \mathcal{A}_n \quad , \quad D \mathcal{A}_n = n \mathcal{A}_n \quad . \tag{2.47}$$

After the simple redefinitions

$$K'^{\dot{\alpha}\alpha} = K^{\dot{\alpha}\alpha} + \sum_i x_i^{\dot{\alpha}\alpha} \quad , \quad S'^{\alpha\mathbf{A}} = S^{\alpha\mathbf{A}} + \sum_i \theta_i^{\alpha\mathbf{A}} \quad , \quad D' = D - n \quad , \tag{2.48}$$

we can really write

$$J'_a \mathcal{A}_n = 0 \quad , \quad \text{for } J'_a \in \{P_{\alpha\dot{\alpha}}, M_{\alpha\beta}, \overline{M}_{\dot{\alpha}\dot{\beta}}, D', K'^{\dot{\alpha}\alpha}, Q_{\alpha A}, \bar{Q}_{\dot{\alpha}}^A, S'^{\alpha A}, \bar{S}_{\dot{A}}^{\dot{\alpha}}, R_B^A\} . \quad (2.49)$$

2.2.3 Yangian symmetry

The dual superconformal generators as operators acting on the full on-shell superspace and commuting with the constraints in (2.39) are given in [35]: the expressions presented in (2.44) are the restriction to the dual on-shell superspace, obtained dropping all terms involving derivatives w.r.t. $\tilde{\lambda}_i$ and η_i ; alternatively, one can consider the restriction to the on-shell superspace dropping all terms involving derivatives w.r.t. x_i and θ_i . Following the latter approach, we discover that the dual generators $P_{\alpha\dot{\alpha}}$ and $Q_{\alpha A}$ become trivial, whereas several others map precisely to generators of the ordinary superconformal algebra, *e.g.*

$$M_{\alpha\beta} \rightarrow \sum_i \lambda_{i(\alpha} \frac{\partial}{\partial \lambda_{i\beta)}} = m_{\alpha\beta} . \quad (2.50)$$

The additional input coming from the dual $\mathfrak{psu}(2, 2|4)$ is encoded in the operators $K'^{\dot{\alpha}\alpha}$ and $S'^{\alpha A}$, which can be used to generate the infinite-dimensional *Yangian algebra* $Y(\mathfrak{psu}(2, 2|4))$.

The notion of Yangian algebra was first introduced by Drinfeld [91, 92]: we will just provide the essential details in the following and refer for additional information to the reviews [93] (on $\mathcal{N} = 4$ SYM amplitudes) and [94] (also focusing on two-dimensional models and spin chains). The generators of a Yangian (super)algebra are organised by levels and we employ the notation $J_a^{(l)}$ for level- l ones; roughly speaking, higher-level generators are yielded by the graded commutator⁴ of lower-level ones. To be more precise, suppose to have a Lie-superalgebra \mathfrak{g} , spanned by the operators $j_a^{(0)}$: they will play the role of level-zero generators, satisfying

$$[j_a^{(0)}, j_b^{(0)}] = f_{ab}^c j_c^{(0)} . \quad (2.51)$$

If one introduces a set of operators $j_a^{(1)}$ such that

$$[j_a^{(0)}, j_b^{(1)}] = f_{ab}^c j_c^{(1)} \quad (2.52)$$

and fulfilling the *Serre relations* – a generalisation of Jacobi relations, see [93, 94] for their precise form – then level-two generators are obtained (anti)commuting level-one generators and in general

$$[j_a^{(l_1)}, j_b^{(l_2)}] = f_{ab}^c j_c^{(l_1+l_2)} , \quad (2.53)$$

⁴Graded commutators are defined as $[O_1, O_2] = O_1 O_2 - (-1)^{|O_1| \cdot |O_2|} O_2 O_1$, where $|O_i|$ is the Grassmann degree of O_i .

up to functions of lower-level generators.

The authors of [36] were able to show that the tree-level superamplitude is invariant under the Yangian of $\mathfrak{psu}(2, 2|4)$. They took at level-zero the superconformal generators of (2.35) and showed that the dual generator S' can be defined to be $q^{(1)}$, up to terms annihilating the amplitude on the support of $\delta^4(p)\delta^{0|8}(q)$; finally, they obtained all the other level-one generators (anti)commuting it with the superconformal ones, according to (2.52). An equally legitimate possibility would have been to supplement the ordinary superconformal generators with K' , which essentially defines $p^{(1)}$. This however leads to the same Yangian, essentially because $[K', \bar{Q}] = S'$, hence the two constructions are equivalent. Let us finally mention that, under certain conditions presented in [95] and fulfilled by $\mathfrak{psu}(2, 2|4)$, level-one generators admit a very convenient representation. Recalling that the $j_a^{(0)}$ are defined as a sum over single-particle generators, *i.e.* $j_a^{(0)} = \sum_i j_{ia}^{(0)}$, we have that

$$j_a^{(1)} = f_a^{bc} \sum_{i < j} j_{ib}^{(0)} j_{jc}^{(0)}, \quad (2.54)$$

where the indices of the structure constants have been raised with the Cartan–Killing metric of the algebra. The latter is called *bi-local* formula, because each summand acts on two legs of the amplitude at a time (contrast this with the case of level-zero generators). Hence tree-level superamplitudes are Yangian-invariant, up to the holomorphic anomaly:

$$y \mathcal{A}_n^{\text{tree}} = 0 \quad , \quad y \in Y(\mathfrak{psu}(2, 2|4)). \quad (2.55)$$

One could wonder whether it would be possible to exchange the roles of the ordinary and dual superconformal algebras and construct a Yangian based on the latter. Indeed this is possible and was investigated in [46]. The level-zero generators were identified with those annihilating \mathcal{P}_n in (2.46) and – mirroring the above procedure – the generator of ordinary special conformal transformations, suitably modified to have it annihilate \mathcal{P}_n , was taken as seed for all the other level-one generators. Finally, one finds

$$\hat{y} \mathcal{P}_n^{\text{tree}} = 0 \quad , \quad \hat{y} \in Y_{\text{dual}}(\mathfrak{psu}(2, 2|4)). \quad (2.56)$$

This dual picture could have been anticipated in light of the AdS/CFT correspondence. The AdS sigma model on $\text{AdS}_5 \times S^5$ is an integrable system and its infinitely many conserved charges are mapped into themselves under T-duality. On the other side of the correspondence, $\mathcal{N} = 4$ SYM ought to display an analogous behaviour and therefore we may think of the mapping of one Yangian onto the other as a kind of T-duality. Furthermore, it is interesting to look at the symmetries of \mathcal{P}_n alone because this is the quantity

of interest in the remarkable duality between MHV scattering amplitudes and expectation values of lightlike polygonal Wilson loops in $\mathcal{N} = 4$ SYM (see [96] for a review).

More explicit expressions for the Yangian generators in both representations will be provided after we introduce supertwistor variables in the next section.

2.3 Twistor variables

2.3.1 Spacetime supertwistors

It is usually seen as a drawback that the generator of the $\mathfrak{psu}(2, 2|4)$ superconformal symmetry range from multiplicative to second order differential operators. Luckily there is a way to overcome this complication introducing new variables called *twistors* [20], especially suited to the description of conformal symmetry. We will stick to an operative definition and refer for more details to the vast literature on the subject (see *e.g.* [97]). Let us thus simply observe that replacing either λ or $\tilde{\lambda}$ in a Fourier transform fashion renders all generators of the conformal algebra first order, homogeneous differential operators. Opposite to what was done in [19], we choose to trade

$$\lambda_i^\alpha \rightarrow -i \frac{\partial}{\partial \tilde{\mu}_{i\alpha}} \quad , \quad \frac{\partial}{\partial \lambda_i^\alpha} \rightarrow -i \tilde{\mu}_{i\alpha} \quad (2.57)$$

and we thus obtain the following form of the superconformal generators:

$$\begin{aligned} p^{\dot{\alpha}\alpha} &= -i \sum_i \tilde{\lambda}_i^{\dot{\alpha}} \frac{\partial}{\partial \tilde{\mu}_{i\alpha}} \quad , \quad k_{\alpha\dot{\alpha}} = -i \sum_i \tilde{\mu}_{i\alpha} \frac{\partial}{\partial \tilde{\lambda}_i^{\dot{\alpha}}} \quad , \quad d = \sum_i \left(-\frac{1}{2} \tilde{\mu}_i^\alpha \frac{\partial}{\partial \tilde{\mu}_i^\alpha} + \frac{1}{2} \tilde{\lambda}_i^{\dot{\alpha}} \frac{\partial}{\partial \tilde{\lambda}_i^{\dot{\alpha}}} \right) \quad , \\ m_{\alpha\beta} &= \sum_i \frac{1}{2} \left(\tilde{\mu}_{i\alpha} \frac{\partial}{\partial \tilde{\mu}_i^\beta} + \tilde{\mu}_{i\beta} \frac{\partial}{\partial \tilde{\mu}_i^\alpha} \right) \quad , \quad \bar{m}_{\dot{\alpha}\dot{\beta}} = \sum_i \frac{1}{2} \left(\tilde{\lambda}_{i\dot{\alpha}} \frac{\partial}{\partial \tilde{\lambda}_i^{\dot{\beta}}} + \tilde{\lambda}_{i\dot{\beta}} \frac{\partial}{\partial \tilde{\lambda}_i^{\dot{\alpha}}} \right) \quad , \\ q^{\alpha A} &= -i \sum_i \eta_i^A \frac{\partial}{\partial \tilde{\mu}_i^\alpha} \quad , \quad \bar{q}_A^{\dot{\alpha}} = \sum_i \tilde{\lambda}_i^{\dot{\alpha}} \frac{\partial}{\partial \eta_i^A} \quad , \quad r_B^A = \sum_i \left(\eta_i^A \frac{\partial}{\partial \eta_i^B} - \frac{1}{4} \delta_B^A \eta_i^C \frac{\partial}{\partial \eta_i^C} \right) \quad , \\ s_{\alpha A} &= -i \sum_i \tilde{\mu}_{i\alpha} \frac{\partial}{\partial \eta_i^A} \quad , \quad \bar{s}_A^{\dot{\alpha}} = \sum_i \frac{\partial}{\partial \tilde{\lambda}_i^{\dot{\alpha}}} \eta_i^A \quad . \end{aligned} \quad (2.58)$$

The four-dimensional objects w_i^a obtained from the new variables $\tilde{\mu}_i^\alpha$ and the old $\tilde{\lambda}_i^{\dot{\alpha}}$ are called twistors; if we consider their supersymmetric extension including the η_i^A – as was first done by Ferber [98] – we obtain the *supertwistors* \mathcal{W}_i^A :

$$w_i^a = \begin{pmatrix} \tilde{\mu}_i^\alpha \\ \tilde{\lambda}_i^{\dot{\alpha}} \end{pmatrix} \quad , \quad \mathcal{W}_i^A = \begin{pmatrix} w_i^a \\ \eta_i^A \end{pmatrix} \quad . \quad (2.59)$$

We used a somewhat funny notation for the variables that replaced the λ helicity spinors: indeed, despite carrying undotted indices, they are denoted by a tilde. This is to highlight that their behaviour under little group scaling is the same as that of $\tilde{\lambda}$, hence we have $\mathcal{W}^{\mathcal{A}} \sim t^{-1} \mathcal{W}^{\mathcal{A}}$: supertwistor space is the complex projective space $\mathbb{CP}^{3|4}$.

The substitution (2.57) has its roots in Penrose's half-Fourier transform, mapping a function of the on-shell superspace variables into one of supertwistor variables: in particular, for the superamplitude,⁵

$$\mathcal{A}_n(\{\tilde{\mu}_i, \tilde{\lambda}_i, \eta_i\}) = \int \left(\prod_i d^2 \lambda_i e^{i \lambda_i^\alpha \tilde{\mu}_{i\alpha}} \right) \mathcal{A}_n(\{\lambda_i, \tilde{\lambda}_i, \eta_i\}) . \quad (2.60)$$

It is relatively easy to perform the half-Fourier transform in the case of a gluon $\overline{\text{MHV}}$ component amplitude, which is a function of $\tilde{\lambda}_i$ only, except for $\delta^4(p)$. Then one finds that such an amplitude only has support when the twistors $w_i = (\tilde{\mu}_i \ \tilde{\lambda}_i)^\text{T}$ lie on a common line in \mathbb{CP}^3 . Observe how moving to twistor space has broken the symmetry between λ and $\tilde{\lambda}$: now gluon amplitudes with different numbers of positive helicity gluons are treated very differently and indeed computing (2.60) is in general a hard task. However, it was conjectured by Witten [19] that for any amplitude the supertwistors of the scattering particles must lie on some algebraic curve, whose degree is determined by the number of positive helicity gluons involved and the loop order.⁶

2.3.2 Momentum supertwistors

Consider the generators of dual superconformal symmetry, spelled out in (2.44). Once again we would like to recast everything in a more homogeneous fashion, by means of appropriate variables. This will lead us to consider the twistor space associated to the dual on-shell superspace. We immediately observe that the relations (2.39) suggest the definitions

$$\mu_i^{\dot{\alpha}} = x_i^{\dot{\alpha}\alpha} \lambda_{i\alpha} = x_{i+1}^{\dot{\alpha}\alpha} \lambda_{i\alpha} \quad , \quad \chi_i^{\text{A}} = \theta_i^{\alpha\text{A}} \lambda_{i\alpha} = \theta_{i+1}^{\alpha\text{A}} \lambda_{i\alpha} , \quad (2.61)$$

also called *incidence relations*. The helicity spinors λ_i^α and the $\mu_i^{\dot{\alpha}}$ build a new kind of twistor variables, which will be called *momentum twistors* z_i^a , because their relation to

⁵Several subtleties are related to this formula: it is well defined when $\lambda, \tilde{\lambda}$ are real variables, which is the case in a spacetime with $(2, 2)$ signature. In $(1, 3)$ signature the most systematic approach is due to Penrose [99] and makes use of cohomology theory. We will not discuss this in the present work.

⁶Beware that in [19] the λ variables are retained, whereas $\tilde{\lambda}$ and η are transformed. This yields a dual description to ours, where MHV amplitudes are in fact the simplest.

momentum space is analogous to that of ordinary twistors to spacetime; including the fermionic χ_i^A gives rise to *momentum supertwistors* \mathcal{Z}_i^A . This name is due to Hodges, who first introduced the concept in [42]. In formulae,

$$z_i^a = \begin{pmatrix} \lambda_i^\alpha \\ \mu_i^{\dot{\alpha}} \end{pmatrix} \quad , \quad \mathcal{Z}_i^A = \begin{pmatrix} z_i^a \\ \chi_i^A \end{pmatrix} . \quad (2.62)$$

Momentum supertwistor space is just another copy of $\mathbb{CP}^{3|4}$: indeed, under little group scaling the new variables change as λ : $\mathcal{Z}^A \sim t\mathcal{Z}^A$, hence we find that also the \mathcal{Z}_i^A are projectively defined.

Once again, these twistor variables can be used to re-cast the generators of dual superconformal symmetry in a less unwieldy form than that in (2.44). We will not present the final result in full detail, because it will not be relevant for the rest of our work. Suffice it to say that at the end of the day one is left with only first-order homogeneous operators, as it had already happened in (2.58) for the generators j_a of $\mathfrak{psu}(2, 2|4)$.

Notice that the construction of momentum twistors – by contrast with spacetime twistors – is purely algebraic. There is no half-Fourier transform relating $\tilde{\lambda}_i$ and μ_i ; rather we have

$$\tilde{\lambda}_i = \frac{\langle i-1\ i \rangle \mu_{i+1} + \langle i\ i+1 \rangle \mu_{i-1} + \langle i+1\ i-1 \rangle \mu_i}{\langle i-1\ i \rangle \langle i\ i+1 \rangle} \quad (2.63)$$

and similarly

$$\eta_i = \frac{\langle i-1\ i \rangle \chi_{i+1} + \langle i\ i+1 \rangle \chi_{i-1} + \langle i+1\ i-1 \rangle \chi_i}{\langle i-1\ i \rangle \langle i\ i+1 \rangle} . \quad (2.64)$$

From the formulae written down so far we can extract the peculiar geometric connection between dual space and momentum twistor space. In introducing the dual variables, we already commented on the fact that the separation of any pair of consecutive points (x_i, x_{i+1}) is lightlike. Not surprisingly, then, we deduce from the definition

$$\mu_i^{\dot{\alpha}} = x_i^{\dot{\alpha}\alpha} \lambda_{i\alpha} = x_{i+1}^{\dot{\alpha}\alpha} \lambda_{i\alpha} \quad (2.65)$$

that two points in dual space are needed to identify the twistor z_i ; conversely, x_i appears in the incidence relations for two different momentum twistors z_{i-1} and z_i ,

$$\mu_{i-1}^{\dot{\alpha}} = x_i^{\dot{\alpha}\alpha} \lambda_{i-1\alpha} \quad , \quad \mu_i^{\dot{\alpha}} = x_i^{\dot{\alpha}\alpha} \lambda_{i\alpha} , \quad (2.66)$$

whence we conclude that

$$x_i^{\dot{\alpha}\alpha} = \frac{\lambda_{i-1}^\alpha \mu_i^{\dot{\alpha}} - \lambda_i^\alpha \mu_{i-1}^{\dot{\alpha}}}{\langle i-1\ i \rangle} . \quad (2.67)$$

Summarising, a point in momentum twistor space corresponds to a null ray in dual space and a point in dual space to a line in momentum twistor space. Of course these considerations extend to the full superspaces.

The basic momentum twistor invariants can be constructed from the bosonic part of the \mathcal{Z}_i^A . They are the brackets

$$\langle ijkl \rangle = \epsilon_{abcd} z_i^a z_j^b z_k^c z_l^d, \quad (2.68)$$

very similar in spirit to the angle- and square-spinor brackets, in that they are determinants too. As such, they also satisfy the Schouten identity

$$\langle ijkl \rangle z_m^a + \langle jklm \rangle z_i^a + \langle klmi \rangle z_j^a + \langle lmi j \rangle z_k^a + \langle mij k \rangle z_l^a = 0. \quad (2.69)$$

We can now prove that two lines in momentum twistor space intersect if and only if the corresponding points in dual space are null-separated. Consider two points x, y in the dual space, described by the pairs of momentum twistors (z_i, z_j) and (z_k, z_l) respectively. Then,

$$\begin{aligned} (x - y)^2 &= \frac{1}{2} (x - y)^{\dot{\alpha}\alpha} (x - y)_{\dot{\alpha}\alpha} = \\ &= \frac{(-\langle ij \rangle [\mu_k \mu_l] + \langle ik \rangle [\mu_j \mu_l] - \langle il \rangle [\mu_j \mu_k] - \langle jk \rangle [\mu_i \mu_l] + \langle jl \rangle [\mu_i \mu_k] - \langle kl \rangle [\mu_i \mu_j])}{\langle ij \rangle \langle kl \rangle}, \end{aligned}$$

where the square brackets are defined as $[\mu_p \mu_q] = \mu_p \dot{\alpha} \mu_q^{\dot{\alpha}}$. The newly introduced four-brackets of momentum twistors allow for a very elegant rewriting of this result, namely

$$(x - y)^2 = \frac{\langle ijkl \rangle}{\langle ij \rangle \langle kl \rangle}. \quad (2.70)$$

We then conclude that the condition of lightlike separation in dual space is equivalent to a coplanarity condition in twistor space, *i.e.* the two lines (z_i, z_j) and (z_k, z_l) intersect. A graphical description of the kinematic setup in terms of dual and momentum twistor coordinates is presented in Figure 2.2. Observe that formula (2.70) comes very handy, because tree-level colour-ordered amplitudes involve propagators precisely of the form

$$\frac{1}{(p_i + p_{i+1} + \dots + p_{j-1})^2} = \frac{1}{(y_i - y_j)^2} = \frac{\langle i-1 \ i \ j-1 \ j \rangle}{\langle i-1 \ i \ j-1 \ j \rangle}. \quad (2.71)$$

Recall that we were on the look for kinematic variables that could encode as much information as possible about the scattering of massless particles. Helicity spinors would

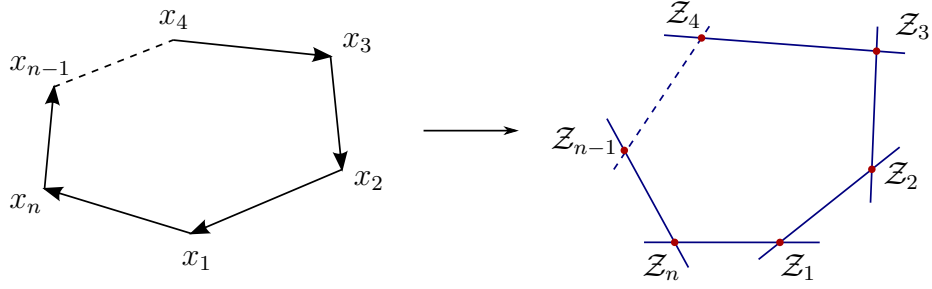


Figure 2.2: This picture has to be taken with a grain of salt: we do not mean that the lines in twistor space bound a polygon.

enforce the on-shell conditions, but not momentum conservation; on the other hand, dual variables would make the latter condition manifest, at the expense of the former. Otherwise said, drawing random numbers and interpreting them as components of either $\lambda_i, \tilde{\lambda}_i$ or x_i variables would in general violate the constraint $\sum_i \lambda_i \tilde{\lambda}_i = 0$ or $(x_i - x_{i+1})^2 = 0$, respectively. Momentum twistors allow to comply with both requirements at the same time and this property alone suggests that they are the best variables to work with to study planar amplitudes: *randomly* specifying n intersection points in momentum twistor space, we can construct the lines $(z_{i-1}, z_i), (z_i, z_{i+1})$ intersecting pairwise at those points and hence the corresponding x_i in dual space; everything else can be derived using the incidence relations (2.65) and the equations (2.63) and (2.64).

2.3.3 Yangian generators in supertwistor formulation

Yet another remarkable feature of supertwistor variables is that they give a very homogeneous appearance to the generators of Yangian symmetry. Level-zero generators will always be first-order operators and from the bi-local formula (2.54) we see that level-one generators will be second-order; from the commutation relations it follows that higher-level generators will correspondingly be higher-order differential operators.

Let us first consider the Yangian based on ordinary superconformal symmetry, annihilating the superamplitude. We then have [36]

$$j^{(0)\mathcal{A}}_{\mathcal{B}} = \sum_i \mathcal{W}_i^{\mathcal{A}} \frac{\partial}{\partial \mathcal{W}_i^{\mathcal{B}}} , \quad (2.72)$$

$$j^{(1)\mathcal{A}}_{\mathcal{B}} = \sum_{i < j} (-1)^{|c|} \left(\mathcal{W}_i^{\mathcal{A}} \frac{\partial}{\partial \mathcal{W}_i^c} \mathcal{W}_j^c \frac{\partial}{\partial \mathcal{W}_j^{\mathcal{B}}} - (i \leftrightarrow j) \right) . \quad (2.73)$$

Turning to the Yangian based on dual superconformal symmetry, annihilating the am-

plitude stripped off of the MHV prefactor, we find [46]

$$J^{(0)\mathcal{A}}_{\mathcal{B}} = \sum_i \mathcal{Z}_i^{\mathcal{A}} \frac{\partial}{\partial \mathcal{Z}_i^{\mathcal{B}}} , \quad (2.74)$$

$$J^{(1)\mathcal{A}}_{\mathcal{B}} = \sum_{i < j} (-1)^{|C|} \left(\mathcal{Z}_i^{\mathcal{A}} \frac{\partial}{\partial \mathcal{Z}_i^{\mathcal{C}}} \mathcal{Z}_j^{\mathcal{C}} \frac{\partial}{\partial \mathcal{Z}_j^{\mathcal{B}}} - (i \leftrightarrow j) \right) . \quad (2.75)$$

In all the above formulae we omitted for brevity a term corresponding to the supertrace. For instance, in (2.72) it reads $-\frac{1}{4}\delta_{\mathcal{B}}^{\mathcal{A}} \sum_i \mathcal{W}_i^{\mathcal{C}} \frac{\partial}{\partial \mathcal{W}_i^{\mathcal{C}}}$ and analogously in (2.74) with momentum supertwistors. The reason why it can be ignored is that it produces a contribution proportional to $\delta_{\mathcal{B}}^{\mathcal{A}}$ and this will vanish if the rest of the operator annihilates the amplitude.

The above formulae, albeit in a bosonised version to be introduced later on, will be central to Chapter 5.

2.4 BCFW recursion relations at tree-level

We have commented on the possibility of analytically continuing the momenta of the scattering particles into the complex plane: one important consequence of this assumption is that three-point on-shell amplitudes are not vanishing anymore. Indeed, momentum conservation implies

$$p_1 \cdot p_2 = \frac{1}{2}(p_1 + p_2)^2 = \frac{1}{2}p_3^2 = 0 \quad \text{and similarly} \quad p_1 \cdot p_3 = p_2 \cdot p_3 = 0 . \quad (2.76)$$

Hence in spinor-helicity variables we have

$$\langle 12 \rangle [21] = \langle 13 \rangle [31] = \langle 23 \rangle [32] = 0 . \quad (2.77)$$

As discussed in (2.10), the helicity spinors associated to real momenta are not independent: hence, all spinor brackets vanish and there is no way to write down a non-zero expression for a three-point amplitude. Instead, if $\lambda, \tilde{\lambda}$ are independent, $\langle ij \rangle [ji] = 0$ only implies that *one* of the brackets is zero. Suppose for instance that $[12] = 0, \langle 12 \rangle \neq 0$: then, always by momentum conservation (2.15),

$$\begin{aligned} \langle 12 \rangle [23] &= -\langle 11 \rangle [13] - \langle 13 \rangle [33] = 0 &\implies & [23] = 0 , \\ [31] \langle 12 \rangle &= -[32] \langle 22 \rangle - [33] \langle 32 \rangle = 0 &\implies & [31] = 0 . \end{aligned} \quad (2.78)$$

Analogously, had we started from $\langle 12 \rangle = 0, [12] \neq 0$, we would have found that all angle brackets are simultaneously vanishing. These two options mean that either $\tilde{\lambda}_1 \sim \tilde{\lambda}_2 \sim \tilde{\lambda}_3$

or $\lambda_1 \sim \lambda_2 \sim \lambda_3$ respectively and a three-point amplitude may depend on spinors of one chirality only. Then, imposing little group scaling constraints (2.19) (and employing some dimensional analysis considerations), we are able to completely fix the three-point MHV and $\overline{\text{MHV}}$ gluon amplitudes, up to an overall constant:

$$A_3^{\text{MHV}}(i^-, j^-) = \frac{\langle ij \rangle^4}{\langle 12 \rangle \langle 23 \rangle \langle 31 \rangle} \quad , \quad A_3^{\overline{\text{MHV}}}(i^+, j^+) = -\frac{[ij]^4}{[12][23][31]} \quad , \quad (2.79)$$

where of course i and j label two of the legs and the third is understood to carry the opposite helicity. Those in (2.79) are the explicit expressions advertised in the comment following (2.23) and can be used as seeds to set up a recursion relation for higher-point tree-level on-shell amplitudes A_n^{tree} .

The idea is to complexify the momenta of the external particles and then express A_n^{tree} , based on the analytic properties of its shifted version. There are many ways to deform the four-momenta p_i^μ in a meaningful way, i.e. such that the new ones are still null and satisfy momentum conservation. It is easy to show that the vectors

$$\hat{p}_i^\mu \equiv p_i^\mu + z q_i^\mu \quad , \quad z \in \mathbb{C} \quad (2.80)$$

will enjoy both properties, provided that the n *complex*⁷ vectors q_i^μ satisfy

$$\begin{aligned} q_1^\mu + q_2^\mu + \cdots + q_n^\mu &= 0 \quad , \\ q_i \cdot q_j &= 0 \quad , \quad q_i \cdot p_i = 0 \quad \forall i, j = 1, \dots, n \quad . \end{aligned} \quad (2.81)$$

Pure Yang–Mills, the traditional derivation We will start our discussion in the non-supersymmetric context. Let $\hat{A}_n^{\text{tree}}(z)$ be the deformed version of an n -point gluon amplitude under a complex shift and discuss its analytical properties. At tree-level it is a rational function of the momenta and of the deformation parameter z : its singularities are then poles corresponding to the vanishing of some propagator. Notice that this amounts to an implicit assumption of locality of the theory, in that we understand the singularities of the deformed amplitude as coming from local propagators blowing up. Moreover, since we are dealing with colour-ordered amplitudes, every propagator involves a sum of momenta of the form $p_i + p_{i+1} + \cdots + p_j$, or rather its deformed version involving shifted momenta. It is immediate to see that $\hat{A}_n^{\text{tree}}(z)$ has only simple poles, as a consequence of (2.81): if $I \subset \{1, \dots, n\}$ is a subset of consecutive labels and we define $P_I = \sum_{i \in I} p_i$, $R_I = \sum_{i \in I} q_i$, we can compute

$$\hat{P}_I(z)^2 = (P_I + z R_I)^2 = P_I^2 + 2z P_I R_I = 0 \quad \longleftrightarrow \quad z = z_I = -\frac{P_I^2}{2P_I R_I} \quad . \quad (2.82)$$

⁷This is crucial, no real vectors exist satisfying (2.81). See also eq. (4) in [69] for an example.

Complex shifts of the momenta are typically introduced in the context of the spinor-helicity formalism, therefore they are defined for λ_i , $\tilde{\lambda}_i$ variables. The two most popular alternatives lead respectively to the *MHV vertex expansion* or *CSW recursion* [25] (after Cachazo, Svrček, Witten) and to the *BCFW recursion* [26, 27] (after Britto, Cachazo, Feng, Witten):

- the former involves a so-called holomorphic all-line shift

$$\lambda_i \rightarrow \lambda_i \quad , \quad \tilde{\lambda}_i \rightarrow \tilde{\lambda}_i + z c_i \tilde{\lambda}_X \quad , \quad (2.83)$$

such that $\sum_i c_i \lambda_i = 0$, for an arbitrary reference spinor $\tilde{\lambda}_X$. As an example, a three-line shift of the form

$$c_1 = \langle 23 \rangle \quad , \quad c_2 = \langle 31 \rangle \quad , \quad c_3 = \langle 12 \rangle \quad , \quad c_4 = \cdots = c_n = 0 \quad . \quad (2.84)$$

is known as a *Risager shift* [100]. The MHV vertex expansion is natural from the point of view of spacetime twistors, as they were introduced in the original paper [19]: if MHV amplitudes are localised on lines in twistor space, which in turn correspond to points in ordinary spacetime, then they can be regarded as local interactions.

- the latter involves a two-line shift

$$\begin{aligned} \lambda_i &\rightarrow \lambda_i & , & \quad \tilde{\lambda}_i \rightarrow \tilde{\lambda}_i + z \tilde{\lambda}_j \\ \lambda_j &\rightarrow \lambda_j - z \lambda_i & , & \quad \tilde{\lambda}_j \rightarrow \tilde{\lambda}_j \end{aligned} \quad , \quad (2.85)$$

typically denoted $[i, j]$ -shift, on which we will focus in the following.

Let us consider the $[n, 1]$ -BCFW-shift for definiteness: by definition we have

$$\begin{aligned} \lambda_n &\rightarrow \lambda_n & , & \quad \tilde{\lambda}_n \rightarrow \hat{\tilde{\lambda}}_n \equiv \tilde{\lambda}_n + z \tilde{\lambda}_1 \\ \lambda_1 &\rightarrow \hat{\lambda}_1 \equiv \lambda_1 - z \lambda_n & , & \quad \tilde{\lambda}_1 \rightarrow \tilde{\lambda}_1 \end{aligned} \quad , \quad (2.86)$$

which means

$$\hat{p}_1 = p_1 - zq \quad , \quad \hat{p}_n = p_n + zq \quad , \quad q = \lambda_n \tilde{\lambda}_1 \quad . \quad (2.87)$$

It is clear that only propagators involving either \hat{p}_1 or \hat{p}_n can exhibit a pole in z and we know that tree-level amplitudes factorise in a product of two on-shell lower-point amplitudes whenever an internal propagator goes on-shell. Let us introduce $P_i \equiv p_1 + \cdots + p_{i-1}$ and focus on its *factorisation channel*, namely the limit in which the corresponding (shifted) propagator becomes singular. Since

$$\hat{P}_i^2(z) = \frac{1}{2} \left(P_i^{\dot{\alpha}\alpha} - z \lambda_n^\alpha \tilde{\lambda}_1^{\dot{\alpha}} \right) \left(P_{i\alpha\dot{\alpha}} - z \lambda_{n\alpha} \tilde{\lambda}_{1\dot{\alpha}} \right) = P_i^2 - z \langle n | P_i | 1 \rangle \quad , \quad (2.88)$$

we obtain

$$\hat{P}_i^2(z) = -\langle n|P_i|1\rangle(z - z_{P_i}) = 0 \quad \longleftrightarrow \quad z = z_{P_i} = \frac{P_i^2}{\langle n|P_i|1\rangle} . \quad (2.89)$$

Looking at (2.89) we see that poles coming from different factorisation channels are located at different points in the complex plane. We will also require them to be away from the origin: this is guaranteed, up to special kinematic configurations that we may disregard. The natural question to ask is what information do the residues encode? On the z_{P_i} pole (see also Figure 2.3),

$$\lim_{z \rightarrow z_{P_i}} \hat{A}_n^{\text{tree}}(z) = -\frac{1}{\langle n|P_i|1\rangle(z - z_{P_i})} \sum_s A_L(\hat{1}, 2, \dots, i-1, -\hat{P}_i^s) A_R(\hat{P}_i^{-s}, i, \dots, n-1, \hat{n}) \Big|_{z_{P_i}} , \quad (2.90)$$

where the sum is over the on-shell degrees of freedom that can propagate along the propagator going on-shell and is therefore theory-dependent. In the case of pure Yang–Mills, we just have to sum over the two possible helicities of the intermediate gluon of momentum P_i , $s \in \{+, -\}$.

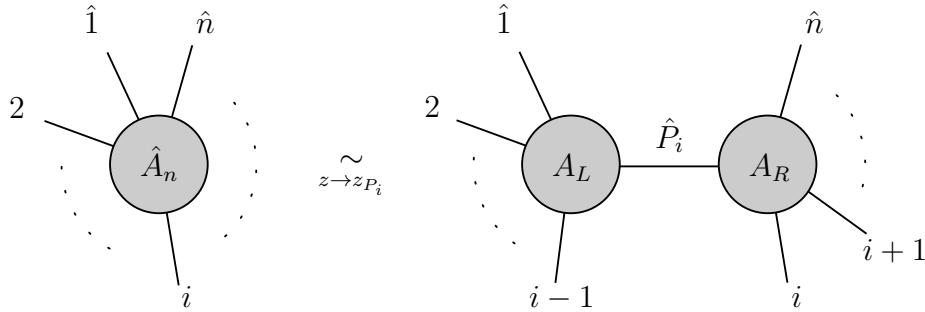


Figure 2.3: Depiction of formula (2.90): on the RHS, a BCFW diagram.

To understand how to obtain the actual scattering amplitude, we need to consider the ratio $\hat{A}_n^{\text{tree}}(z)/z$, which will exhibit all the simple poles of $\hat{A}_n^{\text{tree}}(z)$, plus one at the origin. From (2.90) we have

$$\lim_{z \rightarrow z_{P_i}} \frac{\hat{A}_n^{\text{tree}}(z)}{z} = -\frac{1}{(z - z_{P_i})} \sum_s A_L(\hat{1}, 2, \dots, i-1, -\hat{P}_i^s) \Big|_{z_{P_i}} \frac{1}{P_i^2} A_R(\hat{P}_i^{-s}, i, \dots, n-1, \hat{n}) \Big|_{z_{P_i}} , \quad (2.91)$$

where we remark that the intermediate propagator is unshifted – thus non-zero – and all the shifted quantities are evaluated at $z = z_{P_i}$.

Clearly A_n^{tree} is the residue of $\hat{A}_n^{\text{tree}}(z)/z$ at $z = 0$, to be obtained by integration along a small contour \mathcal{C}_0 surrounding the origin. Equivalently, as portrayed in Figure 2.4, this

can be thought of as the oppositely oriented contour, encircling all the other singularities at finite locations and possibly the one at infinity:

$$\begin{aligned}
 A_n^{\text{tree}} &= \oint_{\mathcal{C}_0} \frac{dz}{2\pi i} \frac{\hat{A}_n^{\text{tree}}(z)}{z} = - \oint_{\mathcal{C}_\infty} \frac{dz}{2\pi i} \frac{\hat{A}_n^{\text{tree}}(z)}{z} - \sum_{z_{P_i}} \oint_{\mathcal{C}_{z_{P_i}}} \frac{dz}{2\pi i} \frac{\hat{A}_n^{\text{tree}}(z)}{z} = \\
 &= \text{Res}_{z \rightarrow \infty} \frac{\hat{A}_n^{\text{tree}}(z)}{z} - \sum_{i=3}^{n-1} \text{Res}_{z \rightarrow z_{P_i}} \frac{\hat{A}_n^{\text{tree}}(z)}{z} .
 \end{aligned} \tag{2.92}$$

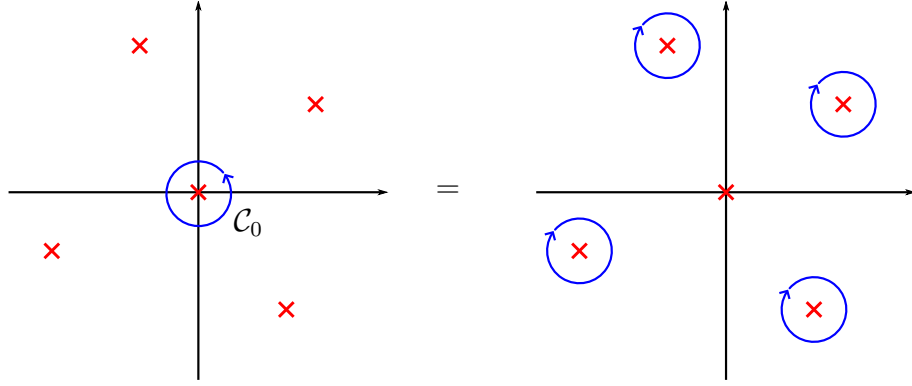


Figure 2.4: Contours of integration. LHS gives the amplitude we are after; in the RHS we already assumed that the A_n^{tree} is regular at infinity.

Assuming for the moment that the amplitude has no singularity at infinity, the first term in the above formula (also called boundary term) can be dropped and, in view of (2.91), we are left with the recursion

$$A_n^{\text{tree}} = \sum_{i=3}^{n-1} \sum_s A_L(z_{P_i}) \frac{1}{P_i^2} A_R(z_{P_i}) \tag{2.93}$$

This formula was obtained from an $[n, 1]$ -shift, but this was just one of many possibilities. We are in principle allowed to consider a variety of shifts, either of adjacent or non-adjacent legs: in the latter case, we will generally have to consider more factorisation channels and hence evaluate more BCFW diagrams. Let us talk about generic $[i, j]$ -shifts from now on. Different choices lead, through (2.93), to distinct representation of the same object; showing their equivalence from an algebraic point of view is in general extremely complicated, however we will see how it follows from an understanding of the underlying geometry, at least in the case of $\mathcal{N} = 4$ SYM.

The most important issue we have to address is the assumption we made that we could discard the boundary term in (2.92). In fact, no recursive construction for it was known at the time when the original articles were published, however in subsequent years much work has been done to extend the scope of this technique, the strongest result having been presented in [101]. We will not delve deeper in the algorithms proposed to compute the residue of the amplitude at infinity – since they will not be relevant for the rest of our discussion – but rather focus on the conditions under which it vanishes.

To better understand the large- z behaviour of the deformed amplitude $\hat{A}_n^{\text{tree}}(z)$, we will perform an analysis based on Feynman diagrams. Clearly, we will not have any boundary term if $\hat{A}_n^{\text{tree}}(z) \rightarrow 0$ as $z \rightarrow 0$. In pure Yang–Mills theory, shifted propagators scale as $\mathcal{O}(1/z)$ (see (2.89)); trivalent vertices, being linear in the momenta, carry at most one factor of z ; quartic vertices cannot involve the shift parameter, since no momentum enters the associated Feynman rule. The worst possible behaviour is then achieved by a diagram having only three-gluon vertices on the path connecting the shifted legs (anywhere else in the diagram the z dependence cancels), see Figure 2.5: since one always has one more vertex than propagators, we have an overall $\mathcal{O}(z)$ behaviour.

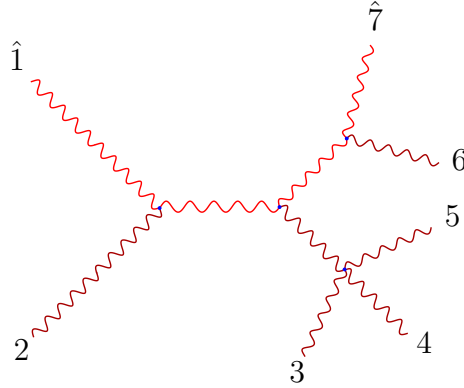


Figure 2.5: Worst-case scenario: a Feynman diagram with only trivalent vertices on the (highlighted) path connecting the shifted legs.

A last (and crucial) source of z -dependence are the polarization vectors of the shifted legs. Based on formulae (2.17), we have

$$\begin{aligned} \varepsilon_{i+} &\sim \frac{\hat{\lambda}_i \mu_i}{\langle \lambda_i \mu_i \rangle} \sim z \quad , & \varepsilon_{j+} &\sim \frac{\tilde{\lambda}_j \mu_j}{\langle \tilde{\lambda}_j \mu_j \rangle} \sim \frac{1}{z} \quad , \\ \varepsilon_{i-} &\sim \frac{\lambda_i \tilde{\mu}_i}{[\hat{\lambda}_i \tilde{\mu}_i]} \sim \frac{1}{z} \quad , & \varepsilon_{j-} &\sim \frac{\hat{\lambda}_j \tilde{\mu}_j}{[\tilde{\lambda}_j \tilde{\mu}_j]} \sim z \quad . \end{aligned} \tag{2.94}$$

Then we conclude that individual diagrams contributing to a deformed helicity amplitude scale at worst as

$$\begin{aligned}\hat{A}_n^{\text{tree}}(\hat{i}^-, \hat{j}^+) &\sim \frac{1}{z} \quad , & \hat{A}_n^{\text{tree}}(\hat{i}^+, \hat{j}^-) &\sim z^3 \quad , \\ \hat{A}_n^{\text{tree}}(\hat{i}^-, \hat{j}^-) &\sim z \quad , & \hat{A}_n^{\text{tree}}(\hat{i}^+, \hat{j}^+) &\sim z \quad ,\end{aligned}\tag{2.95}$$

based on the helicity of the shifted legs. This analysis readily shows that a $[-, +\rangle$ -shift is a safe choice to recursively compute a gluon amplitude. In fact, it can be proven – exploiting either the MHV vertex expansion [27] or the background field method [102] – that shifts of the form $[-, -\rangle$ and $[+, +\rangle$ are equally good: in these cases, cancellations among the badly scaling diagrams occur and the sum of all Feynman diagrams behaves again as $\mathcal{O}(1/z)$. Knowledge of the Parke–Taylor formula (2.24) for MHV amplitudes allows to check this last claim very quickly.

The argument leading to (2.93) is valid for a variety of QFTs. The discussion above using Feynman diagrams, however, explains why the on-shell scattering amplitudes of certain theories cannot be recursed. Consider scalar ϕ^4 theory: its only interaction vertex is quartic and insensitive to complex shifts of the momenta, being just proportional to the coupling constant. For any amplitude that we might try to compute shifting adjacent legs, there will be at least a diagram connecting them via a single vertex; the absence of polarisation vectors will then prevent any z -dependence to appear; finally, any diagram with at least one propagator along the path connecting the shifted legs will be suppressed at large z , so no cancellations are possible. The same happens when shifting non-adjacent legs, since the external legs do not need to be ordered in any particular way. Hence boundary terms in ϕ^4 theory are unavoidable and (2.93) does not hold. In this respect, one may say that Yang–Mills theory is simpler than ϕ^4 . Let us also mention that, even for good theories, BCFW recursion is not applicable to the computation of constant amplitudes, i.e. which have no pole on which to base the recursion. Examples of these are the four point scalar amplitudes in $\mathcal{N} = 4$ SYM, which nonetheless can be inferred from *e.g.* pure gluon amplitudes via supersymmetric Ward identities.

An example: the Parke–Taylor formula To illustrate the power of this method, we can sketch the proof of the formula (2.24) for MHV gluon amplitudes. We can focus on $A_n^{\text{tree}}(1^-, 2^-, 3^+, \dots, n^+)$, because any other case may be simply related to this by the supersymmetric Ward identities. We use induction on n and employ a $[1, 2\rangle$ -shift, observing that the result (2.79) for $A_3^{\text{tree}}(1^-, 2^-, 3^+)$ serves as the base case. For general n , based on (2.23), we have to consider just two factorisation channels, depicted in the BCFW diagrams

of Figure 2.6.

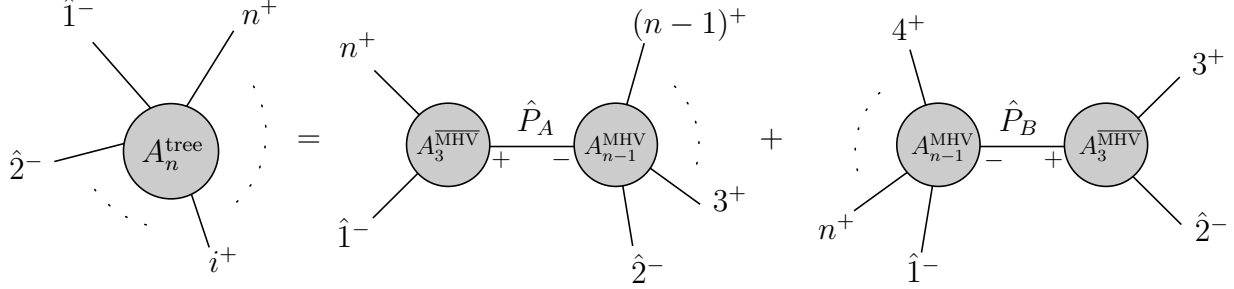


Figure 2.6: An enormous number of colour-ordered Feynman diagrams is replaced by the sum of just two diagrams. Any other partition of the external legs or helicity assignment along the internal leg yields a vanishing subamplitude.

Even more, the first contribution, featuring an $A_3^{\overline{\text{MHV}}}$ left subamplitude, does not contribute. Indeed, the kinematics is forced to satisfy in particular

$$\hat{\lambda}_1 = \lambda_1 \sim \lambda_n \quad \implies \quad \langle 1n \rangle = 0 = p_1 \cdot p_n . \quad (2.96)$$

This is an added collinearity constraint, which does not hold for general kinematics, therefore we can limit ourselves to the evaluation of the second diagram. By the inductive hypothesis we know how to express the $(n-1)$ -point amplitude on the left: combining it with the three-point one on the right, and evaluating everything at the value $z = z_B$ such that $\hat{P}_B(z_B)^2 = 0$, we obtain the desired result:

$$\frac{\langle 1\hat{P}_B \rangle^4}{\langle 1\hat{P}_B \rangle \langle \hat{P}_B 4 \rangle \langle 45 \rangle \cdots \langle n1 \rangle} \frac{1}{P_B^2} \left(-\frac{[3\hat{P}_B]^4}{[3\hat{P}_B][\hat{P}_B 2][23]} \right) \Big|_{z_B} = A_n^{\text{tree}}(1^-, 2^-, 3^+, \dots, n^+) . \quad (2.97)$$

$\mathcal{N} = 4$ SYM, the supersymmetric treatment Let us now move away from pure Yang–Mills theory and come to the realm of maximal supersymmetry. In this case, we need to promote (2.85) to the $[i, j]$ -supershift

$$\tilde{\lambda}_i \rightarrow \tilde{\lambda}_i + z\tilde{\lambda}_j \quad , \quad \lambda_j \rightarrow \lambda_j - z\lambda_i \quad , \quad \eta_i \rightarrow \eta_i + z\eta_j . \quad (2.98)$$

This extension involving the Grassmann-odd η variables is natural from the point of view of supersymmetry, because it corresponds to demand that the supermomentum $q = \sum_i \lambda_i \eta_i$ is conserved as well, as can be immediately checked.

Let us now consider an $[n, 1]$ -supershift: following the same steps as before, we find that the sought-after superamplitude is determined by the residues of its shifted version at each factorisation channel and is given by

$$\mathcal{A}_n^{\text{tree}} = \sum_{i=3}^{n-1} \int d^4 \eta_{\hat{P}_i} \mathcal{A}_L(\hat{1}(z_{P_i}), 2, \dots, i-1, -\hat{P}_i(z_{P_i})) \frac{1}{P_i^2} \mathcal{A}_R(\hat{P}_i(z_{P_i}), i, \dots, n-1, \hat{n}(z_{P_i})) . \quad (2.99)$$

Here each subamplitude is to be stripped of the momentum-conserving $\delta^4(p)$ (whereas the supermomentum-conserving fermionic δ -function has to be taken into account). The most striking difference between (2.99) and (2.93) is the appearance of the integration over the η associated to the internal line of the BCFW diagram, whose shifted momentum vanishes at $z = z_{P_i}$. Intuitively, it ought to replace the sum over the helicities, now that each of the sixteen states of the supermultiplet may be exchanged between the two partial superamplitudes. Breaking them in component amplitudes, it is clear that the possible intermediate states will be different in each case. For instance, if both partial amplitudes involve gluons only, then the internal state will necessarily be a gluon and we will be dealing with an ordinary sum over the two possible helicities. It is however useful to cast it in a different fashion, remembering how component amplitudes are extracted from superamplitudes, namely

$$\left[\left(\prod_A \frac{\partial}{\partial \eta_{P_i}^A} \right) A_L(z_{P_i}) \right] \frac{1}{P_i^2} A_R(z_{P_i}) + A_L(z_{P_i}) \frac{1}{P_i^2} \left[\left(\prod_A \frac{\partial}{\partial \eta_{P_i}^A} \right) A_R(z_{P_i}) \right] \Big|_{\eta_{P_i}=0}, \quad (2.100)$$

the two summands corresponding to the case where the negative-helicity exchanged gluon is attached to the left or to the right subamplitude respectively. If a gluino exchange is allowed, because each partial superamplitude features an odd number of external gluinos, then one of the four derivatives in the first (second) term of (2.100) must be moved from the left (right) subamplitude to the right (left) one, in all possible ways, to account for the different flavours. And similarly, for any scalar exchange, two derivatives must be acting on the left subamplitude and two on the right one. All of this is neatly summarised by

$$\left(\prod_A \frac{\partial}{\partial \eta_{P_i}^A} \right) \left[\mathcal{A}_L(z_{P_i}) \frac{1}{P_i^2} \mathcal{A}_R(z_{P_i}) \right] \Big|_{\eta_{P_i}=0} = \int d^4 \eta_{P_i} \mathcal{A}_L(z_{P_i}) \frac{1}{P_i^2} \mathcal{A}_R(z_{P_i}), \quad (2.101)$$

where we traded derivatives for integrals, since we are dealing with fermionic variables.

An important property of the supersymmetric recursion is that the boundary term always vanishes when shifting neighbouring legs. Let us see how this can be inferred from

the large- z behaviour of a $[+, +\rangle$ -shift. We know that the superamplitude is left invariant by the \bar{q} -supersymmetry, *i.e.*

$$\bar{q}_A^{\dot{\alpha}} \mathcal{A}_n^{\text{tree}} = \sum_i \tilde{\lambda}_i^{\dot{\alpha}} \partial_{\eta_i^A} \mathcal{A}_n^{\text{tree}} = 0 . \quad (2.102)$$

A finite \bar{q} transformation is a translation in the η variables: $\eta_i \rightarrow \eta_i + [\xi^A \tilde{\lambda}_i]$, for $\xi_{\dot{\alpha}}^A$ a fermionic transformation parameter. We can immediately see that

$$\xi_{\dot{\alpha}}^A = \frac{\tilde{\lambda}_{1\dot{\alpha}} \eta_n^A - \tilde{\lambda}_{n\dot{\alpha}} \eta_1^A}{[n1]} \quad (2.103)$$

is not affected by an $[n, 1]$ -supershift and, since

$$[\xi^A \tilde{\lambda}_1] = -\eta_1^A \quad , \quad [\xi^A \tilde{\lambda}_n] = -\eta_n^A , \quad (2.104)$$

we are allowed to set $\eta_1 = \eta_n = 0$, corresponding to a superamplitude featuring two positive-helicity gluons in the first and last leg. This means that the fall-off near infinity of the full superamplitude is $1/z$ and therefore no boundary term will have to be added to (2.99).

An application: all tree-level amplitudes in $\mathcal{N} = 4$ SYM The supersymmetric version of the BCFW recursion relations has been exploited to compute $\mathcal{A}_n^{\text{tree}}$, for any helicity degree k , in [29]. Not surprisingly, the three-point superamplitudes are the fundamental ingredients to solve the recursion. Their expressions are

$$\begin{aligned} \mathcal{A}_3^{\text{MHV}}(1, 2, 3) &= \frac{\delta^4(p)}{\langle 12 \rangle \langle 23 \rangle \langle 31 \rangle} \delta^{0|8}(q) \quad , \\ \mathcal{A}_3^{\overline{\text{MHV}}}(1, 2, 3) &= \frac{\delta^4(p)}{[12][23][31]} \delta^{0|4}([12]\eta_3 + [23]\eta_1 + [31]\eta_2) . \end{aligned} \quad (2.105)$$

Note that we do not need to specify any helicity assignment, since maximal supersymmetry allows to deal with them all at once. If the MHV result is expected from supersymmetry constraints and the requirement (2.22) that $h_i \mathcal{A}_3^{\text{MHV}} = \mathcal{A}_3^{\text{MHV}}$ for any i , the $\overline{\text{MHV}}$ one deserves a brief explanation. We compute it by performing a parity transformation on $\mathcal{A}_3^{\text{MHV}}$, which correctly produces the bosonic part of the result times the fermionic $\delta^{0|8}(\sum_i \tilde{\lambda}_i \bar{\eta}_i)$, involving the parity conjugate of the η_i . As explained in (1.29), one can transform from the former to the latter variables performing a fermionic Fourier transform and this yields the desired expression (more details can be found in [68]). One could wonder why invariance under supersymmetry transformations generated by $q^{\alpha A}$ does not force the appearance of

the usual $\delta^{0|8}(q)$ in $\mathcal{A}_3^{\overline{\text{MHV}}}$ as well. The reason is that in this special case the λ_i spinors involved are proportional, hence we can write $q = \sum_i \lambda_i \eta_i = \lambda_0 \eta_0$ for appropriate λ_0, η_0 and the requirement of q -invariance is just that the $\overline{\text{MHV}}$ amplitude contain $\delta^{0|4}(\eta_0)$, as is indeed the case.⁸

Similarly to the pure Yang–Mills case, the MHV superamplitude can be proven to be

$$\mathcal{A}_n^{\text{MHV}} = \frac{\delta^4(\sum_i \lambda_i \tilde{\lambda}_i) \delta^{0|8}(\sum_i \lambda_i \eta_i)}{\langle 12 \rangle \langle 23 \rangle \cdots \langle n1 \rangle} \quad (2.106)$$

by induction, simply from the knowledge of the three-point (anti)-MHV superamplitude.

Following [29], one can specialise the recursive formula (2.99) to the various helicity sectors, matching the number of η_i appearing on both sides. Recalling that $N^k\text{MHV}$ component amplitudes involve $4(k+2)$ auxiliary variables and observing that the integral removes four of them, we find

$$\mathcal{A}_n^{N^k\text{MHV}} = \sum_{\substack{l,r \\ l+r=k-1}} \sum_{i=3}^{n-1} \int d^4 \eta_{\hat{P}_i} \mathcal{A}_L^{N^l\text{MHV}}(\hat{1}(z_{P_i}), -\hat{P}_i(z_{P_i})) \frac{1}{P_i^2} \mathcal{A}_R^{N^r\text{MHV}}(\hat{P}_i(z_{P_i}), \hat{n}(z_{P_i})) . \quad (2.107)$$

We remark that three-point $\overline{\text{MHV}}$ amplitude – which is not allowed to appear as \mathcal{A}_R for general kinematic configurations – counts as an $N^{-1}\text{MHV}$ amplitude, because it includes only four η_i due to the $\delta^{0|4}$.

Every tree-level amplitude is expressed in terms of special functions called *R-invariants*. In momentum twistor language, they read

$$R_{njk} = \frac{\delta^{0|4}(\langle j-1 \ j \ k-1 \ k \rangle \chi_n + \text{cyclic permutations})}{\langle n \ j-1 \ j \ k-1 \rangle \langle j-1 \ j \ k-1 \ k \rangle \langle j \ k-1 \ k \ n \rangle \langle k-1 \ k \ n \ j-1 \rangle \langle k \ n \ j-1 \ j \rangle} . \quad (2.108)$$

NMHV tree-level superamplitudes, up to the MHV prefactor, are simply sums of *R*-invariants; higher- k superamplitudes, instead, are built out of a generalised version thereof. For future reference, we write down the explicit expression of the NMHV result:

$$\mathcal{A}_n^{\text{NMHV}} = \frac{\delta^4(p) \delta^{0|8}(q)}{\langle 12 \rangle \cdots \langle n1 \rangle} \sum_{b=a+2}^{n-1} \sum_{a=2}^{n-3} R_{nab} . \quad (2.109)$$

In the above, a special role was reserved to the n -th leg: this has to do with having employed an $[n, 1\rangle$ -shift, but it is possible to consider an arbitrary shift of a pair of adjacent legs

⁸By little group scaling arguments, one can show that η_0 must be proportional to the argument of the desired fermionic δ -function.

$(i, i+1)$ and come up with the R_{ijk} invariants. One can for instance perform a $[1, 2\rangle$ -shift and find that

$$\mathcal{A}_n^{\text{NMHV}} = \frac{\delta^4(p)\delta^{0|8}(q)}{\langle 12 \rangle \cdots \langle n1 \rangle} \sum_{b=a+2}^n \sum_{a=3}^{n-2} R_{1ab} . \quad (2.110)$$

Of course, since formulae (2.109) and (2.110) produce the same result, they imply a very non-trivial identity among R-invariants. For instance, we can write

$$\mathcal{A}_6^{\text{NMHV}} = R_{624} + R_{625} + R_{635} = R_{135} + R_{136} + R_{146} . \quad (2.111)$$

It will be possible to give a beautiful interpretation of this fact in the following section.

The authors of [35] had conjectured that the superamplitude should exhibit dual superconformal symmetry and this was proven in [29] showing that every R_{nij} is individually invariant under the action of the generators (2.44). The computation was carried out using dual variables, in terms of which the expression of the R-invariant is more complicated; formula (2.108) shows how momentum supertwistors make it very elegant. The content of the next section constitutes the highlight of this chapter, bringing together both twistor variables and recursion relations to yield a new formalism for the determination of the S-matrix of the theory [43, 44, 50].

2.5 Grassmannian formulation of scattering amplitudes

This section constitutes a review on the so-called *Grassmannian formulation* of scattering amplitudes in planar $\mathcal{N} = 4$ SYM, a field of investigation that was inaugurated by the discovery of a striking connection between them and Grassmannian geometry. In particular, the on-shell formalism serves to expose the simplicity of tree-level amplitudes and generic ℓ -loop *integrand*s, depending on both external and loop momenta q_1, \dots, q_ℓ . Since the q are integrated over, they play the role of dummy variables and it is in general not possible to talk about *the* integrand corresponding to a given loop amplitude, but only about those of the individual Feynman integrals. However, in the planar sector one can come up with a meaningful notion of integrand, based on a consistent assignment of the loop momenta across the multitude of contributing Feynman graphs: for instance one can define q_i for each loop to be carried by the closest propagator to the first external leg.

It was shown [43, 44] that the properties of the integrand are encoded in appropriate contour integrals defined on Grassmannian spaces, which are directly relevant for tree amplitudes as well; furthermore, in [30, 103] it was explained how the all-loop planar

integrand can be derived from a generalisation of the BCFW recursion relations. A new on-shell diagrammatics was developed in parallel, allowing an efficient representation of the BCFW recursions both at tree- and at loop-level, which unveiled an intriguing connection with yet a different Grassmannian space, called *positive Grassmannian*. Before coming to the details of the above concepts, let us start with some introductory mathematical definitions.

Consider the n -dimensional complex vector space \mathbb{C}^n . The space of k -dimensional hyperplanes through its origin is called the *Grassmannian* $G(k, n)$ and it can be given the structure of a smooth manifold. Any such hyperplane \mathcal{C} is spanned by k linearly independent vectors $c_\alpha \in \mathbb{C}^n$, up to an invertible linear transformation thereof. A point in the Grassmannian can therefore be represented via a full rank $k \times n$ matrix C , whose rows are the above c_α vectors, up to the equivalence relation \sim , such that $C \sim C'$ if $C' = A \cdot C$, for some $A \in \text{GL}(k, \mathbb{C})$. The entries $c_{\alpha i}$ of C will then be coordinates on the Grassmannian. If we denote by $M(k, n)$ the set of full rank, $k \times n$ matrices, then

$$G(k, n) = \left\{ C = \begin{pmatrix} c_{11} & c_{12} & \dots & c_{1n} \\ c_{21} & c_{22} & \dots & c_{2n} \\ \vdots & \vdots & & \vdots \\ c_{k1} & c_{k2} & \dots & c_{kn} \end{pmatrix} \in M(k, n) / \sim \right\}. \quad (2.112)$$

Note that Grassmannians with $k = 1$ are simply projective spaces: $G(1, n) = \mathbb{CP}^{n-1}$. Having to mod out by the $\text{GL}(k)$ redundancy, Grassmannian manifolds have dimension $\dim G(k, n) = k(n - k)$. Even more explicitly, observe that fixing the redundancy amounts to set a $k \times k$ submatrix of C – involving columns $\hat{c}_{i_1}, \dots, \hat{c}_{i_k}$ – to the identity matrix. A standard choice fixes the first k columns, so that

$$\mathcal{C} \rightarrow C = \begin{pmatrix} 1 & 0 & \dots & 0 & c_{1k+1} & c_{1k+2} & \dots & c_{1n} \\ 0 & 1 & \dots & 0 & c_{2k+1} & c_{2k+2} & \dots & c_{2n} \\ \vdots & \vdots & \ddots & \vdots & \vdots & \vdots & & \vdots \\ 0 & 0 & \dots & 1 & c_{kk+1} & c_{kk+2} & \dots & c_{kn} \end{pmatrix}, \quad (2.113)$$

which in fact provides just one chart on $G(k, n)$; the collection of $\binom{n}{k}$ different charts having different sets of k columns fixed to $\mathbf{1}_k$ forms an atlas for the whole manifold.

Important quantities in the following will be the (ordered) *maximal minors*, *i.e.* the determinants of $k \times k$ submatrices, of C : we will denote them as $(i_1, \dots, i_k) = \det(\hat{c}_{i_1}, \dots, \hat{c}_{i_k})$,

with $i_1 < \dots < i_k$. Under the transformation $C \rightarrow A \cdot C$, for $A \in \text{GL}(k)$, maximal minors transform simply:

$$(i_1, \dots, i_k) \rightarrow (\det A)(i_1, \dots, i_k) , \quad (2.114)$$

showing that they are actually $\text{SL}(k)$ invariants and their ratios are $\text{GL}(k)$ invariants. However, this also means that maximal minors are projective coordinates on the space of equivalence classes of \sim , *i.e.* the Grassmannian. This motivates a description of $G(k, n)$ as a subspace of a higher-dimensional projective space, namely $\mathbb{CP}^{\binom{n}{k}-1}$, whose (homogeneous) coordinates are the minors: in this context they are referred to as *Plücker coordinates*. This construction goes under the name of *Plücker embedding* [104] and seems bound to fail because there are many more maximal minors than $\dim G(k, n)$. Nevertheless, this is neatly compensated for by the fact that the minors are not all independent, but rather satisfy a large number of (quadratic) *Plücker relations*. For instance, the Plücker coordinates on $G(2, 5)$ satisfy

$$\begin{aligned} (12)(34) - (13)(24) + (14)(23) &= 0 , \\ (12)(35) - (13)(25) + (15)(23) &= 0 , \\ (12)(45) - (14)(25) + (15)(24) &= 0 . \end{aligned} \quad (2.115)$$

Two analogous Plücker relations exist, but are implied by the ones above. Correctly, three degrees of freedom are eliminated by them, so that the embedding $G(2, 5) \hookrightarrow \mathbb{CP}^9$ makes sense. The origin of the Plücker relations is precisely the same as that of the Schouten identities (2.16) and (2.69): consider the $k+1$ columns $\hat{c}_{i_1}, \dots, \hat{c}_{i_k}, \hat{c}_{i_{k+1}}$ of C : since C has rank k , they must be linearly dependent and indeed the following holds:

$$c_{\alpha i_1}(\hat{i}_1, i_2, \dots, i_{k+1}) - c_{\alpha i_2}(i_1, \hat{i}_2, \dots, i_{k+1}) + \dots + (-1)^k c_{\alpha i_{k+1}}(i_1, i_2, \dots, \hat{i}_{k+1}) = 0 , \quad (2.116)$$

or equivalently

$$\begin{aligned} (a_1, \dots, a_{k-1}, i_1)(\hat{i}_1, i_2, \dots, i_{k+1}) - (a_1, \dots, a_{k-1}, i_2)(i_1, \hat{i}_2, \dots, i_{k+1}) + \dots + \\ + (-1)^k (a_1, \dots, a_{k-1}, i_{k+1})(i_1, i_2, \dots, \hat{i}_{k+1}) = 0 , \end{aligned} \quad (2.117)$$

yielding in particular (2.115).

2.5.1 Geometric interpretation of momentum conservation

A basic instance of Grassmannian geometry in the physics of scattering concerns the helicity spinors of Section 2.1. We normally think of them as a collection of n pairs of

two-component vectors $\lambda_i^{\alpha=1,2}, \tilde{\lambda}_i^{\dot{\alpha}=1,2}$; however, a sensible thing to do is to interpret their components as those of n -component vectors and organise them as rows of the $2 \times n$ matrices

$$\mathbf{\Lambda} = \begin{pmatrix} \lambda_1^1 & \lambda_2^1 & \dots & \lambda_n^1 \\ \lambda_1^2 & \lambda_2^2 & \dots & \lambda_n^2 \end{pmatrix}, \quad \tilde{\mathbf{\Lambda}} = \begin{pmatrix} \tilde{\lambda}_1^{\dot{1}} & \tilde{\lambda}_2^{\dot{1}} & \dots & \tilde{\lambda}_n^{\dot{1}} \\ \tilde{\lambda}_1^{\dot{2}} & \tilde{\lambda}_2^{\dot{2}} & \dots & \tilde{\lambda}_n^{\dot{2}} \end{pmatrix}. \quad (2.118)$$

The invariant information encoded by λ_i ($\tilde{\lambda}_i$) is thus the 2-plane spanned by the rows of $\mathbf{\Lambda}$ ($\tilde{\mathbf{\Lambda}}$), an element of $G(2, n)$ [43]. A drawback of the spinor-helicity formalism that is typically emphasised is that momentum conservation is not a linear constraint anymore:

$$p_1 + p_2 + \dots + p_n = 0 \quad \longleftrightarrow \quad \sum_i \lambda_i^\alpha \tilde{\lambda}_i^{\dot{\alpha}} = 0. \quad (2.119)$$

Geometrically, this is interpreted as the perpendicularity of the planes $\mathbf{\Lambda}, \tilde{\mathbf{\Lambda}}$. Alternatively, we can enforce the same condition in a linear fashion by introducing an auxiliary k -plane $\mathcal{C} \in G(k, n)$, together with its $(n-k)$ -dimensional orthogonal complement $\mathcal{C}^\perp \in G(n-k, n)$, and requiring that \mathcal{C} (\mathcal{C}^\perp) be orthogonal to $\tilde{\mathbf{\Lambda}}$ ($\mathbf{\Lambda}$). Otherwise said, $\mathbf{\Lambda}$ ($\tilde{\mathbf{\Lambda}}$) must be contained in the k -plane \mathcal{C} (\mathcal{C}^\perp). Observe that these requirements are impossible to satisfy for general kinematics if $k = 0, 1, n-1, n$, as either \mathcal{C} or \mathcal{C}^\perp are points or lines: this will be related with the vanishing of those helicity amplitudes with less than two negative- or positive-helicity gluons. If \mathcal{C} is represented as in (2.113), then \mathcal{C}^\perp is associated to the $(n-k) \times n$ matrix

$$C^\perp = \begin{pmatrix} -c_{1\,k+1} & -c_{2\,k+1} & \dots & -c_{k\,k+1} & 1 & 0 & \dots & 0 \\ -c_{1\,k+2} & -c_{2\,k+2} & \dots & -c_{k\,k+2} & 0 & 1 & \dots & 0 \\ \vdots & \vdots & & \vdots & \vdots & \vdots & \ddots & \vdots \\ -c_{1n} & -c_{2n} & \dots & -c_{kn} & 0 & 0 & \dots & 1 \end{pmatrix}, \quad (2.120)$$

and it is immediate to check that this structure ensures that $C \cdot C^\perp = C(C^\perp)^T = 0$.

A second nice feature of such a reformulation of momentum conservation is that it explains the special kinematics of three-particle scattering. There is no way for the 2-planes $\mathcal{C}, \mathcal{C}^\perp$ to be orthogonal in three dimensions, unless one of them is degenerate, which in turn corresponds to having either $\lambda_1 \sim \lambda_2 \sim \lambda_3$ or $\tilde{\lambda}_1 \sim \tilde{\lambda}_2 \sim \tilde{\lambda}_3$. By means of the Schouten identity, it is immediate to check that

- if the λ_i are proportional, then \mathcal{C} is a line and $C \cdot \tilde{\lambda} = 0$ has the solution

$$C \sim \begin{pmatrix} [23] & [31] & [12] \end{pmatrix}; \quad (2.121)$$

- if the $\tilde{\lambda}_i$ are proportional, then C^\perp is a line and $C^\perp \cdot \lambda = 0$ is solved by

$$C^\perp \sim \begin{pmatrix} \langle 23 \rangle & \langle 31 \rangle & \langle 12 \rangle \end{pmatrix} . \quad (2.122)$$

In both cases there is an obvious leftover $\text{GL}(1, \mathbb{C})$ rescaling symmetry.

2.5.2 Grassmannian integrals

Arkani-Hamed, Cachazo, Cheung and Kaplan [43] were the first to employ a Grassmannian integral as an object encoding tree-level superamplitudes as well as data related to the integrand of any loop-level amplitude. Their proposal for $\mathcal{A}_n^{\text{N}^k\text{MHV}}$ at all loops, making use of spacetime supertwistors (2.59), reads

$$\mathcal{L}_{n,\tilde{k}}^{(\text{ACCK})} = \frac{1}{\text{GL}(\tilde{k}, \mathbb{C})} \int_{\tilde{\gamma}} \frac{d^{\tilde{k} \times n} \tilde{c}_{\alpha i}}{(1, \dots, \tilde{k})(2, \dots, \tilde{k} + 1) \cdots (n, \dots, \tilde{k} - 1)} \prod_{\alpha=1}^{\tilde{k}} \delta^{4|4} \left(\sum_i \tilde{c}_{\alpha i} \mathcal{W}_i^{\mathcal{A}} \right) , \quad (2.123)$$

where $\tilde{k} = k + 2$. Shortly after, Mason and Skinner [44] suggested another representation of the superamplitude – or rather of the $\mathcal{P}_n^{\text{N}^k\text{MHV}}$ function defined in (2.36) – in momentum supertwistor space (2.62), namely

$$\mathcal{L}_{n,k}^{(\text{MS})} = \frac{1}{\text{GL}(k, \mathbb{C})} \int_{\gamma} \frac{d^{k \times n} c_{\alpha i}}{(1, \dots, k)(2, \dots, k + 1) \cdots (n, \dots, k - 1)} \prod_{\alpha=1}^k \delta^{4|4} \left(\sum_i c_{\alpha i} \mathcal{Z}_i^{\mathcal{A}} \right) . \quad (2.124)$$

The two formulae share several common traits. To start with, they feature integrals over Grassmannian manifolds (hence the name *Grassmannian integrals*), along some contour to be discussed further: indeed, the integration variables are the entries of some rectangular matrix \tilde{C} or C , up to a symmetry under general linear transformations that can be fixed as in (2.113). Secondly, their denominators are precisely the product of all n *consecutive* maximal minors of the matrix, over whose elements we are integrating. We will soon explain the origin of such a structure. Most importantly, both $\mathcal{L}_{n,\tilde{k}}^{(\text{ACCK})}$ and $\mathcal{L}_{n,k}^{(\text{MS})}$ make certain symmetries manifest: in both cases, cyclic symmetry – required as a consequence of colour-ordering – is rather clear (a cyclic permutation of the supertwistors can be undone by accordingly redefining the integration variables, a change of variables with unit Jacobian); furthermore, the δ -functions expose the ordinary and dual superconformal symmetries respectively. As shown in (2.72) and (2.74), the generators of both symmetries take an especially simple form when expressed in terms of supertwistor variables: we thus learn

that superconformal symmetry is nothing but linear $\text{SL}(4|4, \mathbb{C})$ transformations in the right variables and in fact any δ -function whose argument is a linear combination of supertwistors is automatically invariant under them. Focusing on \mathcal{W}_i for definiteness, we have

$$\begin{aligned} j^{(0)\mathcal{A}}_{\mathcal{B}} \delta^{4|4} \left(\sum_j c_{\alpha j} \mathcal{W}_j^{\mathcal{C}} \right) &= \sum_i \mathcal{W}_i^{\mathcal{A}} \frac{\partial}{\partial \mathcal{W}_i^{\mathcal{B}}} \delta^{4|4} \left(\sum_j c_{\alpha j} \mathcal{W}_j^{\mathcal{C}} \right) = \\ &= \sum_i \mathcal{W}_i^{\mathcal{A}} \frac{\partial W^{\mathcal{C}}}{\partial \mathcal{W}_i^{\mathcal{B}}} \frac{\partial}{\partial W^{\mathcal{C}}} \delta^{4|4} (W^{\mathcal{C}}) = \\ &= \sum_i c_{\alpha i} \mathcal{W}_i^{\mathcal{A}} \frac{\partial}{\partial W^{\mathcal{B}}} \delta^{4|4} (W^{\mathcal{C}}) = W^{\mathcal{A}} \frac{\partial}{\partial W^{\mathcal{B}}} \delta^{4|4} (W^{\mathcal{C}}) , \end{aligned} \quad (2.125)$$

where we introduced W to denote the argument of the $\delta^{4|4}$. Integrating by parts, we obtain

$$W^{\mathcal{A}} \frac{\partial}{\partial W^{\mathcal{B}}} \delta^{4|4} (W^{\mathcal{C}}) = (-1)^{|\mathcal{A}||\mathcal{B}|} \left[\frac{\partial}{\partial W^{\mathcal{B}}} W^{\mathcal{A}} - \delta^{\mathcal{A}}_{\mathcal{B}} \right] \delta^{4|4} (W^{\mathcal{C}}) = -(-1)^{|\mathcal{A}||\mathcal{B}|} \delta^{\mathcal{A}}_{\mathcal{B}} \delta^{4|4} (W^{\mathcal{C}}) . \quad (2.126)$$

We dropped the first term, because $W^{\mathcal{A}} \delta^{4|4} (W^{\mathcal{C}}) = 0$ on the support of the $\delta^{4|4}$ and the final result is effectively zero, once we enforce that the $j^{(0)\mathcal{A}}_{\mathcal{B}}$ are traceless. Having a product over \tilde{k} (or k) different $\delta^{4|4}$ also serves the purpose of constructing an object with the correct polynomial dependence on the fermionic variables η_i (or χ_i). Up to now, we only discussed invariance under superconformal symmetry, but if $\mathcal{L}_{n,k}^{\text{ACCK}}$ and $\mathcal{L}_{n,k}^{\text{MS}}$ are to compute superamplitudes (possibly stripped of the tree-level MHV prefactor) then they better know about the full Yangian symmetry enjoyed by them. This is precisely the constraint that was used in [47], together with the requirements of cyclicity and scaling, to uniquely fix the form of the Grassmannian integrals. An alternative approach appeared in [48].

The formulae for $\mathcal{L}_{n,k}^{\text{ACCK}}$ and $\mathcal{L}_{n,k}^{\text{MS}}$ look compellingly similar and in fact were shown to be simply related by the authors of [45]. After Fourier transforming (2.123) to momentum space, they could arrange for a partial gauge-fixing that would leave intact a $\text{GL}(k, \mathbb{C})$ subgroup of the original $\text{GL}(\tilde{k}, \mathbb{C}) = \text{GL}(k+2, \mathbb{C})$. Exploiting a factorisation property of the $\tilde{k} \times \tilde{k}$ minors of C , namely

$$(i, \dots, i+k-1)_C = \left(\prod_{k=i}^{i+k-2} \langle k \ k+1 \rangle \right) (i+1, \dots, i+k-2)_{k \times k} , \quad (2.127)$$

they could prove that in fact

$$\mathcal{L}_{n,k+2}^{(\text{ACCK})} = \frac{\delta^4(p) \delta^{0|8}(q)}{\langle 12 \rangle \langle 23 \rangle \dots \langle n1 \rangle} \mathcal{L}_{n,k}^{(\text{MS})} . \quad (2.128)$$

The conclusion is thus that the Grassmannian integral of (2.123) also enjoys dual superconformal symmetry and hence Yangian invariance. To be precise, the symmetry holds up to total derivatives, which integrate to zero along a closed contour [47].

$\mathcal{N} = 4$ SYM theory is UV-finite, still its ℓ -loop amplitudes suffer from IR divergencies, arising in the integration of the (rational) integrands over loop momenta for soft or collinear configurations: one could say that the trouble comes from having to integrate over the bad-behaved contour $(-\infty, +\infty)^{4\ell} = (\mathbb{R}^4)^\ell$. The idea is to think instead of $\mathcal{L}_{n,\tilde{k}}^{\text{ACCK}}$ and $\mathcal{L}_{n,k}^{\text{MS}}$ as contour integrals and focus on quantities that are simple rational functions of the kinematic invariants and yet encode all the information about $\mathcal{A}_n^{\ell\text{-L}}$, the so-called *leading singularities*. Multi-loop amplitudes have branch cuts as functions of the kinematic invariants and it is therefore natural to consider the discontinuities across such singularities; in turn, these may also have branch cuts and so the procedure can be iterated, until we reach what is called the discontinuity across a leading singularity (leading singularity for short), a concept dating back to the analytic S-matrix program [7]. The procedure generalises the Cutkosky cutting rules [8], putting on the mass shell not just two, but in general 4ℓ propagators (working in four dimensions, this is referred to as a *maximal cut*) and reducing the integral to be computed to a product of tree-level amplitudes. We remark that leading singularities alone allow to reconstruct the amplitude in $\mathcal{N} = 4$ SYM by virtue of maximal supersymmetry, whereas in more general theories their input is required, but not sufficient; for additional details we refer to [105] and the discussions in [69, 43]. From the mathematical point of view, cutting propagators amounts to taking residues of the integrand and in particular cutting a maximal number of them implies that the integral is completely localised on the solutions of a set of quadratic equations. Consider for example the one-loop box integral $I_{\text{box}}(p_1, p_2, p_3, p_4)$ contributing to the four-point gluon amplitude: its leading singularity will be given by the product of four three-point on-shell amplitudes as shown in Figure 2.7, where the loop momentum q has to solve⁹

$$q^2 = (q - p_1)^2 = (q - p_1 - p_2)^2 = (q + p_4)^2 = 0 . \quad (2.129)$$

Coming back to the Grassmannian integrals, after solving the δ -functions one is left with a contour integral over $k(n-k-4)$ variables (see (2.124)), to be computed as an appropriate sum of residues. The conjecture put forward in [43] was that residues of $\mathcal{L}_{n,k+2}^{\text{ACCK}}$ are in one-to-one correspondence with leading singularities of n -point N^kMHV superamplitudes *at*

⁹There are actually two solutions, but a special feature of the four-point case is that they both yield the same result: there is only one leading singularity at four points.

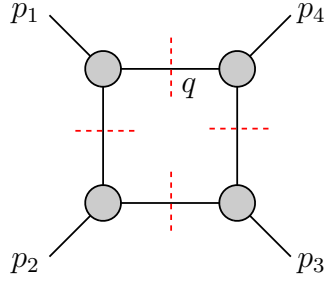


Figure 2.7: This is in fact an on-shell diagram, as will be discussed in the next section.

all loops! The authors provided non-trivial evidence for their claim up to two loops; such evidence was then heavily corroborated by subsequent papers [106, 107]. In particular, Bullimore, Mason and Skinner [106] showed that for $N^k\text{MHV}$ amplitudes no new leading singularity can appear beyond $3k$ -loop order. This is remarkable, because it would be natural to expect that an infinite number of Feynman diagrams at all loops would give rise to an infinite number of leading singularities. This is not the case: in fact, for MHV amplitudes, all leading singularities coincide with the Parke–Taylor prefactor of (2.128), consistently with $\mathcal{L}_{n,k}^{(\text{MS})}$ simply not being there for $k = 0$. What will be most important for us is that tree-level amplitudes can be expressed as sums of one-loop leading singularities (see [26] and references therein). Then, when computing them with the Grassmannian integrals, we will have to set up a contour of integration – $\tilde{\gamma}$ or γ respectively – encircling a proper subset of the singularities, consequently picking up the residues at those poles. There is no real distinction between these two contours, because it is immediate to translate from one to the other: as explained in [45], a singularity characterised by the vanishing of the minor $(i, \dots, i + \tilde{k} - 1) = (i, \dots, i + k + 1)$ in $\mathcal{L}_{n,k}^{(\text{ACCK})}$ corresponds to one where $(i + 1, \dots, i + k) = 0$ in $\mathcal{L}_{n,k}^{(\text{MS})}$.

It turns out that residues of the Grassmannian integrals precisely match the expressions corresponding to super-BCFW diagrams. The correct integration contours are those which produce a combination of residues corresponding to a BCFW recursion. A very important goal achieved by proper sums of such Yangian invariants is that non-local poles – not corresponding to sums of adjacent momenta going on-shell – appearing in individual terms disappear: this phenomenon is referred to as cancellation of spurious singularities [42]. Importantly, integration cycles guaranteeing this are not unique and – as anticipated – this implies linear relations among the residues: they are very non-trivial from the algebraic point of view, but geometrically clear. An instructive example of this is provided by the explicit computation of a tree-level six-point NMHV gluon amplitude, presented in [43]

and reviewed in [64]. We start from

$$\mathcal{L}_{6,3}^{(\text{ACCK})} = \int_{\tilde{\gamma}} \frac{d^9 \tilde{c}_{\alpha i}}{(123) \cdots (612)} \prod_{\beta=1}^3 \delta^2 \left(\sum_i \tilde{c}_{\beta i}^\perp \lambda_i \right) \prod_{\alpha=1}^3 \delta^2 \left(\sum_i \tilde{c}_{\alpha i} \tilde{\lambda}_i \right) \delta^{0|4} \left(\sum_i \tilde{c}_{\alpha i} \eta_i \right), \quad (2.130)$$

after having Fourier-transformed back the $\tilde{\mu}$ components of the supertwistors to the helicity spinors λ_i and fixed the $\text{GL}(3, \mathbb{C})$ redundancy conveniently (*i.e.* setting the columns of C corresponding to negative-helicity gluons to the identity). After solving eight bosonic δ -functions and keeping four others to enforce momentum conservation, we are left with a single integration to perform, for a single entry \tilde{c}_\star of \tilde{C} . Now, focusing on the alternating-helicity configuration, we have

$$A_6(1^+, 2^-, 3^+, 4^-, 5^+, 6^-) = \{M_2\} + \{M_4\} + \{M_6\} = -\{M_1\} - \{M_3\} - \{M_5\}, \quad (2.131)$$

up to the $\delta^4(p)$, where the $\{M_i\}$ are the residues corresponding to the vanishing of the i -th minor. In spinor-helicity variables they read

$$\{M_i\} = \frac{\langle i i + 2 \rangle^4 [i + 3 i - 1]^4}{\tilde{P}_i^2 \langle i | \tilde{P}_i | i + 3 \rangle \langle i + 2 | \tilde{P}_i | i - 1 \rangle \langle i i + 1 \rangle \langle i + 1 i + 2 \rangle [i + 3 i - 2] [i - 2 i - 1]}, \quad (2.132)$$

with $\tilde{P}_i = p_i + p_{i+1} + p_{i+2}$. The situation is schematically portrayed in Figure 2.8.

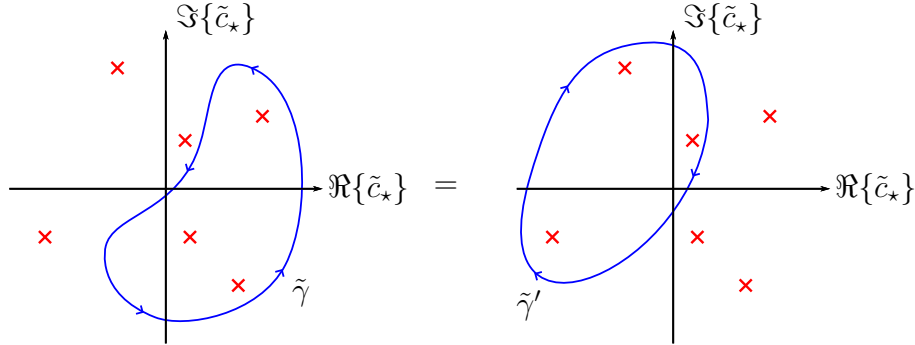


Figure 2.8: Two possible contours encircling a proper set of leading singularities of the Grassmannian integral $\mathcal{L}_{6,3}^{(\text{ACCK})}$.

As the external kinematics is varied, the poles in the left-over integration variable c_\star move around the complex plane and a singularity arises whenever two of them collide. Spurious singularities correspond to the case in which the two colliding poles lie both inside or outside the integration contour and are bound to disappear in the sum of residues because either $\tilde{\gamma}$ or $\tilde{\gamma}'$ does not see them at all. On the contrary, physical singularities demand that the contour be pinched between a pair of poles separated by it. A more complete discussion of this can be found in [43].

2.5.3 On-shell diagrams

We have already discussed in the previous sections how Poincaré invariance, together with little group scaling properties, uniquely fixes the form of the three-point on-shell scattering amplitudes to the form (2.105), which we repeat here for convenience:

$$\begin{aligned}\mathcal{A}_3^{\text{MHV}}(1, 2, 3) &= \frac{\delta^{0|8}(\lambda_1\eta_1 + \lambda_2\eta_2 + \lambda_3\eta_3)}{\langle 12 \rangle \langle 23 \rangle \langle 31 \rangle} \delta^4(\lambda_1\tilde{\lambda}_1 + \lambda_2\tilde{\lambda}_2 + \lambda_3\tilde{\lambda}_3) \quad , \\ \mathcal{A}_3^{\overline{\text{MHV}}}(1, 2, 3) &= \frac{\delta^{0|4}([12]\eta_3 + [23]\eta_1 + [31]\eta_2)}{[12][23][31]} \delta^4(\lambda_1\tilde{\lambda}_1 + \lambda_2\tilde{\lambda}_2 + \lambda_3\tilde{\lambda}_3) \quad .\end{aligned}\tag{2.133}$$

These are in fact supersymmetric expressions, accounting at once for all possible states in $\mathcal{N} = 4$ SYM, but one can quickly recover those for MHV and $\overline{\text{MHV}}$ gluon amplitudes by extracting from the fermionic δ 's the relevant factors. We will represent (2.133) as three-point black or white vertices, respectively, as in Figure 2.9.



Figure 2.9: The trivalent vertices which will be used to build all on-shell diagrams.

While discussing BCFW recursion relations, we argued that three-point superamplitudes are the building blocks for constructing any $\mathcal{A}_n^{\text{N}^k\text{MHV}}$. This suggests that the cubic vertices we just introduced can be combined into objects encoding information about generic on-shell scattering amplitudes. In fact, it is possible to glue them together to yield *on-shell diagrams*, such as those in Figure 2.10. We draw only planar examples, because those will be relevant in our planar setup, but non-planar diagrams are legitimate [108].

Despite the Feynman-diagram-like appearance, on-shell diagrams are really different. As the name indicates, all internal lines are on-shell and both momentum and supermomentum are conserved at every vertex. The gluing procedure consists in integrating over the internal degrees of freedom via the measure

$$\prod_I \int d^4\eta_I \int \frac{d^2\lambda_I d^2\tilde{\lambda}_I}{\text{GL}(1, \mathbb{C})} \quad ,\tag{2.134}$$

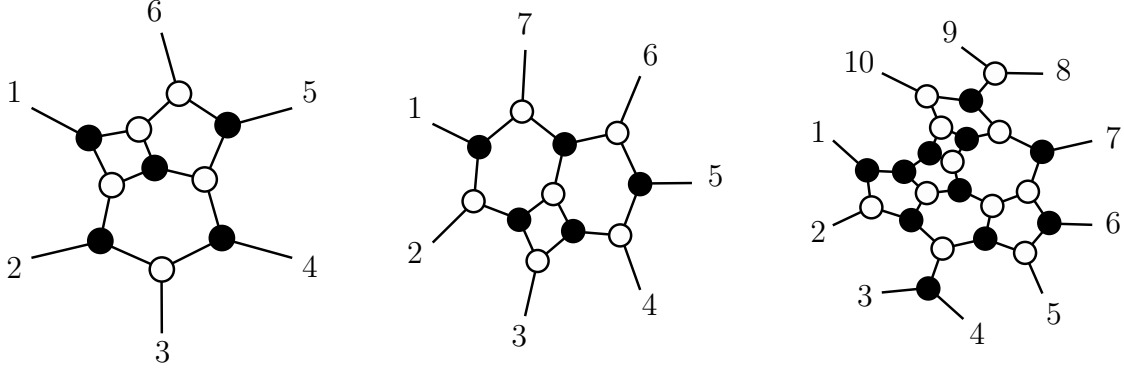


Figure 2.10: Examples of planar on-shell diagrams.

with the $\text{GL}(1, \mathbb{C})$ factor accounting for the little group scaling freedom. As already pointed out discussing the super-BCFW recursion, the external integration replaces a sum over the possible states of $\mathcal{N} = 4$ SYM which can propagate along internal lines: in the case of pure Yang–Mills, it would simply be replaced by a sum over the two possible helicity states of the gluons. In fact, the on-shell diagrams machinery is not inextricably tied to $\mathcal{N} = 4$ SYM: they can be introduced for a multitude of QFTs at the only extra cost of having to decorate the legs to keep track of the different states of their spectrum.

It is instructive to start from some of the most elementary on-shell diagrams and to discuss the physics involved. The simplest thing we can do is to join a white to a black vertex, see Figure 2.11. Gluing either two black or two white vertices is not so interesting,

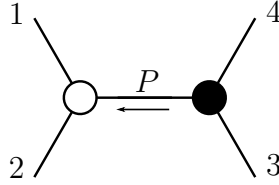


Figure 2.11: A very simple on-shell diagram.

because having only one kind of vertices forces the helicity spinors of the external legs (the $\tilde{\lambda}_i$ or λ_i respectively) to be proportional to each other. In fact, we will now show that also the diagram with oppositely coloured vertices vanishes for general kinematics, but in a less trivial way. Indeed we have $\lambda_1 \sim \lambda_2 \sim \lambda_P$ and $\tilde{\lambda}_3 \sim \tilde{\lambda}_4 \sim \tilde{\lambda}_P$ and the diagram reads

$$\int d^4\eta_P \int \frac{d^2\lambda_P d^2\tilde{\lambda}_P}{\text{GL}(1, \mathbb{C})} \frac{\delta^4(\lambda_1\tilde{\lambda}_1 + \lambda_2\tilde{\lambda}_2 - \lambda_P\tilde{\lambda}_P)\delta^{0|4}([12]\eta_P + [2P]\eta_1 + [P1]\eta_2)}{[12][2P][P1]} \times \quad (2.135)$$

$$\times \frac{\delta^4(\lambda_3\tilde{\lambda}_3 + \lambda_4\tilde{\lambda}_4 + \lambda_P\tilde{\lambda}_P)\delta^{0|8}(\lambda_3\eta_3 + \lambda_4\eta_4 + \lambda_P\eta_P)}{\langle 34 \rangle \langle 4P \rangle \langle P3 \rangle}.$$

The fermionic integrations can be easily carried out and produce $\delta^{0|8}(\sum_i \lambda_i \eta_i)$ and it is immediate to see that on the support of one bosonic δ -function, the other becomes $\delta^4(\sum_i \lambda_i \tilde{\lambda}_i)$. The final result is

$$\frac{\delta^4(p)\delta^{0|8}(q)}{\langle 12 \rangle \langle 23 \rangle \langle 34 \rangle \langle 41 \rangle} \delta((p_1 + p_2)^2), \quad (2.136)$$

where, beside the $\mathcal{A}_4^{\text{tree}}$ factor, the left-over δ enforces the on-shellness of the internal leg and was thus to be expected. Hence the diagram of Figure 2.11 represents a factorisation channel, although it was not introduced as the cut of a four-point graph, but rather as the gluing of two three-point ones.

Let us now move to the diagram of Figure 2.12, evaluating to the product of four three-point on-shell amplitudes, integrated over the internal on-shell degrees of freedom. Counting the number of constraints, *i.e.* (super)momentum-conserving δ -functions, and of

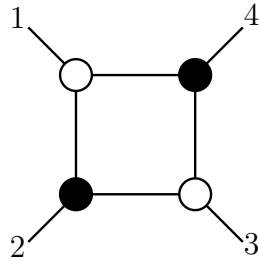


Figure 2.12: The “next-to-simplest” thing.

integrations (2.134), we rapidly conclude that the result will involve four bosonic and eight fermionic δ ’s. In fact, going through the computation, one precisely finds

$$\frac{\delta^4(p)\delta^{0|8}(q)}{\langle 12 \rangle \langle 23 \rangle \langle 34 \rangle \langle 41 \rangle} = \mathcal{A}_4^{\text{tree}}. \quad (2.137)$$

Hence the above diagram actually computes a tree-level amplitude: we remark that there is no relation between the number of loops appearing in an on-shell graph and the loop-order of the amplitude it is contributing to, as various forthcoming examples will illustrate.

An arbitrary diagram involves several integration variables corresponding to internal null momenta and (super)momentum conservation constraints, enforced by Dirac δ ’s, are imposed at each vertex. The interplay between the number of variables and constraints allows for three different situations:

- We may have as many constraints as internal variables, leading to a fully localised integral, *i.e.* a function (or rather a distribution) of the external kinematics alone; this is the case of the box diagram above.

- The number of constraints may exceed that of variables: then, as for the factorisation channel of before, we would have a function of external kinematics, further constrained by additional δ -functions.
- If the constraints are not enough to localise the internal data, we will be left with a differential form to be integrated over some contour.

The scenarios above are not fundamentally different, hence we say somewhat loosely that on-shell diagrams all evaluate to an *on-shell form* \mathcal{F} (after stripping off any remaining integral sign). Other than gluing three-point on-shell amplitudes, a more traditional way to think of on-shell diagrams – which further elucidates the classification above – is as cuts of ℓ -loop amplitudes. Then, denoting the number of internal lines as I , we have constrained external kinematics if $I > 4\ell$, left-over internal degrees of freedom if $I < 4\ell$ and what has previously been called a leading singularity if $I = 4\ell$. From this point of view, Figure 2.12 represents a maximal cut of a one-loop four-point amplitude; non-maximal cuts yield instead honest differential forms: Figure 2.13 provides the simplest example of an on-shell diagram where \mathcal{F} is a 1-form.

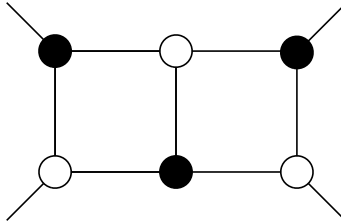
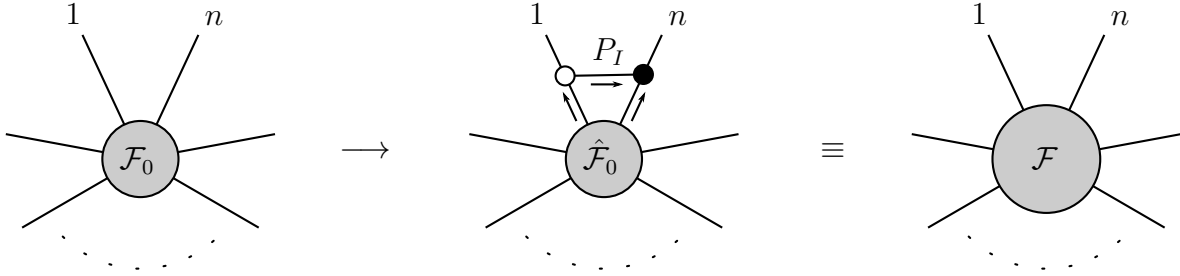


Figure 2.13: This on-shell diagram can be thought of as the heptacut of a two-loop four-point amplitude, one constraint too few to localise the eight components of the two loop momenta.

Before moving further, it is necessary to discuss how BCFW shifts are implemented in the on-shell diagrams formalism, which is also the typical way of building more complicated graphs from simpler ones. Consider an on-shell diagram with n external legs and suppose it evaluates to the on-shell form \mathcal{F}_0 . Now, consider a modified version of the same diagram where *e.g.* legs 1 and n are bridged via a white-black pair of vertices, see Figure 2.14. The internal null momentum $P_I = \lambda_I \tilde{\lambda}_I$ is constrained by the special three-point kinematics, such that $\lambda_I \sim \lambda_1$, $\tilde{\lambda}_I \sim \tilde{\lambda}_n$, *i.e.* $P_I = \alpha \lambda_1 \tilde{\lambda}_n$, for some α . By (super)momentum conservation at the two new vertices, the on-shell momenta \hat{p}_1, \hat{p}_n exiting the rest of the diagram

Figure 2.14: An $[n, 1]$ -shift in the on-shell diagrams language.

(denoted by the grey blob) must fulfil

$$\begin{cases} \hat{p}_1 = p_1 + P_I \\ \hat{p}_n = p_n - P_I \end{cases}, \quad i.e. \quad \begin{cases} \hat{\lambda}_1 \hat{\tilde{\lambda}}_1 = \lambda_1 (\tilde{\lambda}_1 + \alpha \tilde{\lambda}_n) \\ \hat{\lambda}_n \hat{\tilde{\lambda}}_n = (\lambda_n - \alpha \lambda_1) \tilde{\lambda}_n \end{cases}, \quad (2.138)$$

which is precisely the prescription for a $[1, n]$ -shift, or rather supershift, once the η_i are taken into account enforcing supermomentum conservation. The upshot of this analysis is that adding a BCFW bridge introduces a new variable α and the on-shell form \mathcal{F} of the bridged diagram is related to the original \mathcal{F}_0 as

$$\begin{aligned} \mathcal{F}(\lambda_1, \tilde{\lambda}_1, \eta_1; \dots; \lambda_n, \tilde{\lambda}_n, \eta_n; \alpha) &= \frac{d\alpha}{\alpha} \hat{\mathcal{F}}_0(\hat{\lambda}_1, \tilde{\lambda}_1, \eta_1; \dots; \lambda_n, \hat{\tilde{\lambda}}_n, \hat{\eta}_n) = \\ &= \frac{d\alpha}{\alpha} \mathcal{F}_0(\lambda_1, \tilde{\lambda}_1 + \alpha \tilde{\lambda}_n, \eta_1 + \alpha \eta_n; \dots; \lambda_n - \alpha \lambda_1, \tilde{\lambda}_n, \eta_n). \end{aligned} \quad (2.139)$$

The appearance of an extra degree of freedom was to be expected, because the new diagram has one more loop and three more δ 's to be enforced than the original one. The new form has poles in α , a trivial one at $\alpha = 0$ corresponding to the original \mathcal{F}_0 – *i.e.* to erasing the BCFW bridge – and one at a factorisation channel, corresponding to the deletion of another internal edge. Altogether, on-shell diagrams provide a graphical implementation of the BCFW recursion relations. To be more precise, we need to explain how do the parameters n and k of a superamplitude appear. The first is pretty self-explanatory, being the number of external legs (colour-ordered, as usual); the second follows by counting the polynomial degree of the on-shell form in the η_i variables and is given by the following formula:

$$k + 2 = \tilde{k} = 2N_B + N_W - I, \quad (2.140)$$

where, beside the number of internal legs I , we have to take into account the number of black and white vertices appearing in the graph. Notice that inserting a BCFW bridge does

not alter k . Then the graphical representation of formula (2.107) instructs us to recurse n -point amplitudes considering all possible products of lower-point amplitudes, yielding the correct k counting, bridged together with a pair of trivalent vertices as described above, see Figure 2.15 in the case of a $[1, n]$ -shift. The blobs on the left- and right-hand side of the factorisation channels are to be replaced with the on-shell diagrams at lower points!

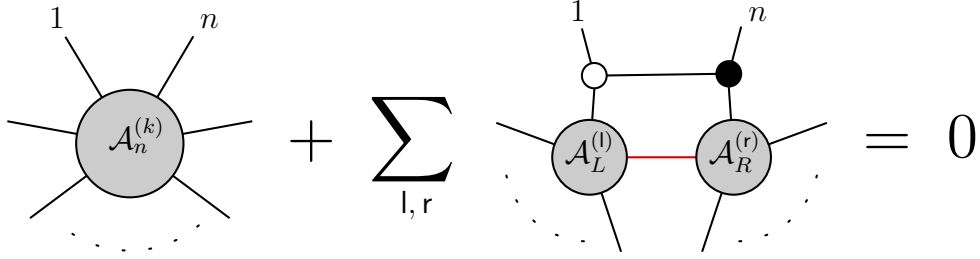


Figure 2.15: Recycling lower-point to evaluate higher-point amplitudes at tree-level, with on-shell diagrams. We employ the shorthand notation $\mathcal{A}^{(\star)} = \mathcal{A}^{\mathcal{N}^{\star}\text{MHV}}$, where as usual $\star = -1$ corresponds to $\mathcal{A}^{\overline{\text{MHV}}}$ and the indices l, r are constrained by $l + r = k - 1$.

Let us discuss some examples. First, we deduce that $\mathcal{A}_4^{\text{tree}}$ must be given by the product $\mathcal{A}_3^{\text{MHV}} \otimes \mathcal{A}_3^{\overline{\text{MHV}}}$, plus the BCFW bridge to connect the shifted legs. This is precisely¹⁰ the content of Figure 2.12, although the box graph can be equivalently seen as the result of attaching a BCFW bridge on any other factorisation channel. Iterating, always at tree-level, all MHV and $\overline{\text{MHV}}$ amplitudes are computed by a single on-shell diagram: in general, as illustrated in Figure 2.16, $\mathcal{A}_n^{\text{MHV}} = \mathcal{A}_{n-1}^{\text{MHV}} \otimes \mathcal{A}_3^{\overline{\text{MHV}}}$ and $\mathcal{A}_n^{\overline{\text{MHV}}} = \mathcal{A}_3^{\text{MHV}} \otimes \mathcal{A}_{n-1}^{\overline{\text{MHV}}}$.

The first amplitude which is actually represented by a sum of on-shell diagrams is $\mathcal{A}_6^{\text{NMHV}}$: this is not surprising, given the discussion at the end of the previous section about the alternating-helicity component amplitude (2.131). Correspondingly, here we have to consider a sum of three terms:

$$\mathcal{A}_6^{\text{NMHV}} = \mathcal{A}_5^{\text{NMHV}} \otimes \mathcal{A}_3^{\overline{\text{MHV}}} + \mathcal{A}_4^{\text{MHV}} \otimes \mathcal{A}_4^{\text{MHV}} + \mathcal{A}_3^{\text{MHV}} \otimes \mathcal{A}_5^{\text{MHV}}, \quad (2.141)$$

depicted in Figure 2.17.

The powerful *Mathematica* package `positroids` [109] generates on-shell diagrams and automates a host of calculations related to them. However, the graphs of Figures 2.16 and 2.17 can be given a different appearance, tuning several optional parameters. Indeed, any given graph is amenable to a class of transformations that do not affect its physical

¹⁰Actually one has to write down two separate contributions, but only one is non-vanishing for general kinematics.

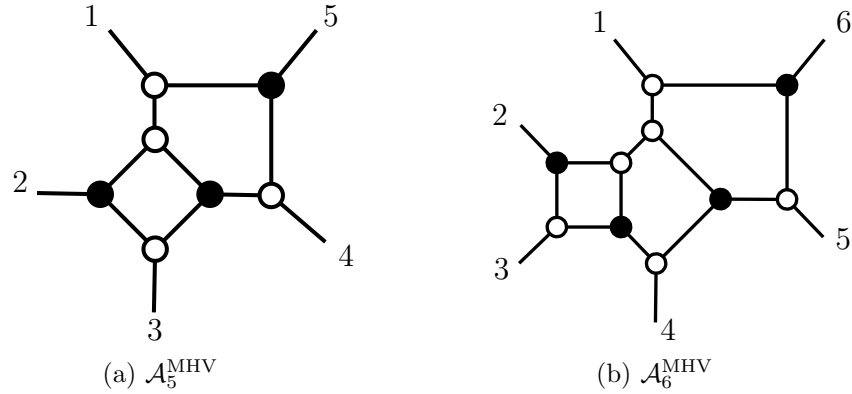


Figure 2.16: Five- and six-point MHV superamplitudes recursed via on-shell diagrams. The $\overline{\text{MHV}}$ ones are obtained similarly.

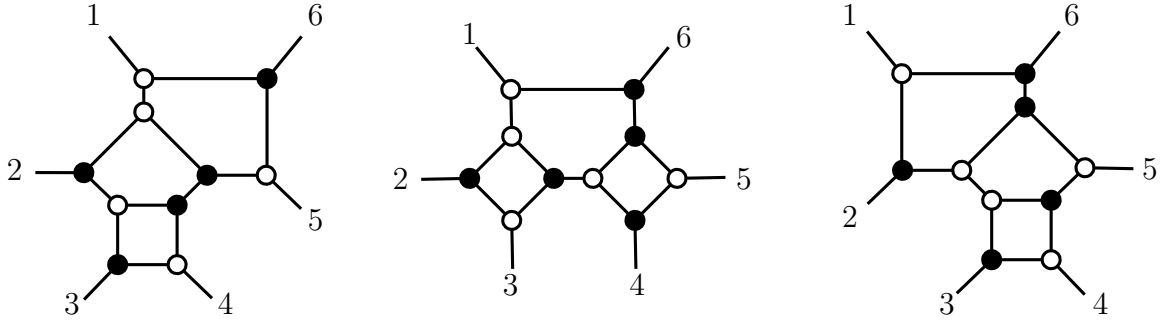


Figure 2.17: The three on-shell graphs building up the six-point NMHV superamplitude.

content. Indeed, one might have wondered how could this formalism be of any advantage as compared to the traditional one based on Feynman diagrams, since of course one can write down an infinite number of on-shell graphs as well. The basic equivalence transformations are called *flip move* and *square move*, shown in Figure 2.18. Their validity can be checked by explicit computation (they all amount to a change of variables); on the other hand, flip moves have to hold because both sides of the equality enforce the same proportionality constraints among λ or $\tilde{\lambda}$ spinors, whereas the square move is a consequence of the existence of a unique leading singularity at four points.

This is not yet the end of the story, since both flip and square moves do not change the number of faces of the graphs. A last operation that can be performed on planar on-shell diagrams is the *bubble deletion*, illustrated in Figure 2.19. Here in fact the on-shell form associated to the diagram before and after the removal of the bubble cannot be the same: indeed, the original one (with the bubble) has three more internal lines and a pair of white-black vertices more than the new one, resulting in one more bosonic integration variable

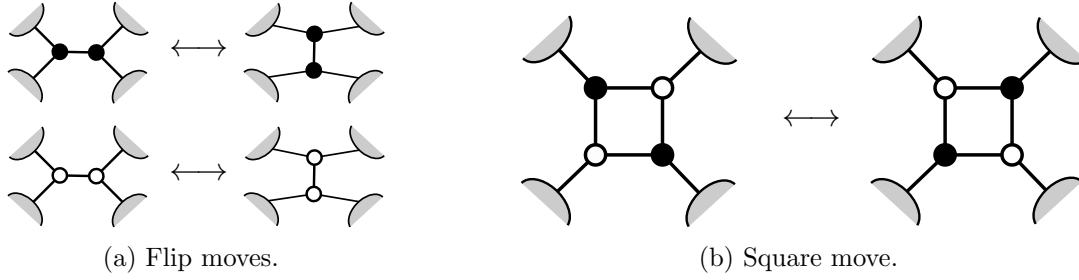


Figure 2.18: Transformations that leave the physical properties of on-shell diagrams invariant.

to be taken into account. Nevertheless, it turns out that the extra degree of freedom α can be factored out cleanly from the on-shell form, namely

$$\mathcal{F}_{\text{orig}} = \frac{d\alpha}{\alpha} \mathcal{F}_{\text{new}} . \quad (2.142)$$



Figure 2.19: Reducing a diagram, removing one of its faces by erasing a bubble.

We will not be concerned with the details of this property, because it is only relevant for constructing loop integrands. The upshot of the discussion is that the seemingly infinite complexity of on-shell diagrams is illusory and, for any number n of external legs, there exists only a *finite* number of *reduced on-shell diagrams*, such that all bubbles have been deleted, up to flip and square moves. On shell forms of reduced diagrams are the residue at $\alpha = 0$ of the on-shell form of the same diagram with an extra bubble, as clearly shown in (2.142). This begs the question of how to characterise the invariant information represented by a class of equivalent on-shell diagrams, *i.e.* by the corresponding on-shell form. The surprising answer is that all of it is encoded in a permutation of the external labels!

As illustrated in Figure 2.20b via an example, constructing the permutation corresponding to an on-shell graph is very easy: one just needs to follow the path leading from each external leg to another one (its image), moving along the internal lines, turning right (left) at every white (black) vertex. This guarantees that on-shell graphs yield a well defined

permutation

$$\sigma = \{\sigma(1), \sigma(2), \dots, \sigma(n)\} = \begin{pmatrix} 1 & 2 & \dots & n \\ \sigma(1) & \sigma(2) & \dots & \sigma(n) \end{pmatrix}, \quad (2.143)$$

which importantly is not altered by any flip or square move. It should be noted that it is actually necessary to work with *decorated permutations*: they are defined according to the constraint $i \leq \sigma(i) \leq i + n$, *i.e.* images must not be smaller than their preimages. The number of legs whose image is bigger than n is denoted \tilde{k} , since those diagrams will be related to $N^k\text{MHV}$ amplitudes. A fixed point i_0 of the permutation σ can be mapped either

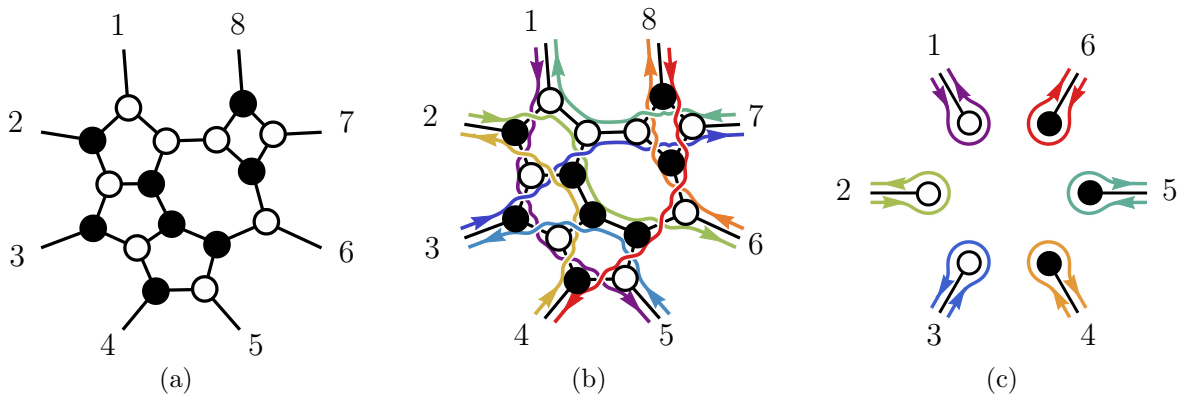


Figure 2.20: In the first two pictures, an on-shell diagram contributing to the eight-point $N^2\text{MHV}$ amplitude, with the left-right paths used to derive the associated decorated permutation, reading $\{5, 6, 7, 10, 11, 8, 9, 12\}$. On the right, an example of identity graph, whose associated permutation is a decoration of the identity, in this case $\{7, 8, 9, 4, 5, 6\}$.

to itself or to $i_0 + n$. To better understand the significance of this ambiguity, we have to allow for unphysical on-shell diagrams involving bivalent and monovalent vertices as well. This is of little concern, since bivalent vertices along any internal line do not change σ ; monovalent ones do not have any effect either, unless they are directly attached to an external leg. Indeed, the fundamental objects we still have to introduce are a special class of on-shell diagrams associated to some decoration of the identity permutation $\sigma_{\text{id}} = \{1, 2, \dots, n\}$, to be denoted $\hat{\sigma}_{\text{id}}$, see for instance the one in Figure 2.20c. We will call them *identity graphs* and their permutations are such that $\sigma(i) = i$ or $\sigma(i) = i + n$ for legs attached to monovalent black or white vertices respectively. The useful thing about such unphysical graphs is that they serve as starting point to construct any other on-shell diagram, whose permutation is obtained from the original decoration of σ_{id} composing a number of transposition, namely

those 2-cycles swapping a pair of labels. Indeed, on the level of the on-shell diagrams, the swap amounts to the insertion of a BCFW bridge on the corresponding legs: looking for instance at Figure 2.14, we realise that the transposition (ij) is implemented inserting a white-black bridge on legs i and j respectively and this will cause the preimages of σ to be interchanged. The precise description of this procedure goes as follows:

- Starting with any permutation σ , rewrite it as $\sigma = (ac) \circ \sigma'$, where the transposition affects the lexicographically first pair of labels in positions a, c , such that $1 \leq a < c \leq n$ and $\sigma(a) < \sigma(c)$, separated only by labels $\sigma(b)$ self-identified under the permutation, *i.e.* such that $\sigma(b) = b \bmod n$ (for this reason, they are called *adjacent transpositions*); iterate until σ' is a decoration of the identity. We will have obtained a decomposition of the form

$$\sigma = (i_1 j_1) \circ (i_2 j_2) \circ \cdots \circ (i_N j_N) \circ \hat{\sigma}_{\text{id}} . \quad (2.144)$$

- The resulting on-shell diagram can be drawn successively adding BCFW bridges to the identity graph corresponding to $\hat{\sigma}_{\text{id}}$, similar to that of Figure 2.20c. Along the way, monovalent vertices not anymore attached to an external leg and bivalent vertices are to be erased.

For the sake of clarity, here is an example of the above: the step-by-step decomposition of the permutation $\sigma = \{4, 6, 5, 7, 8, 9\}$ is

$$\begin{aligned} \sigma &= (12) \circ \{6, 4, 5, 7, 8, 9\} = \\ &= (12) \circ (23) \circ \{6, 5, 4, 7, 8, 9\} = \\ &= (12) \circ (23) \circ (34) \circ \{6, 5, 7, \mathbf{4}, 8, 9\} = \\ &= (12) \circ (23) \circ (34) \circ (23) \circ \{6, 7, 5, \mathbf{4}, 8, 9\} = \\ &= (12) \circ (23) \circ (34) \circ (23) \circ (12) \circ \{\mathbf{7}, 6, 5, \mathbf{4}, 8, 9\} = \\ &= (12) \circ (23) \circ (34) \circ (23) \circ (12) \circ (35) \circ \{\mathbf{7}, 6, 8, \mathbf{4}, \mathbf{5}, 9\} = \\ &= (12) \circ (23) \circ (34) \circ (23) \circ (12) \circ (35) \circ (23) \circ \{\mathbf{7}, \mathbf{8}, 6, \mathbf{4}, \mathbf{5}, 9\} = \\ &= (12) \circ (23) \circ (34) \circ (23) \circ (12) \circ (35) \circ (23) \circ (36) \circ \{\mathbf{7}, \mathbf{8}, \mathbf{9}, \mathbf{4}, \mathbf{5}, \mathbf{6}\} , \end{aligned} \quad (2.145)$$

where in boldface we denoted the labels that “fell in the right place”. Observe that the composition of transpositions as written acts on the images of the permutations, but reading it in reverse (*i.e.* $(36) \circ (23) \circ \cdots \circ (12)$) is equivalent if we act on the preimages of σ instead. In Figure 2.21 we illustrate how adding bridge by bridge brings us to the desired

diagram, equivalent to the one already appeared on the right in Figure 2.17 (to see the equivalence it is sufficient to perform a flip move on the two pairs of like-coloured adjacent vertices).

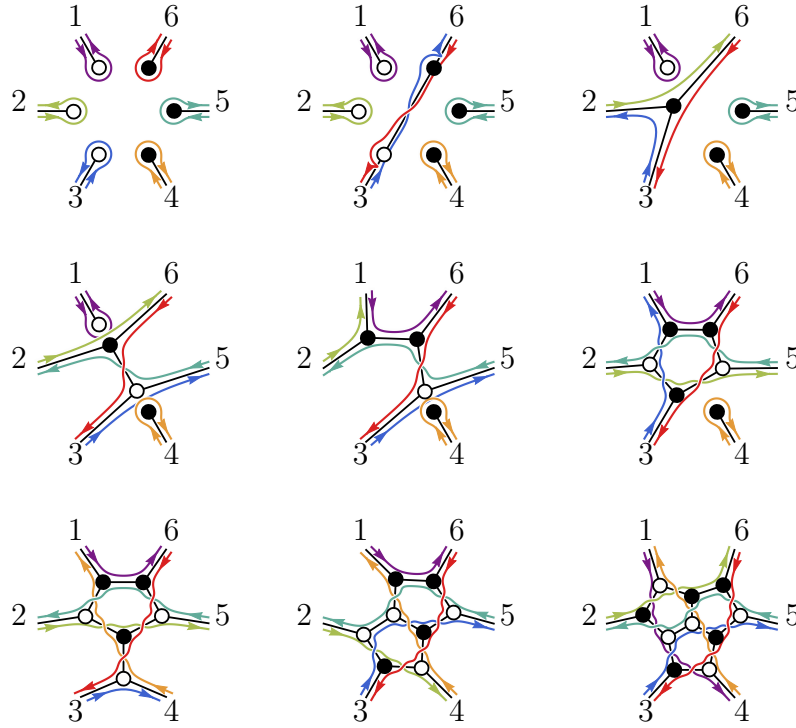


Figure 2.21: Bridge-by-bridge construction of the graph associated to $\sigma = \{4, 6, 5, 7, 8, 9\}$.

We are now finally ready to establish the connection between on-shell diagrams and Grassmannian geometry. First, we will present a much more efficient way to evaluate on-shell graphs than just multiplying three-point amplitudes, which will yield Grassmannian integrals of the form (2.123). Secondly, we will sketch the prescription to bijectively associate to each on-shell graph a submanifold of a suitable Grassmannian. These observations will constitute the backbone of the amplituhedron conjecture, to be introduced in the next chapter.

The first thing to do is to give a manifestly Grassmannian look to the on-shell form of the elementary trivalent vertices, following the reasoning of Section 2.5.1. Recalling the definitions of the 2-planes Λ and $\tilde{\Lambda}$ – and writing $\eta = (\eta_1 \ \eta_2 \ \eta_3)$ in the same spirit – we

introduce auxiliary planes $W \in G(1, 3)$ and $B \in G(2, 3)$ and find

$$\begin{aligned} \mathcal{A}_3^{\overline{\text{MHV}}} &= \frac{\delta^{2 \times 2}(\Lambda \cdot \tilde{\Lambda})}{[12][23][31]} \delta^{0|4}([12]\eta_3 + [23]\eta_1 + [31]\eta_2) \\ &= \frac{1}{\text{GL}(1, \mathbb{C})} \int d^{1 \times 3} W \frac{\delta^{2 \times 2}(\Lambda \cdot W^\perp) \delta^{1 \times 4}(W \cdot \eta)}{(1)(2)(3)} \delta^{1 \times 2}(W \cdot \tilde{\Lambda}) \end{aligned} \quad (2.146)$$

$$\begin{aligned} \mathcal{A}_3^{\text{MHV}} &= \frac{\delta^{2 \times 2}(\Lambda \cdot \tilde{\Lambda})}{\langle 12 \rangle \langle 23 \rangle \langle 31 \rangle} \delta^{0|8}(\lambda_2 \eta_1 + \lambda_2 \eta_2 + \lambda_3 \eta_3) \\ &= \frac{1}{\text{GL}(2, \mathbb{C})} \int d^{2 \times 3} B \frac{\delta^{2 \times 2}(B \cdot \tilde{\Lambda}) \delta^{2 \times 4}(B \cdot \eta)}{(12)(23)(31)} \delta^{2 \times 1}(\Lambda \cdot B^\perp) \end{aligned}$$

In the $\overline{\text{MHV}}$ case, solving $\delta^{1 \times 2}(W \cdot \tilde{\Lambda})$ fixes W to $\begin{pmatrix} [23] & [31] & [12] \end{pmatrix}$, as in (2.121). Then the 1×1 minors in the denominator take the correct value and also the other δ -functions guarantee (super)momentum conservation, since of course $W^\perp = \tilde{\Lambda}$. Similarly, in the MHV case, $\delta^{2 \times 1}(\Lambda \cdot B^\perp)$ implies $B = \Lambda$, whose minors are precisely the desired angle brackets. The nice feature of these integral representations is that the quadratic momentum-conservation constraint has now decoupled and both Λ and $\tilde{\Lambda}$ appear linearly in the δ -functions, making it straightforward to solve for as many degrees of freedom of the internal lines of an on-shell diagram as possible.

Evaluating a generic on-shell diagrams with N_W (N_B) white (black) trivalent vertices and I internal lines amounts to combine all the W and B Grassmannians to yield a set of constraints on the helicity spinors of the external legs. One can show that $\tilde{k} = 2N_B + N_W - I$ relations among the external helicity spinors $\tilde{\lambda}_i$ (and therefore also among the η_i) survive the integration and can be grouped together by means of a $\tilde{k} \times n$ matrix. The latter is in fact a point in $G(\tilde{k}, n)$, because it clearly enjoys a $\text{GL}(\tilde{k}, \mathbb{C})$ symmetry reshuffling the constraints. Similarly, the Dirac δ 's involving the orthogonal complements W^\perp, B^\perp give rise to $n - \tilde{k}$ constraints among the λ_i , implemented by \tilde{C}^\perp . The process by which smaller Grassmannians combine together to yield bigger ones is called *amalgamation* and explained in detail in [50]. At the end of the day, the on-shell form \mathcal{F} is found to be the integral of

$$\left(\prod_{\text{vert}} \frac{1}{\text{GL}(1, \mathbb{C})} \right) \left(\prod_{\text{edges } e} \frac{d\alpha_e}{\alpha_e} \right) \delta^{2 \times (n - \tilde{k})} (\tilde{C}^\perp \cdot \Lambda) \delta^{2 \times \tilde{k}} (\tilde{C} \cdot \tilde{\Lambda}) \delta^{0|4 \times \tilde{k}} (\tilde{C} \cdot \eta) . \quad (2.147)$$

Based on (2.146), every vertex would carry two degrees of freedom, but it is useful to attach one to each leg converging in it, compensating the redundancy with a $\text{GL}(1, \mathbb{C})$ factor. The aforementioned degrees of freedom are called *edge variables* α_e and the \tilde{C}

matrix depends on them. This formula is to be contrasted with (2.130) as for the structure of the δ -functions.

To determine the form of $\tilde{C}(\{\alpha_e\})$, we first need to endow the graph with a *perfect orientation*: this amounts to a decoration of each edge with an arrow, so that each white (black) vertex has one (two) incoming lines and two (one) outgoing ones. As argued in the original reference, physically relevant diagrams always admit a perfect orientation. In fact, more than one, corresponding to different ways of fixing the $\text{GL}(k, \mathbb{C})$ redundancy of \tilde{C} . Furthermore, every perfect orientation will cause exactly \tilde{k} external legs to be oriented inwards and $n - \tilde{k}$ outwards; ingoing legs will correspond to the \tilde{k} columns of \tilde{C} gauge-fixed to the identity, *e.g.* as in (2.113) (we will make this choice for definiteness). Then the remaining matrix elements of \tilde{C} can be computed from the perfectly oriented paths $\gamma_{\alpha i}$ leading from every ingoing leg to an outgoing one. The precise formula is

$$\tilde{c}_{\alpha i} = - \sum_{\gamma_{\alpha i}} \left(\prod_{\alpha_e \in \gamma_{\alpha i}} \alpha_e \right) . \quad (2.148)$$

Should a closed loop be involved – as can be the case when giving a perfect orientation to the diagram of Figure 2.12 – one should sum the resulting geometric series. We provide an example for the (by now familiar) on-shell diagram labelled by the permutation $\sigma = \{4, 6, 5, 7, 8, 9\}$ in Figure 2.22, from which we read off the matrix elements

$$\begin{aligned} \tilde{c}_{25} &= -\alpha_4 \alpha_8 (\alpha_{17} \alpha_{18} + \alpha_9 \alpha_{10} \alpha_{11}) \alpha_{12} \alpha_5 , \\ \tilde{c}_{34} &= -\alpha_3 \alpha_{10} \alpha_4 , \\ \tilde{c}_{36} &= -\alpha_3 \alpha_{10} \alpha_{11} \alpha_{12} \alpha_{13} \alpha_6 . \end{aligned} \quad (2.149)$$

Let us briefly mention that an alternative (and less redundant) way to parametrise the matrix \tilde{C} exploits variables associated to the faces of the on-shell diagrams, indeed called *face variables*. More details about this may be found in the original reference [50].

Up to now we explained how on-shell forms admit a representation in terms of Grassmannian integrals. The final step of this section will be to relate these integrals to those of the form (2.123). To this end, we must take a detour and talk about another type of Grassmannian spaces, the *positive Grassmannians*. The most important difference with respect to those discussed until now is that these will be *real* manifolds, as an obvious requirement to be able to talk about positivity. We call a rectangular real matrix $M \in \mathbb{R}^{\tilde{k} \times n}$ *positive* if its ordered maximal minors $(a_1, \dots, a_{\tilde{k}})$, where $a_1 < \dots < a_{\tilde{k}}$, are all non-negative. Such positive matrices will be coordinates on the positive Grassmannian $G_+(\tilde{k}, n)$, which can

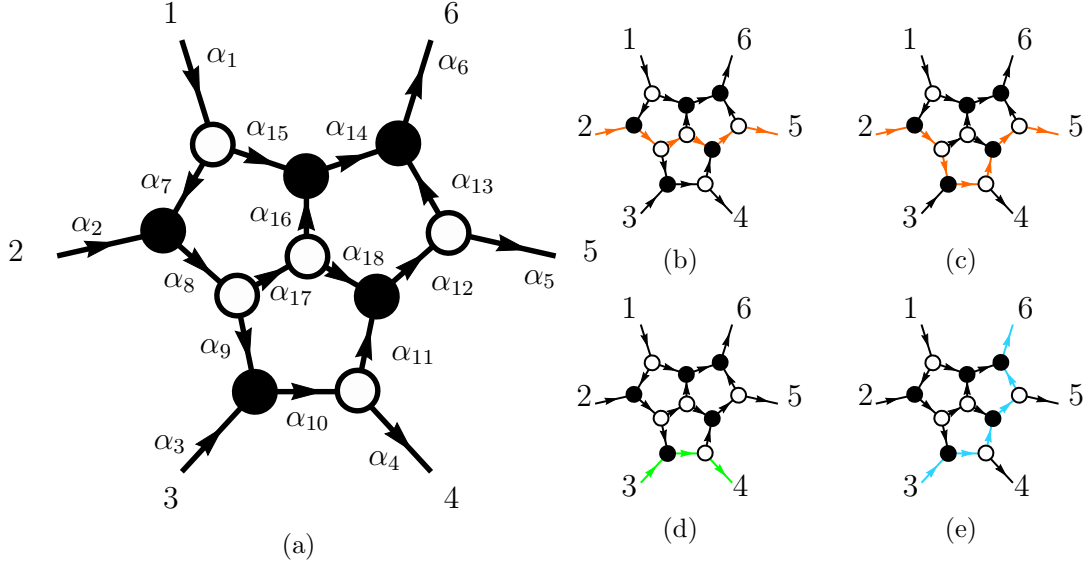


Figure 2.22: Edge variables on each leg of the on-shell diagram and the paths to be considered to compute some entries of the \tilde{C} matrix, namely \tilde{c}_{25} , \tilde{c}_{34} and \tilde{c}_{36} .

be thought of as the submanifold of the real $G(\tilde{k}, n)$ where the Plücker coordinates are non-negative.

Positive Grassmannians have long been studied by mathematicians [49], because of their rich geometrical structure, which quite remarkably has proven to be important in the context of scattering amplitudes. As a subspace of a regular Grassmannian, $G_+(\tilde{k}, n)$ has dimension $\tilde{k}(n - \tilde{k})$. Pretty much like a polyhedron with faces, edges and vertices, then, we can consider its subspaces of various dimensions, generically called *cells*. Lower dimensional cells can be understood as *boundaries* of higher-dimensional ones and the collection of all cells constitutes the so-called *positroid stratification* of the positive Grassmannian.

Every cell of $G_+(\tilde{k}, n)$ can be labelled by a permutation σ of the symmetric group S_n and can be parametrised by a set of canonical coordinates β_i , real and positive. The astounding fact is that the same cell can be precisely associated to the reduced on-shell diagram labelled by the same permutation and a subset of its edge variables will be canonical coordinates on that cell!¹¹ In particular, the top-dimensional cell of $G_+(\tilde{k}, n)$ – *top cell* for short – is matched to the cyclic decorated permutation

$$\sigma_{n,\tilde{k}}^{\text{top}} = \{1 + \tilde{k}, 2 + \tilde{k}, \dots, n + \tilde{k}\} = \{1, 2, \dots, n\} + \tilde{k}. \quad (2.150)$$

¹¹One has to fix the $\text{GL}(1, \mathbb{C})$ redundancies at the vertices and it is possible to do so in such a way that the positivity of the leftover edge variables implies the positivity of the matrix $\tilde{C}(\{\alpha_e\})$.

To the latter is in turn associated an on-shell graph evaluating to the Grassmannian integral $\mathcal{L}_{n,\tilde{k}}^{(\text{ACCK})}$. Figure 2.23 is an example of this.

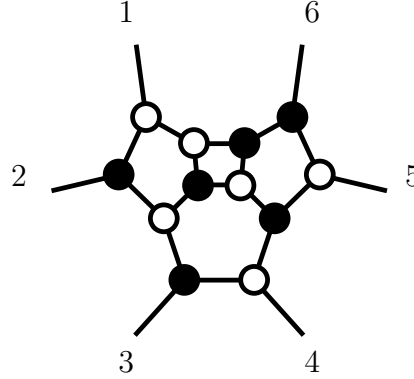


Figure 2.23: The reduced on-shell graph corresponding to the top-cell permutation $\sigma_{6,3}^{\text{top}} = \{4, 5, 6, 7, 8, 9\}$, evaluating to the Grassmannian integral (2.130).

Boundaries of the top cell are reached as one of its canonical coordinates approaches zero: diagrammatically this amounts to removing an edge from the on-shell graph, whereas on the level of the on-shell form one has to take the residue at some $\alpha_\star \rightarrow 0$. Some technicalities are involved here, such as the notion of removability of an edge (since it is not guaranteed that removing an edge from a reduced graph will yield another reduced graph) and we will not attempt to discuss them: suffice it to say that the authors of [50] have argued that all boundaries of a given cell of $G_+(\tilde{k}, n)$ can be reached in this way, provided one adopts the BCFW bridge construction to parametrise it.

In closing, let us remark that the on-shell diagram formalism discussed in the present section has been originally developed for spinor-helicity or spacetime twistor variables. However, an analogous one has been proposed in [110]: the authors presented momentum twistors on-shell diagrams, associated to cells of a positive Grassmannian $G_+(k, n)$.¹²

¹²Notice that the first argument is really the k of $N^k\text{MHV}$ here. From now on, we will stick to k throughout.

Chapter 3

The Amplituhedron proposal

We devoted Chapter 2 to the description of a number of tools that were developed to more efficiently compute scattering amplitudes in $\mathcal{N} = 4$ SYM theory. In particular, the BCFW recursion relations exploit the fact that tree-level amplitudes are fully determined by their analytic properties, *i.e.* the structure of their singularities. We could also understand them within the framework of Grassmannian integrals and on-shell diagrams, bearing unexpected connections to combinatorics and the geometry of positive Grassmannians. The unsatisfactory aspect of this reformulation is that its central players are individual on-shell processes rather than amplitudes. Despite all of them being meaningful quantities – well understood from the point of view of the positroid stratification – some external input is still needed to understand how they should be combined to yield the final result. Such input is the requirement that the amplitudes be free from non-local poles and have correct factorisation properties, as implied by the on-shell recursions. We would like instead to have a more natural understanding of why only some combinations of on-shell processes should represent the quantities we are after and how physical properties of scattering amplitudes as locality and unitarity emerge, rather than being postulated from the start. This will lead us to the *amplituhedron* idea.

In the famous paper [42] that inaugurated the use of momentum twistors for studying scattering amplitudes, Hodges observed that an NMHV amplitude can be interpreted as the volume of a polytope in a *dual* momentum twistor space. The various terms coming from *e.g.* BCFW recursion relations correspond to a particular triangulation of the polytope: reassembling them, spurious singularities cancel as they correspond to boundaries not of the full object, but just of some of the pieces in which it got partitioned. Therefore the idea arose that *all* scattering amplitude can be viewed in such a purely geometric fashion,

as volumes of “some region of some space”, in a sense to be made precise. Coming up with a sharp proposal has proven highly non-trivial, until Arkani-Hamed and Trnka presented a couple of papers [52, 53] initiating this new line of exploration. The amplituhedron construction is specific to planar $\mathcal{N} = 4$ SYM and to date – despite much progress – only some circumstantial evidence has been presented with regards to an extension to the non-planar sector [111]; no analogue for other theories is known.

In this chapter we will largely base our presentation on the original amplituhedron paper, motivating its definition both at tree-level and at loop-level. We will explain how to compute scattering amplitudes in this framework and discuss towards the end some unpublished work [55].

3.1 Positive geometry in arbitrary dimensions

The central concept that will allow us to come to define the amplituhedron is the idea of *positivity*: in particular, we will see how positive matrices naturally come into play when talking about volumes. Our discussion will start from the analysis of simple geometrical settings, which will pave the way towards the physically relevant ones. Let us denote by $M_+(m, n)$ the space of $m \times n$ positive matrices, *i.e.* those with only positive ordered maximal minors. Since eventually we are going to make contact with kinematic variables such as momentum supertwistors, we will think all the time in terms of projective spaces.

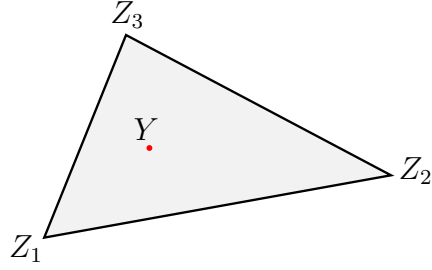
The easiest example one can consider is a triangle $\mathcal{S}^{(2)}$ in a real two-dimensional space, namely \mathbb{RP}^2 . Any point in \mathbb{RP}^2 can be represented as a linear combination of its vertices Z_i^A ($A = 1, 2, 3$),

$$Y^A = c_1 Z_1^A + c_2 Z_2^A + c_3 Z_3^A . \quad (3.1)$$

We are interested in characterising the interior $\mathcal{I}_{\mathcal{S}^{(2)}}$ of $\mathcal{S}^{(2)}$: a moment of reflection tells us that this is parametrised by all the triplets $(c_1, c_2, c_3)/\text{GL}(1, \mathbb{R})$ such that all the ratios c_i/c_j are positive. This is achieved if the c_i are either all negative or all positive: for simplicity we will just talk of positivity of the coefficients and write

$$\mathcal{I}_{\mathcal{S}^{(2)}} = \{Y \in \mathbb{RP}^2 : Y = c_1 Z_1 + c_2 Z_2 + c_3 Z_3, c_1, c_2, c_3 > 0\} . \quad (3.2)$$

It might be useful to note that, given the freedom we have to rescale Y by any factor, this expression is equivalent in particular to that of the center of mass of a system of three point-like objects of masses c_i at positions Z_i .

Figure 3.1: A point inside a triangle in \mathbb{RP}^2 .

This simple construction admits a twofold generalisation. On the one hand, we can observe that a triangle is actually a 2-simplex (hence the name $\mathcal{S}^{(2)}$ we used) and move to higher-dimensional simplices in higher-dimensional spaces; on the other hand, we can discuss generic polygons in two dimensions.

In the first case, let Z_1^A, \dots, Z_n^A define a $(n-1)$ -simplex $\mathcal{S}^{(n-1)}$ in \mathbb{RP}^{n-1} ($A = 1, \dots, n$). Similarly to the above,

$$Y^A = c_1 Z_1^A + \dots + c_n Z_n^A = \sum_i c_i Z_i^A \quad (3.3)$$

is a point inside the simplex if the coefficients of its representation are positive, hence

$$\mathfrak{I}_{\mathcal{S}^{(n-1)}} = \left\{ Y \in \mathbb{RP}^n : Y = \sum_i c_i Z_i, \ c_1, \dots, c_n > 0 \right\}. \quad (3.4)$$

Now, once again we are free to rescale the coefficients of the linear combination of the Z_i by an arbitrary factor. We can thus think of the n -tuple (c_1, \dots, c_n) projectively, *i.e.* as an element of the Grassmannian $G(1, n) = \mathbb{RP}^{n-1}$. Furthermore, the additional positivity requirement restricts it to the positive part of this space, namely the positive Grassmannian $G_+(1, n)$.

When considering a n -gon $\mathcal{P}_n^{(2)}$ in \mathbb{RP}^2 with vertices Z_1^A, \dots, Z_n^A ($A = 1, 2, 3$), one has to make sure that a well defined notion of interior exists. This is the case only if the polygon is *convex*: it turns out that this corresponds to a positivity constraint on the matrix Z whose columns are the vertices Z_i : we demand that

$$Z = \begin{pmatrix} Z_1 & \dots & Z_n \\ \downarrow & \dots & \downarrow \end{pmatrix} \in M_+(3, n), \quad (3.5)$$

or – otherwise said – that $\langle i_1 i_2 i_3 \rangle = \langle Z_{i_1} Z_{i_2} Z_{i_3} \rangle > 0$ for all $i_1 < i_2 < i_3$. After defining the amplituhedron we will provide another reason for this positivity requirement.

Observe that there is no real difference between the two-dimensional and a generic m -dimensional space: also when working in \mathbb{RP}^m , we have to require the positivity of the matrix Z of vertices, and the interior of a polytope $\mathcal{P}_n^{(m)}$ will be described by

$$\mathfrak{I}_{\mathcal{P}_n^{(m)}} = \left\{ Y \in \mathbb{RP}^m : Y = \sum_i c_i Z_i, \begin{array}{l} (c_1 \dots c_n) \in G_+(1, n) \\ (Z_1 \dots Z_n) \in M_+(1+m, n) \end{array} \right\}. \quad (3.6)$$

Knowing how to characterise the inside of a region of projective space, we can introduce a well-defined – *i.e.* projective – notion of volume (or even area, in two dimensions). We talk about a *volume form*, an m -form defined by the requirement of having only *logarithmic singularities* on the boundaries of our space. This last requirement means that, when approaching any boundary, the form must behave as $dx/x = d \log x$ in terms of some local coordinate. Let us once again start illustrating this concept from the triangle example. Looking at the parametrisation (3.2), it is clear that boundaries of the space are reached as $c_i \rightarrow 0$. Since we are working in \mathbb{RP}^2 , however, we are free to write $Y = Z_1 + c_2 Z_2 + c_3 Z_3$, for instance. Then the volume form we are after reads

$$\Omega_{\mathcal{S}^{(2)}} = \frac{dc_2}{c_2} \wedge \frac{dc_3}{c_3}, \quad (3.7)$$

which can be rewritten as

$$\Omega_{\mathcal{S}^{(2)}}(Y, Z_1, Z_2, Z_3) = \frac{1}{2} \frac{\langle 123 \rangle^2}{\langle Y12 \rangle \langle Y23 \rangle \langle Y31 \rangle} \langle Y d^2 Y \rangle, \quad (3.8)$$

as can be quickly checked, since

$$\begin{aligned} \langle Y12 \rangle &= \langle 123 \rangle c_3, \quad \langle Y23 \rangle = \langle 123 \rangle, \quad \langle Y31 \rangle = \langle 123 \rangle c_2, \\ \langle Y d^2 Y \rangle &= \epsilon_{ABC} Y^A dY^B \wedge dY^C = 2 \langle 123 \rangle dc_2 \wedge dc_3. \end{aligned} \quad (3.9)$$

In the rest of this section we will leave sometimes the dependence of the volume form on Y understood. Moving to an arbitrary convex polygon $\mathcal{P}_n^{(2)}$ in the projective plane, the most natural thing to do is to construct a triangulation $\mathcal{T} = \{\Gamma\}$, and obtain $\Omega_{\mathcal{P}_n^{(2)}}$ as the sum of the triangle volume forms calculating the area of each cell:

$$\Omega_{\mathcal{P}_n^{(2)}}(Z_1, \dots, Z_n) = \sum_{\Gamma} \Omega_{\mathcal{S}^{(2)}}^{\Gamma}(Z_a, Z_b, Z_c). \quad (3.10)$$

Consider a concrete example, *e.g.* a pentagon as the one shown in Figure 3.2: we can employ two different kinds of triangulations of $\mathcal{P}_5^{(2)}$, so-called *internal* and *external* trian-

gulations. Based on them, the volume form can be written as

$$\begin{aligned}
 \Omega_{\mathcal{P}_5^{(2)}}(Z_1, \dots, Z_5) &= \Omega_{\mathcal{S}^{(2)}}(Z_1, Z_2, Z_5) + \Omega_{\mathcal{S}^{(2)}}(Z_2, Z_3, Z_5) + \Omega_{\mathcal{S}^{(2)}}(Z_3, Z_4, Z_5) \\
 &= \Omega_{\mathcal{S}^{(2)}}(Z_\star, Z_1, Z_2) + \Omega_{\mathcal{S}^{(2)}}(Z_\star, Z_2, Z_3) + \Omega_{\mathcal{S}^{(2)}}(Z_\star, Z_3, Z_4) + \\
 &\quad + \Omega_{\mathcal{S}^{(2)}}(Z_\star, Z_4, Z_5) + \Omega_{\mathcal{S}^{(2)}}(Z_\star, Z_5, Z_1)
 \end{aligned} \tag{3.11}$$

Of course we could make several alternative choices for the “pivoting” point of the tri-

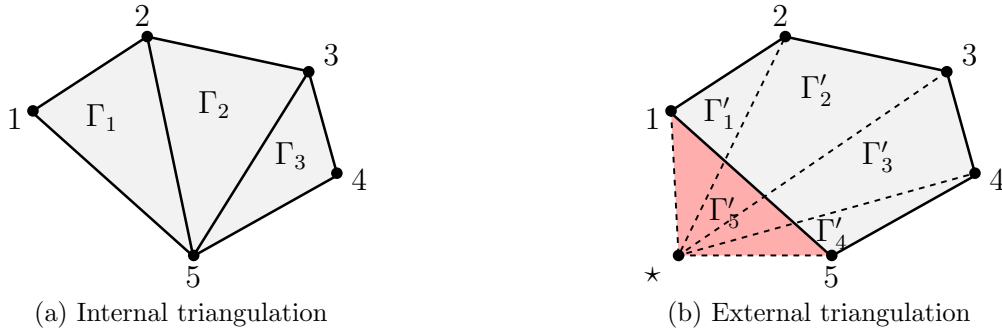


Figure 3.2: A natural way to evaluate the volume form for a polygon is by triangulating it. This can be done in several equivalent ways: in particular, external triangulations require using a point outside $\mathcal{P}_n^{(2)}$. The red-shaded area comes with a negative sign as a result of a flip in the orientation of the triangle contributing to $\Omega_{\mathcal{S}^{(2)}}(Z_\star, Z_5, Z_1)$.

angulation (Z_5 or Z_\star in the previous examples), yielding exactly the same result. An important remark is that – no matter how we triangulate the polygon – we will introduce some spurious singularities, which correctly cancel in the sum. With reference to (3.11), for instance, it is clear that the partial sum $\Omega_{\mathcal{S}^{(2)}}(Z_1, Z_2, Z_5) + \Omega_{\mathcal{S}^{(2)}}(Z_2, Z_3, Z_5)$ already gets rid of the singularity along the (Z_2, Z_5) diagonal, whereas the one along the (Z_3, Z_5) survives until we add the volume form associated to the triangle (Z_3, Z_4, Z_5) .

The reason why it makes sense to call Ω a volume form is that it indeeds computes a volume (or rather an area, in this case), albeit in a dual space. Let us focus as usual on the triangle, the generalisation to higher-dimensional simplices is straightforward (not so for arbitrary polytopes). Given the triangle of vertices Z_1, Z_2, Z_3 , we can consider a map to a dual copy of \mathbb{RP}^2 , such that points are sent to lines and viceversa, see Figure 3.3. Let W_a be dual to the line (Z_1, Z_2) , W_b to the line (Z_2, Z_3) and W_c to the line (Z_3, Z_1) ; conversely, Z_1 will be the preimage of the line (W_c, W_a) , Z_2 of (W_a, W_b) , Z_3 of (W_b, W_c) . In formulae, these relations are described by a set of incidence relations of the form

$$Z_1^A W_{aA} = 0, \quad Z_2^A W_{aA} = 0, \quad Z_1^A W_{cA} = 0 \tag{3.12}$$

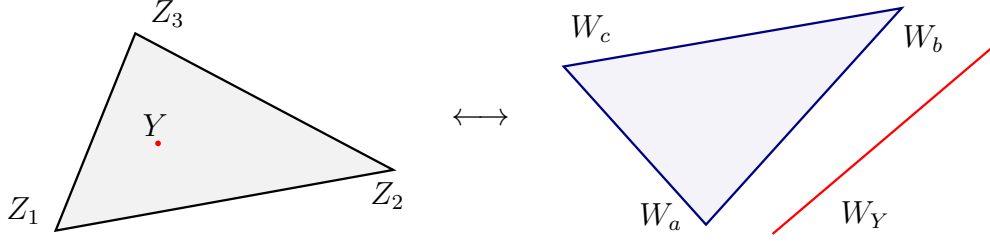


Figure 3.3: Mapping a triangle to its dual.

and so on. From these we deduce that

$$W_{aA} = \epsilon_{ABC} Z_1^B Z_2^C, \quad Z_1^A = \epsilon^{ABC} W_{cB} W_{aC}, \quad (3.13)$$

as well as the analogous cyclic relations. Now, it is not hard to convince oneself – by means of a kind of external triangulation – that the area of the triangle of vertices W_a, W_b, W_c (fixing w.l.o.g. their third component to 1) in dual space is given by

$$A(W_a, W_b, W_c) = \frac{1}{2} \begin{vmatrix} W_{a1} & W_{b1} & W_{c1} \\ W_{a2} & W_{b2} & W_{c2} \\ 1 & 1 & 1 \end{vmatrix}, \quad (3.14)$$

which can be rewritten in a more useful fashion as

$$A(W_a, W_b, W_c) = \frac{1}{2} \frac{\langle W_a W_b W_c \rangle}{(W_0 \cdot W_a)(W_0 \cdot W_b)(W_0 \cdot W_c)}. \quad (3.15)$$

Here $W_0^A = (0 \ 0 \ 1)^\top$ is a reference vector: while the denominator factors in (3.15) look unnecessary in light of our choice to set $W_{i3} = 1$, introducing them makes the whole expression invariant under rescalings and therefore a projectively sound quantity. Observing that

$$\langle W_a W_b W_c \rangle = \langle 123 \rangle^2, \quad W_0 \cdot W_a = \langle W_0 12 \rangle, \quad W_0 \cdot W_b = \langle W_0 23 \rangle, \quad W_0 \cdot W_c = \langle W_0 31 \rangle, \quad (3.16)$$

we see at once that

$$A(W_a, W_b, W_c) = \frac{\langle 123 \rangle^2}{\langle Y 12 \rangle \langle Y 23 \rangle \langle Y 31 \rangle}, \quad (3.17)$$

in the limit $Y \rightarrow Y^* = W_0$, *i.e.* the volume form $\Omega_{S^{(2)}}(Z_1, Z_2, Z_3)$ up to the factor $\langle Y d^2 Y \rangle$ involving the differentials. We will write in general

$$\Omega_{S^{(2)}}(Y, Z_1, Z_2, Z_3) = \Omega_{S^{(2)}}(Y, Z_1, Z_2, Z_3) \langle Y d^2 Y \rangle \quad (3.18)$$

and call $\Omega_{\mathcal{S}(2)}$ the *volume function*. The bottom line of this discussion is that the volume function computes an actual volume (area) in the dual space, in the limit $Y \rightarrow Y^*$. For a simplex in \mathbb{RP}^m , the analogous formula reads

$$\Omega_{\mathcal{S}(m)}(Y, Z_1, \dots, Z_{m+1}) = \frac{1}{m!} \frac{\langle 1 \dots m+1 \rangle^m}{\langle Y 1 \dots m \rangle \dots \langle Y m+1 \dots m-1 \rangle} \langle Y d^m Y \rangle. \quad (3.19)$$

In the next section we will argue that the volume functions $\Omega(Y, Z)$, computing actual volumes in dual space, can be interpreted as scattering amplitudes; when expressed as sums of volume functions of simplices, as in (3.2), the individual summands correspond to R-invariants.

3.2 Tree amplituhedron and scattering amplitudes

This geometric story so far seems to bear little to no connection to scattering amplitudes. However, before we can establish a precise correspondence, we need to fit into this framework a further parameter k , which will eventually be interpreted as the MHV degree of an amplitude: this generalisation will take us away from what can be visualised and will affect both the Z and the C matrices. The vertices of the generalised polytopes will be called *external data* and they will still be organised in columns of Z , but this time we will have $Z \in M_+(m+k, n)$. Most importantly, the row vector $C = (c_1 \dots c_n) \in G_+(1, n)$ (positive projective space) will be promoted to an element of a fully fledged Grassmannian, namely $G_+(k, n)$. Clearly this operation is non-trivial, as it does not amount to just stacking k copies of the same space on top of each other, because the positivity conditions in the two cases are really different!

Drawing from the definition (3.6) of $\mathfrak{J}_{\mathcal{P}_n^{(m)}}$, the *tree-level amplituhedron* (or *tree amplituhedron* for short) is defined as the space

$$\mathfrak{A}_{n,k;m}^{\text{tree}}[Z] = \left\{ Y \in G(k, m+k) : Y = C \cdot Z, \begin{array}{l} C \in G_+(k, n) \\ Z \in M_+(m+k, n) \end{array} \right\}, \quad (3.20)$$

where the k -plane Y is spanned by the vectors Y_α and $Y = C \cdot Z$ is shorthand for

$$Y_\alpha^A = \sum_i c_{\alpha i} Z_i^A. \quad (3.21)$$

Therefore the tree amplituhedron is a subspace of the (ordinary) Grassmannian $G(k, m+k)$ determined by positive linear combination of positive external data. One can think of it as

being the image of the map $\mu_Z : G_+(k, n) \rightarrow G(k, m+k)$ through the external data Z [112] and this point of view sheds more light on why the amplituhedron is desirable at all. Indeed, the cells of $G_+(k, n)$ corresponding to the various BCFW terms building up the amplitude have dimension $m \cdot k$, (significantly) lower than that of the full positive Grassmannian, namely $k(n-k)$. Beside depending on the choice of legs on which to base the recursion – and therefore lacking an intrinsic meaning – they also do not fit together very naturally and the cancellation of spurious singularities appears somewhat magical and geometrically unclear. The projection to the smaller Grassmannian, having precisely the dimension of the BCFW cells, recombines the various pieces, eliminating the redundancies and relating spurious poles to spurious boundaries. In particular, the positivity requirement on Z is a sufficient condition to ensure that Y has full rank [113].

There is a non-trivial constraint on the number of dimensions m to be taken into account: it has to be an even number, otherwise the definition of $\mathfrak{A}_{n,k;m}^{\text{tree}}$ is not cyclic under the following twisted action on the columns of C and Z :

$$\begin{aligned} \hat{c}_1 &\rightarrow \hat{c}_2, \hat{c}_2 \rightarrow \hat{c}_3, \dots, \hat{c}_n \rightarrow (-1)^{k-1} \hat{c}_1, \\ Z_1 &\rightarrow Z_2, Z_2 \rightarrow Z_3, \dots, Z_n \rightarrow (-1)^{m+k-1} Z_1. \end{aligned} \quad (3.22)$$

The above transformation preserves the positivity of C and Z and clearly leaves the product (3.21) invariant. This proves to be a necessary condition to eventually obtain cyclically invariant amplitudes, as we want. As will be discussed in a while, $m=4$ is the physically relevant value of the parameter; nevertheless, the $m=2$ amplituhedron is a useful toy model and will appear prominently in later parts of this work.

An important remark is in order, concerning the role of positivity in identifying the boundaries of the amplituhedron. It is not difficult to convince oneself that the relevant quantities to look at are the brackets $\langle Y i_1 \dots i_m \rangle = \langle Y_1 \dots Y_k i_1 \dots i_m \rangle$, with $i_1 < \dots < i_m$. Their vanishing is to be interpreted as a (generalised) coplanarity condition among the points $Y, Z_{i_1}, \dots, Z_{i_m}$. Let us look at the two-dimensional polygon case first, where $\langle Y Z_i Z_j \rangle = 0$ means that Y is collinear with Z_i and Z_j : depending on which side of the line (Z_i, Z_j) Y is on, the bracket can take either sign. The boundaries of the polygon are those lines for which it has always definite sign and it is immediate to check that

$$\langle Y Z_i Z_j \rangle = \sum_a c_a \langle Z_a Z_i Z_j \rangle > 0 \quad \longleftrightarrow \quad j = i+1. \quad (3.23)$$

Hence from the positivity of C and Z we learn that the boundaries of the polygon are precisely the lines (Z_i, Z_{i+1}) . Moving on to the four-dimensional case (keeping $k=1$), we

can repeat the exercise and find

$$\langle Y Z_i Z_j Z_k Z_l \rangle = \sum_a c_a \langle Z_a Z_i Z_j Z_k Z_l \rangle > 0 \quad \longleftrightarrow \quad j = i + 1, l = k + 1. \quad (3.24)$$

It will be worth looking back at the form of these boundaries after having computed the NMHV volume form: it will then be clear how these correspond to the physical poles of the corresponding amplitude, a fact that can be rephrased saying that locality properties are *emergent* from the positive geometry! In full generality, boundaries of the tree amplituhedron are given by

$$\begin{aligned} \langle Y Z_i Z_j Z_k Z_l \rangle &= \sum_{a_1, \dots, a_k} c_{1a_1} \cdots c_{ka_k} \langle Z_{a_1} \cdots Z_{a_k} Z_i Z_j Z_k Z_l \rangle = \\ &= \sum_{a_1 < \dots < a_k} (c_{a_1}, \dots, c_{a_k}) \langle Z_{a_1} \cdots Z_{a_k} Z_i Z_j Z_k Z_l \rangle, \end{aligned} \quad (3.25)$$

which, just as before, has positive sign inside the whole amplituhedron if and only if $(Z_i, Z_j, Z_k, Z_l) = (Z_i, Z_{i+1}, Z_j, Z_{j+1})$, which are therefore the boundaries.

Unitarity is encoded in the amplituhedron in a subtler way. Suppose to be looking at the boundary where $\langle Y Z_i Z_{i+1} Z_j Z_{j+1} \rangle \rightarrow 0$, which means that some Y_α is a linear combination of $Z_i, Z_{i+1}, Z_j, Z_{j+1}$. Then the α -th row of C will have zeroes everywhere but in positions $i, i+1, j, j+1$. As a consequence of positivity, the whole matrix will then split in a left and a right block, involving k_L and k_R rows respectively, such that $k_L + k_R = k - 1$, in every possible way: the first block stretches from the i -th to the $(j+1)$ -th column, the second from the j -th to the $(i+1)$ -th, wrapping around. Summarising, C will look as follows:

$$C = \begin{pmatrix} & i & i+1 & & j & j+1 & & \\ \begin{matrix} 0 & \cdots & 0 \\ 0 & \cdots & 0 \\ 0 & \cdots & 0 \end{matrix} & \begin{matrix} \updownarrow k_L \\ \text{L} \end{matrix} & \begin{matrix} 0 & 0 & \cdots & 0 \\ 0 & 0 & \cdots & 0 \\ 0 & 0 & \cdots & 0 \end{matrix} & \\ \begin{matrix} 0 & \cdots & 0 & \star & \star & 0 & \cdots & 0 \end{matrix} & \begin{matrix} \star & \star & 0 & 0 & \cdots & 0 \end{matrix} & & \\ \begin{matrix} \text{ } & \text{ } & \text{ } & \text{ } & \text{ } & \text{ } & \text{ } & \text{ } \end{matrix} & \begin{matrix} 0 & \cdots & 0 \\ 0 & \cdots & 0 \\ 0 & \cdots & 0 \end{matrix} & \begin{matrix} \updownarrow k_R \\ \text{R} \end{matrix} & \end{pmatrix} \quad \alpha\text{-th row} \quad .$$

Such splitting at the boundary $\langle Y Z_i Z_{i+1} Z_j Z_{j+1} \rangle \rightarrow 0$ can be interpreted as a splitting of the amplituhedron $\mathfrak{A}_{n,k;4}^{\text{tree}}$ into two smaller amplituhedra $\mathfrak{A}_{n_L, k_L;4}^{\text{tree}}$ and $\mathfrak{A}_{n_R, k_R;4}^{\text{tree}}$ reflecting the expected factorisation properties.

The amplituhedron is a subspace of an $(m \cdot k)$ -dimensional Grassmannian, therefore the associated volume form will be an $(m \cdot k)$ -form. Again, to construct it we can triangulate $\mathfrak{A}_{n,k;m}^{\text{tree}}$: by this we mean identifying a set of $(m \cdot k)$ -dimensional cells of $G_+(k, n)$ such that the corresponding regions on the tree amplituhedron are non-overlapping and cover it completely. This is a complicated problem, not solved in general, as a drawback of the genuinely complicated geometry of the amplituhedron. However, assuming to have constructed a triangulation $\mathcal{T} = \{\Gamma\}$ of $\mathfrak{A}_{n,k;m}^{\text{tree}}$, we have

$$\Omega_{n,k}^{(m)}(Y, Z) = \sum_{\Gamma \in \mathcal{T}} \Omega_{n,k}^{(m)\Gamma}(Y, Z) . \quad (3.26)$$

On each cell Γ of \mathcal{T} – parametrised by the real, positive, local coordinates $(\beta_1^\Gamma, \dots, \beta_{m \cdot k}^\Gamma)$ – the volume form is

$$\Omega_{n,k}^{(m)\Gamma} = \frac{d\beta_1^\Gamma}{\beta_1^\Gamma} \wedge \dots \wedge \frac{d\beta_{m \cdot k}^\Gamma}{\beta_{m \cdot k}^\Gamma} , \quad (3.27)$$

in complete analogy with the previous simpler examples, manifestly showing logarithmic singularities at the boundaries of the cell. The dependence on Y 's and Z 's comes from solving the amplituhedron constraint (3.21) in terms of the $c_{\alpha i}$, which in turn are functions of the β_i^Γ . Some partial results in determining $\Omega_{n,k}^{(m)}$ without resorting to any kind of triangulation are available: a first method [114] fixes its form imposing regularity *outside* the amplituhedron, at the intersections of boundaries; an alternative strategy was presented in [54] for the $k = 1$ case and will be explained in detail in Chapter 4.

At the beginning of the chapter, we advertised the central guiding idea of interpreting a generic scattering amplitude as the volume of some space, the amplituhedron. Schematically,

$$\mathcal{A}_{n,k} \text{ “} \sim \text{” } \int_{\mathfrak{A}_{n,k;m}^{\text{tree}}} \Omega_{n,k}^{(m)} , \quad (3.28)$$

but this statement – although suggestive – needs to be made more precise. Firstly, as discussed in the simple triangle setting, we should really be talking about the volume of a *dual* amplituhedron, not simply of that defined in (3.20), and that amounts to evaluating the volume function $\Omega_{n,k}^{(m)}$. Secondly, the left hand side needs some care: we cannot literally be talking about the full amplitude, since the tree amplituhedron for $k = 0$ is not even defined, and indeed the LHS should rather be understood as $\mathcal{P}_{n,k} = \mathcal{P}_n^{\text{N}^k \text{MHV}}$. More importantly, though, we need to explain how superamplitudes can be computed within a purely bosonic framework. Describing how to match volume forms and superamplitudes, we will give an interpretation to the parameter m and explain how the kinematics appears in the geometric picture.

We start by observing that the vectors Y_α and Z_i are $(m+k)$ -component objects, hence the physics they describe is invariant under $\mathrm{GL}(m+k, \mathbb{R})$ transformations. In particular, a linear transformation exists mapping Y to a convenient reference k -plane $Y^* \in G(k, m+k)$ of the form

$$Y^* = \begin{pmatrix} 0_{m \times k} \\ \mathbb{1}_{k \times k} \end{pmatrix}. \quad (3.29)$$

This choice breaks the $\mathrm{GL}(m+k, \mathbb{R})$ symmetry of the projective space to a smaller $\mathrm{GL}(m, \mathbb{R})$. We can now decompose the vectors Z_i as the sum of their projections onto Y^* and its m -dimensional orthogonal complement. The latter will receive the interpretation of momentum twistors, whereas the former will give rise to the fermionic degrees of freedom of \mathcal{Z}_i : for this reason the physical value of m is 4 and we refer to the Z_i as *bosonised momentum twistors*. According to the standard choice (3.29) for Y^* , we have $(Z_i^1, Z_i^2, Z_i^3, Z_i^4)^\top = z_i$ (the bosonic components λ_i, μ_i of momentum supertwistors, see (2.62)); on the other hand, it is not possible to directly identify the four fermionic components χ_i among those of their bosonised counterpart, since the Z_i are real vectors and moreover their length crucially depends on k . The solution consists in regarding the last k components of the bosonised momentum twistors as composite Grassmann variables: after introducing k auxiliary fermionic variables $\phi_{\alpha A}$, we let

$$Z_i^{4+\alpha} = \phi_{\alpha A} \chi_i^A \quad , \quad \begin{array}{l} \alpha = 1, \dots, k \\ A = 1, 2, 3, 4 \end{array} \quad (3.30)$$

i.e. the $\phi_{\alpha A}$ bosonise the fermionic part of the supertwistor. To summarize, we defined

$$Z_i^A = \begin{pmatrix} \lambda_i^\alpha \\ \mu_i^{\dot{\alpha}} \\ \phi_1 \cdot \chi_i \\ \vdots \\ \phi_k \cdot \chi_i \end{pmatrix}. \quad (3.31)$$

The scattering amplitude is now computed by localising the volume form to the reference plane Y^* of (3.29) and subsequently integrating out the auxiliary Grassmann-odd degrees of freedom

$$\frac{\mathcal{A}_{n,k}^{\mathrm{tree}}(\mathcal{Z})}{\mathcal{A}_{n,0}^{\mathrm{tree}}(\mathcal{Z})} = \int d^4\phi_1 \cdots d^4\phi_k \int \delta^{4k}(Y; Y^*) \Omega_{n,k}^{(4)}(Y, Z). \quad (3.32)$$

The expression features a projective δ -function, which will be spelled out shortly, whose presence renders the inner integrations actually trivial. Indeed, a $4k$ -form on the Grassmannian $G(k, 4+k)$ can be written in full generality as

$$\begin{aligned}\Omega_{n,k}^{(4)}(Y, Z) &= \langle Y_1 \cdots Y_k d^4 Y_1 \rangle \cdots \langle Y_1 \cdots Y_k d^4 Y_k \rangle \Omega_{n,k}(Y, Z)^{(4)} = \\ &= \prod_{\alpha=1}^k \langle Y_1 \cdots Y_k d^4 Y_\alpha \rangle \Omega_{n,k}^{(4)}(Y, Z),\end{aligned}\quad (3.33)$$

where $\Omega_{n,k}^{(4)}$ is the volume function evaluating the volume of the dual amplituhedron, whatever this space might be. The explicit expression of the constraints localising Y to Y^* is instead

$$\delta^{4k}(Y; Y^*) = \int d^{k \times k} \rho_\alpha^\beta (\det \rho)^4 \delta^{k \times (4+k)} (Y_\alpha^A - \rho_\alpha^\beta Y_\beta^{*A}), \quad (3.34)$$

allowing us to rewrite (3.32) as

$$\frac{\mathcal{A}_{n,k}^{\text{tree}}(\mathcal{Z})}{\mathcal{A}_{n,0}^{\text{tree}}(\mathcal{Z})} = \int d^4 \phi_1 \cdots d^4 \phi_k \Omega_{n,k}^{(4)}(Y^*, Z). \quad (3.35)$$

Let us present an example to illustrate the prescription presented above. We will consider a contribution to the volume function $\Omega_{6,1}^{(4)}$, relevant for the six-point NMHV superamplitude. It reads

$$R(Y, Z_1, Z_2, Z_4, Z_5, Z_6) = \frac{\langle 12456 \rangle^4}{\langle Y1245 \rangle \langle Y1246 \rangle \langle Y1256 \rangle \langle Y1456 \rangle \langle Y2456 \rangle},$$

where the RHS is denoted R because – as will be discussed in Section 3.4 – it arises as a residue and also because it is a bosonised R -invariant, as we now show. Its expression features invariant combinations of bosonised momentum twistors, as usual denoted by angle brackets:

$$\langle i_1 i_2 i_3 i_4 i_5 \rangle = \epsilon_{ABCDE} Z_{i_1}^A Z_{i_2}^B Z_{i_3}^C Z_{i_4}^D Z_{i_5}^E \quad (3.36)$$

and in general we can have

$$\langle i_1 \dots i_{m+k} \rangle = \epsilon_{A_1 \dots A_{m+k}} Z_{i_1}^{A_1} \cdots Z_{i_{m+k}}^{A_{m+k}}. \quad (3.37)$$

Let us make the structure of the 5-brackets in $R(Y, Z_1, Z_2, Z_4, Z_5, Z_6)$ more explicit. We have (employing the shorthand $Z_{ijkl}^{ABCD} = Z_i^A Z_j^B Z_k^C Z_l^D$)

$$\begin{aligned}\langle 12456 \rangle &= \epsilon_{ABCDE} Z_1^A Z_2^B Z_4^C Z_5^D Z_6^E = \\ &= \epsilon_{ABCD5} Z_{1245}^{ABCD} Z_6^5 - \epsilon_{ABCE5} Z_{1246}^{ABCE} Z_5^5 + \epsilon_{ABDE5} Z_{1256}^{ABDE} Z_4^5 + \\ &\quad - \epsilon_{ACDE5} Z_{1456}^{ACDE} Z_2^5 + \epsilon_{BCDE5} Z_{2456}^{BCDE} Z_1^5 = \\ &= \phi_A (\langle 1245 \rangle \chi_6^A + \langle 6124 \rangle \chi_5^A + \langle 5612 \rangle \chi_4^A + \langle 4561 \rangle \chi_2^A + \langle 2456 \rangle \chi_1^A)\end{aligned}\quad (3.38)$$

One can observe that any power of a 5-bracket higher than 4 is bound to vanish: indeed, it would contain too many auxiliary ϕ^A , so that at least two would carry the same $SU(4)$ index. Moreover, for $Y \rightarrow Y^*$ we get

$$\langle Y1245 \rangle \rightarrow \langle 1245 \rangle, \quad \langle Y1246 \rangle \rightarrow \langle 1246 \rangle, \quad \text{and so on.} \quad (3.39)$$

Therefore we obtain

$$\begin{aligned} \mathcal{R}(\mathcal{Z}_1, \mathcal{Z}_2, \mathcal{Z}_4, \mathcal{Z}_5, \mathcal{Z}_6) &= \int d^4\phi \, R(Y^*, Z_1, Z_2, Z_4, Z_5, Z_6) = \\ &= \frac{\delta^{0|4}(\langle 1245 \rangle \chi_6^A + \text{cyclic permutations})}{\langle 1245 \rangle \langle 2456 \rangle \langle 4561 \rangle \langle 5612 \rangle \langle 6124 \rangle} = R_{625} \end{aligned} \quad (3.40)$$

an R-invariant (see (2.108)).

For future convenience, let us introduce the notation

$$[i_1 \cdots i_{m+k}] = \frac{\langle i_1 \cdots i_{m+k} \rangle^m}{\langle Y_1 \cdots Y_k i_1 \cdots i_m \rangle \langle Y_1 \cdots Y_k i_2 \cdots i_{m+1} \rangle \cdots \langle Y_1 \cdots Y_k i_{m+k} \cdots i_{m-1} \rangle}. \quad (3.41)$$

In particular, when discussing NMHV volume functions, we will be interested in the quantities $[i_1 i_2 i_3]$ and $[i_1 i_2 i_3 i_4 i_5]$ for the toy model $m = 2$ and the physical case $m = 4$ respectively; in the example above, $R(Y, Z_1, Z_2, Z_4, Z_5, Z_6) = [12456]$. In light of the above result, we will be a bit sloppy and refer directly to the quantities $[i_1 \cdots i_{m+1}]$ as R-invariants. The expressions for NMHV volume functions in terms of R-invariants are known [51]:

$$\Omega_{n,1}^{(2)} = \sum_j [\star j j + 1] \quad , \quad \Omega_{n,1}^{(4)} = \sum_{j < k} [\star j j + 1 k k + 1], \quad (3.42)$$

where \star denotes any of the Z_i .

3.3 Loop-level amplituhedron

As discussed at the beginning of Section 2.5, planarity of $\mathcal{N} = 4$ SYM theory allows us to define an object called the integrand $\mathcal{I}_{n,k}^{(\ell)}(p_1, \dots, p_n, l_1, \dots, l_\ell)$ associated to an ℓ -loop, n -point $N^k\text{MHV}$ amplitude, depending on the momenta of the external particles and the loop momenta. Performing the integrations over l_1, \dots, l_ℓ to get to the amplitude $\mathcal{A}_{n,k}^{(\ell)}$ is a whole different business, forcing us to confront infrared divergences, responsible for the complicated analytic structure of the amplitude and the breaking of Yangian invariance. On the contrary, $\mathcal{I}_{n,k}^{(\ell)}$ is just a rational function and in particular it is still a Yangian invariant. In [30] it was discussed how the full integrand $\mathcal{I}_{n,k}^{(\ell)}$ of any planar $\mathcal{N} = 4$ SYM

amplitude $\mathcal{A}_{n,k}^{(\ell)}$ could be computed via a BCFW-like recursion relation, also admitting a representation in terms of on-shell diagrams [50].

The *loop amplituhedron* $\mathfrak{A}_{n,k}^{\ell\text{-loop}}$ is an object computing the loop-level integrand $\mathcal{I}_{n,k}^{(\ell)}$ in the same spirit of what was done for tree amplitudes,¹ but the degrees of freedom of the loop momenta must be accounted for by considering more general spaces than the ones entering the definition (3.20). In particular, let $G_+(k, n; \ell)$ be the space of k -planes C in n dimensions together with ℓ 2-planes $D^{(i)}$ living in the $(n-k)$ -dimensional complement of C , satisfying what are known as *extended positivity conditions*, to be defined in a moment. We chose to denote it as in the original references, however we emphasise from the start that this is not a Grassmannian space. A point in $G_+(k, n; \ell)$ is represented via a $(k+2\ell) \times n$ matrix \mathcal{C} , which can be organised as

$$\mathcal{C} = \begin{pmatrix} \frac{D^{(1)}}{\hline} \\ \vdots \\ \frac{D^{(\ell)}}{\hline} \\ C \end{pmatrix} \quad (3.43)$$

Extended positivity means that, beside C being a positive matrix, all matrices obtained by stacking any number of $D^{(i)}$ on top of C – as long as the resulting matrix has at least as many columns as rows – ought to be positive:

$$C \in G_+(k, n), \quad \begin{pmatrix} D^{(i)} \\ C \end{pmatrix} \in M_+(k+2, n), \quad \begin{pmatrix} D^{(i)} \\ D^{(j)} \\ C \end{pmatrix} \in M_+(k+4, n), \quad \dots, \quad \mathcal{C} \in M_+(k+2\ell, n). \quad (3.44)$$

These peculiar positivity constraints can be seen as the “echo” of standard positivity of a bigger $(k+2\ell) \times (n+2\ell)$ matrix, ℓ pairs of adjacent columns of which have been removed. As argued in [30] the removal (or hiding) of pairs of adjacent external particles from a lower-loop Yangian invariant could yield a higher-loop, lower-point invariant and it is remarkable that this operation (which amounts to take a residue using a particular contour) reflects itself in terms of positivity conditions.

The loop amplituhedron is then the image of $G_+(k, n; \ell)$ through the external data,

¹We decide to work in the physical setting ($m=4$), but everything can be generalised to any even m .

collected as usual in the positive matrix $Z \in M_+(m+k, n)$. We define

$$\mathfrak{A}_{n,k}^{\ell\text{-loop}}[Z] = \left\{ \mathcal{Y} \in G(k, k+4; \ell) : \mathcal{Y} = \mathcal{C} \cdot Z, \begin{array}{l} \mathcal{C} \in G_+(k, n; \ell) \\ Z \in M_+(m+k, n) \end{array} \right\}, \quad (3.45)$$

where \mathcal{Y} lives in the space of k -planes in $k+4$ dimensions, together with ℓ 2-planes $\mathcal{L}^{(\ell)}$ spanning the four-dimensional orthogonal complement to the Y of the tree amplituhedron:

$$\mathcal{Y} = \begin{pmatrix} \overline{\mathcal{L}^{(1)}} \\ \vdots \\ \overline{\mathcal{L}^{(\ell)}} \\ Y \end{pmatrix}, \quad \begin{pmatrix} \mathcal{L}^{(1)} \\ \vdots \\ \mathcal{L}^{(\ell)} \end{pmatrix} = \begin{pmatrix} D^{(1)} \\ \vdots \\ D^{(\ell)} \end{pmatrix} \cdot Z. \quad (3.46)$$

Observe that, coincidentally, $\mathfrak{A}_{n,0}^{1\text{-loop}}$ and $\mathfrak{A}_{n,2;2}^{\text{tree}}$ are formally identical spaces. Hence physical ($m=4$) one-loop MHV integrands are functionally the same as tree-level N^2 MHV volume functions in the toy-model ($m=2$) amplituhedron.

The computation of the integrand proceeds along the same lines as in the tree-level case. We have to determine a volume form behaving correctly in the neighbourhood of any boundary of the loop amplituhedron, localise it sending $Y \rightarrow Y^*$ and finally strip off the auxiliary ϕ_{iA} variables hidden in the bosonised momentum twistors. It goes without saying, however, that the difficulties at loop-level increase considerably, because the geometry of $\mathfrak{A}_{n,k}^{\ell\text{-loop}}$ is way more involved than that of its tree-level counterpart, therefore only special cases have been treated. In particular, MHV integrands are accessible in the framework of the loop amplituhedron: the matrix C is not there, but \mathcal{C} is well defined as a stack of $D^{(i)}$ matrices, fulfilling mutual positivity conditions. This situation is referred to as *pure loop geometry* and it is the only case where extended positivity involves $D^{(i)}$ matrices alone: in particular, it implies that each of them lives in the positive Grassmannian $G_+(2, n)$; moreover, when $n=4$, the only additional constraints are of the form $\det \begin{pmatrix} D^{(i)} \\ D^{(j)} \end{pmatrix} > 0$, for all pairs (i, j) . The positroid stratification of the loop amplituhedron² in this simplified context was thoroughly investigated in [112] and [115], highlighting a rich structure and hints of simplicity. The four-point MHV integrand up to three loops was constructed in [53].

²In this case and generally when $n=4+k$, the matrix Z can be set to the identity via a change of basis, hence the boundary structure of $G_+(k, n; \ell)$ coincides with that of the loop amplituhedron $\mathfrak{A}_{n,k}^{\ell\text{-loop}}$.

3.4 An $i\epsilon$ -prescription for volume functions

An amplituhedron version of the Grassmannian integral (2.124) exists, such that appropriate sums of its residues reconstruct all tree-level volume forms [54, 116]:

$$\Omega_{n,k}^{(m)}(Y, Z) = \int_{\gamma} \frac{d^{k \times n} c_{\alpha i}}{(1, \dots, k)(2, \dots, k+1) \cdots (n, \dots, k-1)} \prod_{\alpha=1}^k \delta^{m+k} \left(Y_{\alpha}^A - \sum_i c_{\alpha i} Z_i^A \right). \quad (3.47)$$

It manifestly shares many features with the integral over the momentum twistors Grassmannian $G_+(k, n)$, up to the different constraint enforced by the Dirac δ -functions, coming from (3.21). In fact, it looks like the all important $1/\text{GL}(k, \mathbb{R})$ factor is missing: however, this issue can be dealt with, regarding (3.47) as a gauge-fixed version of an honest Grassmannian integral over $G(k, k+n)$. For additional details we refer to [117].

It is thus reasonable to ask whether we can find a criterion to identify the residues of the above integral representation adding up to the correct volume function, *i.e.* the amplituhedron version of the BCFW terms arising from (2.124). As in the usual setting, we expect of course quite some freedom in the choice of the contour γ : the different representations of $\Omega_{n,k}^{(m)}$ would be related to one another via residue theorems.

The strategy we pursued [55] was to calculate multiple real integrals, whose singularities had been moved away from the real axis via a carefully introduced $i\epsilon$ -prescription. This would automatically select for us a distinguished (minimal) set of singularities and the residues at these poles would finally yield the desired result. We have full control on the NMHV volume functions, however the method falls short of our expectations starting at N²MHV level, even for $m = 2$: in the remaining part of the chapter we will illustrate where we stand via examples.

3.4.1 A mathematical prelude: multivariate residues

Although we will be carrying out our computations iteratively, *i.e.* integrating one variable after the other, it is worth reviewing the very basics of residues in several complex variables. The advantage of our approach is that it does not require any *a priori* knowledge of the set of residues needed to express a given volume function, but being able to calculate them by other means serves of course as a useful cross-check. Our exposition follows [43], which in turn draws from [104].

Suppose we want to define a notion of residue for the function

$$f(z_1, z_2) = \frac{h(z_1, z_2)}{(\alpha_1 z_1 + \alpha_2 z_2 + \alpha_3)(\beta_1 z_1 + \beta_2 z_2 + \beta_3)} . \quad (3.48)$$

In analogy with single-variable complex analysis, this amounts to identifying a suitable contour for the integral

$$\mathcal{I} = \frac{1}{(2\pi i)^2} \int dz_1 dz_2 f(z_1, z_2) = \frac{1}{(2\pi i)^2} \int \frac{dz_1 dz_2 h(z_1, z_2)}{(\alpha_1 z_1 + \alpha_2 z_2 + \alpha_3)(\beta_1 z_1 + \beta_2 z_2 + \beta_3)} . \quad (3.49)$$

One is led to consider the change of variables

$$u_1 = \alpha_1 z_1 + \alpha_2 z_2 + \alpha_3 \quad , \quad u_2 = \beta_1 z_1 + \beta_2 z_2 + \beta_3 , \quad (3.50)$$

transforming the integral to

$$\mathcal{I} = \frac{1}{(2\pi i)^2} \int \frac{du_1 du_2}{u_1 u_2} \frac{h(z_1(u_{1,2}), z_2(u_{1,2}))}{\det \left(\frac{\partial(u_{1,2})}{\partial(z_{1,2})} \right)} . \quad (3.51)$$

Then it is natural to define $\text{Res } f$ fixing the contour to encircle³ the point $(u_1, u_2) = (0, 0)$. Otherwise said, the integration is to be performed on the torus $\mathbb{T}^2 = \{(u_1, u_2) \in \mathbb{C}^2 : |u_1|, |u_2| = \epsilon\}$, yielding

$$\text{Res } f = \left[\det \left(\frac{\partial(u_{1,2})}{\partial(z_{1,2})} \right) \Big|_{(z_1^*, z_2^*)} \right]^{-1} h(z_1^*, z_2^*) , \quad (3.52)$$

where of course (z_1^*, z_2^*) is the solution to $u_1(z_1, z_2) = u_2(z_1, z_2) = 0$. It is straightforward to repeat this argument for functions of k variables z_1, \dots, z_k , involving an arbitrary number n of denominator factors linear in the z_i , provided $n \geq k$. Let

$$f(z_1, \dots, z_k) = \frac{h(z_1, \dots, z_k)}{F_1(z_1, \dots, z_k) \cdots F_n(z_1, \dots, z_k)} . \quad (3.53)$$

Then each residue of f is calculated as the integral

$$\mathcal{I} = \frac{1}{(2\pi i)^k} \int \frac{dz_1 \cdots dz_k h(z_1, \dots, z_k)}{F_1(z_1, \dots, z_k) \cdots F_n(z_1, \dots, z_k)} \quad (3.54)$$

for a contour encircling the point $z^* = (z_1^*, \dots, z_k^*)$, solution to the system of algebraic equations obtained setting to 0 a specific set of k factors F_i . We denote it as

$$\{i_1 \dots i_k\} = \text{Res}_{F_{i_1, \dots, i_k} = 0} f = \mathcal{J} \Big|_{(z_1^*, \dots, z_k^*)} \frac{h(z_1^*, \dots, z_k^*)}{\prod_{j \neq i_1, \dots, i_k} F_j \Big|_{(z_1^*, \dots, z_k^*)}} , \quad (3.55)$$

³Not really, see below.

where the Jacobian factor is given by

$$\frac{1}{\mathcal{J}} = \det \begin{pmatrix} \partial_{z_1} F_{i_1} & \cdots & \partial_{z_k} F_{i_1} \\ \vdots & \ddots & \vdots \\ \partial_{z_1} F_{i_k} & \cdots & \partial_{z_k} F_{i_k} \end{pmatrix}. \quad (3.56)$$

Observe that the presence of Jacobian determinants makes the order of the labels i_1, \dots, i_k important. Namely, residues taken “in different orders” coincide up to a sign:

$$\{i_{\sigma(1)}, \dots, i_{\sigma(k)}\} = (-1)^{\text{sgn}(\sigma)} \{i_1, \dots, i_k\} \quad (3.57)$$

In the mathematical literature the quantity $\{i_1, \dots, i_k\}$ is also called the (local) residue of the function h w.r.t. the mapping $F = (F_1, \dots, F_n)$ and coincides with the Grothendieck residue symbol [118].

A small remark concerns the notion of “contour encircling some singularity”. To enclose a point in a $2n$ -dimensional space (we are talking about real dimensions here), one needs a $(2n - 1)$ -dimensional contour. This is the case in standard one-variable complex analysis, but not anymore starting from two variables: for instance, the contour chosen for (3.49) is a two-dimensional torus and the problem persists increasing the number of variables. To emphasise this fact, mathematicians talk about *distinguished contours*.

3.4.2 NMHV amplitudes

For NMHV volume functions, we can recast (3.47) into an n -fold real integral introducing an $i\epsilon$ -prescription, first advocated by Arkani-Hamed, see *e.g.* [119] and recently [116]: explicitly,

$$\Omega_{n,1}^{(m)}(Y, Z) = \frac{1}{(-2\pi i)^{n-m-1}} \int_{-\infty}^{+\infty} \prod_{i=1}^n \frac{dc_i}{c_i + i\epsilon_i} \delta^{m+1} \left(Y^A - \sum_i c_i Z_i^A \right). \quad (3.58)$$

We will provide a justification of this formula in Chapter 4. Here we will explain how to deal with integrals such as (3.58) by complexifying the (initially real) integration variables and using Cauchy residue theorem.

The deformations ϵ_i will be taken positive and small: according to the original proposal one should really introduce a $k \times n$ matrix of deformations and demand that it be positive. We will not insist on this subtlety, as it will be largely immaterial for what we are going to discuss and moreover it is still partially unclear; in the following we will employ the shorthand notation $F_i = c_i + i\epsilon_i$.

We found that the integral (3.58) could be correctly evaluated adopting two alternative prescriptions for the deformations:

- the deformations ϵ_i have the same magnitude and are therefore simply denoted by ϵ ;
- the deformations are strongly ordered, *e.g.* $\epsilon_1 \gg \epsilon_2 \gg \dots \gg \epsilon_n > 0$.

We will present both, highlighting their advantages and drawbacks, in the following two subsections. Either way, we will always start by solving the $m + 1$ δ -functions at our disposal to reduce the number of integrations needed to $n - m - 1$. This is done observing that the amplituhedron constraint (3.21) implies many different index-free relations among the c_i , obtained contracting m bosonised momentum twistors:

$$Y^A = \sum_i c_i Z_i^A \longrightarrow \langle Y j_1 \dots j_m \rangle = \sum_i \langle i j_1 \dots j_m \rangle c_i \quad , \quad j_1, \dots, j_m \in \{1, \dots, n\} . \quad (3.59)$$

Choosing an appropriate subset of the equations (3.59), it is always possible to solve for $c_{n-m}, c_{n-m+1}, \dots, c_n$ in terms of $c_1, c_2, \dots, c_{n-m-1}$.⁴ In particular, it is immediate to notice that the volume functions $\Omega_{3,1}^{(2)}$ and $\Omega_{5,1}^{(4)}$ are completely localised and independent from any $i\epsilon$ -prescription. Focusing on the $m = 4$ volume function, for instance, we find

$$\begin{aligned} c_1 &= \frac{\langle Y 2345 \rangle}{\langle 12345 \rangle} \quad , \quad c_2 = -\frac{\langle Y 1345 \rangle}{\langle 12345 \rangle} \quad , \quad c_3 = \frac{\langle Y 1245 \rangle}{\langle 12345 \rangle} \quad , \\ c_4 &= -\frac{\langle Y 1235 \rangle}{\langle 12345 \rangle} \quad , \quad c_5 = \frac{\langle Y 1234 \rangle}{\langle 12345 \rangle} . \end{aligned} \quad (3.60)$$

Including the Jacobian factor $\langle 12345 \rangle^{-1}$ coming from solving the δ -functions, we immediately obtain the expected result,

$$\Omega_{5,1}^{(4)} = \frac{\langle 12345 \rangle^4}{\langle Y 1234 \rangle \langle Y 2345 \rangle \langle Y 3451 \rangle \langle Y 4512 \rangle \langle Y 5123 \rangle} = [12345] . \quad (3.61)$$

At several stages, finally, we will make use of Schouten identities among $(m + 1)$ -brackets. We have already written them down in the form of Plücker relations in (2.117) and will not repeat them here. We are now ready to understand how the introduced ϵ -deformations point at the correct residues to be picked up. We will always work with physically relevant volume functions, *i.e.* $m = 4$.

⁴Despite it not being in any way mandatory, we will always make this choice and then integrate all remaining c_i starting from c_{n-m-1} all the way down to c_1 . This will help us to have a lighter notation.

Same magnitude deformations

Six points Things get more interesting at six points, when one integration still has to be performed after solving the δ -constraints. Without loss of generality, we choose to solve for c_2, \dots, c_6 in terms of c_1 , finding

$$\begin{aligned} c_2 &= \frac{\langle Y3456 \rangle}{\langle 23456 \rangle} - \frac{\langle 13456 \rangle}{\langle 23456 \rangle} c_1, \quad c_3 = \frac{\langle Y2456 \rangle}{\langle 23456 \rangle} + \frac{\langle 12456 \rangle}{\langle 23456 \rangle} c_1, \quad c_4 = \frac{\langle Y2356 \rangle}{\langle 23456 \rangle} - \frac{\langle 12356 \rangle}{\langle 23456 \rangle} c_1, \\ c_5 &= \frac{\langle Y2346 \rangle}{\langle 23456 \rangle} + \frac{\langle 12346 \rangle}{\langle 23456 \rangle} c_1, \quad c_6 = \frac{\langle Y2345 \rangle}{\langle 23456 \rangle} - \frac{\langle 12345 \rangle}{\langle 23456 \rangle} c_1. \end{aligned} \quad (3.62)$$

and therefore

$$\begin{aligned} \Omega_{6,1}^{(4)} &= -\frac{1}{2\pi i} \int_{-\infty}^{+\infty} \frac{\langle 23456 \rangle^4 \, dc_1}{(c_1 + i\epsilon)(\langle Y3456 \rangle - \langle 13456 \rangle c_1 + i\epsilon)(\langle Y2456 \rangle + \langle 12456 \rangle c_1 + i\epsilon)} \times \\ &\quad \times \frac{1}{(\langle Y2356 \rangle - \langle 12356 \rangle c_1 + i\epsilon)(\langle Y2346 \rangle + \langle 12346 \rangle c_1 + i\epsilon)(\langle Y2345 \rangle - \langle 12345 \rangle c_1 + i\epsilon)}. \end{aligned} \quad (3.63)$$

Looking at the form of the factors F_i , we see that the integrand has six simple poles in the complex c_1 -plane: their exact location depends on the external data, but – as a consequence of the $i\epsilon$ -prescription – we always have that those coming from F_1, F_3, F_5 (F_2, F_4, F_6) lie below (above) $\Re\{c_1\}$.

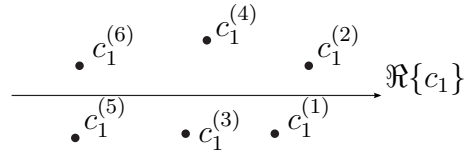


Figure 3.4: Distribution of the singularities in the c_1 -complex plane. We indicate in the superscript which factor F_i vanishes on a specific pole.

Closing the contour below the real axis, we compute the three residues

$$\begin{aligned} \{1_{c_1}\} &= \frac{\langle 23456 \rangle^4}{\langle Y2345 \rangle \langle Y3456 \rangle \langle Y4562 \rangle \langle Y5623 \rangle \langle Y6234 \rangle}, \\ \{3_{c_1}\} &= \frac{\langle 12456 \rangle^4}{\langle Y1245 \rangle \langle Y1246 \rangle \langle Y1256 \rangle \langle Y1456 \rangle \langle Y2456 \rangle}, \\ \{5_{c_1}\} &= \frac{\langle 12346 \rangle^4}{\langle Y1234 \rangle \langle Y2346 \rangle \langle Y3461 \rangle \langle Y4612 \rangle \langle Y6123 \rangle}. \end{aligned} \quad (3.64)$$

The notation $\{i_{c_1}\}$ signifies that the residue is computed at the pole $c_1^{(i)}$, associated to the vanishing of the denominator factor F_i . The reader might recognise $\{3_{c_1}\}$ as the example

expression presented before, evaluating – upon integration against $d^4\phi$ – to the R-invariant R_{625} . Then it is immediate to write down the full result

$$\Omega_{6,1}^{(4)} = \{1_{c_1}\} + \{3_{c_1}\} + \{5_{c_1}\} , \quad (3.65)$$

matching (3.42) for $Z_\star = Z_6$. Had we chosen to close the contour above the real axis, we would have computed

$$\Omega_{6,1}^{(4)} = -\{2_{c_1}\} - \{4_{c_1}\} - \{6_{c_1}\} , \quad (3.66)$$

yielding the (algebraically) non-trivial six-term identity $\sum_i \{i_{c_1}\} = 0$. This identity, upon integration of the auxiliary $\phi_{\alpha A}$ variables, is analogous to the one immediately following from (2.131).

Seven points At seven points the strategy is the same, but we are left with the double integral

$$\Omega_{7,1}^{(4)} = \frac{1}{(2\pi i)^2} \frac{1}{\langle 34567 \rangle} \int_{-\infty}^{+\infty} \frac{dc_1}{F_1} \int_{-\infty}^{+\infty} \frac{dc_2}{F_2 F_3 F_4 F_5 F_6 F_7} , \quad (3.67)$$

where

$$F_1 = c_1 + i\epsilon$$

$$F_2 = c_2 + i\epsilon$$

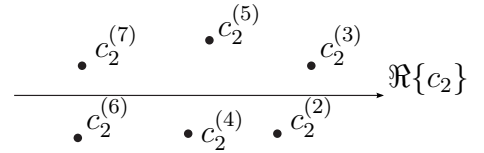
$$F_3 = \frac{1}{\langle 34567 \rangle} (\langle Y4567 \rangle - \langle 14567 \rangle c_1 - \langle 24567 \rangle c_2) + i\epsilon$$

$$F_4 = -\frac{1}{\langle 34567 \rangle} (\langle Y3567 \rangle - \langle 13567 \rangle c_1 - \langle 23567 \rangle c_2) + i\epsilon$$

$$F_5 = \frac{1}{\langle 34567 \rangle} (\langle Y3467 \rangle - \langle 13467 \rangle c_1 - \langle 23467 \rangle c_2) + i\epsilon$$

$$F_6 = -\frac{1}{\langle 34567 \rangle} (\langle Y3457 \rangle - \langle 13457 \rangle c_1 - \langle 23457 \rangle c_2) + i\epsilon$$

$$F_7 = \frac{1}{\langle 34567 \rangle} (\langle Y3456 \rangle - \langle 13456 \rangle c_1 - \langle 23456 \rangle c_2) + i\epsilon$$



and we have fixed an order of integration. In the complex c_2 -plane, the singularities of F_2, F_4, F_6 lie below the real axis, the others lie above it. Closing the contour around the former ones leaves us with

$$\Omega_{7,1}^{(4)} = -\frac{1}{2\pi i} \int_{-\infty}^{+\infty} dc_1 \operatorname{res}_{c_2}(c_1) \quad , \quad \operatorname{res}_{c_2}(c_1) = \{2_{c_2}\} + \{4_{c_2}\} + \{6_{c_2}\} . \quad (3.68)$$

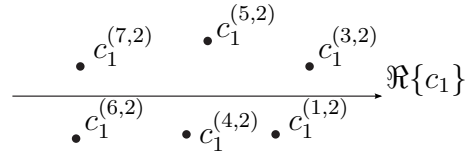
Every partial residue $\{i_{c_2}\}$ is obviously a function of c_1 and includes the factor F_1 . Similarly to what we had before, we find

$$\begin{aligned}\{2_{c_2}\} &= \frac{\langle 34567 \rangle^4}{c_1(\langle Y3456 \rangle - \langle 13456 \rangle c_1)(\langle Y3457 \rangle - \langle 13457 \rangle c_1)(\langle Y3467 \rangle - \langle 13467 \rangle c_1)(\langle Y3567 \rangle - \langle 13567 \rangle c_1)(\langle Y4567 \rangle - \langle 14567 \rangle c_1)} , \\ \{4_{c_2}\} &= \frac{\langle 23567 \rangle^4}{c_1(\langle Y2356 \rangle - \langle 12356 \rangle c_1)(\langle Y2357 \rangle - \langle 12357 \rangle c_1)(\langle Y2367 \rangle - \langle 12367 \rangle c_1)(\langle Y2567 \rangle - \langle 12567 \rangle c_1)(\langle Y3567 \rangle - \langle 13567 \rangle c_1)} , \\ \{6_{c_2}\} &= \frac{\langle 23457 \rangle^4}{c_1(\langle Y2345 \rangle - \langle 12345 \rangle c_1)(\langle Y2357 \rangle - \langle 12357 \rangle c_1)(\langle Y3457 \rangle - \langle 13457 \rangle c_1)(\langle Y2347 \rangle - c_1 \langle 12347 \rangle)(\langle Y2457 \rangle - c_1 \langle 12457 \rangle)} .\end{aligned}\tag{3.69}$$

These are ordinary residues obtained regarding c_1 as a parameter and finally switching off the deformation: indeed, the small imaginary parts introduced in formula (3.58) are important only to understand which poles lie in which half-plane; in every other step of the calculation, we can safely send $\epsilon \rightarrow 0$. Now, reinstating the deformations, we need to carry out the second integration and this requires a separate analysis for the three contributions to res_{c_2} .

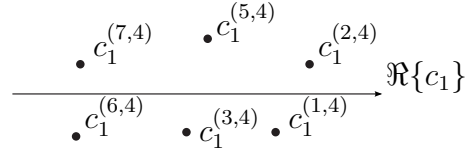
On the pole corresponding to $F_2 = 0$,

$$\begin{aligned}F_1 &= c_1 + i\epsilon \\ F_3|_{c_2^{(2)}} &= \frac{1}{\langle 34567 \rangle} (\langle Y4567 \rangle - \langle 14567 \rangle c_1) + i\epsilon \\ F_4|_{c_2^{(2)}} &= -\frac{1}{\langle 34567 \rangle} (\langle Y3567 \rangle - \langle 13567 \rangle c_1) + i\epsilon \\ F_5|_{c_2^{(2)}} &= \frac{1}{\langle 34567 \rangle} (\langle Y3467 \rangle - \langle 13467 \rangle c_1) + i\epsilon \\ F_6|_{c_2^{(2)}} &= -\frac{1}{\langle 34567 \rangle} (\langle Y3457 \rangle - \langle 13457 \rangle c_1) + i\epsilon \\ F_7|_{c_2^{(2)}} &= \frac{1}{\langle 34567 \rangle} (\langle Y3456 \rangle - \langle 13456 \rangle c_1) + i\epsilon\end{aligned}$$



On the pole corresponding to $F_4 = 0$,

$$\begin{aligned}F_1 &= c_1 + i\epsilon \\ F_2|_{c_2^{(4)}} &= \frac{1}{\langle 23567 \rangle} (\langle Y3567 \rangle - \langle 13567 \rangle c_1) + i\epsilon \\ F_3|_{c_2^{(4)}} &= -\frac{1}{\langle 23567 \rangle} (\langle Y2567 \rangle - \langle 12567 \rangle c_1) + i\epsilon \\ F_5|_{c_2^{(4)}} &= \frac{1}{\langle 23567 \rangle} (\langle Y2367 \rangle - \langle 12367 \rangle c_1) + i\epsilon \\ F_6|_{c_2^{(4)}} &= -\frac{1}{\langle 23567 \rangle} (\langle Y2357 \rangle - \langle 12357 \rangle c_1) + i\epsilon \\ F_7|_{c_2^{(4)}} &= \frac{1}{\langle 23567 \rangle} (\langle Y2356 \rangle - \langle 12356 \rangle c_1) + i\epsilon\end{aligned}$$



On the pole corresponding to $F_6 = 0$,

$$\begin{aligned}
 F_1 &= c_1 + i\epsilon \\
 F_2|_{c_2^{(6)}} &= \frac{1}{\langle 23457 \rangle} (\langle Y3457 \rangle - \langle 13457 \rangle c_1) + i\epsilon \\
 F_3|_{c_2^{(6)}} &= -\frac{1}{\langle 23457 \rangle} (\langle Y2457 \rangle - \langle 12457 \rangle c_1) + i\epsilon \\
 F_4|_{c_2^{(6)}} &= \frac{1}{\langle 23457 \rangle} (\langle Y2357 \rangle - \langle 12357 \rangle c_1) + i\epsilon \\
 F_5|_{c_2^{(6)}} &= -\frac{1}{\langle 23457 \rangle} (\langle Y2347 \rangle - \langle 12347 \rangle c_1) + i\epsilon \\
 F_7|_{c_2^{(6)}} &= \frac{1}{\langle 23457 \rangle} (\langle Y2345 \rangle - \langle 12345 \rangle c_1) + i\epsilon
 \end{aligned}$$

At each pole in the variable c_2 , the resulting integral again has six singularities, three lying above, three below $\Re\{c_1\}$. After choosing to enclose the last ones with the contour of integration, we can evaluate the residues of the summands of res_{c_2} , those supposed to contribute to the volume function. They will be denoted by two labels, *e.g.* $\{1_{c_1}, 2_{c_2}\}$ for the residue calculated at the pole $c_2^{(2)}$ where $F_2 = 0$ and, subsequently, at the pole $c_1^{(1,2)}$ where in addition $F_1 = 0$. Some of them will cancel in pairs due to property (3.57), the others build up the final answer:

$$\Omega_{7,1}^{(4)} = \{1_{c_1}, 2_{c_2}\} + \{1_{c_1}, 4_{c_2}\} + \{3_{c_1}, 4_{c_2}\} + \{1_{c_1}, 6_{c_2}\} + \{3_{c_1}, 6_{c_2}\} + \{5_{c_1}, 6_{c_2}\}. \quad (3.70)$$

It is clear that at higher points we will need more labels to characterise the residues contributing to the volume function. The symbol $\{i_{l,c_l}, \dots, i_{n-5,c_{n-5}}\}$ will denote partial residues obtained upon $(n-l-4)$ -fold integration, on the poles corresponding to the vanishing of $F_{i_{n-5}}$ (in the variable c_{n-5}), \dots , F_{i_l} (in the variable c_l), in this order. When $l = 1$ we have arrived at the actual residues we were interested in – see (3.55) – because all the integrations have been carried out.

General patterns Based on the previous couple of examples and the eight-point calculation (which we do not show, since it is just longer and not more insightful), it is immediate to observe certain regularities, which were then tested up to ten points using a *Mathematica* code.

In all the intermediate steps, we found that the ϵ -deformations of the denominator factors caused an even splitting of the integrand poles: half of them were located above, half of them below, the real axis of the relevant complex c_i -plane. This is no accident and we provide a proof in Appendix A.

Moreover, at least within our framework (integrating variables from c_{n-5} to c_1 and always closing the contour in the lower half-planes), we could come up with a graphical representation of all the partial residues appearing in the calculation of any NMHV volume function $\Omega_{n,1}^{(4)}$ at every stage, *i.e.* after any number of integrations has been carried out. We call it *tree of residues* and Figure 3.5 is an example at eight points.

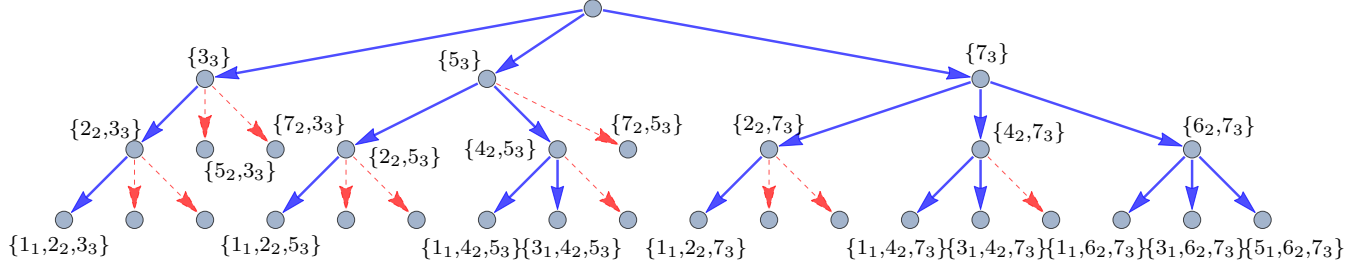


Figure 3.5: The tree of residues for the eight-point NMHV amplitude. On the lowest level, several labels – identifying the residues not contributing to $\Omega_{8,1}^{(4)}$ – were omitted for clarity. Also, in labelling residues we simplified the notation slightly to save space.

The root of the tree corresponds to the original integrand of (3.58) once the δ -functions have been solved. Each level then corresponds to the integration of one variable, starting from c_3 all the way down to c_1 and each node is a (partial) residue. Arrows connect each node to its descendants, *i.e.* the partial residues picked up at the singularities encircled closing the integration contour below the relevant $\Re\{c_l\}$ -axis. Labels of descendant residues are easily determined based on the considerations used in the proof of Appendix A. Nodes connected via red arrows are called sterile: they will not produce descendants and the corresponding (partial) residues have to be discarded. We already encountered an instance of this phenomenon at seven points: there the sterile nodes were showing up at the bottom of the tree, at the level of actual residues of the original integrand, but nothing really changes for partial residues, as will be shown in a moment. The residue functions $\text{res}_{c_3}(c_1, c_2)$, $\text{res}_{c_2, c_3}(c_1)$ are thus sums of all the residues corresponding to non-sterile nodes at the appropriate depth. Observe that the residue trees for the five-, six- and seven-point amplitudes can be read inside the eight-point tree, up to a simple constant shift in the labels. In fact, assume to have a huge residue tree, representing the $\Omega_{N,1}^{(4)}$ computation, for N some big number. Then all the amplitudes $\Omega_{n,1}^{(4)}$ for $n < N$ can be read off at once just looking at the big tree at depth $n - 5$ shifting all the labels back by $N - n$ units.

Let us finally discuss the sterile nodes. Their contributions are picked up on a pole where two summands of the relevant residue function are singular and the two resulting

residues cancel. For example, looking at the eight-point computation, we find that

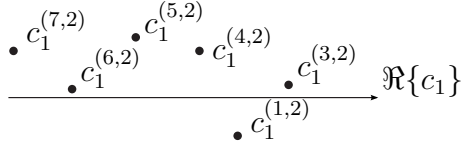
$$\begin{aligned} c_2^{(5,3)} &= \frac{\langle Y4678 \rangle - \langle 14678 \rangle c_1}{\langle 24678 \rangle} = c_2^{(3,5)} \quad \text{and} \quad \{5_{c_2}, 3_{c_3}\} = -\{3_{c_2}, 5_{c_3}\} , \\ c_1^{(7,4,5)} &= \frac{\langle Y2368 \rangle}{\langle 12368 \rangle} = c_1^{(5,4,7)} \quad \text{and} \quad \{7_{c_1}, 4_{c_2}, 5_{c_3}\} = -\{5_{c_1}, 4_{c_2}, 7_{c_3}\} . \end{aligned}$$

By inspection, we have seen that these cancellations always occur at nodes whose leftmost label coincides with the leftmost label of one of the siblings of the parent node. There will thus be two residues cancelling each other according to (3.57).

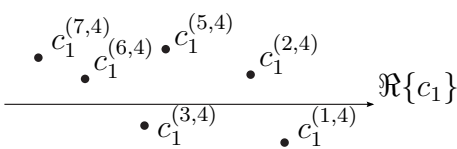
Strongly ordered deformations

The advantage of having ordered positive deformations $\epsilon_1 \gg \epsilon_2 \gg \dots \gg \epsilon_n > 0$ manifests itself when at least a second integration has to be carried out. In fact, the poles cease to evenly distribute themselves above and below the real axes. This – rather than being an obstacle – can save quite some work. Let us see how the method works at seven points.

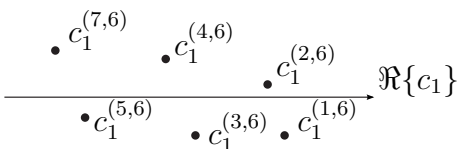
After solving the δ -functions, we have formula (3.67), but the imaginary parts of the F_i factors are now the different ϵ_i . Let us enclose the poles lying below $\Re\{c_2\}$. Here the singularities have to be computed without switching off the deformations, e.g. $\{2_{c_2}\}$ is computed at $c_2^{(2)} = -i\epsilon_2$. On that pole,

$$\begin{aligned} F_1 &= c_1 + i\epsilon_1 \\ F_3|_{c_2^{(2)}} &= \frac{1}{\langle 34567 \rangle} (\langle Y4567 \rangle - \langle 14567 \rangle c_1) + i\epsilon_2 \\ F_4|_{c_2^{(2)}} &= -\frac{1}{\langle 34567 \rangle} (\langle Y3567 \rangle - \langle 13567 \rangle c_1) - i\epsilon_2 \\ F_5|_{c_2^{(2)}} &= \frac{1}{\langle 34567 \rangle} (\langle Y3467 \rangle - \langle 13467 \rangle c_1) + i\epsilon_2 \\ F_6|_{c_2^{(2)}} &= -\frac{1}{\langle 34567 \rangle} (\langle Y3457 \rangle - \langle 13457 \rangle c_1) - i\epsilon_2 \\ F_7|_{c_2^{(2)}} &= \frac{1}{\langle 34567 \rangle} (\langle Y3456 \rangle - \langle 13456 \rangle c_1) + i\epsilon_2 \end{aligned}$$


Indeed, as a consequence of the strong ordering, the imaginary parts proportional to ϵ_2 always dominate the others. It follows that in the c_1 -plane the only singularity below the real axis is the pole of F_1 : closing around it, we immediately get the contribution $\{1_{c_1}, 2_{c_2}\}$ to the solution. Similarly, $\{4_{c_2}\}$ is computed at $c_2^{(4)} = \frac{1}{\langle 23567 \rangle} (\langle Y3567 \rangle - \langle 13567 \rangle c_1) - i\epsilon_4$. On that pole,

$$\begin{aligned}
F_1 &= c_1 + i\epsilon_1 \\
F_2|_{c_2^{(4)}} &= \frac{1}{\langle 23567 \rangle} (\langle Y3567 \rangle - \langle 13567 \rangle c_1) + i\epsilon_2 \\
F_3|_{c_2^{(4)}} &= -\frac{1}{\langle 23567 \rangle} (\langle Y2567 \rangle - \langle 12567 \rangle c_1) + i\epsilon_3 \\
F_5|_{c_2^{(4)}} &= \frac{1}{\langle 23567 \rangle} (\langle Y2367 \rangle - \langle 12367 \rangle c_1) + i\epsilon_4 \\
F_6|_{c_2^{(4)}} &= -\frac{1}{\langle 23567 \rangle} (\langle Y2357 \rangle - \langle 12357 \rangle c_1) - i\epsilon_4 \\
F_7|_{c_2^{(4)}} &= \frac{1}{\langle 23567 \rangle} (\langle Y2356 \rangle - \langle 12356 \rangle c_1) + i\epsilon_4
\end{aligned}$$


Closing the contour below $\Re\{c_1\}$, we pick up the contribution $\{1_{c_1}, 4_{c_2}\} + \{3_{c_1}, 4_{c_2}\}$. Finally, on $c_2^{(6)} = \frac{1}{\langle 23457 \rangle} (\langle Y3457 \rangle - \langle 13457 \rangle c_1) - i\epsilon_6$, we derive

$$\begin{aligned}
F_1 &= c_1 + i\epsilon_1 \\
F_2|_{c_2^{(6)}} &= \frac{1}{\langle 23457 \rangle} (\langle Y3457 \rangle - \langle 13457 \rangle c_1) + i\epsilon_2 \\
F_3|_{c_2^{(6)}} &= -\frac{1}{\langle 23457 \rangle} (\langle Y2457 \rangle - \langle 12457 \rangle c_1) + i\epsilon_3 \\
F_4|_{c_2^{(6)}} &= \frac{1}{\langle 23457 \rangle} (\langle Y2357 \rangle - \langle 12357 \rangle c_1) + i\epsilon_4 \\
F_5|_{c_2^{(6)}} &= -\frac{1}{\langle 23457 \rangle} (\langle Y2347 \rangle - \langle 12347 \rangle c_1) + i\epsilon_5 \\
F_7|_{c_2^{(6)}} &= \frac{1}{\langle 23457 \rangle} (\langle Y2345 \rangle - \langle 12345 \rangle c_1) + i\epsilon_6
\end{aligned}$$


providing us with the last piece $\{1_{c_1}, 6_{c_2}\} + \{3_{c_1}, 6_{c_2}\} + \{5_{c_1}, 6_{c_2}\}$ of $\Omega_{7,1}^{(4)}$.

We checked via explicit computation that this second prescription also produces the correct results up to eight point. Moreover, there is still some freedom to change the ordering of the ϵ_i : for instance, setting $\epsilon_1 \ll \epsilon_2 \ll \dots \ll \epsilon_n$, we could recover the previously computed results. In the example presented above, as well as in its immediate extension to higher points, we quickly realise that the number of poles lying below the various $\Re\{c_i\}$ at the various stages of the calculation is directly related to the number of non-sterile nodes in the various branches of the tree of residues. Making this correspondence precise for an arbitrary ordering of the ϵ_i 's requires further inspection.

We conclude this section mentioning yet another approach to the determination of the residues contributing to $\Omega_{n,1}^{(m)}$. It is based on observing that they are identified by the requirement that certain positivity conditions on the minors of an appropriately defined coefficient matrix are fulfilled. More details about this can be found in [117].

3.4.3 N²MHV amplitudes

At the moment, no complete understanding of N²MHV volume functions is available. However, the ones where $m = 2$ are known, because their expressions coincide with the integrands of one-loop MHV amplitudes in $m = 4$ dimensions, which were studied in [51]:

$$\Omega_{n,2}^{(2)} = \sum_{i < j} \frac{(\langle Y_1 \star i i + 1 \rangle \langle Y_2 \star j j + 1 \rangle - \langle Y_2 \star i i + 1 \rangle \langle Y_1 \star j j + 1 \rangle)^2}{\langle Y_1 Y_2 \star i \rangle \langle Y_1 Y_2 i i + 1 \rangle \langle Y_1 Y_2 i + 1 \star \rangle \langle Y_1 Y_2 \star j \rangle \langle Y_1 Y_2 j j + 1 \rangle \langle Y_1 Y_2 j + 1 \star \rangle} , \quad (3.71)$$

for \star an arbitrary label.

We were able to reproduce the correct result for $\Omega_{5,2}^{(2)}$ by means of an $i\epsilon$ -prescription. The computation goes along the lines of the NMHV case, but this could have been anticipated, since the same volume function can be thought of as an $\overline{\text{NMHV}}$ one and it is thus not surprising that the calculation displays a comparable level of complexity. Indeed, a fundamental reason why it remains simple is that the 2×2 minors of (3.47) are linear functions of the $c_{\alpha i}$, a feature that is lost starting at six points. We refer to Appendix A for the detailed presentation of the five-point N²MHV volume function.

Chapter 4

Volume of the dual tree-level amplituhedron

In Chapter 3 we gave an overview on the amplituhedron, hinting at the difficulties in employing its formalism for actually computing scattering amplitudes. One of the reasons is its complex geometry: for a given number of scattering particles, at a given order in perturbation theory, the amplituhedron defines a complicated region in a high-dimensional space. In order to evaluate the amplitude, we need to determine a differential form with a prescribed singular behaviour at the boundaries of this region. At the moment, no compact formula exists for the volume form and even triangulations of $\mathfrak{A}_{n,k}^{\text{tree}}$ are not known in general. There is, however, a case where we can make much progress, namely tree-level NMHV volume functions. In this case we know how to define a dual amplituhedron and compute its volume. Hodges [42] had already shown how to think of NMHV scattering amplitudes in this way: although he still referred to triangulations, we show in this chapter that this is not necessary; for $N^k\text{MHV}$ volume functions with $k > 1$ a similar volume formula is not known at the moment and we will discuss a possible direction where to look for it.

In Section 4.1 we analyse the symmetries of the amplituhedron tree-level volume functions and derive the differential equations they satisfy. In particular, we will focus on a new set of constraints, called *Capelli differential equations*. Using these, we will be able in Section 4.2 to derive a novel dual space representation of any $\Omega_{n,k}^{(m)}$ and fully fix its form in the NMHV case, before showing several examples in Section 4.3 and commenting on possible extensions in Section 4.4. The chapter is based on the contents of [54].

4.1 Symmetries of the volume function and the Capelli differential equations

We already discussed the properties of tree-level Grassmannian integrals in momentum twistor space. In particular, they are superconformal and dual-superconformal invariants or, equivalently, Yangian invariants. As shown in [47, 48], under certain requirements these symmetries uniquely determine the form of the integrand, up to total derivatives, leaving as the sole ambiguity in (2.124) the contour of integration: in particular the measure is fixed to the inverse of the product of consecutive cyclic minors.¹ Here we also aim at constraining the integral representation (3.47) by means of symmetries, focusing on what can be learned independently of a realisation of Yangian symmetry in the amplituhedron framework. An understanding of the latter only came later [56] and will be discussed at length in Chapter 5. To simplify the notation, let us define the collective variables

$$W_a^A = \begin{cases} Y_a^A & , \quad a = 1, \dots, k \\ Z_{a-k}^A & , \quad a = k+1, \dots, n+k \end{cases} . \quad (4.1)$$

The formal integral (3.47) enjoys two “obvious” kinds of symmetries: to establish a connection with the known mathematical literature, we will state them in both their local and global form. First of all, we observe the $\mathrm{GL}(m+k, \mathbb{R})$ *covariance property*

$$\sum_{a=1}^{n+k} W_a^A \frac{\partial}{\partial W_a^B} \Omega_{n,k}^{(m)}(Y, Z) = -k \delta_B^A \Omega_{n,k}^{(m)}(Y, Z) . \quad (4.2)$$

This statement is analogous to the level-zero Yangian invariance of the Grassmannian formula (2.124), *i.e.*

$$J^{(0)A}_B \Omega_{n,k}^{(m)}(Y, Z) = \left(\sum_{\alpha} Y_{\alpha}^A \frac{\partial}{\partial Y_{\alpha}^B} + \sum_i Z_i^A \frac{\partial}{\partial Z_i^B} \right) \Omega_{n,k}^{(m)}(Y, Z) = 0 , \quad (4.3)$$

upon trace removal. In its global form,

$$\Omega_{n,k}^{(m)}(Y \cdot g, Z \cdot g) = \frac{1}{(\det g)^k} \Omega_{n,k}^{(m)}(Y, Z) , \quad g \in \mathrm{GL}(m+k, \mathbb{R}) . \quad (4.4)$$

Here the action of the linear group is from the right, namely $(W \cdot g)_a^A = \sum_B W_a^B g_B^A$, therefore we talk about right covariance. Secondly, $\Omega_{n,k}^{(m)}$ has a different behaviour under

¹This statement is true for standard bilocal level-one generators, which are relevant for scattering amplitudes. For a discussion on possible deformations of amplitudes and Yangian generators see [120, 121].

rescaling of its variables: on the one hand, it is invariant as far as the Z_i^A are concerned, namely

$$\sum_{A=1}^{m+k} Z_i^A \frac{\partial}{\partial Z_i^A} \Omega_{n,k}^{(m)}(Y, Z) = 0, \text{ for } i = 1, \dots, n; \quad (4.5)$$

on the other hand, it is a $\mathrm{GL}(k, \mathbb{R})$ -covariant homogeneous function of degree $-(m+k)$ in the Y_α^A variables:

$$\sum_{A=1}^{m+k} Y_\alpha^A \frac{\partial}{\partial Y_\beta^A} \Omega_{n,k}^{(m)}(Y, Z) = -(m+k) \delta_\alpha^\beta \Omega_{n,k}^{(m)}(Y, Z), \text{ for } \alpha, \beta = 1, \dots, k. \quad (4.6)$$

Together, these constitute the *scaling properties* of the volume function. In their finite form, we can cast them as a $\mathrm{GL}(k, \mathbb{R})_+ \otimes \mathrm{GL}(1, \mathbb{R})_+ \otimes \dots \otimes \mathrm{GL}(1, \mathbb{R})_+$ left covariance:

$$\Omega_{n,k}^{(m)}(h \cdot Y, \lambda \cdot Z) = \frac{1}{(\det h)^{m+k}} \Omega_{n,k}^{(m)}(Y, Z), \quad (4.7)$$

for $h \in \mathrm{GL}(k, \mathbb{R})_+$ and $\lambda = (\lambda_1, \dots, \lambda_n) \in \mathrm{GL}(1, \mathbb{R})_+ \otimes \dots \otimes \mathrm{GL}(1, \mathbb{R})_+$, where we restricted all possible transformations to be elements of the identity component of linear groups, namely $\mathrm{GL}(l, \mathbb{R})_+ = \{h \in \mathrm{GL}(l, \mathbb{R}) : \det h > 0\}$.

In addition to those above, the volume function $\Omega_{n,k}^{(m)}(Y, Z)$ satisfies further higher-order differential equations: for every $(k+1) \times (k+1)$ minor of the matrix composed of derivatives $\frac{\partial}{\partial W_a^A}$ one can check that

$$\det \left(\frac{\partial}{\partial W_{a_\mu}^{A_\nu}} \right)_{\substack{1 \leq \nu \leq k+1 \\ 1 \leq \mu \leq k+1}} \Omega_{n,k}^{(m)}(Y, Z) = 0, \quad (4.8)$$

for $1 \leq A_1 \leq \dots \leq A_{k+1} \leq m+k$ and $1 \leq a_1 \leq \dots \leq a_{k+1} \leq n+k$. This type of determinant differential equations are usually referred to as the *Capelli differential equations*. In the case at hand, we consider them as defined on the Grassmannian $G(m+k, n+k)$. Interestingly, equations of the form (4.8) – together with covariance and scaling properties like (4.2) and (4.5), (4.6) – were analysed independently in the mathematical literature in various contexts. In particular, Gelfand [122] and Aomoto [123, 124] studied intensively the $k=1$ case, which is related to the so-called GKZ hypergeometric functions (on Grassmannians).

In the context of scattering amplitudes in $\mathcal{N}=4$ SYM, their relevance was suggested in [125]. For the $k=1$ case, the general solution of the above problem was given in [126] and we will present it in the following section. It gives the correct result for $\Omega_{n,1}^{(m)}$ as an

integral over the Grassmannian $G(1, m+1)$. As we will see below, this integral calculates the volume of a simplex in the projective space $G(1, m+1) = \mathbb{RP}^m$ and can be compared to the volume formula proposed by Hodges [42]. An important advantage with respect to the latter is that it can be evaluated without referring to any triangulation of the simplex. For higher k the problem was studied for example in [127], but to our knowledge a general solution suitable for the scaling properties (4.7) is not known.

4.2 Solution for the $k = 1$ case

To look for the solution to (4.8), (4.4) and (4.7), let us first go to Fourier space:

$$\Omega_{n,k}^{(m)}(Y, Z) = \int d\mu(t_A^\alpha, \tilde{t}_A^i) e^{i t_A^\alpha Y_\alpha^A + i \tilde{t}_A^i Z_i^A} f(t_A^\alpha, \tilde{t}_A^i) , \quad (4.9)$$

where the variables t_A^α and \tilde{t}_A^i are Fourier conjugates to Y_α^A and Z_i^A , respectively. Here the flat measure $d\mu(t_A^\alpha, \tilde{t}_A^i)$ is both $\text{GL}(m+k, \mathbb{R})$ - and $\text{GL}(k, \mathbb{R})$ -covariant and $f(t_A^\alpha, \tilde{t}_A^i)$ is a generalised function defined on the product of two matrix spaces:

$$f : M(m+k, k) \times M(m+k, k+n) \rightarrow \mathbb{R} . \quad (4.10)$$

In the $k = 1$ case, relevant for NMHV amplitudes, the index α can take just one value and (4.9) reduces to

$$\Omega_{n,1}^{(m)}(Y, Z) = \int d\mu(t_A, \tilde{t}_A^i) e^{i t_A Y^A + i \tilde{t}_A^i Z_i^A} f(t_A, \tilde{t}_A^i) . \quad (4.11)$$

Then the Capelli differential equations form a system of second-order differential equations. We distinguish two cases: both derivatives are with respect to Z_i^A variables or one derivative is with respect to a Z_i^A and another to Y^A . Explicitly, they read

$$\left(\frac{\partial^2}{\partial Z_i^A \partial Z_j^B} - \frac{\partial^2}{\partial Z_i^B \partial Z_j^A} \right) \Omega_{n,1}^{(m)} = 0 \quad \text{and} \quad \left(\frac{\partial^2}{\partial Y^A \partial Z_j^B} - \frac{\partial^2}{\partial Y^B \partial Z_j^A} \right) \Omega_{n,1}^{(m)} = 0 . \quad (4.12)$$

When applied to the formula (4.11), they can be translated into the following equations for the Fourier variables:

$$\tilde{t}_A^i \tilde{t}_B^j - \tilde{t}_B^i \tilde{t}_A^j = 0 \quad \text{and} \quad t_A \tilde{t}_B^i - t_B \tilde{t}_A^i = 0 . \quad (4.13)$$

It is immediate to verify that

$$\tilde{t}_A^i = -\tilde{s}^i s_A \quad , \quad t_A = s_A \quad (4.14)$$

is a solution of (4.13) for any n and transforms the Fourier integral (4.11) into

$$\Omega_{n,1}^{(m)}(Y, Z) = \int ds_A d\tilde{s}^i e^{i s_A Y^A - i s_A Z_i^A \tilde{s}^i} F(s, \tilde{s}) , \quad (4.15)$$

where we integrate over the space $\mathbb{R}^{m+1} \times \mathbb{R}^n$. Therefore, from the perspective of Capelli differential equations the most convenient and natural variables are not the Fourier ones, but rather the ones we call s_A and \tilde{s}^i . Every \tilde{s}^i can be identified with the corresponding c_i in the integral (3.47) for $k = 1$, while we will refer to s_A as dual variables.

From the definition of the amplituhedron we demand that (4.15) localises on

$$Y^A = \tilde{s}^i Z_i^A , \quad (4.16)$$

as enforced by the δ -function in (3.47). This is only possible if the function $F(s, \tilde{s})$ is independent of s_A : indeed, upon integration over s_A in (4.15), we would end up with the desired δ -function. However, we will refrain from doing it and rather eliminate the \tilde{s}_i . What we obtain is an integral representation of $\Omega_{n,1}^{(m)}(Y, Z)$ depending only on dual variables, namely

$$\Omega_{n,1}^{(m)}(Y, Z) = \int ds_A e^{i s_A Y^A} \tilde{F}(s_A Z_i^A) , \quad (4.17)$$

where $\tilde{F}(s_A Z_i^A)$ is the Fourier transform of the function $F(\tilde{s})$. Notice that the integrand depends on the external data only through the n combinations $s_A Z_i^A$.

Let us observe that, for $k = 1$, the fact that $\Omega_{n,k}^{(m)}$ satisfies the Capelli differential equations and the scaling properties directly implies that it is also invariant under level-one Yangian generators of the form

$$J^{(1)A}_B = \sum_{a < b} \left(W_a^A \frac{\partial}{\partial W_a^C} W_b^C \frac{\partial}{\partial W_b^B} - (a \leftrightarrow b) \right) + (m+1) Y^A \frac{\partial}{\partial Y^B} . \quad (4.18)$$

Together with (4.2), this proves the full Yangian invariance for $k = 1$. This statement is however not true for higher values of k .

This ends the study of the Capelli differential equations. Now we need to supplement it by the invariance and scaling properties, which will constrain the form of the function $\tilde{F}(s_A Z_i^A)$. After careful analysis we find that it has to be a homogeneous (generalised) function of degree zero in each of its variables. Such space of functions is a well studied one. Following [128], we find that for each integer number l there are exactly two independent homogeneous generalized functions of degree l . For $l = 0$, one can pick as a basis the Heaviside step functions $\theta(x)$ and $\theta(-x)$. This yields the general solution

$$\Omega_{n,1}^{(m)}(Y, Z) = \int ds_A e^{i s_A Y^A} \prod_i (C_i \theta(s_A Z_i^A) + D_i \theta(-s_A Z_i^A)) , \quad (4.19)$$

where C_i and D_i are arbitrary complex numbers. The existence of various solutions can be linked with the ambiguity in choosing the integration contour of the Grassmannian integral. By direct calculation – imposing that the resulting integral be finite – we find that those relevant for scattering amplitudes are the ones with either all $D_i = 0$ or all $C_i = 0$. In the first case we end up with

$$\Omega_{n,1}^{(m)}(Y, Z) = \frac{1}{i^{m+1}} \int ds_A e^{i s_A Y^A} \prod_i \theta(s_A Z_i^A). \quad (4.20)$$

As we will show shortly, this is the correct formula for the volume. Before we do it, let us rewrite (4.20) in a way that resembles the formula found by Hodges. First, let us observe that (4.20) is $\mathrm{GL}(m+1, \mathbb{R})$ -covariant and use this to fix $m+1$ of the Z_i 's to form an identity matrix, namely, $\{Z_1, \dots, Z_{m+1}\} = \mathbb{1}_{m+1}$. Then

$$\Omega_{n,1}^{(m)}(Y, Z) = \frac{1}{i^{m+1}} \int_0^{+\infty} \left(\prod_{A=1}^{m+1} ds_A \right) e^{i s_A Y^A} \prod_{i=m+2}^n \theta(s_A Z_i^A), \quad (4.21)$$

where we used $m+1$ of the θ -functions to restrict the domain of integration. Furthermore, we can perform a change of variables $s \rightarrow s'$ such that

$$s_1 = s'_1, \quad s_A = s'_1 s'_A, \quad \text{for } A = 2, \dots, m+1 \quad (4.22)$$

and compute the integral over s'_1 explicitly, to end up with

$$\Omega_{n,1}^{(m)} = \int_0^{+\infty} \left(\prod_{A=2}^{m+1} ds_A \right) \frac{m!}{(s \cdot Y)^{m+1}} \prod_{i=m+2}^n \theta(s \cdot Z_i). \quad (4.23)$$

Here we introduced the compact notation $s \cdot W_a = W_a^1 + s_2 W_a^2 + \dots + s_{k+m} W_a^{k+m}$, where W_a can be either Y or one of the Z_i . Formula (4.23) is the central result of this chapter and features an m -fold integral over the m -dimensional real projective space \mathbb{RP}^m : in view of a forthcoming generalisation to arbitrary k , it is more useful to think of it as an instance of a *dual Grassmannian*. By comparison of (4.23) with the one found in [42] by Hodges, the elements of \mathbb{RP}^m can be identified with the elements of dual momentum twistor space; however, we prefer to think about them rather as elements of $G(1, m+1)$, as anticipated.

Before we show in detail how our master formula evaluates the volume of the dual amplituhedron, we comment on its relation to the formal expression (3.47). Let us consider again the integral (4.20), write the Fourier representation of θ -functions and, subsequently,

integrate over all s_A :

$$\begin{aligned}\Omega_{n,1}^{(m)}(Y, Z) &= \frac{i^{n-m-1}}{(2\pi)^n} \int_{-\infty}^{+\infty} ds_A d\tilde{s}^i e^{i s_A Y^A - i s_A Z_i^A \tilde{s}^i} \prod_i \frac{1}{\tilde{s}^i + i\epsilon^i} = \\ &= \frac{1}{(-2\pi i)^{n-m-1}} \int_{-\infty}^{+\infty} \prod_i \frac{d\tilde{s}^i}{\tilde{s}^i + i\epsilon^i} \delta^{m+1}(Y^A - \tilde{s}^i Z_i^A) \quad ,\end{aligned}\quad (4.24)$$

with all $\epsilon^i > 0$. Hence we recovered the $i\epsilon$ -prescription of (3.58) and from our discussion we see that it has a natural origin in the dual space.

Two important comments on formula (4.23) are in order. First of all, if Y lies inside the amplituhedron, the integral is finite for any value of n . Indeed,

$$s \cdot Y = s \cdot (c_i Z_i) = c_i (s \cdot Z_i) > 0, \quad (4.25)$$

where we used the definition (3.20) and the associated positivity constraints. Hence the poles of the integrand always lie outside the integration region. Additionally, convergence of our representation is ensured by the behaviour of $(s \cdot Y)^{-(m+1)}$ at infinity. Secondly, it is clear that the integrand depends on the number of particles only through the θ -functions, shaping the domain of integration $\mathcal{D}_n^{(m)}$, while the number of integration variables depends uniquely on m : this is in stark contrast with other integral representations, see *e.g.* (3.58). Recall that the $\text{GL}(m+1, \mathbb{R})$ -covariance of the integral (4.20) allows us to fix $m+1$ bosonised momentum twistors to the identity: $\{Z_1, \dots, Z_{m+1}\} = \mathbf{1}_{m+1}$. From now on, we will work in this particular frame and only at the end of our calculation we will lift the results to be valid in general, relaxing this choice. In general, we can describe the domain of integration – convex as a consequence of positivity of the external data Z – as

$$\mathcal{D}_n^{(m)} = \bigcap_{i=1}^n \{s \cdot Z_i > 0\} = \bigcap_{i=m+2}^n \{s \cdot Z_i > 0\} \cap \{s > 0\}, \quad (4.26)$$

where $\{s > 0\}$ means that all s_A 's are positive, as dictated by the aforementioned fixing. We observe that

$$\Omega_{n,1}^{(m)} = m! \int_{\mathcal{D}_n^{(m)}} ds (s \cdot Y)^{-(m+1)} = \Omega_{n-1,1}^{(m)} - m! \int_{\mathcal{D}_{n-1}^{(m)} \cap \{s \cdot Z_n \leq 0\}} ds (s \cdot Y)^{-(m+1)}, \quad (4.27)$$

which will be extensively used later on. We also denote by ℓ_{Z_i} the $(m-1)$ -dimensional subspaces defined by $s \cdot Z_i = 0$ through the θ -functions.

4.3 Applying the master formula

In this section we present a detailed analysis of the volume integral for $k = 1$. Although scattering amplitudes in planar $\mathcal{N} = 4$ SYM correspond to the case $m = 4$, we find it advantageous to first focus on the $m = 2$ setting. In this case, (4.23) takes the explicit form

$$\Omega_{n,1}^{(2)} = \int_0^{+\infty} ds_2 \int_0^{+\infty} ds_3 \frac{2}{(s \cdot Y)^3} \prod_{i=4}^n \theta(s \cdot Z_i) , \quad (4.28)$$

as compared to the physical case

$$\Omega_{n,1}^{(4)} = \int_0^{+\infty} ds_2 \int_0^{+\infty} ds_3 \int_0^{+\infty} ds_4 \int_0^{+\infty} ds_5 \frac{4!}{(s \cdot Y)^5} \prod_{i=6}^n \theta(s \cdot Z_i) , \quad (4.29)$$

to be discussed later on.

4.3.1 Volume in the $m = 2$ case

As already stated in (3.42), a representation of the volume function $\Omega_{n,1}^{(2)}$ is given by [51]

$$\Omega_{n,1}^{(2)} = \sum_{i=2}^{n-1} [1 \ i \ i+1] , \quad \text{with} \quad [i \ j \ k] = \frac{\langle i \ j \ k \rangle^2}{\langle Y \ i \ j \rangle \langle Y \ j \ k \rangle \langle Y \ k \ i \rangle} . \quad (4.30)$$

We will verify that formula (4.28) exactly reproduces this result.

Three points No θ -functions are present in this case and we have to evaluate the integral

$$\Omega_{3,1}^{(2)} = \int_0^{+\infty} ds_2 \int_0^{+\infty} ds_3 \frac{2}{(Y^1 + s_2 Y^2 + s_3 Y^3)^3} , \quad (4.31)$$

where clearly the integration domain $\mathcal{D}_3^{(2)}$ is simply the positive quadrant, see Figure 4.1. As discussed in (4.25), the integrand does not have poles inside $\mathcal{D}_3^{(2)}$. By performing the integral we simply find

$$\Omega_{3,1}^{(2)} = \frac{1}{Y^1 Y^2 Y^3} . \quad (4.32)$$

There is a unique way to lift this formula to the case of generic Z_i by rewriting it in terms of $\text{SL}(3, \mathbb{R})$ -invariant brackets with the proper scaling:

$$\Omega_{3,1}^{(2)} = \frac{\langle 123 \rangle^2}{\langle Y 12 \rangle \langle Y 23 \rangle \langle Y 31 \rangle} = [123] , \quad (4.33)$$

in agreement with formula (4.30).

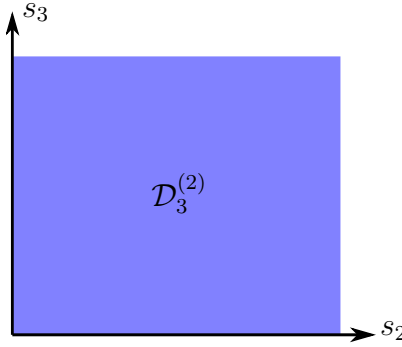


Figure 4.1: Domain of integration at three points.

Four points This is the first non-trivial case, featuring a single θ -function. Explicitly,

$$\Omega_{4,1}^{(2)} = \int_0^{+\infty} ds_2 \int_0^{+\infty} ds_3 \frac{2}{(Y^1 + s_2 Y^2 + s_3 Y^3)^3} \theta(Z_4^1 + s_2 Z_4^2 + s_3 Z_4^3) . \quad (4.34)$$

Demanding positivity of the external data, we see that the components of Z_4 must satisfy $Z_4^1 > 0$, $Z_4^2 < 0$ and $Z_4^3 > 0$. Then, the θ -function simply describes a half-plane in the (s_2, s_3) -plane above the line $\ell_{Z_4} : s \cdot Z_4 = 0$, which has positive slope and intersects the positive s_2 -semiaxis, see Figure 4.2. It is straightforward to evaluate the integral (4.34)

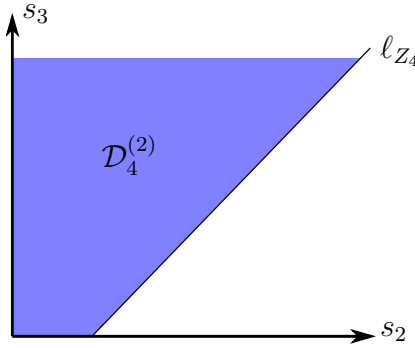


Figure 4.2: Domain of integration for four points.

explicitly, however – in order to make contact with results known in the literature – it is useful to think of the domain $\mathcal{D}_4^{(2)}$ in two different ways, depicted in Figure 4.3. On the one hand, we can split the integration region as in Figure 4.3a, leading to the local (internal) triangulation [51]

$$\Omega_{4,1}^{(2)} = \{3\} + \{4\} , \quad \text{with} \quad \{i\} = \frac{\langle 12i \rangle \langle i-1 \ i \ i+1 \rangle}{\langle Y12 \rangle \langle Y \ i-1 \ i \rangle \langle Y \ i \ i+1 \rangle} . \quad (4.35)$$

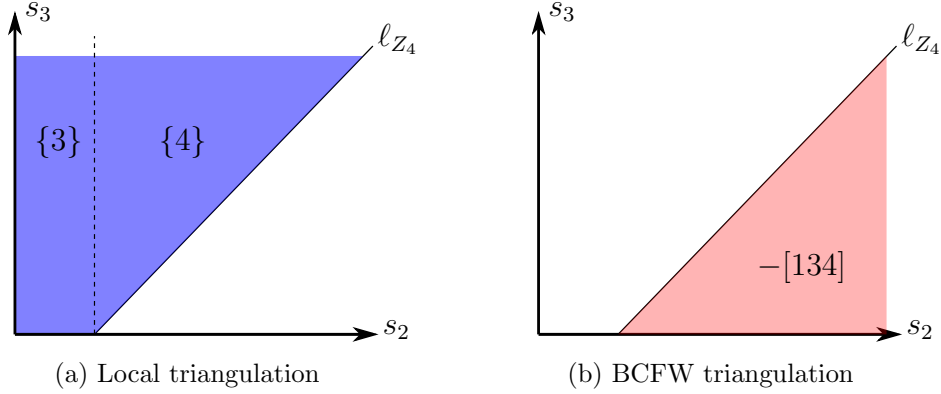


Figure 4.3: Two ways of calculating the four-point integral.

Alternatively, we can obtain it as the difference of $\mathcal{D}_3^{(2)}$ with the region shown in Figure 4.3b. This choice produces an external triangulation, agreeing with the terms coming from BCFW recursion relations:

$$\Omega_{4,1}^{(2)} = [123] + [134]. \quad (4.36)$$

We remark that – in order to be able to perform the integral over the region in Figure 4.3b – one needs to additionally assume that the integrand does not have any pole there, since it is not ensured by the geometry of the amplituhedron.

When the number of points is increased, the presence of more θ -functions guarantees that the domain of integration shrinks, as already explained in [114]. Let us show it on the five-point example. For concreteness, let us choose the following positive configuration

$$Z_4^A = (1, -1, 1)^T, \quad Z_5^A = (3, -2, 1)^T, \quad (4.37)$$

determining the integration domain in Figure 4.4a. As before, we can construct both an internal and an external triangulation (Figure 4.4b and 4.4c, respectively), yielding the known result

$$\Omega_{5,1}^{(2)} = \{3\} + \{4\} + \{5\} = [123] + [134] + [145]. \quad (4.38)$$

General pattern From these examples, we see an elegant pattern emerging. For $m = 2$, the second summand in (4.27) is in fact just an integral over the wedge

$$\mathcal{D}_{n-1}^{(2)} \cap \{s \cdot Z_n \leq 0\} = \{s \cdot Z_{n-1} > 0\} \cap \{s \cdot Z_n \leq 0\}, \quad (4.39)$$

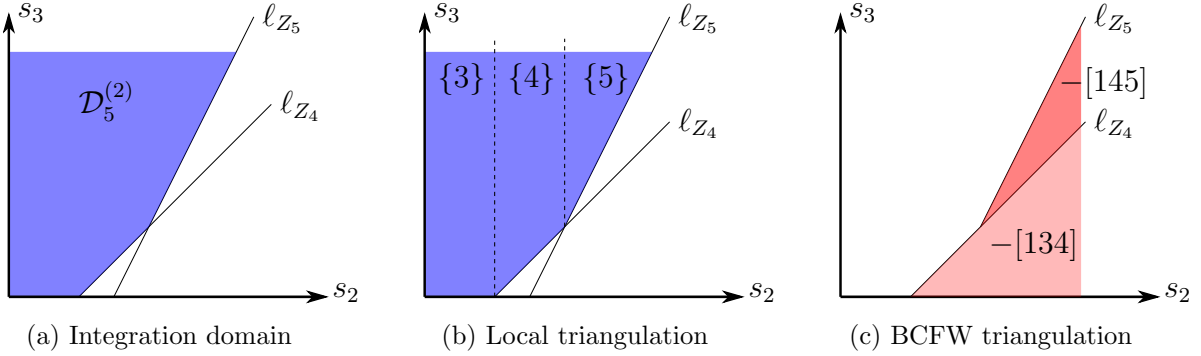


Figure 4.4: The domain $\mathcal{D}_5^{(2)}$ and the two ways of triangulating it.

depicted as the red-shaded area in Figure 4.5. It always evaluates to an R-invariant

$$\int_{\{s \cdot Z_{n-1} > 0\} \cap \{s \cdot Z_n \leq 0\}} ds (s \cdot Y)^{-3} = -[1\ n - 1\ n] . \quad (4.40)$$

This gives a relation between the volume integral (4.23) and the BCFW decomposition of amplitudes for $k = 1$. However, as we pointed out, there is no need to perform this triangulation in order to evaluate the integral (4.23). This fact is even more relevant in the $m = 4$ case, where the BCFW triangulation is more complicated.

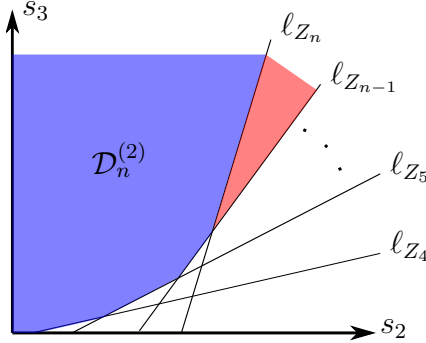


Figure 4.5: Generic domain of integration for n points. We marked in red the wedge which evaluates to (minus) the R-invariant $[1\ n - 1\ n]$.

4.3.2 Volume in the $m = 4$ case

Once again, NMHV volume functions are given by [51]

$$\Omega_{n,1}^{(4)} = \frac{1}{2} \sum_{i,j} [1\ i\ i + 1\ j\ j + 1] = \sum_{i < j} [1\ i\ i + 1\ j\ j + 1] , \quad (4.41)$$

where the R-invariants are defined as

$$[i j k l m] = \frac{\langle i j k l m \rangle^4}{\langle Y i j k l \rangle \langle Y j k l m \rangle \langle Y k l m i \rangle \langle Y l m i j \rangle \langle Y m i j k \rangle} . \quad (4.42)$$

In the following we will check that formula (4.29) yields this result.

Five points The simplest computable volume function involves five particles. This case is the direct generalisation of the three-point volume for $m = 2$, since no θ -functions appear in the integrand of (4.29):

$$\Omega_{5,1}^{(4)} = \int_0^{+\infty} ds_2 \int_0^{+\infty} ds_3 \int_0^{+\infty} ds_4 \int_0^{+\infty} ds_5 \frac{4!}{(Y^1 + s_2 Y^2 + s_3 Y^3 + s_4 Y^4 + s_5 Y^5)^5} . \quad (4.43)$$

The domain of integration is just the region of the four-dimensional real space where all coordinates are positive. The usual argument ensures that the integral is completely well defined and we find

$$\Omega_{5,1}^{(4)} = \frac{1}{Y^1 Y^2 Y^3 Y^4 Y^5} , \quad (4.44)$$

which lifts to the non-fixed form

$$\Omega_{5,1}^{(4)} = \frac{\langle 12345 \rangle^4}{\langle Y 1234 \rangle \langle Y 2345 \rangle \langle Y 3451 \rangle \langle Y 4512 \rangle \langle Y 5123 \rangle} = [12345] , \quad (4.45)$$

as expected.

Six points Formula (4.29) reads in this case

$$\Omega_{6,1}^{(4)} = 4! \int_0^{+\infty} ds_2 \int_0^{+\infty} ds_3 \int_0^{+\infty} ds_4 \int_0^{+\infty} ds_5 \frac{\theta(Z_6^1 + s_2 Z_6^2 + s_3 Z_6^3 + s_4 Z_6^4 + s_5 Z_6^5)}{(Y^1 + s_2 Y^2 + s_3 Y^3 + s_4 Y^4 + s_5 Y^5)^5} . \quad (4.46)$$

To simplify the discussion, we can again choose a particular positive configuration of external data. Let

$$Z_6^A = (1, -1, 1, -1, 1)^\top , \quad (4.47)$$

so that the θ -function defines the hyperplane $\ell_{Z_6} : 1 - s_2 + s_3 - s_4 + s_5 = 0$. Solving the constraint, we can rewrite (4.46) as

$$\Omega_{6,1}^{(4)} = 4! \int_0^{+\infty} ds_3 \int_0^{+\infty} ds_5 \int_0^{1+s_3+s_5} ds_2 \int_0^{1-s_2+s_3+s_5} ds_4 (s \cdot Y)^{-5} , \quad (4.48)$$

which can be easily evaluated and agrees with the correct result for six-point NMHV amplitude (4.41). In order to relate the integral (4.48) term-by-term with the BCFW recursion result

$$\Omega_{6,1}^{(4)} = [12345] + [12356] + [13456], \quad (4.49)$$

let us observe that

$$[12345] = 4! \int_0^{+\infty} ds_3 \int_0^{+\infty} ds_5 \int_0^{+\infty} ds_2 \int_0^{+\infty} ds_4 (s \cdot Y)^{-5}, \quad (4.50)$$

$$[12356] = -4! \int_0^{+\infty} ds_3 \int_0^{+\infty} ds_5 \int_0^{+\infty} ds_2 \int_{a-s_2}^{+\infty} ds_4 (s \cdot Y)^{-5}, \quad (4.51)$$

$$[13456] = 4! \int_0^{+\infty} ds_3 \int_0^{+\infty} ds_5 \int_a^{+\infty} ds_2 \int_{a-s_2}^0 ds_4 (s \cdot Y)^{-5}, \quad (4.52)$$

where $a = 1 + s_3 + s_5 > 0$. It is enough to focus on the integration regions in the (s_2, s_4) -plane since the remaining two variables are integrated over $(0, +\infty)$ in all cases. There the hyperplane ℓ_{Z_6} is represented as a line, the domain of $[12345]$ is simply the positive quadrant, whereas those of $[12356]$ and $[13456]$ are depicted in Figure 4.6. Figure 4.7 shows that the various domains correctly add up to the integration region of $\Omega_{6,1}^{(4)}$, as parametrised in (4.48).

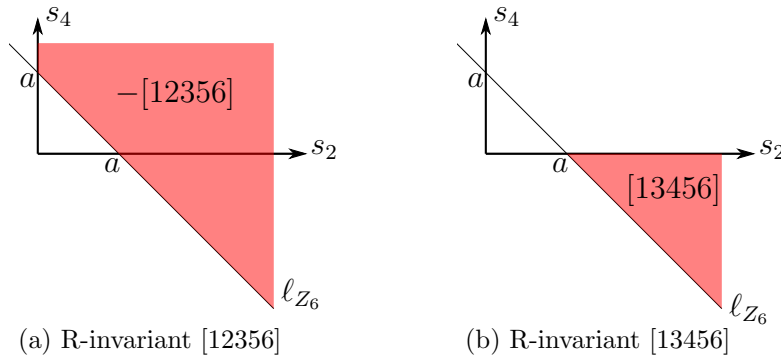


Figure 4.6: Two contributions to the domain of integration for $\Omega_{6,1}^{(4)}$.

For higher number of points the relation to BCFW recursion is more obscure since one has to study the full four-dimensional space in order to identify proper “triangles”: already at seven points, we could not produce any integral representation for all six relevant R-invariants which could be neatly projected down to two or three dimensions as in the above example. In particular, adding new particles does not simply correspond to removing a

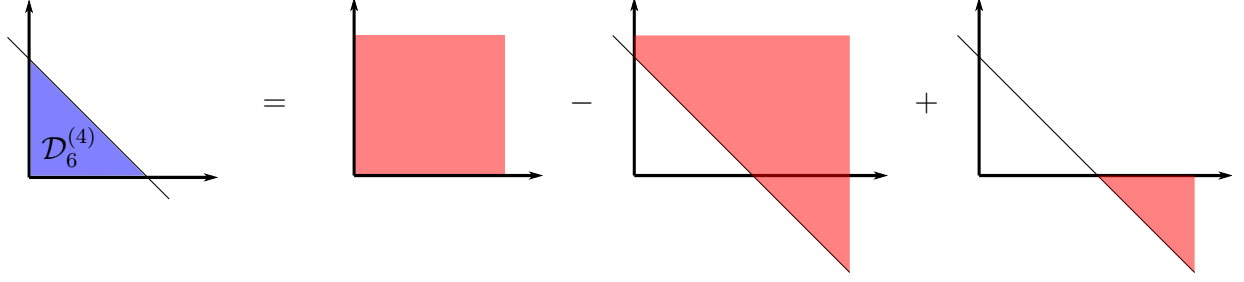


Figure 4.7: $\mathcal{D}_6^{(4)}$ obtained combining the domains of integrations corresponding to the BCFW terms for the six-point NMHV volume function.

single wedge as in Figure 4.5, since (4.39) does not hold anymore. This can be traced back to the difference between formulae (4.30) and (4.41): for $m = 2$ we always add one R-invariant when increasing the number of particles by one, while for $m = 4$ we need $n - 4$ new contributions. However, thanks to formula (4.29), we can be cavalier about this, since the volume can be computed directly without any reference to triangulations.

4.4 Deformations and higher- k amplituhedron volumes

One can consider some natural deformations of the equations we studied so far, drawing inspiration from those introduced in the context of amplitudes in [120, 121]. For $k = 1$ this amounts to more general scaling properties and formula (4.5) is replaced by

$$\sum_{A=1}^{m+1} Z_i^A \frac{\partial}{\partial Z_i^A} \Omega_{n,1}^{(m)}(Y, Z) = \alpha_i \Omega_{n,1}^{(m)}(Y, Z) , \quad \text{for } i = 1, \dots, n , \quad (4.53)$$

with

$$\sum_{i=1}^n \alpha_i = 0 . \quad (4.54)$$

Let us remark that we only modify the weight of the variables Z_i to match the deformed top-cell Grassmannian integral in [125, 129]. In the context of scattering amplitudes, the complex numbers α_i are related to the inhomogeneities of an integrable spin chain, as explained in [130, 57] and level-one Yangian generators (4.18) get modified by local terms with inhomogeneities. In this generalised case, the solution to (4.2), (4.8) and (4.53) can also be found in [126] and reads

$$\Omega_{n,1}^{(m)}(Y, Z) = \int ds_A e^{i s_A Y^A} \prod_i (s_A Z_i^A)_+^{\alpha_i} , \quad (4.55)$$

where

$$x_+^\alpha = \begin{cases} x^\alpha, & x \geq 0 \\ 0, & x < 0 \end{cases} \quad (4.56)$$

is the distribution generalising the Heaviside step function. The integral (4.55) is a GKZ hypergeometric function and its properties were studied in *e.g.* [126]. Importantly, it is convergent for α_i close to zero and can be evaluated explicitly. We can verify at once that in the limit $\alpha_i \rightarrow 0$ the integral (4.55) smoothly approaches the one in (4.20).

Encouraged by the success in determining the volume formula for $k = 1$, it is natural to try to pursue a similar approach for $N^{k>1}$ MHV volume functions. First of all, similarly to the $k = 1$ case, the Capelli equations introduce two sets of natural variables and a general form of the solution can always be written as

$$\Omega_{n,k}^{(m)}(Y, Z) = \int ds_A^\alpha d\tilde{s}_\alpha^i e^{i s_A^\alpha Y_\alpha^A - i s_A^\alpha Z_i^A \tilde{s}_\alpha^i} F(s, \tilde{s}) . \quad (4.57)$$

Then, demanding that all Y_α^A localise on the hyperplanes defined by the external data, namely

$$Y_\alpha^A = \tilde{s}_\alpha^i Z_i^A , \quad (4.58)$$

we again obtain that the function $F(s, \tilde{s})$ is in fact independent on s_A^α and we can derive the following representation:

$$\Omega_{n,k}^{(m)}(Y, Z) = \int ds_A^\alpha e^{i s_A^\alpha Y_\alpha^A} \tilde{F}(s_A^\alpha Z_i^A) . \quad (4.59)$$

Now the variables s_A^α are coordinates on a proper dual Grassmannian $G(k, m+k)$, generalising the dual projective space of the NMHV setting. The function $\tilde{F}(s_A^\alpha Z_i^A)$ involves $k \cdot n$ variables and the scaling property (4.6) implies that it depends on them through their $\text{SL}(k, \mathbb{R})$ -invariant combinations

$$\{i_1 \cdots i_k\} = \det \left((s \cdot Z)_{i_1}, \dots, (s \cdot Z)_{i_k} \right) , \quad (4.60)$$

where the compact notation $(s \cdot Z)_i$ is to be understood as in formula (4.59). Unfortunately, the additional constraints coming from (4.5) and (4.6) are not enough to fix the final answer uniquely, since \tilde{F} is now allowed to be an arbitrary function of what we will generically call *cross-ratios*, weightless ratios of the brackets (4.60), *e.g.* for $k = 2$

$$\frac{\{i_1 i_2\} \{i_3 i_4\}}{\{i_1 i_3\} \{i_2 i_4\}} , \frac{\{i_1 i_3\} \{i_3 i_4\} \{i_5 i_6\}}{\{i_1 i_5\} \{i_3 i_4\} \{i_3 i_6\}} , \dots \quad (4.61)$$

We should mention that solutions to several higher-order systems of Capelli equations supplemented by certain covariance and scaling properties can be found in the literature [127]. Their integral representations in terms of the variables parametrising the dual Grassmannian variables are finite and can be computed for any value of the parameter n . Unfortunately – as anticipated – these are not relevant for tree-level volume functions due to different scaling behaviours. In order to proceed further, help might come from additional symmetries, such as Yangian invariance, which already proved useful in the Grassmannian formulation of scattering amplitudes. This will be the subject of Chapter 5.

Chapter 5

Yangian symmetry for the tree-level amplituhedron

The amplituhedron is defined in a purely bosonic space, whose elements can be obtained from momentum supertwistors by bosonisation of the Grassmann-odd components χ_i^A . Surprisingly, although this new set of variables makes certain geometric properties of the amplitude manifest – *e.g.* it provides an explanation for the cancellation of spurious singularities, beside explaining the presence of physical poles in terms of boundaries of the amplituhedron – it obscures some of the algebraic ones. In particular, it was not clear how Yangian symmetry would be realised in this space. Indeed, the natural idea of trying to trade the supertwistors in (2.74) for their bosonised counterparts does not yield good level-one generators of $Y(\mathfrak{gl}(m+k))$ beyond $k=1$. More generally, it is not obvious that volume functions are Yangian invariants at all, since in going from them to the amplitudes we need to perform the fermionic integrations (3.32), projecting out many terms as the last k components of the Z_i are taken to be composite Grassmann variables. From the perspective of [54] and Chapter 4, this fact is the main obstacle to circumvent in order to be able to derive a volume formula for generic tree-level volume functions.

In this chapter we present the solution to this long-standing problem, first appeared in [56]. Although the generators of $Y(\mathfrak{gl}(m+k))$ do not annihilate $\Omega_{n,k}^{(m)}$, the expressions we get belong to the kernel of a simple differential operator. As a result, we will prove that there exists a matrix of functions closely related to the amplituhedron volume function which is invariant under the Yangian of $\mathfrak{gl}(m+k)$. To this purpose, we follow the steps of [57], where Yangian invariants relevant for tree-level amplitudes in $\mathcal{N}=4$ SYM have been obtained using the Quantum Inverse Scattering Method. Indeed, the infinite-dimensional symmetry

algebra governing planar $\mathcal{N} = 4$ SYM allows us to employ methods and techniques proper to (or inspired by) integrable theories. The first step in this direction was taken in [120, 121]: there, a deformation of scattering amplitudes in terms of a spectral parameter was proposed by considering Yangian generators relevant to inhomogeneous spin chains. This has led, in particular, to a systematic approach for the construction of Yangian invariants relevant to scattering amplitudes from an underlying spin chain description [57, 130, 131, 132]. This story generalizes to the amplituhedron, as we will soon show.

Since we will make use of some concepts coming from the realm of exactly soluble systems, we will devote Section 5.1 to the discussion of the Heisenberg $\text{XXX}_{1/2}$ spin chain. It is one of the most well studied integrable models and it will give us the opportunity to review the *algebraic Bethe ansatz* technique, which will echo in our derivations. To keep this introduction reasonably short, we will collect some computational details and proofs in Appendix B.¹ Going back to the amplituhedron in Section 5.2, we will explain how is it possible to obtain any volume function $\Omega_{n,k}^{(m)}$ acting with some appropriately defined operators on a special object: such action can be graphically interpreted as the addition of a BCFW bridge, yielding a diagrammatics having much in common with that of Section 2.5.3. Finally, in Section 5.3 we will show that it is possible to construct a spin chain for the tree amplituhedron, from which to extract the level-zero and level-one generators of the relevant Yangian. Appendix C will include some technical details.

5.1 The Heisenberg isotropic spin chain and the algebraic Bethe ansatz

5.1.1 Introduction

We consider the prototype of integrable systems, namely the isotropic spin- $\frac{1}{2}$ Heisenberg quantum spin chain, also known as $\text{XXX}_{1/2}$ spin chain. The Heisenberg model was introduced to describe magnetism in solid state physics; its one-dimensional version was considered by Hans Bethe in a seminal paper [135] that inaugurated the study of quantum integrability and of the methods collectively going under the name of *Bethe ansatz*.

A spin chain is a one-dimensional lattice comprising N sites. At each one of those, a quantum magnetic needle is free to rotate: if we assume the spin to be $\frac{1}{2}$, its space of states

¹For additional details we refer to the reviews [133, 134].

is $V = \mathbb{C}^2$ and the natural choice for a basis is clearly

$$|\uparrow\rangle = \begin{pmatrix} 1 \\ 0 \end{pmatrix} \quad , \quad |\downarrow\rangle = \begin{pmatrix} 0 \\ 1 \end{pmatrix} . \quad (5.1)$$

The space of states will then be given by the vector space $V = V_1 \otimes \cdots \otimes V_N = (\mathbb{C}^2)^{\otimes N}$. The physics of the model will depend on the spin operators $\vec{S}_i = (S_i^1, S_i^2, S_i^3)$, expressed in the two-dimensional, fundamental representation of the $\mathfrak{su}(2)$ algebra, *i.e.* $\vec{S}_i = \frac{1}{2}\vec{\sigma}_i$. The subscript refers to the fact that \vec{S}_i acts uniquely on the spin state at the corresponding site and will commute with any other operator \vec{S}_j with $i \neq j$. Indeed the subscript notation is short for

$$\vec{S}_i = \mathbf{1} \otimes \cdots \otimes \underbrace{\frac{1}{2}\vec{\sigma}}_{i\text{-th site}} \otimes \cdots \otimes \mathbf{1} . \quad (5.2)$$

At times it will be useful to employ raising and lowering operators, defined as follows:

$$S_i^\pm = S_i^1 \pm iS_i^2 \quad \text{i.e.} \quad S_i^+ = \begin{pmatrix} 0 & 1 \\ 0 & 0 \end{pmatrix}_i , \quad S_i^- = \begin{pmatrix} 0 & 0 \\ 1 & 0 \end{pmatrix}_i . \quad (5.3)$$

We will assume that every spin interacts only with its nearest neighbours. The Hamiltonian for an XXX spin chain with N sites – involving a constant shift chosen for later convenience – is

$$\mathcal{H}_N = J \sum_i \left(\frac{1}{4} \mathbf{1}^{\otimes N} - \vec{S}_i \cdot \vec{S}_{i+1} \right) = J \sum_i H_{ii+1} , \quad (5.4)$$

where we stress that in fact \mathcal{H}_N is just the sum of two-site Hamiltonians and J is a positive constant in the ferromagnetic case.² $\vec{S}_i \cdot \vec{S}_{i+1}$ denotes the scalar product of the two vectors in the tensor space of two spins $V_i \otimes V_{i+1}$, *i.e.*

$$\vec{S}_i \cdot \vec{S}_{i+1} = S_i^1 S_{i+1}^1 + S_i^2 S_{i+1}^2 + S_i^3 S_{i+1}^3 = \mathbf{1} \otimes \cdots \otimes \left(\frac{1}{4} \sum_{k=1}^3 \sigma_k \otimes \sigma_k \right) \otimes \cdots \otimes \mathbf{1} . \quad (5.5)$$

Let us discuss boundary conditions: the XXX spin chain can only be open or closed, the latter topology being customarily chosen, because it makes calculations easier. In fact, it is a slightly unphysical choice, since there is no reason for the spins at the opposite ends of a (typically long) chain to have anything to do with each other. Nevertheless,

²Had we chosen to have different constants J_1, J_2, J_3 in front of the different components of the scalar product, we would have obtained the (non-isotropic) XYZ model.

thermodynamic properties are independent of such details as long as the interactions are short-ranged: it is therefore justified to impose periodic boundary conditions, letting the sum in (5.4) run over $i = 1, \dots, N$ and performing the identification $\vec{S}_{N+1} = \vec{S}_1$.

Solving the system means computing the spectrum of the Hamiltonian together with its eigenstates. The total-spin operator $\vec{S}_{\text{tot}} = \sum_i \vec{S}_i$ commutes with \mathcal{H}_N , in particular $[S_{\text{tot}}^3, \mathcal{H}_N] = 0$: hence the eigenstates of the Hamiltonian will arrange themselves in multiplets of the symmetry algebra. It is immediate to check that the state $|\Omega\rangle = |\uparrow\uparrow\cdots\uparrow\rangle$ is the ground state of the system and has zero energy thanks to the constant shift introduced in \mathcal{H}_N . Its excited states will involve a certain number of flipped spins, obtained acting with the S_i^- on $|\Omega\rangle$ and they will not mix with others involving a different number of flipped spins, due to the conservation of S_{tot}^3 : they can be interpreted as quasiparticles, called *magnons*, propagating along the chain.

Let us introduce the *permutation operators*

$$\begin{aligned} \mathcal{P}_{ij}: \quad V &\rightarrow V \\ \vec{x}_i \otimes \vec{y}_j &\mapsto \vec{y}_i \otimes \vec{x}_j \end{aligned} \quad (5.6)$$

In the canonical basis of the $\mathbb{C}^2 \otimes \mathbb{C}^2$ subspace on which they act non-trivially, they have the matrix representation

$$\mathcal{P}_{ij} = \frac{1}{2} \left(\mathbb{1} \otimes \mathbb{1} + \sum_{k=1}^3 \sigma_k \otimes \sigma_k \right) = \begin{pmatrix} 1 & 0 & 0 & 0 \\ 0 & 0 & 1 & 0 \\ 0 & 1 & 0 & 0 \\ 0 & 0 & 0 & 1 \end{pmatrix}. \quad (5.7)$$

A more versatile definition of permutation operators, to be employed when studying higher-dimensional representation of the symmetry algebra, is discussed in Appendix B. It allows to quickly prove that they all square to the identity (intuitively) and, more importantly, that not all pairs of permutation operators commute with each other. From now on, we will often restrict our attention to those of the form \mathcal{P}_{ii+1} : it is immediate to understand that $[\mathcal{P}_{ii+1}, \mathcal{P}_{jj+1}] = 0$ if $i = j$ or $\{i, i+1\} \cap \{j, j+1\} = \emptyset$; moreover we have the relations

$$\begin{aligned} \mathcal{P}_{i-1i} \mathcal{P}_{ii+1} &= \mathcal{P}_{i-1,i+1} \mathcal{P}_{i-1i} = \mathcal{P}_{ii+1} \mathcal{P}_{i-1,i+1} \\ \mathcal{P}_{ii+1} \mathcal{P}_{i-1i} &= \mathcal{P}_{i-1,i+1} \mathcal{P}_{ii+1} = \mathcal{P}_{i-1i} \mathcal{P}_{i-1,i+1} \end{aligned} \quad (5.8)$$

Given the form (5.7), we observe that the Hamiltonian of the spin chain can be rewritten as

$$\mathcal{H}_N = \frac{J}{2} \sum_i (\mathbb{1}^{\otimes N} - \mathcal{P}_{ii+1}) \quad (5.9)$$

Another useful tool to introduce is the operator $\mathcal{U}_N = \mathcal{P}_{12}\mathcal{P}_{23}\cdots\mathcal{P}_{N-1N}$. From the defining property

$$\mathcal{P}_{ij}(X_i Y_j) = Y_i X_j \quad \longrightarrow \quad \mathcal{P}_{ij} X_j \mathcal{P}_{ij} = X_i , \quad (5.10)$$

we easily obtain

$$\begin{aligned} X_i \mathcal{U}_N &= \mathcal{P}_{12} \cdots X_i \mathcal{P}_{i-1i} \mathcal{P}_{ii+1} \cdots \mathcal{P}_{N-1N} = \\ &= \mathcal{P}_{12} \cdots \mathcal{P}_{i-1i} X_{i-1} \mathcal{P}_{ii+1} \cdots \mathcal{P}_{N-1N} = \mathcal{U}_N X_{i-1} . \end{aligned} \quad (5.11)$$

Hence \mathcal{U}_N is called *shift operator*: when acting on a generic state of V , it effectively shifts all spins by one site.³ Applying it enough times, then, one comes back to the initial state of the chain: specifically, $(\mathcal{U}_N)^N = \mathbb{1}$, implying that its eigenvalues are the N -th roots of unity. Furthermore, the shift operator is unitary, since the permutation operators are their own complex conjugates and square to the identity. Its most important property, however, is that it commutes with the Hamiltonian of the system:

$$[\mathcal{U}_N, \mathcal{H}_N] = -\frac{J}{2} \sum_{i=1}^N [\mathcal{U}_N, \mathcal{P}_{ii+1}] = 0 , \quad (5.12)$$

see Appendix B for a proof. The commutator would not vanish, were it not for the periodic boundary conditions.

The meaning of this result is that \mathcal{U}_N is the lattice version of the translation operator, producing a shift along one site of the spin chain instead of an infinitesimal one, namely $\mathcal{U}_N^{-1} X_i \mathcal{U}_N = X_{i-1}$. The generator of translational symmetry, *i.e.* the momentum P , is then related to \mathcal{U}_N via

$$\mathcal{U}_N = e^{iP} \quad \longleftrightarrow \quad P = -i \log \mathcal{U}_N . \quad (5.13)$$

Despite the simplicity of the system, diagonalizing the Hamiltonian \mathcal{H}_N – a $2^N \times 2^N$ matrix – is a computationally intractable task already for fairly small values of N . This motivated the development of several other methods, going under the name of *Bethe ansatz* in one of its various declinations. The original approach by Bethe is nowadays known as *coordinate Bethe ansatz*; in the following we will rather focus on the *algebraic Bethe ansatz* developed by the ‘Leningrad School’ under the guide of Ludwig Faddeev, since a similar formalism will be of use in the amplituhedron context as well.

³ \mathcal{U}_N is a right-shift operator and one could of course define a left-shift operator as well, but this detail will not be relevant for us.

5.1.2 Lax operators, R-matrices, monodromy and transfer matrix

In the classical study of the integrable Korteweg–de Vries system, some linear operators appear in the auxiliary spectral problem of the classical inverse scattering method, called *Lax operators*. In this quantum context they also play a central role and their definition requires the introduction of an auxiliary space, typically chosen to be the vector space on which the fundamental representation of the symmetry algebra acts, hence $V_a = \mathbb{C}^2$ in our case. The Lax operator is an endomorphism of the tensor space $V_a \otimes V_i$ depending on a complex variable λ , called *spectral parameter*. We have the equivalent definitions

$$\begin{aligned} \mathcal{L}_{ai}(\lambda) &= \lambda \mathbb{1}_a \otimes \mathbb{1}_i + i \sum_{k=1}^3 \sigma_a^k \otimes S_i^k \\ &= \lambda \mathbb{1}_a \otimes \mathbb{1}_i + i \left(\sum_{s=\pm} S_a^s \otimes S_i^{(-s)} + \sigma_a^3 \otimes S_i^3 \right). \end{aligned} \quad (5.14)$$

We can give further representations of the Lax operators. One can write \mathcal{L}_{ai} as a 2×2 matrix acting on the auxiliary space, with entries being in turn 2×2 matrices acting on the quantum space of the relevant spin: explicitly,

$$\mathcal{L}_{ai}(\lambda) = \begin{pmatrix} \lambda \mathbb{1} + i S_i^3 & i S_i^- \\ i S_i^+ & \lambda \mathbb{1} - i S_i^3 \end{pmatrix}_a. \quad (5.15)$$

Finally, since V_a and V_i coincide, it makes sense to introduce a permutation operator \mathcal{P}_{ai} on their tensor product, allowing for the handy rewriting

$$\mathcal{L}_{ai}(\lambda) = \left(\lambda - \frac{i}{2} \right) \mathbb{1}_a \otimes \mathbb{1}_i + i \mathcal{P}_{ai}. \quad (5.16)$$

The Lax operator can be thought of as a connection on the one-dimensional lattice. If $\psi_i = (\psi_i^1 \ \psi_i^2)_a^T \in V_a \otimes V_i$ are vectors associated to each lattice site, then we say that ψ_i is parallel if the Lax equation

$$\psi_{i+1} = \mathcal{L}_{ai} \psi_i \quad (5.17)$$

holds. Then multiplying several “consecutive” Lax operators, building $\mathcal{L}_{an_2} \cdots \mathcal{L}_{an_1}$, allows to define transport from site n_1 to site $n_2 + 1$ and one can move all the way round the chain with the *monodromy matrix*

$$\mathcal{M}_a(\lambda) = \mathcal{L}_{aN}(\lambda) \mathcal{L}_{aN-1} \cdots \mathcal{L}_{a1}(\lambda), \quad (5.18)$$

defined on $V_a \otimes V_1 \otimes \cdots \otimes V_N$. It is a matrix product on the auxiliary space, but the resulting matrix elements are tensor products (after all, the matrix entries of each Lax operator factor act non trivially only on the associated V_i space). Lax operators constructed out of different auxiliary spaces but the same quantum space do not commute: this is encoded in the Yang–Baxter equation on $V_{a_1} \otimes V_{a_2} \otimes V_i$

$$\mathcal{R}_{a_1 a_2}(\lambda_1 - \lambda_2) \mathcal{L}_{a_1 i}(\lambda_1) \mathcal{L}_{a_2 i}(\lambda_2) = \mathcal{L}_{a_2 i}(\lambda_2) \mathcal{L}_{a_1 i}(\lambda_1) \mathcal{R}_{a_1 a_2}(\lambda_1 - \lambda_2) , \quad (5.19)$$

where we introduced another object, analogous to the Lax operators, called *R-matrix*. Its precise definition is

$$\begin{aligned} \mathcal{R}_{ab}(\lambda) &= \left(\lambda + \frac{i}{2} \right) \mathbb{1}_a \otimes \mathbb{1}_b + 2i \sum_{k=1}^3 S_a^k \otimes S_b^k \\ &= \left(\lambda + \frac{i}{2} \right) \mathbb{1}_a \otimes \mathbb{1}_b + i \left(S_a^+ \otimes S_b^- + S_a^- \otimes S_a^+ + 2S_a^3 \otimes S_b^3 \right) , \end{aligned} \quad (5.20)$$

or in matrix form

$$\mathcal{R}_{ab}(\lambda) = \begin{pmatrix} (\lambda + \frac{i}{2})\mathbb{1} + iS_b^3 & iS_b^- \\ iS_b^+ & (\lambda + \frac{i}{2})\mathbb{1} - iS_b^3 \end{pmatrix}_a . \quad (5.21)$$

Finally, the last matrix representations make it obvious that

$$\mathcal{R}_{ab}(\lambda) = \lambda \mathbb{1}_a \otimes \mathbb{1}_b + i\mathcal{P}_{ab} , \quad (5.22)$$

from which another Yang–Baxter equation follows:

$$\mathcal{R}_{ab}(\lambda_a - \lambda_b) \mathcal{R}_{ac}(\lambda_a - \lambda_c) \mathcal{R}_{bc}(\lambda_b - \lambda_c) = \mathcal{R}_{bc}(\lambda_b - \lambda_c) \mathcal{R}_{ac}(\lambda_a - \lambda_c) \mathcal{R}_{ab}(\lambda_a - \lambda_b) . \quad (5.23)$$

Let us stress that the indices a, b, c need not be related to auxiliary spaces only: \mathcal{R} -matrices are defined also on the tensor spaces $V_i \otimes V_j$. Finally, it is clear that (5.19) implies the existence of a Yang–Baxter equation for the monodromy matrices as well:

$$\mathcal{R}_{ab}(\lambda - \lambda') \mathcal{M}_a(\lambda) \mathcal{M}_b(\lambda') = \mathcal{M}_b(\lambda') \mathcal{M}_a(\lambda) \mathcal{R}_{ab}(\lambda - \lambda') . \quad (5.24)$$

We are now ready to introduce the last bit of notation and understand why our model is integrable. We have seen how the monodromy matrix can be thought as a 2×2 matrix on the auxiliary space, i.e.

$$\mathcal{M}_a(\lambda) = \begin{pmatrix} A(\lambda) & B(\lambda) \\ C(\lambda) & D(\lambda) \end{pmatrix}_a , \quad (5.25)$$

where clearly the entries are polynomials of degree N in the spectral parameter. The transfer matrix is defined taking its trace:

$$T(\lambda) = \text{tr}_a (\mathcal{M}_a(\lambda)) = A(\lambda) + D(\lambda) . \quad (5.26)$$

This is a matrix on the space $V = V_1 \otimes \cdots \otimes V_N$.

Both the shift operator \mathcal{U}_N and the Hamiltonian \mathcal{H}_N can be extracted from the transfer matrix (see Appendix B for the proof):

$$\mathcal{U}_N = i^{-N} T\left(\frac{i}{2}\right) , \quad \mathcal{H}_N = J \left(\frac{N}{2} - \frac{i}{2} \frac{d}{d\lambda} \log T(\lambda) \Big|_{\lambda=\frac{i}{2}} \right) . \quad (5.27)$$

Therefore, if we can diagonalise the transfer matrix, we immediately solve the spectral problem for \mathcal{H}_N as well. Furthermore, transfer matrices commute at different values of the spectral parameter. First, we need to multiply (5.24) by the inverse of the \mathcal{R}_{ab} matrix, then we take the double trace over the two auxiliary spaces, obtaining

$$\text{tr}_a \left(\text{tr}_b (\mathcal{M}_a(\lambda) \mathcal{M}_b(\lambda')) \right) = \text{tr}_a \left(\text{tr}_b \left((\mathcal{R}_{ab}(\lambda - \lambda'))^{-1} \mathcal{M}_b(\lambda') \mathcal{M}_a(\lambda) \mathcal{R}_{ab}(\lambda - \lambda') \right) \right) , \quad (5.28)$$

which by the cyclicity property of the trace implies

$$[T(\lambda), T(\lambda')] = 0 . \quad (5.29)$$

Due to the polynomial nature of the transfer matrices, this commutator ensures that we have N quantities in involution, which is Liouville's definition of classical integrability. In fact, there is a subtlety here, since the next-to-leading term of (5.26) vanishes. However, we can define \mathcal{Q}_{N-1} to be *e.g.* the third component of the total spin – as it commutes with \mathcal{H}_N and thus with $T(\lambda)$ – and recover N mutually commuting charges.

5.1.3 The ansatz and the Bethe equations

Given the results of the previous section, our goal is to diagonalise the transfer matrix $T(\lambda)$. We will present the results in a rather quick fashion, referring as usual to Appendix B for further details. First of all, it is clear that the $C(\lambda)$ block of the monodromy matrix annihilates the ferromagnetic vacuum state $|\Omega\rangle = |\uparrow\rangle \otimes \cdots \otimes |\uparrow\rangle$, due to the presence of S_i^+ operators. Moreover, (5.15) shows that $|\Omega\rangle$ is an eigenvector of both $A(\lambda)$ and $D(\lambda)$:

$$\mathcal{M}_a(\lambda) |\Omega\rangle = \begin{pmatrix} (\lambda + \frac{i}{2})^N & \star \\ 0 & (\lambda - \frac{i}{2})^N \end{pmatrix} |\Omega\rangle , \quad (5.30)$$

where \star stands for something complicated originating from the action of $B(\lambda)$ on our reference state. Equation (5.30) immediately implies that $|\Omega\rangle$ is eigenvector of the transfer matrix as well:

$$T(\lambda) |\Omega\rangle = \left[\left(\lambda + \frac{i}{2} \right)^N + \left(\lambda - \frac{i}{2} \right)^N \right] |\Omega\rangle . \quad (5.31)$$

The all-spin-up configuration can then be thought of as the vacuum state of an harmonic oscillator. We will now argue that the $B(\lambda)$ block of the monodromy can be used as a raising operator and an ansatz for our physical states, or *Bethe states* is formulated as

$$|\psi\rangle = B(\lambda_1)B(\lambda_2) \cdots B(\lambda_n) |\Omega\rangle . \quad (5.32)$$

To study the action on $|\psi\rangle$ of the transfer matrix we need to derive the commutation rules relating the A, B, D operators. To this end we have to look back to the Yang–Baxter equation (5.24): by comparing homologous components on the two sides we find

$$B(\lambda)B(\lambda') = B(\lambda')B(\lambda) , \quad (5.33)$$

$$A(\lambda)B(\lambda') = f(\lambda - \lambda')B(\lambda')A(\lambda) + g(\lambda - \lambda')B(\lambda)A(\lambda') , \quad (5.34)$$

$$D(\lambda)B(\lambda') = h(\lambda - \lambda')B(\lambda')D(\lambda) + k(\lambda - \lambda')B(\lambda)D(\lambda') , \quad (5.35)$$

where we introduced the auxiliary functions

$$f(\xi) = \frac{\xi - i}{\xi} , \quad g(\xi) = \frac{i}{\xi} , \quad h(\xi) = \frac{\xi + i}{\xi} , \quad k(\xi) = -\frac{i}{\xi} . \quad (5.36)$$

It is clear from (5.33) that $|\psi\rangle$ must be a symmetric function of the spectral parameters $\lambda_1, \dots, \lambda_n$. Moreover, it would automatically be an eigenvector of the transfer matrix, were it not for the second summand on the right hand sides of (5.34) and (5.35). Indeed, when computing $T(\lambda) |\psi\rangle$, they generate some extra terms where one of the $B(\lambda_i)$ operators acting on the vacuum $|\Omega\rangle$ is replaced by $B(\lambda)$, which prevents us from reconstructing the potential eigenstate (more details will be given shortly). Demanding that these unwanted pieces cancel yields the *Bethe equations*, *i.e.* the conditions the λ_i 's must fulfil in order for $|\psi\rangle$ to be an eigenstate. They read

$$\left(\frac{\lambda_i + i/2}{\lambda_i - i/2} \right)^N = \prod_{k \neq i} \frac{\lambda_i - \lambda_k + i}{\lambda_i - \lambda_k - i} , \quad i = 1, \dots, n . \quad (5.37)$$

Then the Bethe state of (5.32) satisfies the eigenvalue equation

$$T(\lambda) |\psi\rangle = \left[\prod_{k=1}^n \left(\frac{\lambda - \lambda_k - i}{\lambda - \lambda_k} \right) \left(\lambda + \frac{i}{2} \right)^N + \prod_{k=1}^n \left(\frac{\lambda - \lambda_k + i}{\lambda - \lambda_k} \right) \left(\lambda - \frac{i}{2} \right)^N \right] |\psi\rangle . \quad (5.38)$$

We remark that the Bethe equations also ensure that the poles of the expression in square brackets cancel and the RHS is an analytic function of λ , just as the LHS is. Solutions to the Bethe equations are called *Bethe roots* and we demand that they be distinct from one another: this is sufficient to determine the spectrum of the transfer matrix. Moreover, allowing multiple roots would result in higher order poles to be removed from (5.38): this in turn would require more than n constraints.⁴

It is now possible to express the eigenvalues of various important observables in terms of the Bethe roots, making use of the fact that the corresponding operators are simultaneously diagonalised with the transfer matrix. First of all, let us consider the shift operator: based on the first equation in (5.27),

$$U(\{\lambda_j\}) = i^{-N} \Lambda\left(\frac{i}{2}, \{\lambda_j\}\right) = \prod_{k=1}^n \frac{\lambda_k + i/2}{\lambda_k - i/2}. \quad (5.39)$$

By (5.13), the spectrum of the total momentum operator $P = -i \log \mathcal{U}_N$ is

$$p(\{\lambda_j\}) = -i \sum_{k=1}^n \log \frac{\lambda_k + i/2}{\lambda_k - i/2}. \quad (5.40)$$

Always from (5.27), we can readily calculate the energy eigenvalues, finding

$$E(\{\lambda_j\}) = \frac{J}{2} \sum_{k=1}^n \frac{1}{\lambda_k^2 + \frac{1}{4}}. \quad (5.41)$$

The additivity of the total momentum and energy eigenvalues justifies the quasiparticle interpretation for the spectrum of observables on Bethe states. Each magnon is created by one $B(\lambda_i)$ operator, associated to a specific spectral parameter and Bethe root. Its momentum and energy are

$$p_k(\lambda_k) = -i \log \frac{\lambda_k + i/2}{\lambda_k - i/2}, \quad E_k(\lambda_k) = \frac{J}{2} \frac{1}{\lambda_k^2 + \frac{1}{4}}, \quad (5.42)$$

expressed in terms of the *rapidity* λ_k of the quasiparticle.

As a final important point in this introduction, let us remark that a Yangian may be defined via the Yang–Baxter equation (5.24), a construction sometimes referred to as the *third realisation*, as opposed to the *first realisation* employed in Section 2.2.3 (such terminology is the one adopted *e.g.* in [94]). This is done noting that there is a second

⁴In the *coordinate Bethe ansatz approach*, coinciding Bethe roots would make the ansatz wavefunction vanish, since it has to be antisymmetric in the λ_i .

special value of the spectral parameter for which simplifications are achieved (beyond $\lambda = i/2$, that allowed us to establish a connection between the transfer matrix and physical observables, see (5.27)). Indeed, the large- λ limit is a very interesting one. Looking at the explicit form (5.14) of the Lax operators, the leading terms of the expansion of the monodromy matrix are given by

$$\mathcal{M}_a(\lambda) = \lambda^N \mathbb{1}_a \otimes \mathbb{1} + i\lambda^{N-1} \sum_i \sum_{k=1}^3 \sigma_a^k \otimes S_i^k - \lambda^{N-2} \sum_{i < j} \sum_{k,l=1}^3 (\sigma^k \sigma^l)_a \otimes (S_i^k S_j^l) + \dots \quad (5.43)$$

We already know that the components of the total spin – showing up at order $\mathcal{O}(\lambda^{N-1})$ – generate the $\mathfrak{su}(2)$ symmetry algebra. Moreover, at order $\mathcal{O}(\lambda^{N-2})$ we observe the first occurrence of a non-local operator, *i.e.* acting on more than one site of the spin chain at the same time: they are level-one generators of the Yangian $Y(\mathfrak{su}(2))$. More subleading terms in the large- λ expansion of $\mathcal{M}_a(\lambda)$ involve higher-level Yangian generators, but they are also polluted by powers of the lower-level ones. It is important to stress that the question of Yangian invariance of a spin chain Hamiltonian strongly depends on the boundary conditions of the model. In general, Yangian symmetry is not compatible with periodic boundary conditions (they cause a tension with the need to pick an origin, with respect to which to define an ordering of the sites for the definition of $J^{(1)}, J^{(2)}, \dots$): the symmetry might then be spoiled by boundary terms, but still “effectively hold” if one is interested in phenomena happening in the bulk. If one further imposes that the system is invariant under cyclic permutations of the sites, then one recovers full Yangian invariance provided that the symmetry algebra has vanishing dual Coxeter number \mathfrak{c}_2 , defined via some contraction of the structure constants. This is relevant for discussing scattering in $\mathcal{N} = 4$ SYM, since a spin chain picture is available [40]: the various sites are associated to the external on-shell states in the colour-ordered scattering amplitude and it is clear that such a system is both periodic and cyclically invariant by construction. Then exact Yangian invariance holds, because $\mathfrak{psu}(2, 2|4)$ has $\mathfrak{c}_2 = 0$, as discussed in [36].

5.2 Construction of amplituhedron volume functions

Before discussing the Yangian invariance of amplituhedron volume functions $\Omega_{n,k}^{(m)}(Y, Z)$, we show in this section how to construct (3.47) by introducing an on-shell diagrammatics similar to, but different from, the one established for scattering amplitudes. In the following

section we argue that this diagrammatics follows directly from an underlying spin chain description for the tree-level amplituhedron. The latter derivation will parallel a similar construction [57] for the Grassmannian integral computing $\mathcal{P}_n^{\text{N}^k\text{MHV}}$ featuring momentum supertwistors. The main ingredient there is the operator [136]

$$\mathcal{B}_{ij}(u) = \left(\mathcal{Z}_j^A \partial_{\mathcal{Z}_i^A} \right)^u = \mathcal{N} \int \frac{d\alpha}{\alpha^{1+u}} e^{\alpha \mathcal{Z}_j^A \partial_{\mathcal{Z}_i^A}}, \quad (5.44)$$

where the normalisation \mathcal{N} and the integration contour will not be relevant to our discussion. In the following we will also be using the bosonised version of (5.44): it will be clear from the context which definition we will be working with. Notice that the rightmost expression in (5.44) is well defined even when $u = 0$.

5.2.1 From scattering amplitudes to the amplituhedron

Let us start by reviewing the main steps in the construction of (2.124). We discussed towards the end of Section 2.5.3 that one can associate this Grassmannian integral with the top cell of the positive Grassmannian $G_+(k, n)$. As explained in [49], to each cell of its positroid stratification one can in turn associate a permutation of the symmetric group S_n . For the top cell of $G_+(k, n)$ this takes the particularly simple form

$$\sigma_{n,k}^{\text{top}}(i) = i + k \pmod{n}. \quad (5.45)$$

We need to decompose $\sigma_{n,k}^{\text{top}}$ into adjacent transpositions, as in (2.144). Let us emphasise that such a decomposition is not unique but the function we will associate to the given permutation will be independent of this choice. Moreover, we assume to be working with decompositions with the least number of factors, called *minimal* decompositions. One example we will use in the following is

$$\sigma_{n,k}^{\text{top}} = \underbrace{(k, k+1) \cdots (n-1, n)}_{n-k \text{ factors}} \cdots \underbrace{(23) \cdots (n-k+1, n-k+2)}_{n-k \text{ factors}} \underbrace{(12) \cdots (n-k, n-k+1)}_{n-k \text{ factors}}. \quad (5.46)$$

We remark that the composition of transpositions in (5.46) has to be understood as acting on the identity by swapping preimages (images) when reading from the left (right). It is easy to find an explicit form for the l -th factor (i_l, j_l) of the above decomposition (counting from the right): if we write $l = p(n-k) + q$, where $q \in \{1, 2, \dots, n-k\}$, from the explicit form of $\sigma_{n,k}^{\text{top}}$ we get

$$i_l = n - k + p - q + 1, \quad j_l = i_l + 1. \quad (5.47)$$

Provided the decomposition (5.46), one can show that (2.124) can be constructed as

$$\mathcal{A}_{n,k}(\mathcal{Z}) = \prod_{l=1}^{k(n-k)} \mathcal{B}_{i_l j_l}(0) \prod_{i=1}^k \delta^{4|4}(\mathcal{Z}_i^A), \quad (5.48)$$

where the operators $\mathcal{B}_{i_l j_l}$ appear in the opposite order compared to the order of factors of $\sigma_{n,k}^{\text{top}}$. This construction is based on the possibility of building up any cell of the positive Grassmannian $G_+(k, n)$ – and the associated canonical forms – starting from zero-dimensional cells, which correspond to vacua of the spin chain.

A crucial difference between the integral for volume functions (3.47) and its analogue for scattering amplitudes (2.124) is the presence of the auxiliary variables Y_α^A . It turns out that this difference can be traced back to the choice of “vacuum” on which the operators \mathcal{B}_{ij} act. For scattering amplitudes it is a product of δ -functions which – in the amplituhedron context – has to be replaced by the *seed* $\mathcal{S}_k^{(m)}$:

$$\prod_{i=1}^k \delta^{m|m}(\mathcal{Z}_i^A) \longrightarrow \mathcal{S}_k^{(m)} = \int \frac{d^{k \times k} \beta}{(\det \beta)^k} \prod_{\alpha=1}^k \delta^{m+k} \left(Y_\alpha^A - \sum_{i=1}^k \beta_{\alpha i} Z_i^A \right). \quad (5.49)$$

Notice that $\mathcal{S}_k^{(m)}$ involves only k bosonised momentum twistors, which we chose to be Z_1, \dots, Z_k . The result is independent of this choice, provided that the Z_i are consecutive, which guarantees cyclic invariance of the volume form. It can then be proven that the volume function is given by the formula

$$\Omega_{n,k}^{(m)}(Y, Z) = \prod_{l=1}^{k(n-k)} \mathcal{B}_{i_l j_l}(0) \mathcal{S}_k^{(m)}, \quad (5.50)$$

see Appendix C.1 for details. This is the main formula of this section and we will use it in the following to establish a connection between volume functions and spin chains.

Our discussion focused so far on the top cell of the positive Grassmannian. However, there is a natural way to generalise it to any residue of (3.47). As we mentioned already, all its residues are in one-to-one correspondence with the cells C_σ of the positive Grassmannian $G_+(k, n)$, which in turn are labelled by the permutations $\sigma \in S_n$. In order to find a formula similar to (5.50) for a given residue, which we denote $\Omega_\sigma^{(m)}(Y, Z)$, we first decompose the permutation σ into *generalised* adjacent transpositions

$$\sigma = \prod_{l=1}^{|\sigma|} (i_l, j_l) = (i_{|\sigma|}, j_{|\sigma|}) \dots (i_2, j_2)(i_1, j_1), \quad (5.51)$$

where $|\sigma|$ is the dimension of the cell C_σ . A decomposition into generalized adjacent transpositions is characterized by the following condition: any j_l is allowed to be bigger than $i_l + 1$, provided that for every $q > p$ one has $i_q, j_q \notin \{i_p + 1, \dots, j_p - 1\}$. Then,

$$\Omega_\sigma^{(m)}(Y, Z) = \prod_{l=1}^{|\sigma|} \mathcal{B}_{i_l j_l}(0) \mathcal{S}_k^{(m)}. \quad (5.52)$$

This gives us a very concrete prescription to calculate the volume functions associated to the individual BCFW terms contributing to a given amplitude. The permutations labelling them – which can be computed by means of the program **positroids** [109] – are naturally given in ordinary twistor language, *i.e.* they are related to cells of the Grassmannian $G(\tilde{k}, n)$ of (2.123): after translating to momentum twistor language [50], their decomposition into adjacent transpositions provides us with the labels (i_l, j_l) needed in (5.52). Finally, the sum of the resulting $\Omega_\sigma^{(m)}(Y, Z)$ is the sought-after volume function.

5.2.2 On-shell diagrammatics

The above discussion suggests an on-shell diagrammatics for volume functions bearing several similarities to that relevant to scattering amplitudes. There, one could construct all Yangian invariants using just two vertices corresponding to the MHV and the $\overline{\text{MHV}}$ three-point amplitudes [50]; in the case of the amplituhedron, those vertices are modified and their explicit form can be found in Figure 5.1. Notice that, opposed to the amplitude case, the parameter k associated to the full diagram appears explicitly at each vertex via the δ -functions. Moreover, the arrows on the edges of the diagrams indicate the gauge-fixing we use: we can evaluate only those diagrams which can be given a *perfect orientation*, *i.e.* all of their trivalent vertices can be dressed with arrows as depicted below. We also need to introduce the new seed vertex $\mathcal{S}_k^{(m)}$ corresponding to the vacuum, depicted in Figure 5.2. These three ingredients are enough to graphically represent the residue (5.52) associated to any cell of the positive Grassmannian. Let us mention that, interestingly, a similar new type of seed vertex (for $k = 2$) was introduced in the context of on-shell diagrams for form factors [137]. The permutation labelling a given invariant or, equivalently, a cell of the positive Grassmannian, can be read from the corresponding diagram by following its edges from one external leg to another (its image), taking right (left) turns at every white (black) vertex, as shown in Figure 5.1. Moreover, one has to turn back when encountering the seed vertex $\mathcal{S}_k^{(m)}$.

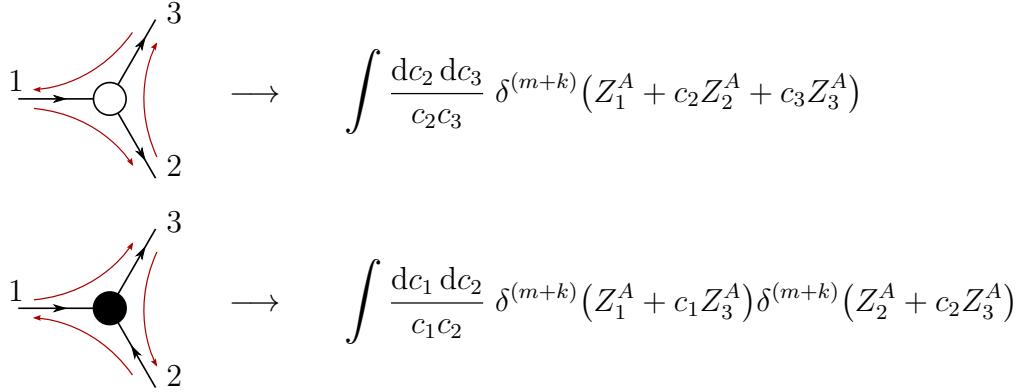


Figure 5.1: Trivalent vertices.

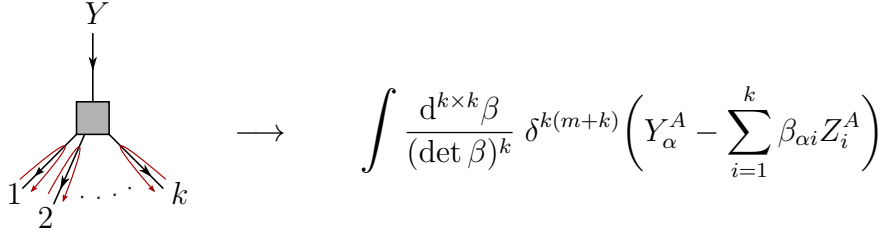
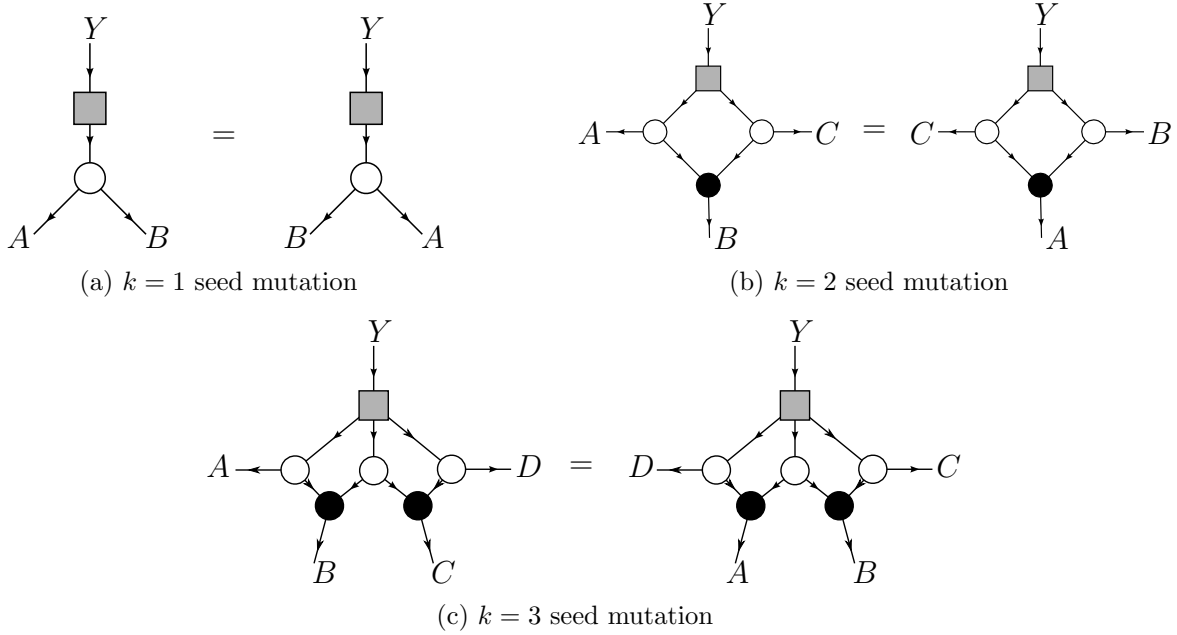


Figure 5.2: Seed vertex, corresponding to the function $\mathcal{S}_k^{(m)}$.

Just as for scattering amplitudes, different on-shell diagrams might evaluate to the same volume function. In the former case, such equivalent graphs can be mapped to each other using transformations preserving the corresponding functions, the square and flip moves of Figure 2.18. Such transformations are collectively called *cluster mutations* since they can be understood in the framework of cluster algebras [138] and they hold in this context as well. In fact, yet another class of transformations exists, under which the amplituhedron on-shell diagrams are invariant, which we call *seed mutations*: their existence was called for, given the presence of a third kind of vertex in our diagrammatics. In Figure 5.3 we portray the simplest seed mutations, relevant for NMHV, N^2 MHV and N^3 MHV volume functions respectively. It is immediate to extrapolate the pattern for arbitrary k and a general proof of their validity is provided in Appendix C.2. Seed mutations allow in particular to prove cyclic invariance of the volume functions: as checked in a variety of examples, an appropriate sequence of flip and square moves and seed mutations maps a given on-shell diagram to a version of itself where the external legs have been cyclically relabelled.

As a further remark, it was shown in [57] that it is also possible to construct deformed

Figure 5.3: Cluster mutations of the seed vertex for $k = 1, 2, 3$.

Grassmannian integrals following a similar procedure to that of (5.52). So far we have used solely the operators $\mathcal{B}_{ij}(0)$: in order to obtain deformed Grassmannian integrals, one needs to allow a non-trivial dependence on u -parameters. Then, demanding that the obtained integrals are Yangian invariants, it was found that they are again in one-to-one correspondence with permutations and they smoothly reduce to undeformed integrals when the deformations are removed. In the next section we will pursue an analogous approach, yielding an explicit construction of *deformed* volume functions.

We conclude this section with a simple example illustrating all concepts introduced so far. Let us consider the case of $\Omega_{4,2}^{(m)}(Y, Z)$. The top-cell permutation is

$$\sigma_{4,2}^{\text{top}} = \begin{pmatrix} 1 & 2 & 3 & 4 \\ 3 & 4 & 1 & 2 \end{pmatrix} = (23)(34)(12)(23) . \quad (5.53)$$

Then, according to (5.50), we can construct the volume function as

$$\Omega_{4,2}^{(m)}(Y, Z) = \mathcal{B}_{23}(0)\mathcal{B}_{12}(0)\mathcal{B}_{34}(0)\mathcal{B}_{23}(0) \mathcal{S}_2^{(m)} . \quad (5.54)$$

This procedure can be depicted as in Figure 5.4 where \mathcal{B}_{ij} is represented as a BCFW bridge, built out of one black and one white trivalent vertex. On the right we depict the corresponding on-shell diagram for $\Omega_{4,2}^{(m)}(Y, Z)$ which can be obtained by removing all bivalent vertices.

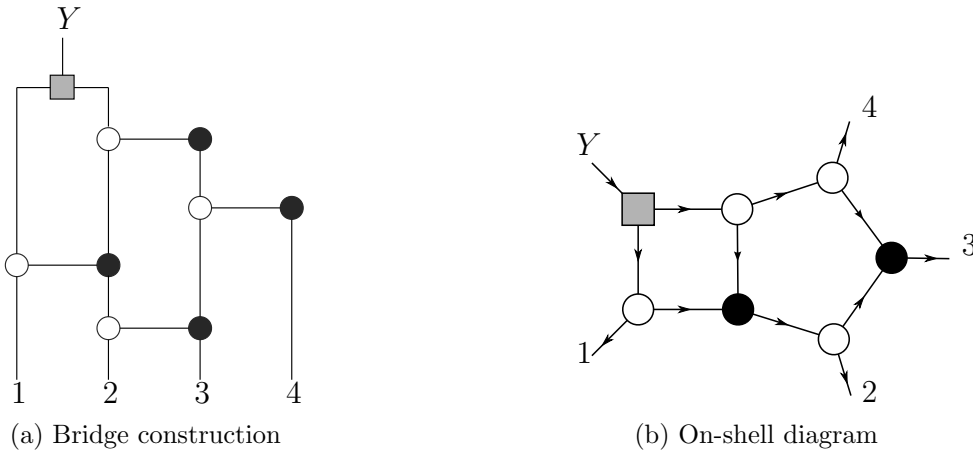


Figure 5.4: Diagrammatic representation for the $n = 4$, $k = 2$ volume function.

Computing the volume form via (5.54), we obtain

$$\Omega_{4,2}^{(m)} = \int \frac{d^4\beta}{(\det \beta)^2} \frac{d\alpha_1 d\alpha_2 d\alpha_3 d\alpha_4}{\alpha_1 \alpha_2 \alpha_3 \alpha_4} \delta^{2 \times (2+m)}(Y - \beta \cdot \tilde{C} \cdot Z), \quad \tilde{C} = \begin{pmatrix} 1 & \alpha_3 & \alpha_3 \alpha_4 & 0 \\ 0 & 1 & \alpha_1 + \alpha_4 & \alpha_1 \alpha_2 \end{pmatrix}, \quad (5.55)$$

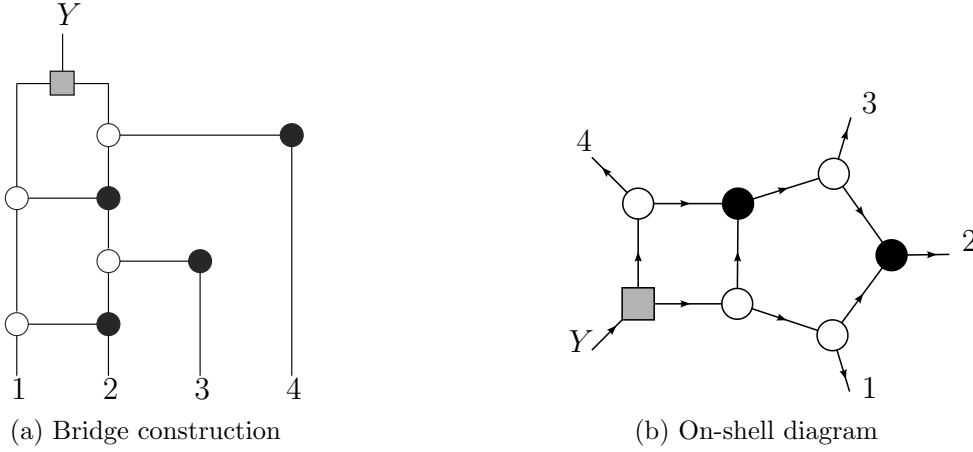
Although for $m = 4$ this function is overly constrained and therefore vanishes for generic external data, for $m = 2$ one gets the well-known result

$$\Omega_{4,2}^{(2)} = \frac{\langle 1234 \rangle^2}{\langle Y12 \rangle \langle Y23 \rangle \langle Y34 \rangle \langle Y41 \rangle} . \quad (5.56)$$

In order to clarify the fact that the volume function does not depend on the representation of the associated permutation in terms of transposition, let us focus on the alternative decomposition $\sigma_{4,2} = (24)(12)(23)(12)$. The corresponding bridge construction and on-shell diagram are depicted in Figure 5.5. It is straightforward to explicitly calculate the function associated to this on-shell diagram and find again (5.56). This equivalence can also be shown using a simple sequence of square and flip moves. Moreover, a seed mutation as in Figure 5.3b yields the diagram in Figure 5.4b with cyclically relabelled external legs, proving diagrammatically the cyclic invariance of (5.56).

5.3 Spin chain picture for the amplituhedron volume

As already mentioned in the introduction to the chapter, the action of the generators of $Y(\mathfrak{gl}(m+k))$ on the volume function is not zero. In this section we will show that there

Figure 5.5: Another decomposition for the $n = 4$, $k = 2$ volume function.

exists an operator, namely

$$(J_Y)^A_B = \sum_{\alpha=1}^k \frac{\partial}{\partial Y^B_\alpha} Y^A_\alpha = \sum_{\alpha=1}^k Y^A_\alpha \frac{\partial}{\partial Y^B_\alpha} + k \delta^A_B, \quad (5.57)$$

for which

$$(J_Y)^A_C (J^{(l)})^C_B \Omega_{n,k}^{(m)} = 0, \quad \ell \in \mathbb{N}, \quad (5.58)$$

for all level- l generators of $Y(\mathfrak{gl}(m+k))$. In particular, we will relate the volume functions to the eigenvectors of the monodromy matrix of a particular spin chain.

Let us start by defining the latter. The quantum space of our spin chain is taken to be

$$V = \overline{V}_1 \otimes \cdots \otimes \overline{V}_k \otimes V_{k+1} \otimes \cdots \otimes V_n, \quad (5.59)$$

where \overline{V}_i and V_i are the spaces where particular $\mathfrak{gl}(m+k)$ representations are defined. These are non-compact and elements of their representation space are functions – or more generally distributions – of bosonised momentum twistors. In the following we demand that the elements of the quantum space are invariant under rescaling of the variables Z_i . For $1 \leq i \leq k$ we identify pairs $\left(-\frac{\partial}{\partial Z^B_i}, Z^A_i\right)$ of creation and annihilation operators acting on \overline{V}_i and define the Fock vacua as

$$Z^A_i |\overline{0}\rangle_i = 0, \quad A = 1, \dots, m+k \quad \Rightarrow \quad |\overline{0}\rangle_i = \delta(Z^A_i). \quad (5.60)$$

For $k+1 \leq i \leq n$, instead, we switch the role of Z and ∂_Z and take pairs $\left(Z^A_i, \frac{\partial}{\partial Z^B_i}\right)$ to be creation and annihilation operators acting on V_i and define the Fock vacua as

$$\frac{\partial}{\partial Z^A_i} |0\rangle_i = 0, \quad A = 1, \dots, m+k \quad \Rightarrow \quad |0\rangle_i = 1. \quad (5.61)$$

Let us remark that the above oscillator representations respectively correspond to the so-called *dual realisations* and *symmetric realisations* in [57]. We also equip each V_i and \bar{V}_i with a complex parameter v_i , called *inhomogeneity*, which will enter our construction as a parameter of the Lax operators. The generators of the $\mathfrak{gl}(m+k)$ algebra are realised on the spaces \bar{V}_i and V_i as

$$\begin{aligned} (\bar{J}_i)_B^A &= \frac{\partial}{\partial Z_i^B} Z_i^A = Z_i^A \frac{\partial}{\partial Z_i^B} + \delta_B^A \quad , \quad i = 1, \dots, k \quad , \\ (J_i)_B^A &= Z_i^A \frac{\partial}{\partial Z_i^B} \quad , \quad i = k+1, \dots, n \end{aligned} \quad (5.62)$$

respectively.

We now want to introduce Lax operators, for which an auxiliary space is needed: let it be a fundamental representation space of $\mathfrak{gl}(m+k)$, called V_{aux} . For every $i = 1, \dots, k$ we define the *dual Lax operators* $\bar{L}_i : V_{\text{aux}} \otimes \bar{V}_i \rightarrow V_{\text{aux}} \otimes \bar{V}_i$, whereas for $i = k+1, \dots, n$ the *symmetric Lax operators* $L_i : V_{\text{aux}} \otimes V_i \rightarrow V_{\text{aux}} \otimes V_i$. Their matrix elements read

$$\bar{L}_i(u - v_i)_B^A = \delta_B^A + (u - v_i - 1)^{-1} \frac{\partial}{\partial Z_i^B} Z_i^A \quad , \quad (5.63)$$

$$L_i(u - v_i)_B^A = \delta_B^A + (u - v_i)^{-1} Z_i^A \frac{\partial}{\partial Z_i^B} \quad . \quad (5.64)$$

It will be useful in the following to introduce the operator

$$\mathcal{L}_i(u)_B^A = (u - v_i) \delta_B^A + Z_i^A \frac{\partial}{\partial Z_i^B} \quad , \quad (5.65)$$

which is easily seen to be related to the two kinds of Lax operators by

$$\bar{L}_i(u) = (u - v_i - 1)^{-1} \mathcal{L}_i(u) \quad , \quad L_i(u) = (u - v_i)^{-1} \mathcal{L}_i(u) \quad . \quad (5.66)$$

Finally we can define a monodromy matrix as

$$M(u; v_1, \dots, v_n) = \bar{L}_1(u - v_1) \cdots \bar{L}_k(u - v_k) L_{k+1}(u - v_{k+1}) \cdots L_n(u - v_n) \quad . \quad (5.67)$$

In the following we will prove that (deformed) volume functions – when acted upon with J_Y – are (left) eigenvectors of the monodromy matrix (5.67). In order to do so, we use the expression for the volume function written in terms of $\mathcal{B}_{ij}(u)$ operators and act on it with $M(u; v_1, \dots, v_n)$. Crucially, we will use the intertwining relation

$$\mathcal{L}_i(u - v_i) \mathcal{L}_j(u - v_j) \mathcal{B}_{ij}(v_j - v_i) = \mathcal{B}_{ij}(v_j - v_i) \mathcal{L}_i(u - v_j) \mathcal{L}_j(u - v_i) \quad , \quad (5.68)$$

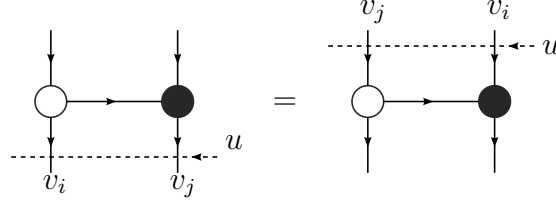


Figure 5.6: Fundamental relation for the construction of monodromy eigenvectors.

which we prove in Appendix C.3. Its meaning is depicted in Figure 5.6, where the dashed line corresponds to the auxiliary space and \mathcal{B}_{ij} is again represented as a BCFW bridge.

We proceed in full generality, keeping the deformation parameters u in (5.44) non-zero. We use the permutation we introduced in (5.45) with decomposition (5.46) and define a sequence of permutations

$$\tau_l = \tau_{l-1} \circ (i_l, j_l) = (i_1 j_1) \dots (i_l, j_l) , \quad (5.69)$$

with the property

$$\tau_{k(n-k)} = (\sigma_{n,k}^{\text{top}})^{-1} . \quad (5.70)$$

Then we can define a *deformed volume function* as

$$\tilde{\Omega}_{n,k}^{(m)}(Y, Z; v_1, \dots, v_n) = \mathcal{B}_{i_1 j_1}(\bar{u}_1) \mathcal{B}_{i_2 j_2}(\bar{u}_2) \dots \mathcal{B}_{i_{k(n-k)} j_{k(n-k)}}(\bar{u}_{k(n-k)}) \mathcal{S}_k^{(m)} , \quad (5.71)$$

with the u parameters being a special combination of inhomogeneities:

$$\bar{u}_l = v_{\tau_l(i_l)} - v_{\tau_l(j_l)} . \quad (5.72)$$

In order for (5.71) to be an element of our quantum space V , $\tilde{\Omega}_{n,k}^{(m)}$ must be invariant under rescalings of the Z_i , which requires the following restriction on the inhomogeneities v_i :

$$v_{\sigma_{n,k}^{\text{top}}(i)} = v_i , \quad (5.73)$$

i.e. a particular case of the condition derived in [57], see also [132]. Then we can show that the following relation holds:

$$M(u; v_1, \dots, v_n)_B^C (J_Y)_C^A \tilde{\Omega}_{n,k}^{(m)} = (J_Y)_B^A \tilde{\Omega}_{n,k}^{(m)} , \quad (5.74)$$

namely, $J_Y \tilde{\Omega}_{n,k}^{(m)}$ is an eigenvector of the monodromy matrix (5.67) with unit eigenvalue. In particular, if $v_i = 0$ for all i , then (5.73) is trivially satisfied and (5.74) holds true for the undeformed $\Omega_{n,k}^{(m)}$. This will lead us to the meaning of Yangian invariance for amplituhedron volume functions.

5.3.1 Proof of the monodromy relation

We now provide the main steps to prove (5.74), which is the most important formula of this chapter. In order to ease the notation, let

$$\mathcal{M}(u; v_1, \dots, v_n) = \mathcal{L}_1(u - v_1) \cdots \mathcal{L}_n(u - v_n), \quad (5.75)$$

allowing the following rewriting of the monodromy matrix:

$$M(u; v_1, \dots, v_n) = \prod_{i=1}^k \frac{1}{u - v_i - 1} \prod_{i=k+1}^n \frac{1}{u - v_i} \mathcal{M}(u; v_1, \dots, v_n). \quad (5.76)$$

We will need a technical result, whose proof we postpone to Appendix C.4:

$$\mathcal{L}_i(u, v_i)_B^C (J_Y)_C^A \mathcal{S}_k^{(m)} = \begin{cases} (u - v_i - 1) (J_Y)_B^A \mathcal{S}_k^{(m)}, & i = 1, \dots, k \\ (u - v_i) (J_Y)_B^A \mathcal{S}_k^{(m)}, & i = k + 1, \dots, n \end{cases}. \quad (5.77)$$

Using this fact, we can show how the monodromy matrix acts on the seed function $\mathcal{S}_k^{(m)}$:

$$\begin{aligned} \mathcal{M}(u; v_1, \dots, v_n)_B^C (J_Y)_C^A \mathcal{S}_k^{(m)} &= (\mathcal{L}_1)_B^C \cdots (\mathcal{L}_n)_B^{D_{n-1}} (J_Y)_C^A \mathcal{S}_k^{(m)} \\ &= \prod_{i=1}^k (u - v_i - 1) \prod_{i=k+1}^n (u - v_i) (J_Y)_B^A \mathcal{S}_k^{(m)}, \end{aligned} \quad (5.78)$$

where we have suppressed all arguments of the Lax operators and we have made repeatedly use of (5.77). We can now prove that $J_Y \tilde{\Omega}_{n,k}^{(m)}$ is indeed an eigenvector of our monodromy matrix. Repeatedly using the intertwining relations (5.68), we have

$$\begin{aligned} M(u; v_1, \dots, v_n)_B^C (J_Y)_C^A \tilde{\Omega}_{n,k}^{(m)} &= \\ &= \prod_{i=1}^k \frac{1}{u - v_i - 1} \prod_{i=k+1}^n \frac{1}{u - v_i} \mathcal{M}(u; v_1, \dots, v_n)_B^C \prod_{l=1}^{k(n-k)} \mathcal{B}_{i_l, j_l}(\bar{u}_l) (J_Y)_C^A \mathcal{S}_k^{(m)} \\ &= \prod_{i=1}^k \frac{1}{u - v_i - 1} \prod_{i=k+1}^n \frac{1}{u - v_i} \prod_{l=1}^{k(n-k)} \mathcal{B}_{i_l, j_l}(\bar{u}_l) \mathcal{M}(u; v_{\sigma_{n,k}^{-1}(1)}, \dots, v_{\sigma_{n,k}^{-1}(n)})_B^C (J_Y)_C^A \mathcal{S}_k^{(m)}, \end{aligned} \quad (5.80)$$

Observe that J_Y commutes with all the $\mathcal{B}_{i_l, j_l}(\bar{u}_l)$, since they depend on Z_i variables only. Making use of (5.78), we finally arrive at the desired result,

$$M(u; v_1, \dots, v_n)_B^C (J_Y)_C^A \tilde{\Omega}_{n,k}^{(m)} = \quad (5.81)$$

$$= \prod_{i=1}^k \frac{u - v_{\sigma_{n,k}^{-1}(i)} - 1}{u - v_i - 1} \prod_{i=k+1}^n \frac{u - v_{\sigma_{n,k}^{-1}(i)}}{u - v_i} \prod_{l=1}^{k(n-k)} \mathcal{B}_{i_l, j_l}(\bar{u}_l) (J_Y)_B^A \mathcal{S}_k^{(m)} = (J_Y)_B^A \tilde{\Omega}_{n,k}^{(m)}, \quad (5.82)$$

where the products over i evaluate to 1 in light of (5.73). This completes the proof of formula (5.74).

5.3.2 Yangian invariance for the amplituhedron volume

We are now in the right position to discuss the Yangian invariance of the tree amplituhedron and, specifically, of the deformed volume functions. By defining⁵

$$\tilde{\Omega}_B^A(Y, Z; v_1, \dots, v_n) = (J_Y)_B^A \tilde{\Omega}_{n,k}^{(m)}(Y, Z; v_1, \dots, v_n) , \quad (5.83)$$

we can rewrite the result (5.74) of the previous section in the following way:

$$M(u; v_1, \dots, v_n)_B^C \tilde{\Omega}_C^A(Y, Z; v_1, \dots, v_n) = \tilde{\Omega}_B^A(Y, Z; v_1, \dots, v_n) . \quad (5.84)$$

If we now expand the monodromy matrix around $u \rightarrow \infty$ using the explicit form of Lax operators (5.63) and (5.64), we find

$$M(u; v_1, \dots, v_n)_B^A = \delta_B^A + \frac{1}{u} (\tilde{J}^{(0)})_B^A + \frac{1}{u^2} (\tilde{J}^{(1)})_B^A + \dots , \quad (5.85)$$

where by $\tilde{J}^{(l)}$ we mean the deformed version of the Yangian generators, involving inhomogeneities. In particular, the leading term cancels the right hand side of (5.84) while the subleading terms lead to the following invariance properties for $\tilde{\Omega}_B^A$:

$$(\tilde{J}^{(0)})_B^C \tilde{\Omega}_C^A = 0 \quad , \quad (\tilde{J}^{(1)})_B^C \tilde{\Omega}_C^A = 0 . \quad (5.86)$$

Setting the inhomogeneities v_i to zero for compactness, we find

$$(J^{(0)})_B^A = \sum_{i=1}^n Z_i^A \frac{\partial}{\partial Z_i^B} + k \delta_B^A , \quad (5.87)$$

$$(J^{(1)})_B^A = \sum_{i < j} Z_i^A \frac{\partial}{\partial Z_i^C} Z_j^C \frac{\partial}{\partial Z_j^B} + k \sum_{i=1}^n Z_i^A \frac{\partial}{\partial Z_i^B} + \frac{k(k+1)}{2} \delta_B^A . \quad (5.88)$$

In order to make a comparison with formulae already present in the literature, one can exploit level-zero invariance and rewrite the level-one generators in the form

$$(J^{(1)})_B^A = \sum_{i < j} \left(Z_i^A \frac{\partial}{\partial Z_i^C} Z_j^C \frac{\partial}{\partial Z_j^B} - (i \leftrightarrow j) \right) . \quad (5.89)$$

⁵Our notation obscures the parameters n , k and m , but this should not generate any confusion.

These generators are known to form the Yangian algebra $Y(\mathfrak{gl}(m+k))$. We have therefore shown that the functions $\tilde{\Omega}_B^A$, related to our original volume function $\tilde{\Omega}_{n,k}^{(m)}$ through (5.83), are Yangian-invariant.

As a final remark, let us mention that it is at the moment unclear what is the explicit relation, if any, between the Yangian for the amplituhedron with $m = 4$, namely $Y(\mathfrak{gl}(4+k))$, and the Yangian for scattering amplitudes, namely $Y(\mathfrak{psu}(2,2|4))$. In particular, it is not known how to directly translate the bosonic generators (5.87) and (5.88) by integrating out the auxiliary fermions ϕ , as in (3.35), in order to get (2.74). It is not even clear whether the bosonic part of $Y(\mathfrak{psu}(2,2|4))$ can be embedded in a larger $Y(\mathfrak{gl}(4+k))$. The statement we proved here is that all volume functions corresponding to Yangian invariants of $Y(\mathfrak{psu}(2,2|4))$ are themselves invariants of $Y(\mathfrak{gl}(4+k))$ in the sense of (5.86).

Different lines of investigation can stem from the results of this chapter. Most urgently, we can now look back at the original question of characterising the dual of the tree amplituhedron in full generality and address the issues discussed in Section 4.4 for higher-helicity volume functions.

Chapter 6

Summary and outlook

In this dissertation we investigated the subject of scattering amplitudes in planar $\mathcal{N} = 4$ SYM, a field that has witnessed tremendous progress especially in the last decades. Despite often not directly suitable for phenomenological applications, the techniques developed and the results achieved for the most symmetric of gauge theories in four dimensions have contributed a great deal to the understanding of the properties of such models. It is in this spirit that we pursued the amplituhedron approach to tree-level scattering amplitudes. We have focused our attention on two main questions: on the one hand, we explored the concept of dual amplituhedron, whose volume has been conjectured to evaluate the amplitudes; on the other, we looked for a notion of Yangian symmetry in this context.

In regard to the first issue, addressed in Chapter 4, we could fully characterise the dual of $\mathfrak{A}_{n,1;m}^{\text{tree}}$, yielding the explicit formula

$$\Omega_{n,1}^{(m)}(Y, Z) = \frac{1}{i^{m+1}} \int_0^{+\infty} \left(\prod_{A=1}^{m+1} ds_A \right) e^{i s_A Y^A} \prod_{i=m+2}^n \theta(s_A Z_i^A)$$

for the computation of NMHV volume functions as integrals over the dual projective space \mathbb{RP}^m : this was achieved enforcing the covariance and scaling properties fulfilled by all $\Omega_{n,k}^{(m)}$ functions, as well as a set of newly introduced PDEs, the Capelli differential equations (4.8), which are second-order in the $k = 1$ case. In general, we observed that the above constraints always allow us to cast $\Omega_{n,k}^{(m)}$ in the form of an integral over the dual Grassmannian manifold $G(k, m + k)$. However, the integrand in this case cannot be fixed unambiguously, because the external data can now be arranged with the coordinates of the dual Grassmannian in non-trivial combinations, that we termed cross-ratios. To attempt bootstrapping the correct integrand for general tree-level volume functions, more constraints were needed

and this was one of the reasons to search for a realisation of Yangian invariance in this framework.

In Chapter 5, we set out to identify suitable generators by proposing a spin chain picture for the amplituhedron. After introducing the matrix Ω_B^A , closely related to the volume function, we find that it is invariant under the Yangian $Y(\mathfrak{gl}(m+k))$, generated by

$$\begin{aligned} (J^{(0)})_B^A &= \sum_{i=1}^n Z_i^A \frac{\partial}{\partial Z_i^B} + k \delta_B^A, \\ (J^{(1)})_B^A &= \sum_{i < j} \left(Z_i^A \frac{\partial}{\partial Z_i^C} Z_j^C \frac{\partial}{\partial Z_j^B} - (i \leftrightarrow j) \right), \end{aligned}$$

i.e. the bosonised version of the usual Yangian generators based on momentum super-twistors, which do not annihilate $\Omega_{n,k}^{(m)}$ on their own. A fundamental ingredient were the intertwining relations (5.68), involving the operators $\mathcal{B}_{ij}(u)$: these provide a way to construct the volume function from the seed $\mathcal{S}_k^{(m)}$, acting as creation operators on a vacuum state:

$$\Omega_{n,k}^{(m)}(Y, Z) = \prod_{l=1}^{k(n-k)} \mathcal{B}_{i_l j_l}(0) \mathcal{S}_k^{(m)}.$$

Because they admit a graphical interpretation as BCFW bridges, we could also derive as a byproduct of our construction an on-shell diagrammatics for $\Omega_{n,k}^{(m)}$ that closely parallels the established one for tree-level amplitudes and loop integrands. In particular, we identified a further class of transformations of the graphs leaving the associated function invariant, called seed mutations. It would naturally be important to investigate whether they – together with flip and square moves – actually correspond to some cluster algebra.

The work presented in this thesis is important in advancing the understanding of the amplituhedron. Despite the relative simplicity of its definition, applications are complicated by many subtleties. Nevertheless, new angles keep emerging, from both the mathematical [139, 140] and the physical [116, 141] communities and suggest that the most beautiful and powerful results are yet to be discovered. Therefore in the following we list a few natural directions for future explorations.

The most obvious problem to tackle is the generalisation of the master formula derived in Chapter 4 for tree-level NMHV volume functions to higher-helicity cases, which would also provide a characterisation of the dual amplituhedron at tree-level. Having at our disposal the additional constraints coming from Yangian invariance, one can hopefully

understand how the cross-ratios have to appear in the ansatz (4.59). Then, assuming to have obtained a properly working formula even for some special value of k , it should be relatively straightforward to repeat the steps that led to (4.24), to understand what the correct generalisation of the $i\epsilon$ -prescription of Section 3.4 is for volume functions with $k > 1$.

Additionally, it is important that a link between the amplituhedron and spin chains could be made concrete, since now the study of the former is more clearly amenable to the methods of integrability, which have proven very powerful in deriving results for planar $\mathcal{N} = 4$ SYM. One possible goal is to start an analysis of loop-level volume functions: indeed, it has been observed in [30] that all integrands of scattering amplitudes are Yangian invariants, nevertheless the analogous statement for their amplituhedron avatars was beyond reach until now. In particular, in [142] it was shown that there exists a generalisation of the Grassmannian measure and of the cell structure for one-loop volume functions. It would be interesting to explore possible implications of our present results in these respects.

On a different note, we stress that our proof of Yangian invariance was carried out in the generalised setting of inhomogeneous spin chains: therefore our statements hold even for deformed volume functions, which upon integration of the auxiliary $\phi_{\alpha A}$ are expected to yield deformed scattering amplitudes (we also briefly commented on this matter towards the end of Chapter 4). The emphasis on deformations of scattering amplitudes might sound unjustified, especially as far as tree amplitudes are concerned, however their relevance is clear at loop-level. The biggest obstacle to the computation of loop amplitudes is that even in UV-safe theories they are plagued by IR-divergencies, calling for a regularisation procedure. Their typical drawback, however, is that they break the symmetries of the model: the most popular regularisation scheme, *dimensional regularisation*, manifestly violates conformal invariance by introducing a mass scale μ . However, it was argued in [121] that the spectral parameter could be used to regulate divergent integrals, such as the one-loop massless box, crucially without having to resort to any mass parameter. As such, the so-called *spectral regularisation* preserves conformal symmetry¹ and it would be very exciting to finally have a way to handle complicated divergent integrals without spoiling their physically relevant symmetries.

More generally, the long-term goal of this program is to extend as much as possible the ideas discussed in this dissertation to other quantum field theories, particularly less

¹It does so at the expense of dual conformal invariance, see the original reference for a discussion of this point.

supersymmetric gauge theories, especially QCD. For several of the concepts introduced along the way, generalisations have been worked out: for instance, on-shell diagrams have been studied in the non-planar sector [108, 143], in $\mathcal{N} < 4$ models [144] and also in the case of $\mathcal{N} = 8$ supergravity [145, 146]. Unfortunately, as already commented upon, nothing like the amplituhedron is known beyond the maximally symmetric Yang–Mills theory. However, as new results are presented, the evidence grows more compelling that this framework to understand QFT is correct and worth investigating in greater depth. We hope to be able to reap the rewards of this collective effort very soon.

Appendix A

More on the $i\epsilon$ -prescription

A.1 Even distribution of poles: a proof

We prove by induction that our iterative procedure to compute the integral (3.58) always produces an even distribution of poles above and below the real axis of the relevant complex c_i -plane. Consider the generic n -point integral (3.58)

$$\Omega_{n,1}^{(4)}(Y, Z) = \frac{1}{(-2\pi i)^{n-5}} \int_{-\infty}^{+\infty} \prod_{i=1}^n \frac{dc_i}{c_i + i\epsilon} \delta^5(Y_\alpha^A - c_i Z_i^A) \quad (\text{A.1})$$

First of all, looking at the argument of the δ -function, we observe that every c_i (hence every F_i) must carry the weight $1/Z_i$. To ease notation, let us denote label $n-j$ simply by $-j$, and use $\langle \bullet \rangle = \langle n-4, n-3, n-2, n-1, n \rangle = \langle -4, -3, -2, -1, 0 \rangle$. Solving the δ -constraints for the last five variables, we find

$$\begin{aligned} c_{-4} &= \frac{1}{\langle \bullet \rangle} \left(\langle Y, -3, -2, -1, 0 \rangle - \sum_{i=1}^{n-5} \langle i, -3, -2, -1, 0 \rangle c_i \right) \\ c_{-3} &= -\frac{1}{\langle \bullet \rangle} \left(\langle Y, -4, -2, -1, 0 \rangle - \sum_{i=1}^{n-5} \langle i, -4, -2, -1, 0 \rangle c_i \right) \\ c_{-2} &= \frac{1}{\langle \bullet \rangle} \left(\langle Y, -4, -3, -1, 0 \rangle - \sum_{i=1}^{n-5} \langle i, -4, -3, -1, 0 \rangle c_i \right) \\ c_{-1} &= -\frac{1}{\langle \bullet \rangle} \left(\langle Y, -4, -3, -2, 0 \rangle - \sum_{i=1}^{n-5} \langle i, -4, -3, -2, 0 \rangle c_i \right) \\ c_0 &= \frac{1}{\langle \bullet \rangle} \left(\langle Y, -4, -3, -2, -1 \rangle - \sum_{i=1}^{n-5} \langle i, -4, -3, -2, -1 \rangle c_i \right) \end{aligned}$$

and the poles in the first integration variable, namely c_{-5} , are split as usual.

This constitutes the base case for our induction. We will now assume that the thesis holds up to the point where the variable c_{l+2} was integrated out ($1 \leq l \leq n-7$) and we are left with

$$\Omega_{n,1}^{(4)}(Y, Z) = \frac{1}{(-2\pi i)^{l+1}} \int_{-\infty}^{+\infty} \prod_{i=1}^{l+1} \frac{dc_i}{F_1 \dots F_l} \text{res}_{c_{l+2}, \dots, c_{-5}}(c_1, \dots, c_{l+1}), \quad (\text{A.2})$$

where $\text{res}_{c_{l+2}, \dots, c_{-5}}$ already includes the denominator factor F_{l+1} and is a sum of partial residues of the form $\{i_{l+2, l+2}, \dots, i_{-5, -5}\}$. This means that

$$\begin{array}{ll} F_{i_{-5}} & \text{had a pole in } c_{-5}^{(i_{-5})} \\ F_{i_{-6}} \big|_{c_{-5}^{(i_{-5})}} & \text{had a pole in } c_{-6}^{(i_{-6}, i_{-5})} \\ \vdots & \vdots \\ F_{i_j} \big|_{c_{-5}^{(i_{-5})}, c_{-6}^{(i_{-6}, i_{-5})}, \dots, c_{j+1}^{(i_{j+1}, \dots, i_{-5})}} & \text{had a pole in } c_j^{(i_j, i_{j+1}, \dots, i_{-5})} \quad \forall j \geq l+2 \end{array}$$

Now, to study the pole structure in the c_{l+1} -plane, we need to understand how the various F_i factors look upon any of the partial residues described above. They are built out of 5-brackets: their entries (but the first one) must range from $l+2$ to n , removing all those corresponding to previously encircled singularities, namely $i_{l+2}, i_{l+3}, \dots, i_{-5}$. This counting leaves us with exactly five free labels: let us call them a, b, c, d, e , such that w.l.o.g. $a < b < c < d < e$. Then each summand of $\text{res}_{c_{l+2}, \dots, c_{-5}}(c_1, \dots, c_{l+1})$ is of the form $(F_{l+1} F_a F_b F_c F_d F_e)^{-1}$. Demanding that each factor has the correct weight, we end up with the following expressions:

$$\begin{aligned} F_{l+1} &= c_{l+1} + i\epsilon \\ F_a &= \frac{1}{\langle abcde \rangle} \left(\langle Ybcde \rangle - \sum_{i=1}^{l+1} \langle ibcde \rangle c_i \right) + i\epsilon \\ F_b &= -\frac{1}{\langle abcde \rangle} \left(\langle Yacde \rangle - \sum_{i=1}^{l+1} \langle iacde \rangle c_i \right) + i\epsilon \\ F_c &= \frac{1}{\langle abcde \rangle} \left(\langle Yabde \rangle - \sum_{i=1}^{l+1} \langle iabde \rangle c_i \right) + i\epsilon \\ F_d &= -\frac{1}{\langle abcde \rangle} \left(\langle Yabce \rangle - \sum_{i=1}^{l+1} \langle iabce \rangle c_i \right) + i\epsilon \\ F_e &= \frac{1}{\langle abcde \rangle} \left(\langle Yabcd \rangle - \sum_{i=1}^{l+1} \langle iabcd \rangle c_i \right) + i\epsilon \end{aligned}$$

We remark that the minus signs in F_b, F_d have to be there to obtain the correct distribution of singularities in the c_{l+1} -plane: indeed, this is still part of our inductive hypothesis.

After this lengthy (mostly notational) introduction, we can now close the contour of integration below $\Re\{c_{l+1}\}$, locate the poles $c_{l+1}^{(i_{l+1}, \dots, i_{-5})}$ and show that – at each one of them – going to the c_l -plane we recover once again the desired splitting of the singularities. The location of the singularities is easily determined: beyond the trivial $c_{l+1}^{(l+1, \dots, l-5)} = 0$,

$$c_{l+1}^{(b, \dots, i_{-5})} = \frac{1}{\langle l+1 \ acde \rangle} \left(\langle Yacde \rangle - \sum_{i=1}^l \langle iacde \rangle c_i \right),$$

$$c_{l+1}^{(d, \dots, i_{-5})} = \frac{1}{\langle l+1 \ abce \rangle} \left(\langle Yabce \rangle - \sum_{i=1}^l \langle iabce \rangle c_i \right).$$

Switching the deformations back on, after performing some simplifications via Schouten identities, we can compute the following expressions for the denominator factors. On the $c_{l+1}^{(l+1, \dots, l-5)}$ pole, we have $F_l = c_l + i\epsilon$ and

$$\begin{aligned} F_a &= \frac{1}{\langle abcde \rangle} \left(\langle Ybcde \rangle - \sum_{i=1}^l \langle ibcde \rangle c_i \right) + i\epsilon \\ F_b &= -\frac{1}{\langle abcde \rangle} \left(\langle Yacde \rangle - \sum_{i=1}^l \langle iacde \rangle c_i \right) + i\epsilon \\ F_c &= \frac{1}{\langle abcde \rangle} \left(\langle Yabde \rangle - \sum_{i=1}^l \langle iabde \rangle c_i \right) + i\epsilon \\ F_d &= -\frac{1}{\langle abcde \rangle} \left(\langle Yabce \rangle - \sum_{i=1}^l \langle iabce \rangle c_i \right) + i\epsilon \\ F_e &= \frac{1}{\langle abcde \rangle} \left(\langle Yabcd \rangle - \sum_{i=1}^l \langle iabcd \rangle c_i \right) + i\epsilon \end{aligned}$$

$$\frac{\begin{array}{ccc} \bullet c_l^{(e, l+1, \dots)} & \bullet c_l^{(c, l+1, \dots)} & \bullet c_l^{(a, l+1, \dots)} \\ \bullet c_l^{(d, l+1, \dots)} & \bullet c_l^{(b, l+1, \dots)} & \bullet c_l^{(l+1, \dots)} \end{array}}{\Re\{c_l\}}$$

On the $c_{l+1}^{(b, \dots, i_{-5})}$ pole, once again $F_l = c_l + i\epsilon$ and we compute

$$\begin{aligned} F_{l+1} &= \frac{1}{\langle l+1 \ acde \rangle} \left(\langle Yacde \rangle - \sum_{i=1}^l \langle iacde \rangle c_i \right) \\ F_a &= -\frac{1}{\langle l+1 \ acde \rangle} \left(\langle Yl+1 \ cde \rangle - \sum_{i=1}^l \langle il+1 \ cde \rangle c_i \right) + i\epsilon \\ F_c &= \frac{1}{\langle l+1 \ acde \rangle} \left(\langle Yl+1 \ ade \rangle - \sum_{i=1}^l \langle il+1 \ ade \rangle c_i \right) + i\epsilon \\ F_d &= -\frac{1}{\langle l+1 \ acde \rangle} \left(\langle Yl+1 \ ace \rangle - \sum_{i=1}^l \langle il+1 \ ace \rangle c_i \right) + i\epsilon \\ F_e &= \frac{1}{\langle l+1 \ acde \rangle} \left(\langle Yl+1 \ acd \rangle - \sum_{i=1}^l \langle il+1 \ acd \rangle c_i \right) + i\epsilon \end{aligned}$$

$$\frac{\begin{array}{ccc} \bullet c_l^{(e, b, \dots)} & \bullet c_l^{(c, b, \dots)} & \bullet c_l^{(l+1, b, \dots)} \\ \bullet c_l^{(d, b, \dots)} & \bullet c_l^{(a, b, \dots)} & \bullet c_l^{(l, b, \dots)} \end{array}}{\Re\{c_l\}}$$

Finally, on the $c_{l+1}^{(d,\dots,i-5)}$ pole, $F_l = c_l + i\epsilon$ as usual and

$$\begin{aligned}
F_{l+1} &= \frac{1}{\langle l+1 \, abce \rangle} \left(\langle Yabce \rangle - \sum_{i=1}^l \langle iabce \rangle c_i \right) + i\epsilon \\
F_a &= -\frac{1}{\langle l+1 \, abce \rangle} \left(\langle Yl+1 \, bce \rangle - \sum_{i=1}^l \langle i \, l+1 \, bce \rangle c_i \right) + i\epsilon \\
F_b &= \frac{1}{\langle l+1 \, abce \rangle} \left(\langle Yl+1 \, ace \rangle - \sum_{i=1}^l \langle i \, l+1 \, ace \rangle c_i \right) + i\epsilon \\
F_c &= -\frac{1}{\langle l+1 \, abce \rangle} \left(\langle Yl+1 \, abe \rangle - \sum_{i=1}^l \langle i \, l+1 \, abe \rangle c_i \right) + i\epsilon \\
F_e &= \frac{1}{\langle l+1 \, abce \rangle} \left(\langle Yl+1 \, abc \rangle - \sum_{i=1}^l \langle i \, l+1 \, abc \rangle c_i \right) + i\epsilon
\end{aligned}$$

The inductive step is complete.

A.2 The five-point N^2 MHV volume function

Focusing on the toy amplituhedron with $m = 2$, the five-point N^2 MHV volume function is given by

$$\Omega_{5,2}^{(2)}(Y, Z) = \int \frac{d^{10} c_{ai}}{(12)(23)(34)(45)(51)} \delta^4(Y_1^A + c_{1i} Z_i^A) \delta^4(Y_2^A + c_{2i} Z_i^A) . \quad (\text{A.3})$$

Before introducing any $i\epsilon$ -prescription, we would like to write down all the residues of the above integral.

Let us solve the two δ -functions (hence producing a total Jacobian factor $1/\langle 2345 \rangle^2$) in terms of c_{11}, c_{21} . Setting $\langle \bullet \rangle = \langle 2345 \rangle$, we find

$$\begin{aligned}
c_{12} &= \frac{1}{\langle \bullet \rangle} (\langle Y_1 345 \rangle - \langle 1345 \rangle c_{11}) & , & & c_{13} &= -\frac{1}{\langle \bullet \rangle} (\langle Y_1 245 \rangle - \langle 1245 \rangle c_{11}) , \\
c_{14} &= \frac{1}{\langle \bullet \rangle} (\langle Y_1 235 \rangle - \langle 1235 \rangle c_{11}) & , & & c_{15} &= -\frac{1}{\langle \bullet \rangle} (\langle Y_1 234 \rangle - \langle 1234 \rangle c_{11}) , \\
c_{22} &= \frac{1}{\langle \bullet \rangle} (\langle Y_2 345 \rangle - \langle 1345 \rangle c_{21}) & , & & c_{23} &= -\frac{1}{\langle \bullet \rangle} (\langle Y_2 245 \rangle - \langle 1245 \rangle c_{21}) , \\
c_{24} &= \frac{1}{\langle \bullet \rangle} (\langle Y_2 235 \rangle - \langle 1235 \rangle c_{21}) & , & & c_{25} &= -\frac{1}{\langle \bullet \rangle} (\langle Y_2 234 \rangle - \langle 1234 \rangle c_{21}) .
\end{aligned}$$

Then the minors are readily computed:

$$\begin{aligned}
(12) &= \frac{1}{\langle \bullet \rangle} (\langle Y_2 345 \rangle c_{11} - \langle Y_1 345 \rangle c_{21}) , \\
(23) &= \frac{1}{\langle \bullet \rangle} (\langle Y_1 Y_2 45 \rangle + \langle Y_2 145 \rangle c_{11} - \langle Y_1 145 \rangle c_{21}) , \\
(34) &= \frac{1}{\langle \bullet \rangle} (\langle Y_1 Y_2 25 \rangle + \langle Y_2 125 \rangle c_{11} - \langle Y_1 125 \rangle c_{21}) , \\
(45) &= \frac{1}{\langle \bullet \rangle} (\langle Y_1 Y_2 23 \rangle + \langle Y_2 123 \rangle c_{11} - \langle Y_1 123 \rangle c_{21}) , \\
(51) &= \frac{1}{\langle \bullet \rangle} (\langle Y_2 234 \rangle c_{11} - \langle Y_1 234 \rangle c_{21}) .
\end{aligned}$$

Notice that all $(i\ i+1)$ stay linear, as anticipated in the main text, a special feature of the five-point computation. The residues of the integrand

$$f(c_{11}, c_{21}) = \frac{1}{\langle 2345 \rangle^2} \frac{1}{(12)(23)(34)(45)(51)} \quad (\text{A.4})$$

can now be computed making use of formula (3.55). We have ten ways $\binom{5}{2} = 10$ of setting two minors to zero in the above formula and we distinguish two situations: either the two are adjacent minors, or not. Furthermore, we introduce the notation (\star, i, j) as a shorthand for each summand in (3.71).

Adjacent minors set to vanish

- For

$$(12) = (23) = 0 \quad \longrightarrow \quad c_{11} = \frac{\langle Y_1 345 \rangle}{\langle 1345 \rangle} , \quad c_{21} = \frac{\langle Y_2 345 \rangle}{\langle 1345 \rangle} ,$$

we find

$$\text{Res}_{(12)=(23)=0} f = (3, 4, 5) = (1, 3, 4) .$$

- For

$$(23) = (34) = 0 \quad \longrightarrow \quad c_{11} = \frac{\langle Y_1 245 \rangle}{\langle 1245 \rangle} , \quad c_{21} = \frac{\langle Y_2 245 \rangle}{\langle 1245 \rangle} ,$$

we find

$$\text{Res}_{(23)=(34)=0} f = (2, 4, 5) = (4, 1, 5) .$$

- For

$$(34) = (45) = 0 \quad \longrightarrow \quad c_{11} = \frac{\langle Y_1 235 \rangle}{\langle 1235 \rangle} , \quad c_{21} = \frac{\langle Y_2 235 \rangle}{\langle 1235 \rangle} ,$$

we find

$$\text{Res}_{(34)=(45)=0} f = (3, 1, 5) = (5, 1, 2) .$$

- For

$$(45) = (51) = 0 \quad \longrightarrow \quad c_{11} = \frac{\langle Y_1 234 \rangle}{\langle 1234 \rangle}, \quad c_{21} = \frac{\langle Y_2 234 \rangle}{\langle 1234 \rangle},$$

we find

$$\text{Res}_{(45)=(51)=0} f = (1, 2, 3) = (4, 1, 2).$$

- For

$$(51) = (12) = 0 \quad \longrightarrow \quad c_{11} = 0, \quad c_{21} = 0,$$

we find

$$\text{Res}_{(51)=(12)=0} f = (2, 3, 4) = (5, 2, 3).$$

Non-adjacent minors set to vanish

- For

$$(34) = (12) = 0 \quad \longrightarrow \quad \begin{aligned} c_{11} &= \frac{\langle Y_1 Y_2 25 \rangle \langle Y_1 345 \rangle}{\langle Y_1 125 \rangle \langle Y_2 345 \rangle - \langle Y_2 125 \rangle \langle Y_1 345 \rangle}, \\ c_{21} &= \frac{\langle Y_1 Y_2 25 \rangle \langle Y_2 345 \rangle}{\langle Y_1 125 \rangle \langle Y_2 345 \rangle - \langle Y_2 125 \rangle \langle Y_1 345 \rangle}, \end{aligned}$$

we find

$$\text{Res}_{(34)=(12)=0} f = (5, 3, 1).$$

- For

$$(12) = (45) = 0 \quad \longrightarrow \quad \begin{aligned} c_{11} &= \frac{\langle Y_1 Y_2 23 \rangle \langle Y_1 345 \rangle}{\langle Y_1 123 \rangle \langle Y_2 345 \rangle - \langle Y_2 123 \rangle \langle Y_1 345 \rangle}, \\ c_{21} &= \frac{\langle Y_1 Y_2 23 \rangle \langle Y_2 345 \rangle}{\langle Y_1 123 \rangle \langle Y_2 345 \rangle - \langle Y_2 123 \rangle \langle Y_1 345 \rangle}, \end{aligned}$$

we find

$$\text{Res}_{(12)=(45)=0} f = (3, 4, 1).$$

- For

$$(45) = (23) = 0 \quad \longrightarrow \quad \begin{aligned} c_{11} &= \frac{\langle Y_1 Y_2 45 \rangle \langle Y_1 123 \rangle - \langle Y_1 Y_2 23 \rangle \langle Y_1 145 \rangle}{\langle Y_1 145 \rangle \langle Y_2 123 \rangle - \langle Y_1 123 \rangle \langle Y_2 145 \rangle}, \\ c_{21} &= \frac{\langle Y_1 Y_2 45 \rangle \langle Y_2 123 \rangle - \langle Y_1 Y_2 23 \rangle \langle Y_2 145 \rangle}{\langle Y_1 145 \rangle \langle Y_2 123 \rangle - \langle Y_1 123 \rangle \langle Y_2 145 \rangle}, \end{aligned}$$

we find

$$\text{Res}_{(45)=(23)=0} f = (1, 4, 2).$$

- For

$$(23) = (51) = 0 \quad \longrightarrow \quad \begin{aligned} c_{11} &= \frac{\langle Y_1 Y_2 45 \rangle \langle Y_1 234 \rangle}{\langle Y_1 145 \rangle \langle Y_2 234 \rangle - \langle Y_2 145 \rangle \langle Y_1 234 \rangle} \\ c_{21} &= \frac{\langle Y_1 Y_2 45 \rangle \langle Y_2 234 \rangle}{\langle Y_1 145 \rangle \langle Y_2 234 \rangle - \langle Y_2 145 \rangle \langle Y_1 234 \rangle} \end{aligned} ,$$

we find

$$\text{Res}_{(23)=(51)=0} f = (4, 2, 5) .$$

- For

$$(51) = (34) = 0 \quad \longrightarrow \quad \begin{aligned} c_{11} &= \frac{\langle Y_1 Y_2 25 \rangle \langle Y_1 234 \rangle}{\langle Y_1 125 \rangle \langle Y_2 234 \rangle - \langle Y_2 125 \rangle \langle Y_1 234 \rangle} \\ c_{21} &= \frac{\langle Y_1 Y_2 25 \rangle \langle Y_2 234 \rangle}{\langle Y_1 125 \rangle \langle Y_2 234 \rangle - \langle Y_2 125 \rangle \langle Y_1 234 \rangle} \end{aligned} ,$$

we find

$$\text{Res}_{(51)=(34)=0} f = (2, 3, 5) .$$

Observe that, in order to match the contributions (\star, i, j) with the correct sign, we had to set non-adjacent minors to zero in an prescribed order. In fact, this reveals a nice pattern: writing down the correct sum of residues for each value of \star according to (3.71), we always pick up two adjacent and one non-adjacent residues. Schematically, the \star representation of $\Omega_{5,2}^{(2)}$ is

$$\left((\star-2, \star-1), (\star-1, \star) = 0 \right) + \left((\star-2, \star-1), (\star+1, \star+2) = 0 \right) + \left((\star, \star+1), (\star+1, \star+2) = 0 \right) . \quad (\text{A.5})$$

The five-point N^2 MHV volume function from an $i\epsilon$ -prescription We were able to come up with an $i\epsilon$ -prescription producing the correct result for $\Omega_{5,2}^{(2)}$, consisting in deforming the minors in the denominator. Starting from the formula (A.3), we change variables from c_{11}, c_{21} to $w_1 = (12)$ and $w_2 = (23)$. After this change of variables, and solving the δ -functions, we find

$$\Omega_{5,2}^{(2)} = \int \frac{dw_1 dw_2}{w_1 w_2 w_3 w_4 w_5} , \quad (\text{A.6})$$

where

$$\begin{aligned}
w_3 = (34) &= -\frac{\langle Y_1 Y_2 15 \rangle \langle 1245 \rangle}{\langle Y_1 Y_2 45 \rangle \langle 1345 \rangle} w_1 + \frac{\langle Y_1 125 \rangle \langle Y_2 345 \rangle - \langle Y_2 125 \rangle \langle Y_1 345 \rangle}{\langle Y_1 Y_2 45 \rangle \langle 1345 \rangle} w_2 + \dots, \\
w_4 = (45) &= -\frac{\langle Y_1 123 \rangle \langle Y_2 145 \rangle - \langle Y_2 123 \rangle \langle Y_1 145 \rangle}{\langle Y_1 Y_2 45 \rangle \langle 1345 \rangle} w_1 + \frac{\langle Y_1 123 \rangle \langle Y_2 345 \rangle - \langle Y_2 123 \rangle \langle Y_1 345 \rangle}{\langle Y_1 Y_2 45 \rangle \langle 1345 \rangle} w_2 + \dots, \\
w_5 = (15) &= \frac{\langle Y_1 234 \rangle \langle Y_2 145 \rangle - \langle Y_2 234 \rangle \langle Y_1 145 \rangle}{\langle Y_1 Y_2 45 \rangle \langle 1345 \rangle} w_1 - \frac{\langle Y_1 Y_2 34 \rangle \langle 2345 \rangle}{\langle Y_1 Y_2 45 \rangle \langle 1345 \rangle} w_2 + \dots,
\end{aligned}$$

and the dots represent constants in w_1 and w_2 , irrelevant for this analysis. Observe that we intentionally flipped the last wrapping minor. One can quickly prove, using $Y_\alpha = c_{\alpha i} Z_i$ and the positivity of the matrix C , that

$$\begin{aligned}
&\langle Y_1 Y_2 i j \rangle > 0 \quad \text{for all } i, j \text{ (cyclic) neighbours, } i < j, \\
&\langle Y_1 123 \rangle \langle Y_2 145 \rangle - \langle Y_2 123 \rangle \langle Y_1 145 \rangle < 0, \\
&\langle Y_1 234 \rangle \langle Y_2 145 \rangle - \langle Y_2 234 \rangle \langle Y_1 145 \rangle < 0, \\
&\langle Y_1 125 \rangle \langle Y_2 345 \rangle - \langle Y_2 125 \rangle \langle Y_1 345 \rangle < 0, \\
&\langle Y_1 123 \rangle \langle Y_2 345 \rangle - \langle Y_2 123 \rangle \langle Y_1 345 \rangle > 0.
\end{aligned} \tag{A.7}$$

Then the coefficients of both w_1, w_2 in the denominator factors have alternating signs, *i.e.* the pattern is $\{w_k, w_3, w_4, w_5\} = \{+, -, +, -\}$ for $k = 1, 2$.

Now, let us introduce the deformations $w_i \rightarrow w_i + i\epsilon_i$. Performing the integration over w_1 first, we are led to pick up the poles at $w_1 = 0$ and $w_4 = 0$ and we can move on to study

$$\int_{-\infty}^{+\infty} dw_2 \operatorname{res}_{w_1}(w_2) \quad , \quad \operatorname{res}_{w_1}(w_2) = \{(w_1)_{w_1}\} + \{(w_4)_{w_1}\}, \tag{A.8}$$

having adapted the notation used for the NMHV residues. At $w_1^{(1)} = 0$ we trivially get

$$\begin{aligned}
w_3|_{w_1^{(1)}} &= \frac{\langle Y_1 125 \rangle \langle Y_2 345 \rangle - \langle Y_2 125 \rangle \langle Y_1 345 \rangle}{\langle Y_1 Y_2 45 \rangle \langle 1345 \rangle} w_2 + \dots + i\epsilon_3, \\
w_4|_{w_1^{(1)}} &= \frac{\langle Y_1 123 \rangle \langle Y_2 345 \rangle - \langle Y_2 123 \rangle \langle Y_1 345 \rangle}{\langle Y_1 Y_2 45 \rangle \langle 1345 \rangle} w_2 + \dots + i\epsilon_4, \\
w_5|_{w_1^{(1)}} &= -\frac{\langle Y_1 Y_2 34 \rangle \langle 2345 \rangle}{\langle Y_1 Y_2 45 \rangle \langle 1345 \rangle} w_2 + \dots + i\epsilon_5,
\end{aligned}$$

hence the signs of the coefficients of w_2 follow the pattern $\{w_2, w_3, w_4, w_5\} = \{+, -, +, -\}$.

Similarly, at the point $w_1^{(4)}$ where $w_4 = 0$, we compute

$$\begin{aligned} w_1|_{w_1^{(4)}} &= \frac{\langle Y_1 123 \rangle \langle Y_2 345 \rangle - \langle Y_2 123 \rangle \langle Y_1 345 \rangle}{\langle Y_1 123 \rangle \langle Y_2 145 \rangle - \langle Y_2 123 \rangle \langle Y_1 145 \rangle} w_2 + \cdots + i\epsilon_1 , \\ w_3|_{w_1^{(4)}} &= \frac{\langle Y_1 Y_2 12 \rangle \langle 1235 \rangle}{\langle Y_1 123 \rangle \langle Y_2 145 \rangle - \langle Y_2 123 \rangle \langle Y_1 145 \rangle} w_2 + \cdots + i\epsilon_3 , \\ w_5|_{w_1^{(4)}} &= -\frac{\langle Y_1 Y_2 23 \rangle \langle 1234 \rangle}{\langle Y_1 123 \rangle \langle Y_2 145 \rangle - \langle Y_2 123 \rangle \langle Y_1 145 \rangle} w_2 + \cdots + i\epsilon_5 , \end{aligned}$$

yielding once again the alternating signs pattern $\{w_1, w_2, w_3, w_5\} = \{-, +, -, +\}$.

We are ready to compute the residues summing to the amplitude we are interested in. We have to consider four singularities, but only three of them will actually contribute: in fact, the solution of $w_4|_{w_1^{(1)}} = 0$ is a singularity of $\{(w_4)_{w_1}\}$ as well and the two residues cancel against each other. This can also be understood drawing the relevant tree of residues.¹

Finally our volume function will be the sum of residues

$$\begin{aligned} \Omega_{5,2}^{(2)} &= \{(w_1)_{w_1}, (w_2)_{w_2}\} + \{(w_4)_{w_1}, (w_2)_{w_2}\} + \{(w_4)_{w_1}, (w_5)_{w_2}\} = \\ &= \left((12), (23) = 0 \right) + \left((45), (23) = 0 \right) + \left((45), (51) = 0 \right) , \end{aligned} \tag{A.9}$$

in agreement with (3.71) and (A.5), setting $\star = 1$.

¹Although this is probably just an artifact of the five-point calculation being in fact a $\overline{\text{NMHV}}_5$ for $m = 2$.

Appendix B

Details on the solution of the Heisenberg spin chain

This Appendix serves as a complement to the introduction to Chapter 5. We will present a few calculations that were skipped in the main text.

We make use of the standard definition of tensor product. Tensor products of states and matrix operators are built according to

$$x \otimes y = \begin{pmatrix} x_1 \\ x_2 \end{pmatrix} \otimes \begin{pmatrix} y_1 \\ y_2 \end{pmatrix} = \begin{pmatrix} x_1 y_1 \\ x_1 y_2 \\ x_2 y_1 \\ x_2 y_2 \end{pmatrix} \quad (\text{B.1})$$

and

$$A \otimes B = \begin{pmatrix} a_{11} & a_{12} \\ a_{21} & a_{22} \end{pmatrix} \otimes \begin{pmatrix} b_{11} & b_{12} \\ b_{21} & b_{22} \end{pmatrix} = \begin{pmatrix} a_{11}B & a_{12}B \\ a_{21}B & a_{22}B \end{pmatrix} = \begin{pmatrix} a_{11}b_{11} & a_{11}b_{12} & a_{12}b_{11} & a_{12}b_{12} \\ a_{11}b_{21} & a_{11}b_{22} & a_{12}b_{21} & a_{12}b_{22} \\ a_{21}b_{11} & a_{21}b_{12} & a_{22}b_{11} & a_{22}b_{12} \\ a_{21}b_{21} & a_{21}b_{22} & a_{22}b_{21} & a_{22}b_{22} \end{pmatrix}. \quad (\text{B.2})$$

It is also useful to recall the identity $(A \otimes B) \cdot (C \otimes D) = (A \cdot C) \otimes (B \cdot D)$, where \cdot denotes the matrix product.

B.1 Permutation and shift operators

The generalised definition of the permutation operator mentioned in the main text reads

$$\mathcal{P}_{ij} = \sum_{m,n=1}^n \mathbb{1} \otimes \cdots \otimes \underbrace{e_{mn}}_{i\text{-th site}} \otimes \cdots \otimes \underbrace{e_{nm}}_{j\text{-th site}} \otimes \cdots \otimes \mathbb{1} \quad (\text{B.3})$$

where $\{e_{mn}\}$ is the collection of sparse matrices having a single 1 as the (m, n) -th entry, forming a basis for the $n \times n$ matrices. We have $(e_{mn})_{pq} = \delta_{mp}\delta_{nq}$ and thus $e_{kl}e_{mn} = \delta_{lm}e_{kn}$. Hence it is easy to show that any \mathcal{P}_{ij} squares to the identity:

$$\mathcal{P}_{ij}^2 = \sum_{k,l,m,n} (e_{kl}e_{mn}) \otimes (e_{lk}e_{nm}) = \sum_{k,l,m,n} (\delta_{lm}e_{kn}) \otimes (\delta_{kn}e_{lm}) = \sum_k e_{kk} \otimes \sum_l e_{ll} = \mathbb{1} \otimes \mathbb{1} , \quad (\text{B.4})$$

where of course we left the many identity factors in the tensor product understood. It is then apparent that $[\mathcal{P}_{ii+1}, \mathcal{P}_{jj+1}] = 0$ if there is no overlap among the labels. However, we have

$$\mathcal{P}_{ab}\mathcal{P}_{ac} = \mathcal{P}_{bc}\mathcal{P}_{ab} = \mathcal{P}_{ac}\mathcal{P}_{bc} . \quad (\text{B.5})$$

Indeed, assuming that $a < b < c$ (the other cases work identically),

$$\begin{aligned} \mathcal{P}_{ab}\mathcal{P}_{ac} &= \sum_{i,j,k,l} e_{ij}e_{kl} \otimes e_{ji} \otimes e_{lk} = \sum_{i,j,l} e_{il} \otimes e_{ji} \otimes e_{lj} , \\ \mathcal{P}_{bc}\mathcal{P}_{ab} &= \sum_{i,j,k,l} e_{kl} \otimes e_{ij}e_{lk} \otimes e_{ji} = \sum_{i,j,k} e_{kj} \otimes e_{ik} \otimes e_{ji} , \\ \mathcal{P}_{ac}\mathcal{P}_{bc} &= \sum_{i,j,k,l} e_{ij} \otimes e_{kl} \otimes e_{ji}e_{lk} = \sum_{i,j,k} e_{ij} \otimes e_{ki} \otimes e_{jk} , \end{aligned} \quad (\text{B.6})$$

the three expressions being equal upon relabelling.

That the shift operator \mathcal{U}_N commutes with the Hamiltonian is seen as follows:

$$\begin{aligned} [\mathcal{U}_N, \mathcal{H}_N] &= -\frac{J}{2} \sum_{i=1}^N [\mathcal{U}, \mathcal{P}_{ii+1}] = -\frac{J}{2} \sum_{i=1}^N (\mathcal{P}_{12} \cdots \mathcal{P}_{N-1N} \mathcal{P}_{ii+1} - \mathcal{P}_{ii+1} \mathcal{P}_{12} \cdots \mathcal{P}_{N-1N}) = \\ &= -\frac{J}{2} \left[(\mathcal{P}_{13} \mathcal{P}_{34} \cdots \mathcal{P}_{N-1N} - \mathcal{P}_{23} \mathcal{P}_{34} \cdots \mathcal{P}_{N-1N}) + \right. \\ &\quad + \sum_{i=2}^{N-2} (\mathcal{P}_{12} \cdots \mathcal{P}_{ii+2} \cdots \mathcal{P}_{N-1N} - \mathcal{P}_{12} \cdots \mathcal{P}_{i-1i+1} \cdots \mathcal{P}_{N-1N}) + \\ &\quad + (\mathcal{P}_{12} \cdots \mathcal{P}_{N-2N-1} - \mathcal{P}_{12} \cdots \mathcal{P}_{N-2N}) + \\ &\quad \left. + (\mathcal{P}_{23} \mathcal{P}_{34} \cdots \mathcal{P}_{N-1N} - \mathcal{P}_{12} \cdots \mathcal{P}_{N-2N-1}) \right] = 0 . \end{aligned} \quad (\text{B.7})$$

Here we highlighted the terms coming from the values $i = 1, N-1, N$ of the sum index and the last two terms – cancelling against previous ones – are the result of manipulations based on the commutation relations (B.5). Were the spin chain open, they would be missing and hence the commutator would fail to vanish despite the telescopic sum.

B.2 \mathcal{U}_N and \mathcal{H}_N from the transfer matrix

Let us consider the transfer matrix $T(\lambda) = \text{tr}_a(\mathcal{M}_a(\lambda))$, looking at a special value of the spectral parameter, namely $\lambda = i/2$. We can compute

$$\mathcal{M}_a\left(\frac{i}{2}\right) = i^N \mathcal{P}_{aN} \mathcal{P}_{aN-1} \cdots \mathcal{P}_{a1} = i^N \mathcal{P}_{12} \mathcal{P}_{23} \cdots \mathcal{P}_{N-1N} \mathcal{P}_{aN}, \quad (\text{B.8})$$

exploiting the commutation relations of permutation operators. Then, taking the trace over the auxiliary space and using that

$$\text{tr}_a(\mathcal{P}_{ai}) = \text{tr}_a \begin{pmatrix} \frac{1}{2}\mathbb{1} + S_i^3 & S_i^- \\ S_i^+ & \frac{1}{2}\mathbb{1} - S_i^3 \end{pmatrix}_a = \mathbb{1},$$

we obtain the shift operator:

$$T\left(\frac{i}{2}\right) = i^N \mathcal{P}_{12} \mathcal{P}_{23} \cdots \mathcal{P}_{N-1N} \longrightarrow \mathcal{U}_N = i^{-N} T\left(\frac{i}{2}\right). \quad (\text{B.9})$$

On the other hand, we find

$$\frac{dT}{d\lambda}(\lambda) = \text{tr}_a \left(\frac{d\mathcal{M}_a(\lambda)}{d\lambda} \right) = \sum_{k=1}^N \text{tr}_a \left(\mathcal{L}_{aN}(\lambda) \cdots \widehat{\mathcal{L}_{ak}(\lambda)} \cdots \mathcal{L}_{a1}(\lambda) \right) \quad (\text{B.10})$$

and thus, using the same manipulations of (B.8),

$$\begin{aligned} \frac{dT}{d\lambda} \left(\frac{i}{2} \right) &= i^{N-1} \sum_k \text{tr}_a \left(\mathcal{P}_{aN} \cdots \widehat{\mathcal{P}_{ak}} \cdots \mathcal{P}_{a1} \right) = \\ &= i^{N-1} \sum_k \mathcal{P}_{12} \cdots \mathcal{P}_{k-2k-1} \mathcal{P}_{k-1k+1} \mathcal{P}_{k+1k+2} \cdots \mathcal{P}_{N-1N}. \end{aligned} \quad (\text{B.11})$$

Then, it follows that the Hamiltonian is the logarithmic derivative of the transfer matrix:

$$\mathcal{H}_N = J \left(\frac{N}{2} - \frac{i}{2} \frac{dT}{d\lambda} T^{-1}(\lambda) \Big|_{\lambda=\frac{i}{2}} \right) = J \left(\frac{N}{2} - \frac{i}{2} \frac{d}{d\lambda} \log T(\lambda) \Big|_{\lambda=\frac{i}{2}} \right), \quad (\text{B.12})$$

where it should be noted that – in light of $[T(\lambda), T(\lambda')] = 0$ – such logarithmic derivative is unambiguous.

B.3 On the ansatz and the Bethe equations

A quick proof of equation (5.30) can be given observing that

$$\mathcal{L}_{ai}(\lambda) |\uparrow\rangle_i = \begin{pmatrix} (\lambda + iS_i^3) |\uparrow\rangle & iS_i^- |\uparrow\rangle \\ iS_i^+ |\uparrow\rangle & (\lambda - iS_i^3) |\uparrow\rangle \end{pmatrix}_a = \begin{pmatrix} \lambda + \frac{i}{2} & \star \\ 0 & \lambda - \frac{i}{2} \end{pmatrix}_a |\uparrow\rangle_i, \quad (\text{B.13})$$

implying

$$\begin{aligned} \mathcal{M}_a(\lambda) |\Omega\rangle &= (\mathcal{L}_{aN}(\lambda) |\uparrow\rangle_N) (\mathcal{L}_{a,N-1}(\lambda) |\uparrow\rangle_{N-1}) \cdots (\mathcal{L}_{a1}(\lambda) |\uparrow\rangle_1) = \\ &= \begin{pmatrix} (\lambda + \frac{i}{2})^N & \star \\ 0 & (\lambda - \frac{i}{2})^N \end{pmatrix}_a |\Omega\rangle. \end{aligned} \quad (\text{B.14})$$

To derive the commutation rules relating the A, B, D operators, we can simply compute the two sides of the Yang–Baxter equation for monodromy matrices, which we reproduce here:

$$\mathcal{R}_{ab}(\lambda - \lambda') \mathcal{M}_a(\lambda) \mathcal{M}_b(\lambda') = \mathcal{M}_b(\lambda') \mathcal{M}_a(\lambda) \mathcal{R}_{ab}(\lambda - \lambda').$$

Setting $\kappa = \lambda - \lambda'$, $\kappa' = \kappa + i$, we have

$$\begin{aligned} \mathcal{R}_{ab}(\lambda - \lambda') &= \begin{pmatrix} \kappa' & & \\ & \kappa & i \\ & i & \kappa \\ & & & \kappa' \end{pmatrix}, \\ \mathcal{M}_a(\lambda) &= \begin{pmatrix} A(\lambda) & & B(\lambda) \\ & A(\lambda) & B(\lambda) \\ C(\lambda) & & D(\lambda) \\ & C(\lambda) & D(\lambda) \end{pmatrix}, \quad \mathcal{M}_b(\lambda') = \begin{pmatrix} A(\lambda') & B(\lambda') & & \\ C(\lambda') & D(\lambda') & & \\ & & A(\lambda') & B(\lambda') \\ & & C(\lambda') & D(\lambda') \end{pmatrix}. \end{aligned} \quad (\text{B.15})$$

By comparing the (1, 4)-, (1, 3)- and (3, 4)-components on the two sides, we obtain respectively equations (5.33), (5.34) and (5.35).

Let us now discuss how the Bethe equations arise by demanding that the generic Bethe state $|\psi\rangle$ of (5.32) is indeed an eigenvector of the transfer matrix. One can convince oneself

by going through a few examples that

$$\begin{aligned}
A(\lambda) |\psi\rangle &= \prod_{i=1}^n f(\lambda - \lambda_i) \left(\lambda + \frac{i}{2} \right)^N B(\lambda_1) \cdots B(\lambda_n) |\Omega\rangle + \\
&\quad + \sum_{i=1}^n a_i(\lambda, \{\lambda_j\}) \left(\lambda_i + \frac{i}{2} \right)^N B(\lambda_1) \cdots \widehat{B(\lambda_i)} \cdots B(\lambda_n) B(\lambda) |\Omega\rangle , \\
D(\lambda) |\psi\rangle &= \prod_{i=1}^n h(\lambda - \lambda_i) \left(\lambda - \frac{i}{2} \right)^N B(\lambda_1) \cdots B(\lambda_n) |\Omega\rangle + \\
&\quad + \sum_{i=1}^n d_i(\lambda, \{\lambda_j\}) \left(\lambda_i - \frac{i}{2} \right)^N B(\lambda_1) \cdots \widehat{B(\lambda_i)} \cdots B(\lambda_n) B(\lambda) |\Omega\rangle .
\end{aligned} \tag{B.16}$$

Each coefficient $a_k(\lambda, \{\lambda_j\})$, $d_k(\lambda, \{\lambda_j\})$ is the sum of 2^{k-1} contributions, products of f, g and h, k functions respectively: their structure depends on which terms of (5.34), (5.35) are picked in commuting $A(\lambda)$ and $D(\lambda)$ past the various $B(\lambda_i)$. In particular, a_1 and d_1 are given by a single term, namely

$$\begin{aligned}
a_1 &= g(\lambda - \lambda_1) \prod_{k \neq 1} f(\lambda_1 - \lambda_k) = \frac{i}{\lambda - \lambda_1} \prod_{k \neq 1} \frac{\lambda_1 - \lambda_k - i}{\lambda_1 - \lambda_k} , \\
d_1 &= k(\lambda - \lambda_1) \prod_{k \neq 1} h(\lambda_1 - \lambda_k) = \frac{-i}{\lambda - \lambda_1} \prod_{k \neq 1} \frac{\lambda_1 - \lambda_k + i}{\lambda_1 - \lambda_k} .
\end{aligned} \tag{B.17}$$

It is easy to convince oneself that the simplicity of a_1 and d_1 is a consequence of having written $|\psi\rangle = B(\lambda_1) \cdots |\Omega\rangle$, i.e. of having $B(\lambda_1)$ appear to the far left in our ansatz. In view of (5.33), however, we know that the order of the $B(\lambda_i)$ is immaterial, hence in full generality

$$\begin{aligned}
a_i &= g(\lambda - \lambda_i) \prod_{k \neq i} f(\lambda_i - \lambda_k) = \frac{i}{\lambda - \lambda_i} \prod_{k \neq i} \frac{\lambda_i - \lambda_k - i}{\lambda_i - \lambda_k} , \\
d_i &= k(\lambda - \lambda_i) \prod_{k \neq i} h(\lambda_i - \lambda_k) = \frac{-i}{\lambda - \lambda_i} \prod_{k \neq i} \frac{\lambda_i - \lambda_k + i}{\lambda_i - \lambda_k} .
\end{aligned} \tag{B.18}$$

Notice that $k(\lambda - \lambda_i) = -g(\lambda - \lambda_i)$: hence in summing the two expressions in (B.16) we obtain that the Bethe state $|\psi\rangle$ is an eigenvector of the transfer matrix if and only if

$$\left(\lambda_i + \frac{i}{2} \right)^N \prod_{k \neq i} \frac{\lambda_i - \lambda_k - i}{\lambda_i - \lambda_k} = \left(\lambda_i - \frac{i}{2} \right)^N \prod_{k \neq i} \frac{\lambda_i - \lambda_k + i}{\lambda_i - \lambda_k} , \quad i = 1, \dots, n . \tag{B.19}$$

i.e. the Bethe equations. Let us now argue that these are precisely the conditions for the

cancellation of the superficial poles in the eigenvalues of (5.38). We have

$$\begin{aligned}
\Lambda(\lambda, \{\lambda_j\}) &= \\
&= \left(\lambda + \frac{i}{2}\right)^N \frac{\lambda - \lambda_i - i}{\lambda - \lambda_i} \prod_{k \neq i} \left(\frac{\lambda - \lambda_k - i}{\lambda - \lambda_k}\right) + \left(\lambda - \frac{i}{2}\right)^N \frac{\lambda - \lambda_i + i}{\lambda - \lambda_i} \prod_{k \neq i} \left(\frac{\lambda - \lambda_k + i}{\lambda - \lambda_k}\right) = \\
&= \left[\left(\lambda + \frac{i}{2}\right)^N \prod_{k \neq i} \left(\frac{\lambda - \lambda_k - i}{\lambda - \lambda_k}\right) + \left(\lambda - \frac{i}{2}\right)^N \prod_{k \neq i} \left(\frac{\lambda - \lambda_k + i}{\lambda - \lambda_k}\right) \right] + \\
&\quad - \frac{i}{\lambda - \lambda_i} \left[\left(\lambda + \frac{i}{2}\right)^N \prod_{k \neq i} \left(\frac{\lambda - \lambda_k - i}{\lambda - \lambda_k}\right) + \left(\lambda - \frac{i}{2}\right)^N \prod_{k \neq i} \left(\frac{\lambda - \lambda_k + i}{\lambda - \lambda_k}\right) \right],
\end{aligned}$$

where we chose to single out the i -th factor from the products. We observe that the first summand of the above rewriting is regular for $\lambda = \lambda_i$, whereas the second is of course not: to avoid the divergence, we have to make sure that the coefficient of $(\lambda - \lambda_i)^{-1}$ vanishes. This argument holds of course for each choice of i , producing the full set of n Bethe equations.

Appendix C

Yangian for the tree amplituhedron

This Appendix collects some derivations relevant to Sections 5.2 and 5.3.

C.1 Construction of volume functions

We will prove the identity (5.50)

$$\Omega_{n,k}^{(m)}(Y, Z) = \prod_{l=1}^{k(n-k)} \mathcal{B}_{i_l j_l}(0) \mathcal{S}_k^{(m)} . \quad (\text{C.1})$$

First of all, we know [57] that in the case of amplitudes

$$\prod_{l=1}^{k(n-k)} \mathcal{B}_{i_l j_l}(0) \prod_{i=1}^k \delta^{4|4}(\mathcal{Z}_i^{\mathcal{A}}) = \int \frac{\mathrm{d}^{k \times (n-k)} \tilde{C}}{\widetilde{\mathcal{M}}_1 \cdots \widetilde{\mathcal{M}}_n} \delta^{4|4}(\tilde{C} \cdot \mathcal{Z}) , \quad (\text{C.2})$$

i.e. after changing variables, we can recover a gauge-fixed version of the Grassmannian formula (2.124), with $\tilde{C} = (\mathbb{1}_{k \times k} | F_{k \times (n-k)})$ a matrix with the first k columns fixed to the identity and $\widetilde{\mathcal{M}}_i$ its consecutive maximal minors. We can now use this result and act with the $\mathcal{B}_{i_l j_l}(0)$ operators on the seed $\mathcal{S}_k^{(m)}$ instead of the δ -functions:

$$\begin{aligned} \prod_{l=1}^{k(n-k)} \mathcal{B}_{i_l j_l}(0) \mathcal{S}_k^{(m)} &= \int \frac{\mathrm{d}^{k \times k} \beta}{(\det \beta)^k} \prod_{l=1}^{k(n-k)} \mathcal{B}_{i_l j_l}(0) \delta^{k(m+k)}(Y - \beta \cdot Z) = \\ &= \int \frac{\mathrm{d}^{k \times k} \beta}{(\det \beta)^k} \int \frac{\mathrm{d}^{k \times (n-k)} \tilde{C}}{\widetilde{\mathcal{M}}_1 \cdots \widetilde{\mathcal{M}}_n} \delta^{k(m+k)}(Y - \beta \cdot \tilde{C} \cdot Z) . \end{aligned} \quad (\text{C.3})$$

The amplituhedron volume function can be reconstructed by the following change of variables: $\beta' = \beta$ and $F' = \beta \cdot F$, such that the new variables are rearranged in the matrix

$C = (\beta' | F') = \beta \cdot \tilde{C}$. The related Jacobian is $(\det \beta)^{-(n-k)}$, whereas each of the n minors $\tilde{\mathcal{M}}_i$ of \tilde{C} equals the corresponding \mathcal{M}_i of C , up to a factor $(\det \beta)^{-1}$. In the end,

$$\prod_{l=1}^{k(n-k)} \mathcal{B}_{i_l j_l}(0) \mathcal{S}_k^{(m)} = \int \frac{d^{k \times n} C}{\mathcal{M}_1 \cdots \mathcal{M}_n} \delta^{k(m+k)}(Y - C \cdot Z) = \Omega_{n,k}^{(m)}. \quad (\text{C.4})$$

C.2 Seed mutations

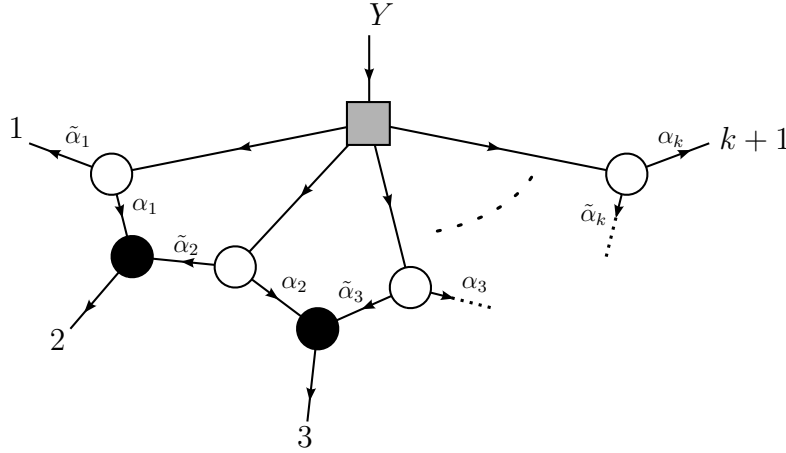


Figure C.1: On-shell diagram

In this appendix we prove that the seed mutations depicted in Fig. 5.3 hold true for any k . We consider the on-shell diagram portrayed in Figure C.1 and show that we can cyclically relabel particles $1, \dots, k+1$ and the diagram evaluates to the same Grassmannian integral. Using the rules of Figure 5.1 and solving the δ -functions arising from the trivalent vertices, we obtain an integral representation involving both $\alpha, \tilde{\alpha}$ and $\gamma, \tilde{\gamma}$ variables, respectively associated to white and black vertices. The latter can be eliminated fixing $2(k-1)$ of the $\text{GL}(1, \mathbb{R})$ redundancies due to the projective nature of the bosonized twistors running along the internal lines and we arrive at

$$\int \prod_{a=1}^k \frac{d\alpha_a}{\alpha_a} \prod_{a=1}^k \frac{d\tilde{\alpha}_a}{\tilde{\alpha}_a} \int \frac{d^{k \times k} \beta}{(\det \beta)^k} \delta^{k(m+k)}(Y - \beta \cdot C \cdot Z), \quad (\text{C.5})$$

where C is a matrix whose entries read $C(\tilde{\alpha}, \alpha)_{ai} = \delta_{ai} \tilde{\alpha}_a + \delta_{a,i-1} \alpha_a$. Using the last k $\text{GL}(1, \mathbb{R})$ redundancies, we can eliminate the $\tilde{\alpha}$ variables too, which yields an even simpler

form for C , namely $C(\alpha)_{ai} = \delta_{ai} + \delta_{a,i-1}\alpha_{k+1-a}$. In formulae,

$$C(\alpha, \tilde{\alpha}) = \begin{pmatrix} \tilde{\alpha}_1 & \alpha_1 & & \\ & \tilde{\alpha}_2 & \alpha_2 & \\ & & \ddots & \\ & & & \tilde{\alpha}_k & \alpha_k \end{pmatrix} \longrightarrow C(\alpha) = \begin{pmatrix} 1 & \alpha_1 & & \\ & 1 & \alpha_2 & \\ & & \ddots & \\ & & & 1 & \alpha_k \end{pmatrix}, \quad (\text{C.6})$$

resulting in the following expression for the on-shell diagram of Figure C.1:

$$\int \prod_{a=1}^k \frac{d\alpha_a}{\alpha_a} \int \frac{d^{k \times k} \beta}{(\det \beta)^k} \delta^{k(m+k)}(Y - \beta \cdot C(\alpha) \cdot Z). \quad (\text{C.7})$$

We would like to give C an even simpler structure, such that its first k columns form an identity matrix and only the last one is non-trivial. This is achieved using the following $\text{GL}(k, \mathbb{R})$ transformation: if A is the square matrix formed by the first k columns of C , then $A^{-1}C = (\mathbb{1}_{k \times k} | F_{k \times 1})$, with $F(\alpha)_a = (-1)^{k-a} \alpha_1 \cdots \alpha_{k+1-a}$. At this point we change variables from α 's to c 's, namely $c_{a,k+1} = F_a(\alpha)$, and from β_{aj} to $\beta'_{ab} = (\beta \cdot A)_{ab}$. Calling $\widetilde{\mathcal{M}}_i$ the minor $(i, \dots, i+k-1)$ of the matrix $\tilde{C} = (\mathbb{1}_{k \times k} | c_{a,k+1})$, we observe that

$$\prod_{a=1}^k \frac{d\alpha_a}{\alpha_a} = \prod_{a=1}^k \frac{dc_{a,k+1}}{c_{a,k+1}} = \frac{d^k c}{\prod_{i=1}^{k+1} \widetilde{\mathcal{M}}_i}, \quad (\text{C.8})$$

and we recover the gauge-fixed version of the Grassmannian integral over C already appeared in (C.3). Following the same steps presented in Appendix A, we can thus bring (C.7) to the form

$$\int \frac{d^{k \times (k+1)} c}{\mathcal{M}_1 \cdots \mathcal{M}_{k+1}} \delta^{k(m+k)}(Y - C \cdot Z) = \Omega_{k+1,k}^{(m)}(Y, Z), \quad (\text{C.9})$$

which exhibits a manifest cyclic symmetry in Z_1, \dots, Z_{k+1} .

C.3 Intertwining relations

In this appendix we will prove formula (5.68), assuming $i \neq j$

$$\mathcal{L}_i(u - v_i) \mathcal{L}_j(u - v_j) \mathcal{B}_{ij}(v_j - v_i) = \mathcal{B}_{ij}(v_j - v_i) \mathcal{L}_i(u - v_j) \mathcal{L}_j(u - v_i). \quad (\text{C.10})$$

We observe that on both sides we get the same contribution proportional to δ_B^A , namely

$$(u - v_i)(u - v_j) \mathcal{B}_{ij}(v_j - v_i). \quad (\text{C.11})$$

Focusing on the other terms, we have (denoting $\nu_i = u - v_i$ and $\nu = \nu_i - \nu_j = v_j - v_i$)

$$\begin{aligned} & \left(\nu_i Z_j^A \frac{\partial}{\partial Z_j^B} + \nu_j Z_i^A \frac{\partial}{\partial Z_i^B} + Z_i^A \frac{\partial}{\partial Z_i^C} Z_j^C \frac{\partial}{\partial Z_j^B} \right) \left(Z_j^D \frac{\partial}{\partial Z_i^D} \right)^\nu = \\ & = \left(Z_j^D \frac{\partial}{\partial Z_i^D} \right)^\nu \left(\nu_j Z_j^A \frac{\partial}{\partial Z_j^B} + \nu_i Z_i^A \frac{\partial}{\partial Z_i^B} + Z_i^A \frac{\partial}{\partial Z_i^C} Z_j^C \frac{\partial}{\partial Z_j^B} \right). \end{aligned} \quad (\text{C.12})$$

First, we observe that

$$\left[Z_l^A \frac{\partial}{\partial Z_l^B}, Z_j^D \frac{\partial}{\partial Z_i^D} \right] = (\delta_{jl} - \delta_{il}) Z_j^A \frac{\partial}{\partial Z_i^B}. \quad (\text{C.13})$$

The RHS trivially commutes with $Z_j^D \frac{\partial}{\partial Z_i^D}$, thus we can use the formula

$$[[A, B], B] = 0 \quad \Rightarrow \quad [A, B^\nu] = \nu[A, B]B^{\nu-1}. \quad (\text{C.14})$$

to perform the commutation in the first two summands of the LHS of (C.12), obtaining

$$\nu(\nu_i - \nu_j) Z_j^A \frac{\partial}{\partial Z_i^B} \left(Z_j^D \frac{\partial}{\partial Z_i^D} \right)^{\nu-1}. \quad (\text{C.15})$$

Manipulating the third one in a similar fashion, one arrives at

$$\nu \left(Z_j^D \frac{\partial}{\partial Z_i^D} \right)^\nu \left(Z_i^A \frac{\partial}{\partial Z_i^B} - Z_j^A \frac{\partial}{\partial Z_j^B} \right) - \nu^2 \left(Z_j^D \frac{\partial}{\partial Z_i^D} \right)^{\nu-1} Z_j^A \frac{\partial}{\partial Z_i^B}. \quad (\text{C.16})$$

Now it is immediate to check that (C.12) turns into

$$(\nu + \nu_j - \nu_i) \left[\left(Z_j^D \frac{\partial}{\partial Z_i^D} \right)^\nu \left(Z_i^A \frac{\partial}{\partial Z_i^B} - Z_j^A \frac{\partial}{\partial Z_j^B} \right) - \nu \left(Z_j^D \frac{\partial}{\partial Z_i^D} \right)^{\nu-1} Z_j^A \frac{\partial}{\partial Z_i^B} \right] = 0, \quad (\text{C.17})$$

which holds true since $\nu = \nu_i - \nu_j$.

C.4 Action of the monodromy matrix on the seed

We will prove the identity (5.77)

$$\mathcal{L}_i(u, v_i)_B^C (J_Y)_C^A \mathcal{S}_k^{(m)} = \begin{cases} (u - v_i - 1) (J_Y)_B^A \mathcal{S}_k^{(m)}, & i = 1, \dots, k \\ (u - v_i) (J_Y)_B^A \mathcal{S}_k^{(m)}, & i = k + 1, \dots, n. \end{cases} \quad (\text{C.18})$$

In the following we will work with the matrix elements and suppress the arguments of the \mathcal{L}_i operators. We start with

$$\begin{aligned}\mathcal{L}_i(u, v_i) {}^C_B (J_Y) {}^A_C \mathcal{S}_k^{(m)} &= \left((u - v_i) \delta_B^C + Z_i^C \frac{\partial}{\partial Z_i^B} \right) \left(\sum_{\alpha=1}^k Y_\alpha^A \frac{\partial}{\partial Y_\alpha^C} + k \delta_C^A \right) \mathcal{S}_k^{(m)} = \\ &= (u - v_i) (J_Y) {}^A_B \mathcal{S}_k^{(m)} + Z_i^C \frac{\partial}{\partial Z_i^B} \left(\sum_{\alpha=1}^k Y_\alpha^A \frac{\partial}{\partial Y_\alpha^C} + k \delta_C^A \right) \mathcal{S}_k^{(m)}.\end{aligned}\tag{C.19}$$

We argue that the second summand is trivially zero for $i > k$, since $\mathcal{S}_k^{(m)}$ just depends on Z_1, \dots, Z_k , whereas it is equal to $-(J_Y) {}^A_B \mathcal{S}_k^{(m)}$ for $i = 1, \dots, k$. Using the fact that the seed $\mathcal{S}_k^{(m)}$ is $\text{GL}(m+k, \mathbb{R})$ -covariant in the same way as $\Omega_{n,k}^{(m)}$ is, see (4.2), we can write the second summand as

$$-Z_i^C \frac{\partial}{\partial Z_i^B} \left(\sum_{l=1}^k Z_l^A \frac{\partial}{\partial Z_l^C} \right) \mathcal{S}_k^{(m)}.\tag{C.20}$$

Now we recast the operators acting on Z_i into ones acting on the integration variables $\beta_{\alpha i}$:

$$\sum_{l=1}^k Z_i^C \frac{\partial}{\partial Z_i^B} Z_l^A \frac{\partial}{\partial Z_l^C} = \sum_{l=1}^k \frac{\partial}{\partial Z_i^B} Z_l^A Z_i^C \frac{\partial}{\partial Z_l^C} - \sum_{l=1}^k Z_l^A \frac{\partial}{\partial Z_l^B},\tag{C.21}$$

finally noticing that

$$Z_i^C \frac{\partial}{\partial Z_l^C} \mathcal{S}_k^{(m)} = \int \frac{d^{k \times k} \beta}{(\det \beta)^k} \mathbb{O}_l^i \delta^{k(m+k)}(Y - \beta \cdot Z), \quad \mathbb{O}_l^i = \beta_{\alpha l} \frac{\partial}{\partial \beta_{\alpha i}}.\tag{C.22}$$

Suppressing the argument of the δ -function,

$$\begin{aligned}\int \frac{d^{k \times k} \beta}{(\det \beta)^k} \mathbb{O}_l^i \delta^{k(m+k)} &= \int d^{k \times k} \beta \left(\mathbb{O}_l^i (\det \beta)^{-k} - [\mathbb{O}_l^i, (\det \beta)^{-k}] \right) \delta^{k(m+k)} = \\ &= \int d^{k \times k} \beta \left(\frac{\partial}{\partial \beta_{\alpha i}} \beta_{\alpha l} - k \delta_l^i \right) (\det \beta)^{-k} \delta^{k(m+k)} + k \delta_l^i \int d^{k \times k} \beta (\det \beta)^{-k} \delta^{k(m+k)} = 0,\end{aligned}\tag{C.23}$$

where in the first integral we have dropped the total derivative term and in the second one we used

$$[\mathbb{O}_l^i, (\det \beta)^{-k}] = -k (\det \beta)^{-k-1} [\mathbb{O}_l^i, \det \beta] = -k \delta_l^i (\det \beta)^{-k},$$

since the operator \mathbb{O}_l^i acts on the determinant simply substituting the i -th with the l -th row. Substituting back all the intermediate results and using again $\text{GL}(m+k, \mathbb{R})$ covariance of the seed to rewrite the second term in the LHS of (C.21), we readily obtain the desired identity (C.18).

Bibliography

- [1] H. Goldstein, C. Poole and J. Safko, “*Classical Mechanics*”, Addison Wesley (2002).
- [2] W. Pauli, “*Über das Wasserstoffspektrum vom Standpunkt der neuen Quantenmechanik*”, Z. Phys. 36, 336 (1926).
- [3] J. J. Sakurai and J. Napolitano, “*Modern quantum physics*”, Addison-Wesley (2011).
- [4] R. P. Feynman, “*Space-Time approach to quantum electrodynamics*”, Phys. Rev. 76, 769 (1949).
- [5] S. J. Parke and T. R. Taylor, “*The Cross Section for Four-Gluon Production by Gluon-Gluon Fusion*”, Nucl. Phys. B269, 410 (1986).
- [6] S. J. Parke and T. R. Taylor, “*Amplitude for n -Gluon Scattering*”, Phys. Rev. Lett. 56, 2459 (1986).
- [7] R. J. Eden, P. V. Landshoff, D. I. Olive and J. C. Polkinghorne, “*The analytic S-matrix*”, Cambridge University Press (2002).
- [8] R. E. Cutkosky, “*Singularities and discontinuities of Feynman amplitudes*”, J. Math. Phys. 1, 429 (1960).
- [9] Z. Bern, L. J. Dixon, D. C. Dunbar and D. A. Kosower, “*One-Loop n -Point Gauge Theory Amplitudes, Unitarity and Collinear Limits*”, Nucl. Phys. B425, 217 (1994), hep-ph/9403226.
- [10] Z. Bern, L. J. Dixon, D. C. Dunbar and D. A. Kosower, “*Fusing gauge theory tree amplitudes into loop amplitudes*”, Nucl. Phys. B435, 59 (1995), hep-ph/9409265.
- [11] Z. Bern, L. J. Dixon and D. A. Kosower, “*One-loop amplitudes for $e^+ e^-$ to four partons*”, Nucl. Phys. B513, 3 (1998), hep-ph/9708239.
- [12] S. Badger, G. Mogull and T. Peraro, “*Local integrands for two-loop all-plus Yang–Mills amplitudes*”, JHEP 1608, 063 (2016), arxiv:1606.02244.
- [13] D. C. Dunbar, G. R. Jehu and W. B. Perkins, “*Two-loop six gluon all plus helicity amplitude*”, Phys. Rev. Lett. 117, 061602 (2016), arxiv:1605.06351.

- [14] Z. Bern, J. J. M. Carrasco, L. J. Dixon, H. Johansson and R. Roiban, “*The Complete Four-Loop Four-Point Amplitude in $\mathcal{N} = 4$ super Yang–Mills Theory*”, Phys. Rev. D82, 125040 (2010), [arxiv:1008.3327](#).
- [15] Z. Bern, J. J. M. Carrasco, H. Johansson and R. Roiban, “*The Five-Loop Four-Point Amplitude of $\mathcal{N} = 4$ super Yang–Mills Theory*”, Phys. Rev. Lett. 109, 241602 (2012), [arxiv:1207.6666](#).
- [16] Z. Bern, L. J. Dixon and V. A. Smirnov, “*Iteration of planar amplitudes in maximally supersymmetric Yang–Mills theory at three loops and beyond*”, Phys. Rev. D72, 085001 (2005), [hep-th/0505205](#).
- [17] Z. Bern and Y.-t. Huang, “*Basics of Generalized Unitarity*”, J. Phys. A44, 454003 (2011), [arxiv:1103.1869](#).
- [18] J. J. M. Carrasco and H. Johansson, “*Generic multiloop methods and application to $\mathcal{N} = 4$ super Yang–Mills*”, J. Phys. A44, 454004 (2011), [arxiv:1103.3298](#).
- [19] E. Witten, “*Perturbative gauge theory as a string theory in twistor space*”, Commun. Math. Phys. 252, 189 (2004), [hep-th/0312171](#).
- [20] R. Penrose, “*Twistor algebra*”, J. Math. Phys. 8, 345 (1967).
- [21] R. Penrose and M. A. MacCallum, “*Twistor theory: An Approach to the quantization of fields and space-time*”, Phys.Rept. 6, 241 (1972).
- [22] N. Berkovits, “*An Alternative string theory in twistor space for $\mathcal{N} = 4$ super Yang–Mills*”, Phys. Rev. Lett. 93, 011601 (2004), [hep-th/0402045](#).
- [23] R. Roiban and A. Volovich, “*All conjugate-maximal-helicity-violating amplitudes from topological open string theory in twistor space*”, Phys. Rev. Lett. 93, 131602 (2004), [hep-th/0402121](#).
- [24] R. Roiban, M. Spradlin and A. Volovich, “*On the tree-level S-matrix of Yang–Mills theory*”, Phys. Rev. D70, 026009 (2004), [hep-th/0403190](#).
- [25] F. Cachazo, P. Svrček and E. Witten, “*MHV vertices and tree amplitudes in gauge theory*”, JHEP 0409, 006 (2004), [hep-th/0403047](#).
- [26] R. Britto, F. Cachazo and B. Feng, “*New recursion relations for tree amplitudes of gluons*”, Nucl. Phys. B715, 499 (2005), [hep-th/0412308](#).
- [27] R. Britto, F. Cachazo, B. Feng and E. Witten, “*Direct proof of tree-level recursion relation in Yang–Mills theory*”, Phys. Rev. Lett. 94, 181602 (2005), [hep-th/0501052](#).
- [28] H. Elvang, D. Z. Freedman and M. Kiermaier, “*Proof of the MHV vertex expansion for all tree amplitudes in $\mathcal{N} = 4$ SYM theory*”, JHEP 0906, 068 (2009), [arxiv:0811.3624](#).

- [29] J. M. Drummond and J. M. Henn, “*All tree-level amplitudes in $\mathcal{N} = 4$ SYM*”, JHEP 0904, 018 (2009), [arxiv:0808.2475](#).
- [30] N. Arkani-Hamed, J. L. Bourjaily, F. Cachazo, S. Caron-Huot and J. Trnka, “*The All-Loop Integrand For Scattering Amplitudes in Planar $\mathcal{N} = 4$ SYM*”, JHEP 1101, 041 (2011), [arxiv:1008.2958](#).
- [31] J. M. Maldacena, “*The Large- N limit of superconformal field theories and supergravity*”, Int. J. Theor. Phys. 38, 1113 (1999), [hep-th/9711200](#), [Adv. Theor. Math. Phys. 2, 231 (1998)].
- [32] L. F. Alday and J. M. Maldacena, “*Gluon scattering amplitudes at strong coupling*”, JHEP 0706, 064 (2007), [arxiv:0705.0303](#).
- [33] L. F. Alday and J. Maldacena, “*Comments on gluon scattering amplitudes via AdS/CFT* ”, JHEP 0711, 068 (2007), [arxiv:0710.1060](#).
- [34] M. Ammon and J. Erdmenger, “*Gauge/Gravity Duality*”, Cambridge University Press (2015).
- [35] J. M. Drummond, J. M. Henn, G. P. Korchemsky and E. Sokatchev, “*Dual superconformal symmetry of scattering amplitudes in $\mathcal{N} = 4$ super-Yang-Mills theory*”, Nucl. Phys. B828, 317 (2010), [arxiv:0807.1095](#).
- [36] J. M. Drummond, J. M. Henn and J. Plefka, “*Yangian symmetry of scattering amplitudes in $\mathcal{N} = 4$ super Yang-Mills theory*”, JHEP 0905, 046 (2009), [arxiv:0902.2987](#).
- [37] N. Beisert, C. Ahn, L. F. Alday, Z. Bajnok, J. M. Drummond et al., “*Review of AdS/CFT Integrability: An Overview*”, Lett.Math.Phys. 99, 3 (2012), [arxiv:1012.3982](#).
- [38] J. A. Minahan and K. Zarembo, “*The Bethe-Ansatz for $\mathcal{N} = 4$ super Yang-Mills*”, JHEP 0303, 013 (2003), [hep-th/0212208](#).
- [39] N. Beisert, “*The Complete One-Loop Dilatation Operator of $\mathcal{N} = 4$ Super Yang-Mills Theory*”, Nucl. Phys. B676, 3 (2004), [hep-th/0307015](#).
- [40] J. A. Minahan, “*Review of AdS/CFT Integrability, Chapter I.1: Spin Chains in $\mathcal{N} = 4$ Super Yang-Mills*”, Lett. Math. Phys. 99, 33 (2012), [arxiv:1012.3983](#).
- [41] B. Basso, A. Sever and P. Vieira, “*Spacetime and Flux Tube S -Matrices at Finite Coupling for $\mathcal{N} = 4$ Supersymmetric Yang-Mills Theory*”, Phys. Rev. Lett. 111, 091602 (2013), [arxiv:1303.1396](#).
- [42] A. Hodges, “*Eliminating spurious poles from gauge-theoretic amplitudes*”, JHEP 1305, 135 (2013), [arxiv:0905.1473](#).

- [43] N. Arkani-Hamed, F. Cachazo, C. Cheung and J. Kaplan, “*A Duality For The S Matrix*”, JHEP 1003, 020 (2010), [arxiv:0907.5418](#).
- [44] L. J. Mason and D. Skinner, “*Dual Superconformal Invariance, Momentum Twistors and Grassmannians*”, JHEP 0911, 045 (2009), [arxiv:0909.0250](#).
- [45] N. Arkani-Hamed, F. Cachazo and C. Cheung, “*The Grassmannian Origin Of Dual Superconformal Invariance*”, JHEP 1003, 036 (2010), [arxiv:0909.0483](#).
- [46] J. M. Drummond and L. Ferro, “*Yangians, Grassmannians and T-duality*”, JHEP 1007, 027 (2010), [arxiv:1001.3348](#).
- [47] J. M. Drummond and L. Ferro, “*The Yangian origin of the Grassmannian integral*”, JHEP 1012, 010 (2010), [arxiv:1002.4622](#).
- [48] G. Korchemsky and E. Sokatchev, “*Superconformal invariants for scattering amplitudes in $\mathcal{N} = 4$ SYM theory*”, Nucl.Phys. B839, 377 (2010), [arxiv:1002.4625](#).
- [49] A. Postnikov, “*Total positivity, Grassmannians, and networks*”, [math/0609764](#).
- [50] N. Arkani-Hamed, J. L. Bourjaily, F. Cachazo, A. B. Goncharov, A. Postnikov and J. Trnka, “*Scattering Amplitudes and the Positive Grassmannian*”, Cambridge University Press (2012), [arxiv:1212.5605](#).
- [51] N. Arkani-Hamed, J. L. Bourjaily, F. Cachazo, A. Hodges and J. Trnka, “*A Note on Polytopes for Scattering Amplitudes*”, JHEP 1204, 081 (2012), [arxiv:1012.6030](#).
- [52] N. Arkani-Hamed and J. Trnka, “*The Amplituhedron*”, JHEP 1410, 030 (2014), [arxiv:1312.2007](#).
- [53] N. Arkani-Hamed and J. Trnka, “*Into the Amplituhedron*”, JHEP 1412, 182 (2014), [arxiv:1312.7878](#).
- [54] L. Ferro, T. Lukowski, A. Orta and M. Parisi, “*Towards the Amplituhedron Volume*”, JHEP 1603, 014 (2016), [arxiv:1512.04954](#).
- [55] L. Ferro, T. Lukowski, J. F. Morales, A. Orta and C. Wen, unpublished notes.
- [56] L. Ferro, T. Lukowski, A. Orta and M. Parisi, “*Yangian Symmetry for the Tree Amplituhedron*”, [arxiv:1612.04378](#).
- [57] N. Kanning, T. Lukowski and M. Staudacher, “*A shortcut to general tree-level scattering amplitudes In $\mathcal{N} = 4$ SYM via integrability*”, Fortsch.Phys. 62, 556 (2014), [arxiv:1403.3382](#).
- [58] M. Gell-Mann and F. Low, “*Bound states in quantum field theory*”, Phys. Rev. 84, 350 (1951).

- [59] R. Kleiss and H. Kuijf, “*Multi - Gluon Cross-sections and Five Jet Production at Hadron Colliders*”, Nucl. Phys. B312, 616 (1989).
- [60] G. 't Hooft, “*A Planar Diagram Theory for Strong Interactions*”, Nucl. Phys. B72, 461 (1974).
- [61] M. L. Mangano and S. J. Parke, “*Multi-Parton Amplitudes in Gauge Theories*”, Phys. Rept. 200, 301 (1991), [hep-th/0509223](#).
- [62] Z. Bern and D. A. Kosower, “*Color decomposition of one loop amplitudes in gauge theories*”, Nucl. Phys. B362, 389 (1991).
- [63] J. E. Paton and H.-M. Chan, “*Generalized Veneziano model with isospin*”, Nucl. Phys. B10, 516 (1969).
- [64] H. Elvang and Y.-t. Huang, “*Scattering Amplitudes in Gauge Theory and Gravity*”, Cambridge University Press (2015), [arxiv:1308.1697](#).
- [65] V. Del Duca, A. Frizzo and F. Maltoni, “*Factorization of tree QCD amplitudes in the high-energy limit and in the collinear limit*”, Nucl. Phys. B568, 211 (2000), [hep-ph/9909464](#).
- [66] V. Del Duca, L. J. Dixon and F. Maltoni, “*New color decompositions for gauge amplitudes at tree and loop level*”, Nucl. Phys. B571, 51 (2000), [hep-ph/9910563](#).
- [67] Z. Bern, J. J. M. Carrasco and H. Johansson, “*New Relations for Gauge-Theory Amplitudes*”, Phys. Rev. D78, 085011 (2008), [arxiv:0805.3993](#).
- [68] J. M. Henn and J. C. Plefka, “*Scattering Amplitudes in Gauge Theories*”, Lect. Notes Phys. 883, pp.1 (2014).
- [69] N. Arkani-Hamed, F. Cachazo and J. Kaplan, “*What is the Simplest Quantum Field Theory?*”, JHEP 1009, 016 (2010), [arxiv:0808.1446](#).
- [70] L. Brink, J. H. Schwarz and J. Scherk, “*Supersymmetric Yang-Mills Theories*”, Nucl. Phys. B121, 77 (1977).
- [71] M. F. Sohnius, “*Introducing Supersymmetry*”, Phys. Rept. 128, 39 (1985).
- [72] V. P. Nair, “*A Current Algebra for Some Gauge Theory Amplitudes*”, Phys. Lett. B214, 215 (1988).
- [73] J. M. Drummond, J. Henn, G. P. Korchemsky and E. Sokatchev, “*Generalized unitarity for $N=4$ super-amplitudes*”, Nucl. Phys. B869, 452 (2013), [arxiv:0808.0491](#).
- [74] M. T. Grisaru and H. N. Pendleton, “*Some Properties of Scattering Amplitudes in Supersymmetric Theories*”, Nucl. Phys. B124, 81 (1977).

- [75] M. T. Grisaru, H. N. Pendleton and P. van Nieuwenhuizen, “*Supergravity and the S Matrix*”, Phys. Rev. D15, 996 (1977).
- [76] P. De Causmaecker, R. Gastmans, W. Troost and T. T. Wu, “*Multiple Bremsstrahlung in Gauge Theories at High-Energies. 1. General Formalism for Quantum Electrodynamics*”, Nucl. Phys. B206, 53 (1982).
- [77] F. A. Berends, R. Kleiss, P. De Causmaecker, R. Gastmans, W. Troost and T. T. Wu, “*Multiple Bremsstrahlung in Gauge Theories at High-Energies. 2. Single Bremsstrahlung*”, Nucl. Phys. B206, 61 (1982).
- [78] R. Kleiss and W. J. Stirling, “*Spinor Techniques for Calculating $p\bar{p} \rightarrow W^\pm/Z^0 + \text{Jets}$* ”, Nucl. Phys. B262, 235 (1985).
- [79] F. A. Berends and W. T. Giele, “*Recursive Calculations for Processes with n Gluons*”, Nucl. Phys. B306, 759 (1988).
- [80] F. Cachazo, P. Svrček and E. Witten, “*Gauge theory amplitudes in twistor space and holomorphic anomaly*”, JHEP 0410, 077 (2004), [hep-th/0409245](#).
- [81] F. Cachazo, “*Holomorphic anomaly of unitarity cuts and one-loop gauge theory amplitudes*”, [hep-th/0410077](#).
- [82] R. Britto, F. Cachazo and B. Feng, “*Computing one-loop amplitudes from the holomorphic anomaly of unitarity cuts*”, Phys. Rev. D71, 025012 (2005), [hep-th/0410179](#).
- [83] T. Bargheer, N. Beisert, W. Galleas, F. Loebbert and T. McLoughlin, “*Exacting $\mathcal{N} = 4$ Superconformal Symmetry*”, JHEP 0911, 056 (2009), [arxiv:0905.3738](#).
- [84] A. Sever and P. Vieira, “*Symmetries of the $\mathcal{N} = 4$ SYM S-matrix*”, [arxiv:0908.2437](#).
- [85] C. Anastasiou, Z. Bern, L. J. Dixon and D. A. Kosower, “*Planar amplitudes in maximally supersymmetric Yang–Mills theory*”, Phys. Rev. Lett. 91, 251602 (2003), [hep-th/0309040](#).
- [86] J. M. Drummond, J. Henn, V. A. Smirnov and E. Sokatchev, “*Magic identities for conformal four-point integrals*”, JHEP 0701, 064 (2007), [hep-th/0607160](#).
- [87] J. M. Drummond, G. P. Korchemsky and E. Sokatchev, “*Conformal properties of four-gluon planar amplitudes and Wilson loops*”, Nucl. Phys. B795, 385 (2008), [arxiv:0707.0243](#).
- [88] J. M. Drummond, J. M. Henn, G. P. Korchemsky and E. Sokatchev, “*On planar gluon amplitudes/Wilson loops duality*”, Nucl. Phys. B795, 52 (2008), [arxiv:0709.2368](#).
- [89] D. Nguyen, M. Spradlin and A. Volovich, “*New Dual Conformally Invariant Off-Shell Integrals*”, Phys. Rev. D77, 025018 (2008), [arxiv:0709.4665](#).

- [90] Z. Bern, L. J. Dixon, D. A. Kosower, R. Roiban, M. Spradlin, C. Vergu and A. Volovich, “*The Two-Loop Six-Gluon MHV Amplitude in Maximally Supersymmetric Yang–Mills Theory*”, Phys. Rev. D78, 045007 (2008), [arxiv:0803.1465](#).
- [91] V. G. Drinfeld, “*Hopf algebras and the quantum Yang-Baxter equation*”, Sov. Math. Dokl. 32, 254 (1985).
- [92] V. G. Drinfeld, “*Quantum groups*”, J. Math. Sci. 41, 898 (1988).
- [93] L. Ferro, “*Yangian Symmetry in $\mathcal{N} = 4$ super Yang–Mills*”, [arxiv:1107.1776](#).
- [94] F. Loebbert, “*Lectures on Yangian Symmetry*”, J. Phys. A49, 323002 (2016), [arxiv:1606.02947](#).
- [95] L. Dolan, C. R. Nappi and E. Witten, “*Yangian symmetry in $D = 4$ superconformal Yang–Mills theory*”, [hep-th/0401243](#), in: “*Quantum Theory and Symmetries*”, World Scientific (2004).
- [96] J. M. Henn, “*Duality between Wilson loops and gluon amplitudes*”, Fortsch. Phys. 57, 729 (2009), [arxiv:0903.0522](#).
- [97] S. A. Huggett and K. P. Tod, “*An Introduction to Twistor Theory*”, Cambridge University Press (1986).
- [98] A. Ferber, “*Supertwistors and Conformal Supersymmetry*”, Nucl. Phys. B132, 55 (1978).
- [99] R. Penrose, “*Twistor quantization and curved space-time*”, Int. J. Theor. Phys. 1, 61 (1968).
- [100] K. Risager, “*A Direct proof of the CSW rules*”, JHEP 0512, 003 (2005), [hep-th/0508206](#).
- [101] Q. Jin and B. Feng, “*Recursion Relation for Boundary Contribution*”, JHEP 1506, 018 (2015), [arxiv:1412.8170](#).
- [102] N. Arkani-Hamed and J. Kaplan, “*On Tree Amplitudes in Gauge Theory and Gravity*”, JHEP 0804, 076 (2008), [arxiv:0801.2385](#).
- [103] S. Caron-Huot, “*Loops and trees*”, JHEP 1105, 080 (2011), [arxiv:1007.3224](#).
- [104] P. Griffiths and J. Harris, “*Principles of algebraic geometry*”, John Wiley & Sons (2014).
- [105] F. Cachazo, “*Sharpening The Leading Singularity*”, [arxiv:0803.1988](#).
- [106] M. Bullimore, L. J. Mason and D. Skinner, “*Twistor-Strings, Grassmannians and Leading Singularities*”, JHEP 1003, 070 (2010), [arxiv:0912.0539](#).
- [107] J. Kaplan, “*Unraveling $\mathcal{L}_{n,k}$: Grassmannian Kinematics*”, JHEP 1003, 025 (2010), [arxiv:0912.0957](#).

- [108] S. Franco, D. Galloni, B. Penante and C. Wen, “*Non-Planar On-Shell Diagrams*”, JHEP 1506, 199 (2015), [arxiv:1502.02034](#).
- [109] J. L. Bourjaily, “*Positroids, Plabic Graphs, and Scattering Amplitudes in Mathematica*”, [arxiv:1212.6974](#).
- [110] Y. Bai and S. He, “*The Amplituhedron from Momentum Twistor Diagrams*”, JHEP 1502, 065 (2015), [arxiv:1408.2459](#).
- [111] Z. Bern, E. Herrmann, S. Litsey, J. Stankowicz and J. Trnka, “*Evidence for a Nonplanar Amplituhedron*”, JHEP 1606, 098 (2016), [arxiv:1512.08591](#).
- [112] S. Franco, D. Galloni, A. Mariotti and J. Trnka, “*Anatomy of the Amplituhedron*”, JHEP 1503, 128 (2015), [arxiv:1408.3410](#).
- [113] S. N. Karp, “*Sign variation, the Grassmannian, and total positivity*”, [arxiv:1503.05622](#).
- [114] N. Arkani-Hamed, A. Hodges and J. Trnka, “*Positive Amplitudes In The Amplituhedron*”, JHEP 1508, 030 (2015), [arxiv:1412.8478](#).
- [115] D. Galloni, “*Positivity Sectors and the Amplituhedron*”, [arxiv:1601.02639](#).
- [116] N. Arkani-Hamed, Y. Bai and T. Lam, “*Positive Geometries and Canonical Forms*”, [arxiv:1703.04541](#).
- [117] M. Parisi, “*Symmetries of the Tree Amplituhedron*”, 2016, author’s MSc Thesis.
- [118] A. K. Tsikh, “*Multidimensional residues and their applications*”, AMS (1992).
- [119] N. Arkani-Hamed, “*The amplituhedron, scattering amplitudes and Ψ_U* ”, New geometric structures in scattering amplitudes, <http://tinyurl.com/ya3k6j6f>.
- [120] L. Ferro, T. Lukowski, C. Meneghelli, J. Plefka and M. Staudacher, “*Harmonic R-matrices for Scattering Amplitudes and Spectral Regularization*”, Phys.Rev.Lett. 110, 121602 (2013), [arxiv:1212.0850](#).
- [121] L. Ferro, T. Lukowski, C. Meneghelli, J. Plefka and M. Staudacher, “*Spectral Parameters for Scattering Amplitudes in $N=4$ Super Yang–Mills Theory*”, JHEP 1401, 094 (2014), [arxiv:1308.3494](#).
- [122] I. Gelfand, “*General theory of hypergeometric functions*”, Dokl. Akad. Nauk SSSR 288, 14 (1986).
- [123] K. Aomoto, “*Les équations aux différences linéaires et les intégrales des fonctions multiformes*”, J. Fac. Sci. Univ. Tokyo, Sect. IA Math. 22, 271 (1975).
- [124] M. Kita and K. Aomoto, “*Theory of hypergeometric functions*”, Springer-Verlag (2011).

- [125] L. Ferro, T. Lukowski and M. Staudacher, “ $\mathcal{N} = 4$ scattering amplitudes and the deformed Grassmannian”, Nucl. Phys. B889, 192 (2014), [arxiv:1407.6736](#).
- [126] I. M. Gelfand, M. I. Graev and V. S. Retakh, “General hypergeometric systems of equations and series of hypergeometric type”, Uspekhi Mat. Nauk SSSR 47:4, 3 (1992).
- [127] T. Oshima, “Capelli Identities, Degenerate Series and Hypergeometric Functions”, in: “Proceedings of a symposium on Representation Theory at Okinawa (1995)”, 1-19p.
- [128] I. Gelfand and G. Shilov, “Generalized Functions: Properties and operations, translated by E. Saletan”, Academic Press (1964).
- [129] T. Bargheer, Y.-t. Huang, F. Loebbert and M. Yamazaki, “Integrable Amplitude Deformations for $N=4$ Super Yang–Mills and ABJM Theory”, Phys. Rev. D91, 026004 (2015), [arxiv:1407.4449](#).
- [130] R. Frassek, N. Kanning, Y. Ko and M. Staudacher, “Bethe Ansatz for Yangian Invariants: Towards Super Yang–Mills Scattering Amplitudes”, Nucl. Phys. B883, 373 (2014), [arxiv:1312.1693](#).
- [131] N. Beisert, J. Broedel and M. Rosso, “On Yangian-invariant regularization of deformed on-shell diagrams in $\mathcal{N} = 4$ super-Yang-Mills theory”, J. Phys. A47, 365402 (2014), [arxiv:1401.7274](#).
- [132] J. Broedel, M. de Leeuw and M. Rosso, “A dictionary between R -operators, on-shell graphs and Yangian algebras”, JHEP 1406, 170 (2014), [arxiv:1403.3670](#).
- [133] L. D. Faddeev, “How algebraic Bethe ansatz works for integrable model”, [hep-th/9605187](#), in: “Relativistic gravitation and gravitational radiation”, 149-219p.
- [134] M. Staudacher, “Review of AdS/CFT Integrability, Chapter III.1: Bethe Ansätze and the R -Matrix Formalism”, Lett. Math. Phys. 99, 191 (2012), [arxiv:1012.3990](#).
- [135] H. Bethe, “Zur Theorie der Metalle. I. Eigenwerte und Eigenfunktionen der lineare Atomkette”, Z. Phys. 71, 205 (1931).
- [136] D. Chicherin, S. Derkachov and R. Kirschner, “Yang-Baxter operators and scattering amplitudes in $\mathcal{N} = 4$ super-Yang–Mills theory”, Nucl.Phys. B881, 467 (2014), [arxiv:1309.5748](#).
- [137] R. Frassek, D. Meidinger, D. Nandan and M. Wilhelm, “On-shell diagrams, Grammannians and integrability for form factors”, JHEP 1601, 182 (2016), [arxiv:1506.08192](#).
- [138] S. Fomin and A. Zelevinsky, “Cluster algebras I: foundations”, J. Am. Math. Soc. 15, 497 (2002), [math/0104151](#).

- [139] S. N. Karp and L. K. Williams, “*The $m=1$ amplituhedron and cyclic hyperplane arrangements*”, [arxiv:1608.08288](#).
- [140] S. N. Karp, L. K. Williams and Y. X. Zhang, “*Decompositions of amplituhedra*”, [arxiv:1708.09525](#).
- [141] N. Arkani-Hamed, H. Thomas and J. Trnka, “*Unwinding the Amplituhedron in Binary*”, [arxiv:1704.05069](#).
- [142] Y. Bai, S. He and T. Lam, “*The Amplituhedron and the One-loop Grassmannian Measure*”, JHEP 1601, 112 (2016), [arxiv:1510.03553](#).
- [143] J. L. Bourjaily, S. Franco, D. Galloni and C. Wen, “*Stratifying On-Shell Cluster Varieties: the Geometry of Non-Planar On-Shell Diagrams*”, JHEP 1610, 003 (2016), [arxiv:1607.01781](#).
- [144] P. Benincasa and D. Gordo, “*On-shell diagrams and the geometry of planar $\mathcal{N} < 4$ SYM theories*”, [arxiv:1609.01923](#).
- [145] P. Heslop and A. E. Lipstein, “*On-shell diagrams for $\mathcal{N} = 8$ supergravity amplitudes*”, JHEP 1606, 069 (2016), [arxiv:1604.03046](#).
- [146] E. Herrmann and J. Trnka, “*Gravity On-shell Diagrams*”, JHEP 1611, 136 (2016), [arxiv:1604.03479](#).